2015-3

Optimisation of Isolation Methods for the AZA Group of Marine Biotoxins and the Development of Accurate and Precise Methods of Analysis

Jane Kilcoyne
Technological University Dublin, jane.kilcoyne@marine.ie

Optimisation of isolation methods for the azaspiracid group of marine biotoxins and the development of accurate and precise methods of analysis.

Jane Kilcoyne

School of Chemical & Pharmaceutical Sciences

College of Sciences & Health

Dublin Institute of Technology

Marine Environment and Food Safety Services

Marine Institute

March 2015

Thesis submitted for the award of Doctor of Philosophy

Supervisors

Professor Christopher O. Miles

Dr. Barry Foley

DECLARATION PAGE

I certify that this thesis which I now submit for examination for the award of PhD, is entirely my own work and has not been taken from the work of others, save and to the extent that such work has been cited and acknowledged within the text of my work.

This thesis was prepared according to the regulations for postgraduate study by research of the Dublin Institute of Technology and has not been submitted in whole or in part for another award in any Institute.

The work reported on in this thesis conforms to the principles and requirements of the Institute's guidelines for ethics in research.

The Institute has permission to keep, lend or copy this thesis in whole or in part, on condition that any such use of the material of the thesis be duly acknowledged.

Signature _____ Date _____ Candidate

ACKNOWLEDGEMENTS

Firstly I would like to thank Margaret Rae – thankyou for putting the idea of doing a PhD into my head and for being so enthusiastic and supportive.

I am very fortunate and I appreciate very much that I have had the support of the Marine Institute who enabled me to carry out my studies while also providing me with a full time job.

I couldn't have wished for a better supervisor than Christopher Miles. Thankyou so much Chris for imparting all your wisdom, being so patient, kind, inspiring and motivating. I feel so privileged to have had you as my mentor.

Thanks to present and past colleagues at the Marine Institute; Conor Duffy, Stephen Burrell, Sinead O' Brien, Pat Costello, Ciara Nulty, Ger Clancy, Adela Stan, Orla Finch, Olivia Fitzgerald and Agnieszka Rupnik. Thanks also to Dermot Hurst for encouragement and advice. Special thanks to Stephen for all the support and the laughs – I am very lucky to have such a great hard working colleague who makes every work day fun! Also thanks so much to Ciara for all your help with the isolations and for being so conscientious.

I want to thank Philipp Hess – your work ethic and passion for the subject has been inspiring and again I feel very privileged to have worked with you. Thanks also for your encouragement and guidance through my studies.

I was extremely lucky to have had the chance to spend two 3 month placements at the NRC laboratories in Canada and I want to thank the following people for hosting me and being so helpful and welcoming during my time there; Michael Quilliam, Pat LeBlanc, Pearse McCarron, Krista Thomas, Ian Burton, Sabrina Giddings, Elliot Wright, Sheila Crain, Ruth Perez, Bill Hardstaff, Dian Marciniak, Khalida Bekri and Jeremy Melanson. Thanks to Pat and Pearse for supervising me– it was great working with you and I learned so much. Thanks also to Pearse for help with editing manuscripts, Ian for performing the NMR work on AZA6 and Sheila for doing the qNMR.

I spent a short period at the Ifremer laboratories in Nantes and would like to thank Philipp, Fabienne Herve and Thierry Jauffrais for looking after me.

Also thanks to Alistair Wilkins, Ingunn Samdal and Frode Rise who I had the pleasure of working with on a visit to the Norwegian Veterinary Institute. Both Chris and Alistair performed all the NMR structure elucidation work and Frode provided lots of instrument time on very busy instruments, which is very much appreciated.

Thanks to my publication co-authors Mike Twiner for performing all the *in vitro* testing and Elie Fux for all your input into the matrix effects study; your expertise has added significant value to the publications and it was a pleasure working with you both.

Thanks to Barry Foley for all the help and advice and finally, thanks to Professor Bill Baker and Professor John Cassidy for agreeing to be my examiners.

TABLE OF CONTENTS

ABBREVIATIONS

AOAC	Association of Analytical Communities
ADAM	9-anthryldiazomethane
ANOVA	analysis of variance
ASP	amnesic shellfish poisoning
AZA	azaspiracid
AZP	azaspiracid poisoning
CH_3CN	acetonitrile
CGC	cerebellar granular cell
COSY	correlation spectroscopy
CRM	certified reference material
DSP	diarrhetic shellfish poisoning
DTX1	dinophysistoxin -1
DTX2	dinophysistoxin -2
EC_{50}	half maximal effective concentration
EFSA	European Food Safety Authority
ESI	electrospray ionisation
Et_2O	diethyl ether
EtOAc	ethyl acetate
EtOH	ethanol
EU	European Union
FAO	Food and Agricultural Organisation
FDA	Federal Drug Administration
FIA	flow injection analysis
FIS	fragment ion scan
FSAI	Food Safety Authority Ireland
HABs	harmful algal blooms
HPLC	high performance liquid chromatography
HMBC	heteronuclear multiple bond correlation
HRMS	high resolution mass spectrometry
HSQC	heteronuclear single quantum coherence
ICH	International Conference on Harmonisation
INAB	Irish National Accreditation Board
JNK	c-Jun-N-terminal kinase
LC-FLD	liquid chromatography – fluorescence detection
LC-MS/MS	liquid chromatography - mass spectrometry
LC-PDA	liquid chromatography – photo diode array
LC-UVD	liquid chromatography – ultra violet detection
LLE	liquid-liquid extraction
LOD	limit of detection
LOQ	limit of quantitation
LRM	laboratory reference material
MBA	mouse bioassay
Me	methyl
MeOH	methanol
MS	mass spectrometry
MTS	3-(4,5-dimethylthiazol-2-yl)-5-(3-carboxymethoxyphenyl)-2-(4-sulfophenyl)-2H-tetrazolium
NDP	National Development Plan

NOESY	nuclear overhause effect spectroscopy
NMR	nuclear magnetic resonance
OA	okadaic acid
PBS	phosphate buffered saline
PMS	phenazine methosulfate
PSP	paralytic shellfish poisoning
PTX	pectenotoxin
QC	quality control
qNMR	quantitative nuclear magnetic resonance
QToF	quadrupole time of flight
QUASIMEME	quality assurance for marine environmental monitoring in Europe
RDA	retro-Diels Alder
RM	reference material
ROESY	rotating frame overhause effect spectroscopy
RSD	relative standard deviation
SD	standard deviation
SE	standard error
SIM	selected ion monitoring
SPE	solid phase extraction
SRM	selected reaction monitoring
SSR	sample to solvent ratio
STX	saxitoxin
TEF	toxic equivalent factor
TOCSY	total correlated spectroscopy
TSQ	triple stage quadrupole
UV	ultra violet
W	weight
YTX	yessotoxin

LIST OF THESIS PUBLICATIONS

The work presented in the following chapters has been published in peer reviewed scientific journals with one manuscript in preparation:

Kilcoyne, J., McCarron, Hess, P., Miles, C. O. Effects of heating on proportions of azaspiracids 1–10 in mussels (*Mytilus edulis*) and identification of novel carboxylated analogues. *Manuscript in preparation.*

Kilcoyne, J., Twiner, M., McCarron, P., Crain, S., Giddings, S. D., Foley, B., Rise, F., Hess, P., Wilkins, A. L., Miles, C. O. Structure elucidation, relative LC-MS response and *in vitro* toxicity of azaspiracids isolated from mussels (*Mytilus edulis*). **Journal of Agriculture and Food Chemistry**, 2015, DOI: 10.1021/acs.jafc.5b01320.

Kilcoyne, J., Nulty, C., Jauffrais, T., McCarron, P., Herve, F., Foley, B., Rise, F., Crain, S., Wilkins, A. L., Twiner, M., Hess, P., Miles, C. O. Isolation, structure elucidation, relative LC-MS response, and *in vitro* toxicity of azaspiracids from the dinoflagellate *Azadinium spinosum*. **Journal of Natural products**, 2014, 77, 2465–2474.

Kilcoyne, J., McCarron, P., Twiner, M., Nulty, C., Rise, F., Crain, S., Quilliam, M. A., Wilkins, A. L., Miles, C. O. Epimers of azaspiracids: Isolation, structural elucidation and relative response of 37-*epi*-azaspiracid1. **Chemical Research in Toxicology**, 2014, 27, 587−600.

Kilcoyne, J., Keogh, A., Clancy, G., LeBlanc, P., Burton, I., Quilliam, M.A., Hess, P., Miles, C. O. Optimisation of an isolation procedure for azaspiracids from shellfish and structural elucidation of AZA6. **Journal of Agriculture and Food Chemistry,** 2012, 60, 2447−2455.

Kilcoyne, J. and Fux, E. Strategies for the elimination of matrix effects in the LC-MS/MS analysis of the lipophilic toxins okadaic acid and azaspiracid-1 in molluscan shellfish. **Journal of Chromatography A,** 2010, 1217, 7123–7130.

Other publications associated with this work are listed below.

Kilcoyne, J.; Twiner, M. J.; McCarron, P.; Giddings, S. D.; Hess, P.; Miles, C. O. Structural elucidation and toxicity of a unique azaspiracid isolated from shellfish (*Mytilus edulis*). *Manuscript in preparation.* .

Jauffrais T., **Kilcoyne J.,** Herrenknecht C., Truquet P., Séchet V., Miles C. O., Hess P. Dissolved azaspiracids are absorbed and metabolized by blue mussels (*Mytilus edulis*). **Toxicon**, 2013, 65, 81–89.

Jauffrais, T., **Kilcoyne, J.,** Séchet, S., Herrenknecht, C., Truquet, P., Hervé, F., Bérard, J., Nulty, C., Taylor, S., Tillmann, U., Miles, C., Hess, P. Production and preparative isolation of azaspiracid-1 and -2 from *Azadinium spinosum* culture in pilot scale photobioreactors. **Marine Drugs,** 2012, 10, 1360–1382**.**

Twiner, M., El-Ladki, R., **Kilcoyne, J.,** and Doucette, G. Comparative effects of the marine algal toxins azaspiracid-1, -2, and -3 on Jurkat T lymphocyte cells. **Chemical Research in Toxicology,** 2012, 25, 747–754.

Salas, R., Tillmann, U., Uwe, J., **Kilcoyne, J.,** Burson, A., Cantwell, C., Hess, P., Jauffrais, T., Silke, J. The role of *Azadinium spinosum* (Dinophyceae) in the production of azaspiracid shellfish poisoning in mussels. **Harmful Algae,** 2011, 10, 774–783.

Kilcoyne, J., Jauffrais, T., Krock, B., Uwe, John., Twiner, M. J., Doucette, G. J., Aasen Bunæs, J. A., Nulty, C., Salas, R., Clarke, D., Geraghty, J., Sosa, S., McCarron, P., Quilliam, M., Miles, C. O., Silke, J., Cembella, A., Tillmann, U. and Hess, P. Azaspiracids - toxicological evaluation, test methods and identification of the source organisms (ASTOX II). **Marine Institute – Marine Research Sub-Programme (NDP 2007−2013) series** (http:/oar.marine.ie/handle/10793/970)

Hess, P., McCarron, P., Krock, B., **Kilcoyne, J.,** Miles, C. O. Azaspiracids: chemistry, biosynthesis, metabolism and detection. In: **Seafood and Freshwater toxins, 3rd Ed.** Botana, L. M. (Ed.), CRC Press, Boca Raton, FL. 2014, pp799−821.

ABSTRACT

The two main groups of biotoxins which affect the Irish shellfish industry are azaspiracids (AZAs) and the okadaic acid (OA) group (OA, DTX2, DTX1 and their esters) toxins. Since AZAs were first identified in 1998, well over 30 analogues have been reported. Structural and toxicological data have been described for AZA1–5 (isolated from shellfish). LC-MS/MS is the EU reference method for detection of the AZAs (AZA1, -2 and -3) and the OA group toxins in raw shellfish with the regulatory limit set at 160 µg/kg for each toxin group. Limited supplies of purified toxins for certified reference materials (CRMs) were available for AZA1−3. Little knowledge was also available on the relevance of the additional AZA analogues that had been reported, in terms of human health protection.

The analysis of marine biotoxins by LC-MS/MS can be severely affected by matrix interferences. Here, a study was performed on two instruments; a quadrapole time of flight (QToF) and a triple stage quadrupole (TSQ) to assess matrix interferences for AZA1 and OA using a number of tissue types. Enhancement was observed for OA on the QToF while matrix suppression was observed for AZA1 on TSQ. The enhancement on the QToF was overcome by use of an on-line SPE method and matrix matched calibrants, while the suppression on the TSQ was found to be due to late eluting compounds from previous injections and was overcome by employing either a column flush method or an alkaline mobile phase.

The isolation of 11 AZA analogues (AZA1−10 and 37-*epi*-AZA1) from shellfish using an improved procedure (7 steps) is described. Recoveries increased ~2-fold (~ 52%) from previously described isolation procedures.

The preparative isolation procedure developed for shellfish was optimised for *Azadinium spinosum* bulk culture extracts such that only four steps were necessary to obtain purified AZA1 and -2. A purification efficiency of ~70% was achieved, and isolation from 1,200 L of culture yielded 9.3 mg of AZA1 and 2.2 mg of AZA2 (purities >95%). This work demonstrated the

feasibility of sustainably producing AZA1 and -2 from *A. spinosum* cultures. In addition to AZA1 and -2, the novel analogues AZA33, -34 were isolated (also from *A. spinosum*).

Sufficient quantities were purified to enable full structural elucidation, the preparation of reference standards and CRMs, and toxicity studies. Nine of these analogues were fully characterised for the first time (Table 7.1). Structural determination was achieved by NMR and chemical analysis, while toxicity was assessed using the Jurkat T lymphocyte cell assay, mouse intraperitoneal (AZA1−3 and -6) and mouse oral (AZA1−3) administration.

The preparation of reference standards for the analogues AZA4−10, 37-*epi*-AZA1, AZA33 and -34 enabled their relevance in terms of human health protection to be determined. The *in vitro* and *in vivo* toxicity studies performed confirmed AZA toxicity. Using the Jurkat T lymphocyte assay the order of potency is: AZA2 > AZA6 > AZA34 ≈ 37-*epi*-AZA1 > AZA8 ≈ AZA3 > AZA1 > AZA4 ≈ AZA9 > AZA5 ≈ AZA10 > AZA33.

The results from the oral and intraperitoneal mice studies correlated very well, contradicting previous reports and showing that AZA1 is more toxic than AZA2 and -3 and that AZA6 is slightly less toxic than AZA1 i.e., AZA1 > AZA6 > AZA2 > AZA3.

Analysis of shellfish (*Mytilus edulis*) submitted to the Irish biotoxin monitoring programme using the reference standards confirmed previous reports showing that levels of AZA3, -4, -6 and -9 increase following cooking due to heat induced decarboxylation of AZA17, -21, -19 and -23. Very high levels of AZA3 (up to 3-fold that of AZA1) and -6 (up to 3- fold that of AZA2) were detected in some samples (with levels varying most likely due to different rates of metabolism and time of harvesting). As the concentrations of AZA3 and -6 are negligible in raw mussels, yet can increase significantly during the cooking of mussels, the overall concentrations are underestimated by methods used according to current legislation.

In cooked shellfish the AZA analogues -4, -5, -7–10, as well as AZA33 and -34, comprise on average ~5% of the total AZA content, however in some samples levels of AZA4 were higher

than AZA6. Levels of the 37-epimers in the cooked shellfish extracts were ~ 15% that of the parent analogues.

CHAPTER 1 - INTRODUCTION

1.1. The Irish shellfish industry

Since the 1970s the Irish shellfish industry has expanded rapidly. The value was estimated to be worth over €60 million in 2012[1] and there is significant potential for further growth. The main products are mussels, oysters, scallops and clams. Currently there are ~ 90 shellfish harvesting sites around the coasts of Ireland. 76% of all aquaculture production is conducted along the Western seaboard and is an important contributor to job creation and the economy for these coastal communities.

Mussels account for the biggest production – 6,000 tonnes of bottom and 9,000 tonnes of rope mussels were produced in 2012. Total employment in the mussel industry was 444 in the same year with exports valued at over €20 million. Over 50% of the mussels produced in Ireland are certified organic.

Oysters are the second largest shellfish product produced in Ireland with ~ 7,600 tonnes produced in 2012 and employing 933 people. Oyster exports in 2012 were valued at over €35 million. France was the biggest export market accounting for 86% of oyster exports.

Other varieties produced are scallops, clams, razor fish, cockles and limpets.

One of the limiting factors for the industry is the occurrence of biotoxin producing algae on which the shellfish feed. These algae can accumulate in shellfish to toxic levels (for human health) over a very short time period.

The adverse impacts of harmful algal blooms (HABs) on farmed shellfish in Europe was estimated to cost €53.78 million per annum from 2001 to 2009. In Ireland, the figure was estimated at €1.64 million over the same period.[2]

1.2. EU regulated marine biotoxins

1.2.1. Hydrophilic toxins

1.2.1.1. Domoic acid

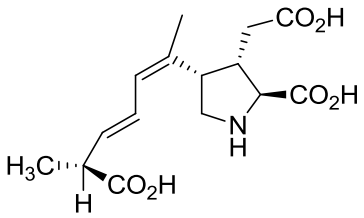

Figure 1.1. Structure of domoic acid.

The first reported case of an amnesic shellfish poisoning (ASP) event was in 1987 in Canada following the consumption of mussels. The symptoms included nausea, vomiting, abdominal cramps and diarrhoea which appeared within the first 24 h following consumption. Neurological systems then kicked in within 48–72 h and included confusion, disorientation, loss of short term memory, seizures and coma. A number of people were hospitalised and four people died as a result of this poisoning event. Domoic acid (a tricarboxylic acid) was soon discovered as the toxin responsible[3] and has since been found worldwide, although no other poisoning incident associated with this toxin group has since been reported.

The toxin is produced by the genus *Pseudo-nitzchia*,[4] a marine diatom and is typically associated with mussels and scallops in Ireland.[5] Domoic acid induces toxicity by activating the kainite class of glutamate neurotransmitter receptors.[6] The EU regulatory limit is set at 20 µg/g for domoic acid and *epi*-domoic acid.

1.2.1.2. Paralytic shellfish poisoning toxins

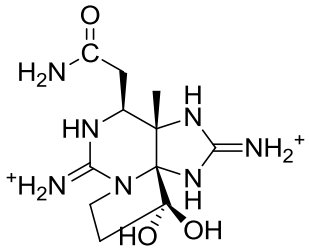

Figure 1.2. Structure of saxitoxin.

The paralytic shellfish poisoning (PSP) toxins are the most serious shellfish toxins in terms of effects on human health with very low levels capable of inducing human fatalities. These toxins are produced by the dinoflagellates *Alexandrium* spp[7] and *Gymnodinium* spp[8] and are distributed globally. More than 20 analogues have been reported to occur naturally, with saxitoxin (STX) being the parent analogue.

The basic structure consists of a tetrahydropurine skeleton with two guanidinium groups (Figure 1.2). They exert their toxic effects by blocking the sodium ion channel and symptoms include tingling sensations, numbness of the extremities, headache, dizziness, nausea, vomiting, diarrhoea and in severe cases, death by asphyxiation.[9] The EU regulatory limit for PSP toxins is 800 µg/kg STX equivalents.

1.2.2. Lipophilic toxins

1.2.2.1. Azaspiracids

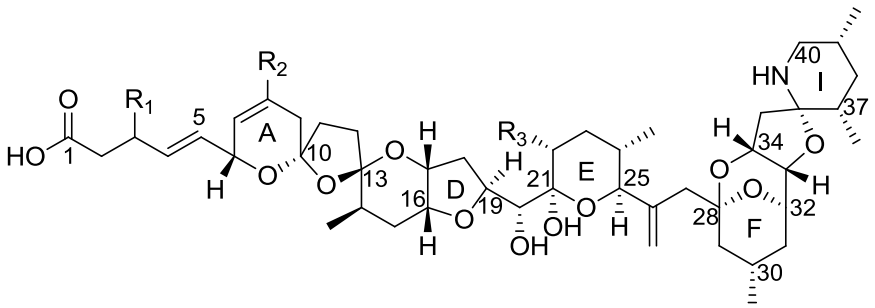

Toxin	R_1	R_2	R_3
AZA1	H	H	CH_3
AZA2	H	CH_3	CH_3
AZA3	H	H	H

Figure 1.3. Structure of azaspiracid1−3.

AZAs were first discovered in 1998 following a poisoning outbreak in 1995 in the Netherlands associated with Irish shellfish.[10] Symptoms included nausea, vomiting, abdominal cramps and diarrhoea which appeared within the first 24 h following consumption.[11] AZA1 was initially isolated and characterised[10] followed by the analogues AZA2 and -3[12] in 1999 and AZA4 and -5 in 2001.[13] The AZAs were found to have highly oxygenated polyether structures with a spiro ring, a cyclic amine and a carboxylic acid moiety. More than 20 additional analogues were subsequently observed in shellfish by LC-MS/MS.[14] It was not until 2009 that the producer of these toxins was identified – a small (5 µm in width) thecate dinoflagellate, subsequently named *Azadinium spinosum*.[15] *A. spinosum* was found to produce only AZA1 and -2 in culture[16] and it is believed that many of the other analogues are produced in the shellfish via metabolism.[14,17] AZAs have been detected globally and there have been a number of poisoning events associated with this toxin group since the first report in 1995, all of which were sourced back to Irish shellfish.[18] The EU regulatory limit is set at 160 µg/kg for AZA1, -2 and -3.

1.2.2.2. Okadaic acid group

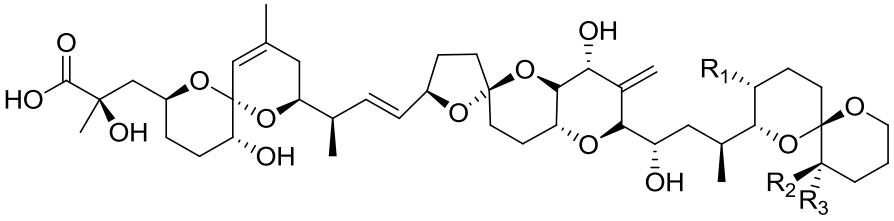

Toxin	R_1	R_2	R_3
OA	CH_3	H	H
DTX1	CH_3	CH_3	H
DTX2	H	H	CH_3

Figure 1.4. Structure of OA group.

OA group toxins result in a syndrome known as diarrhetic shellfish poisoning (DSP), the symptoms of which mimic those of AZAs; nausea, vomiting, abdominal cramps and diarrhoea which appear within the first 24 h following consumption. The first poisoning incident associated with this toxin group occurred in Japan in 1976 following the consumption of mussels.[19] The OA group consists of OA, dinophysis toxin 1 (DTX1), dinophysis toxin 2 (DTX2) and their esters. Structurally they consist of long chain compounds containing trans-fused or spiro-linked cyclic polyether rings (Figure 1.4). The induced toxicity is due to inhibition of protein phosphatases PP1 and PP2A. This toxin group has been detected globally[5,20–22] and is produced by the marine dinoflagellate species of the genus *Dinophysis*[20,23] and *Prorocentrum.*[24.25] The EU regulatory limit is set at 160 µg/kg for OA, DTX1, DTX2 and their esters.

1.2.2.3. Pectenotoxins

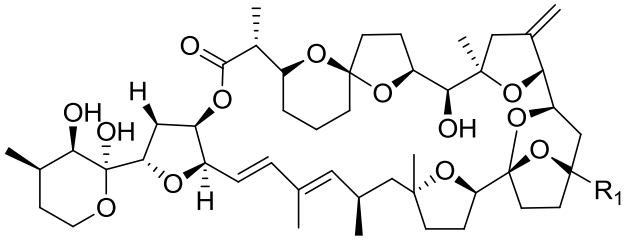

Toxin	R_1
PTX1	CH_2OH
PTX2	CH_3

Figure 1.5. Structure of PTX1 and PTX2 group.

Pectenotoxins (PTXs) are produced by some of the algae (*Dinophysis*[26–30]) that also produce the OA group toxins and these toxins regularly co-occur in shellfish. PTX1 and PTX2 were originally isolated from shellfish in 1984[31] and are included with the OA group toxins for regulation i.e., the limit is 160 µg/kg for the OA group and PTX1 and PTX2. They have also been found in *Protoperidinium*.[32] They are cyclic polyether lactone compounds. PTX2 is the most common analogue which is metabolised in shellfish to produce other derivatives, such as PTX1, PTX3 PTX6[23] and PTX2 seco acid.[32]

These toxins have not been shown to be toxic when administered orally.[30,32] In addition no human poisoning events have been associated with this toxin group hence these compounds are not considered of major concern to human health.

1.2.2.4. Yessotoxins

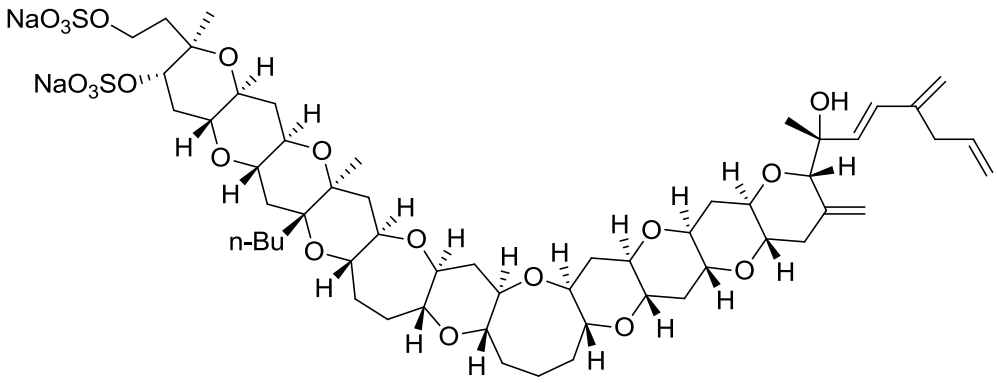

Figure 1.6. Structure of yessotoxin.

Yessotoxins (YTXs) were first discovered in 1986 in scallops from Japan.[33] They are produced by *Prorocentrum reticulatum*,[34] *Lingulodinium polyedrum*[35] and *Gonyaulax spinifera*.[36] A wide range of compounds belonging to the YTX group have been identified. The basic structure consists of a disulphated polyether with an unsaturated side chain. YTX was initially classified as a DSP toxin[33] however it has since been found not to induce toxic effects in oral mouse studies[37,38] and is therefore not deemed to be of significance to human health. Furthermore, studies investigating the combined effects of AZAs and YTXs found that YTX does not have any synergistic effects when administered orally with AZA1.[39] Recently EU legislation was amended increasing the limit to 3.75 mg/kg.[40]

1.3. Toxic episodes in Ireland

AZAs have been detected in shellfish since the monitoring programme was established in 2001. Since that time there was only one year (2004) in which there were no closures due to AZAs being over the regulatory limit (160 µg/kg), Figure 1.7. Typically onset of toxicity occurs mid to late summer. Those sites that are affected can remain closed for long periods due to the slow

depuration rates of AZAs from shellfish. The highest recorded levels in shellfish were in 2005 where concentrations reached 9 µg/g (60 times over the regulatory limit) at a site in Donegal. Mussels are the worst affected shellfish. 2012 was the most extensive and protracted toxicity period with sites all along the West coast being closed, some of which were closed for almost one year. This trend was repeated in 2013 and is causing severe economic hardship for shellfish farmers. Interestingly, the AZAs appear to be only problematic in Ireland and all of the poisoning incidents associated with these toxins can be sourced back to shellfish harvested in Ireland. Norway and the UK are the only other countries to date that have reported AZAs being just over the regulatory limit in shellfish.

The second most important toxin group which affects the shellfish industry in Ireland is the OA group toxins. Since 2002 these toxins have been detected in shellfish every year resulting from blooms of *Dinophysis acuta* or *Dinophysis acuminata* (which produce OA and DTX2). The Southwest of the country is particularly prone to accumulation of both OA group and AZA toxins in shellfish, Figure 1.7. Typically OA group toxicity occurs early to mid-summer and regularly there is co-occurrence with the AZAs. Again mussels are the worst affected shellfish, however the OA group toxins are quicker to depurate than the AZAs.

Closure of sites has also resulted due to levels of domoic acid being over the regulatory limit (20 µg/g). Typically only scallops are tested for this toxin group however at certain times of the year (usually spring time) large blooms of the producing species *Pseudo-nitzchias* result in high levels of domoic acid in mussels. Such onsets occur quickly but also the concentration levels in the shellfish reduce very quickly.

Fortunately the PSP toxins are not problematic for the Irish shellfish industry, to date, with closures only ever occurring in Cork Harbour due to these toxins being over the regulatory limit (>800 µg/kg STX equivalents). The PSPs have been detected in shellfish from other parts of the country, however, levels have been extremely low.

PTXs were detected for the first time in Irish shellfish in 2014, while YTXs have not been detected to date.[5]

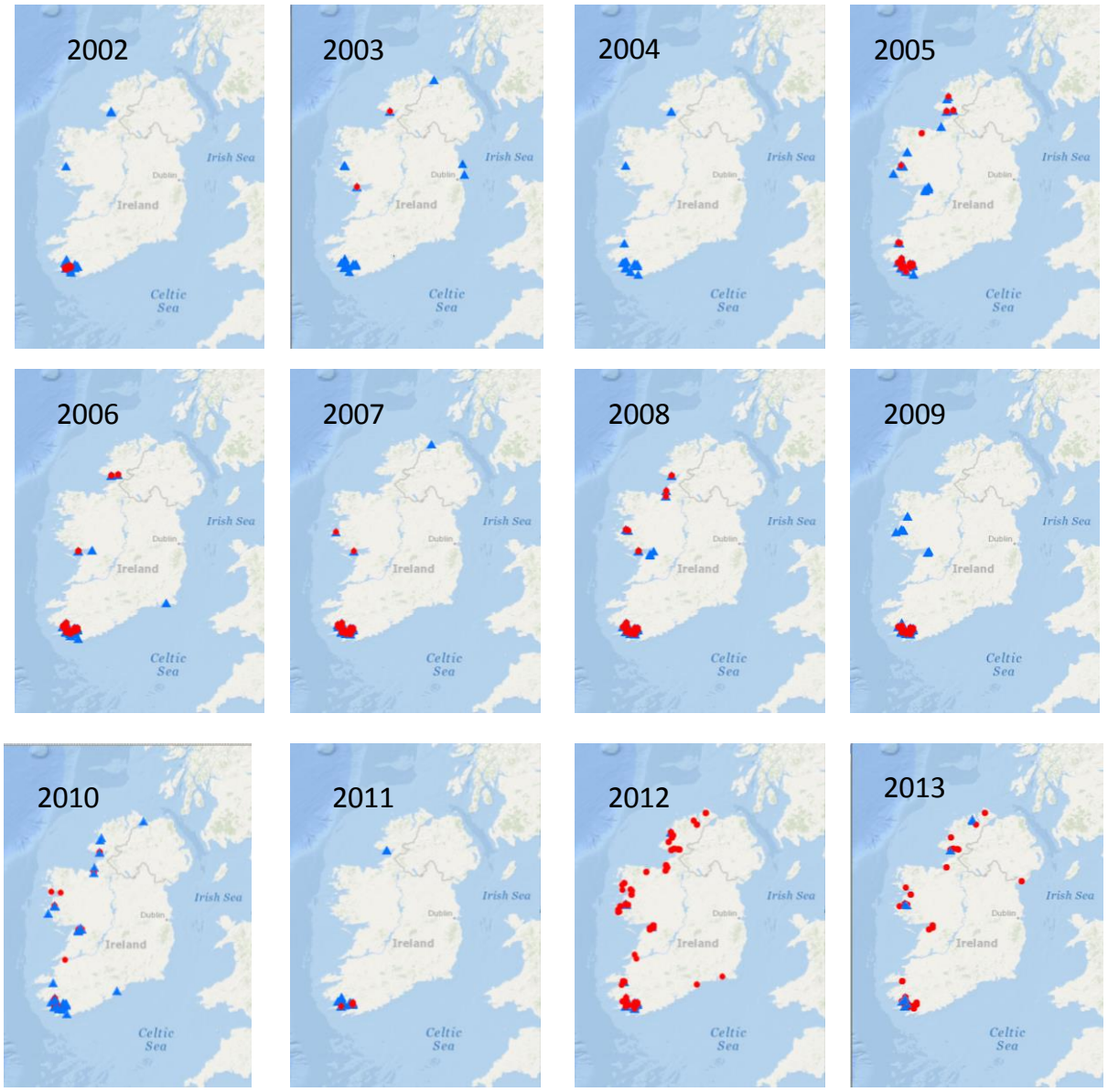

Figure 1.7. Closure of Irish shellfish harvesting sites due to AZAs and OA group toxins from 2002–2013.

1.4. Methods of analysis

The marine biotoxin monitoring programme was set up in Ireland in 2001. At that time the EU regulatory method for the monitoring of the lipophilic toxins and PSPs in shellfish was by the Mouse BioAssay (MBA).[41] Along with the MBA, phytoplankton monitoring and analysis of shellfish extracts (for the lipophilic toxins) by LC-MS/MS was performed in parallel. Domoic acid was monitored by a HPLC-UV method.

The LC-MS/MS method was limited by the lack of CRMs for all the regulated toxins with standard calibrants only available for OA (certified) and AZA1 (non-certified). In 2003 the Marine Institute received National Development Plan (NDP) funding for a three year project on AZAs named ASTOX.[42] One of the main aims of the project was to purify sufficient amounts of AZA1–3 to produce CRMs to aid in the monitoring of these toxins. Through collaborations with other international research teams the project aims were achieved; successful isolations of AZA1–3 from shellfish, enabling the production of CRMs.[43] A number of tissue CRMs were also prepared for the first time over the course of the project.[44,45] In addition to preparing CRMs for the AZAs the project was also successful in producing a CRM for DTX2.[42] CRMs are essential to ensure accurate results are being produced by monitoring laboratories. The availability of these CRMs enabled more accurate analysis to be performed by LC-MS/MS and facilitated the introduction of new legislation replacing the MBA and implementing LC-MS/MS as the regulatory method.[46] In parallel the PSP MBA was replaced by a HPLC-FLD method.

Currently at the Marine Institute, Irish National Accreditation Board (INAB) accredited methods are employed for the analysis of all the EU regulated toxins. Proficiency testing schemes are also used to ensure the validity of results being produced – the Marine Institute subscribes to QUASIMEME (Quality Assurance of Information for Marine Environmental Monitoring in Europe) twice yearly for all the toxin groups and a Community Reference Laboratory (CRL) intercomparison, which is run annually.

In parallel with the chemistry methods, the phytoplankton monitoring programme provides a complementary service in providing valuable information on the presence of toxin producing algae in the water.

1.4.1. LC-MS/MS

LC-MS/MS with electrospray ionisation (ESI) is the technique of choice for the analysis of many of the regulated marine biotoxins offering specificity, selectivity and high sensitivity, particularly with the newer instruments. The most common instruments used for quantitative, high throughput analysis are the tandem mass spectrometers (QqQ), also known as a TSQ, consisting of two quadrupole mass spectrometers in series, with a (non mass-resolving) radio frequency (RF)-only quadrupole between them to act as a cell for collision-induced dissociation. Precursor ions selected in the first quadrupole (Q1) are dissociated in the collision cell (Q2) in the presence of an inert gas such as Ar, He, or N_2, with the generated fragment ions from the precursor ion being scanned in the second quadrupole (Q3).

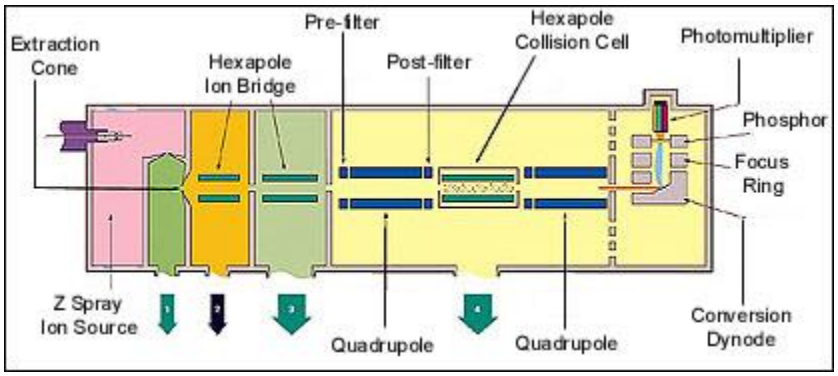

Figure 1.8. Schematic of a Micromass tandem mass spectrometer. Courtesy of Micromass-Waters

Such instruments can be operated in selected reaction monitoring mode (SRM) whereby the precursor and fragment ions are selected or selected ion monitoring (SIM) mode where only the

precursor ion is selected (no fragmentation). Due to the targeted nature of SRM, tandem mass spectrometers have mostly contributed to confirmation of known analytes, and not to the discovery of novel compounds. Numerous multitoxin MS methods have been developed using such instruments.[47–49] The emergence of fast scanning instruments in parallel with UPLC systems has enabled rapid sample turnaround time for monitoring laboratories.

High resolution mass spectrometers (HRMS), such as QToF instruments are required for the detection and characterisation of novel compounds. These instruments have a quadrupole where the precursor ions are selected, a collision cell followed by a time of flight (TOF) sector. The TOF has an extended flight path (V or W) through which the ions travel and separate based on their mass-to-charge ratio, enabling mass spectral data and accurate mass measurements to be produced. A mass resolution of ~ 10,000 can be obtained with older QToF instruments (Figure 1.9), whereas newer instruments offer resolutions of ≥ 50,000. The discovery of novel AZA analogues was reported using the QToF shown in Figure 1.9.[14]

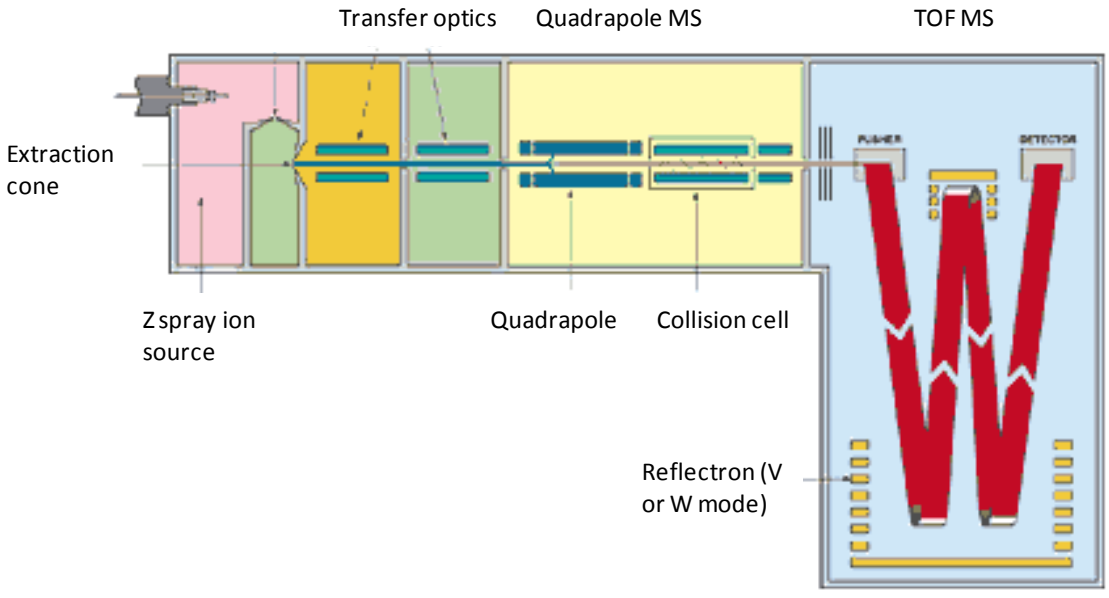

Figure 1.9. Schematic of a Micromass quadrupole time of flight mass spectrometer. Courtesy of Micromass-Waters

The increasing complexity of samples and increasing detection of novel compounds has led to more advanced MS instruments that are robust with high resolving power, mass accuracy, sensitivity and dynamic range. Non targeted HRMS screening using Orbitrap instruments has been reported recently for the detection of marine biotoxins.[50,51] Such instruments allow for effective screening of complex samples for known and unknown compounds, however, additional analysis by a QToF is required for structural characterisation.

1.4.2. NMR

Many of the marine biotoxins are cyclic polyethers consisting of long carbon chains substituted with hydrogen atoms. Such structures lend themselves well to ^{1}H and ^{13}C NMR spectroscopy, and it is this method, supplemented by mass spectrometry, that has primarily been used for structure determination.[10,12,52,53] Typically the minimum amount of highly purified (>95%) sample required is 100 µg for purity assessment and structural elucidation. Full stereochemical elucidation may not always be possible by NMR alone but requires chemical synthesis and/or X-ray crystallography. The stereochemistry of OA and AZA were only confirmed following synthesis of the compounds by Forsyth *et al.*[54] and Nicolaou *et al.*,[55–57] respectively.

1.5. Toxicology of AZAs

1.5.1. *In vivo*

Mice exposed to mussel extracts containing AZA via intraperitoneal injection exhibited "neurotoxin-like" symptoms characterized by sluggishness, respiratory difficulties, spasms, progressive paralysis, and death within 20–90 min.[11,58] The intraperitoneal minimum lethal dose of partially purified AZA1 was originally determined to be 150 µg/kg,[11] while from the first purified AZA1 a lethal dose was identified to be 200 µg/kg.[10] The intraperitoneal minimum lethal doses of AZA2 and -3 were 110 and 140 µg/kg, respectively,[12] suggesting higher potency

relative to AZA1. These results have since been used for toxic equivalent factor (TEF) determination and application for regulatory purposes.[59] The more polar AZA4 and -5 (hydroxylated versions of AZA3) were less potent with lethal dose values of 470 and <1,000 µg/kg, respectively.[13]

Due to the lack of purified AZAs, limited studies on their acute oral toxicity have been performed. Previous studies focused only on AZA1. These studies found that the gastrointestinal tract, liver, spleen and thymus were the main organs affected.[37,39,60–63]

Studies by Aasen *et al.*[61] and Aune *et al.*[64] using female NMRI mice demonstrated that doses of 100–540 µg/kg were insufficient to kill any of the tested animals but doses above 600 µg/kg resulted in some mortality. The experimentally determined LD_{10} and LD_{50} levels (with 95% confidence intervals) were 570 (435–735) and 775 (596–1,055) µg/kg, respectively.[64]

In separate experiments, severe injuries were induced by two repeated doses of 250, 300, 350, or 450 µg/kg, two days apart, and recovery was monitored for up to 90 days. Of the 16 mice receiving 450 µg/kg, 11 died prior to the second dose, suggesting a revised minimum oral lethal dose of <450 µg/kg. [65]

The most common pathological effect of AZA1 following oral exposure is degradation of the lining surrounding the upper small intestine.[60–64] Despite known uptake and systemic distribution of AZA1 following oral exposure, only limited and less severe histopathological changes were observed in other internal organs/tissues. Moderate doses of AZA1 (100–300 µg/kg) resulted in the liver being abnormally pale in coloration,[64] which may be the result of fatty acid droplet accumulation.[60] Higher doses (500–700 µg/kg) increased liver weight by 38%. There were time- and dose-dependent effects on the number of necrotic lymphocytes in the thymus, spleen, and the Peyer's patches of the small intestine, which was supported by quantitation of the number of non-granulocytes (lymphocytes, monocytes, macrophages) in the spleen. AZA1 treatments of 600 and 700 µg/kg resulted in a 33% decrease in the number of non-granulocytes, which were

primarily T and B lymphocytes.[60] There were no reported histological changes associated with the kidney, heart, lung, and brain.[60,61,64]

1.5.2. *In vitro*

Preliminary experiments performed by Flanagan *et al.*[66–68] using HepG2 hepatoblastoma cells and human bladder carcinoma cells (ECV-304) exposed to contaminated crude mussel extracts showed AZAs to have a cytotoxic effect. In the ASTOX project,[42] cellular and molecular studies were designed to investigate the mode of action underlying the toxicity of AZAs. Studies conducted on seven different mammalian cell lines showed that AZAs strongly affect most cell types. A functional assay was developed in the project for the specific detection of AZAs using morphological changes of pseudopodia in lymphocyte T cells (Jurkat). It was subsequently found to be the most sensitive for AZAs of all the assays tested.[42] In T lymphocytes, cells initially responded to AZA1 by a reduction in membrane integrity, organelle protrusion concurrent with flattening of cells, and a retraction of their pseudopodia or lamellipodia.[69] This was followed by protracted cell lysis. Using this assay the relative toxicities of the regulated AZAs were: AZA2>AZA1>AZA3,[70] which confirmed the original mouse intraperitoneal relative toxicities.[10,12]

In leukaemia cells, AZA2 caused DNA synthesis phase arrest.[71] In neuroblastoma cells, AZA1 induced cell rounding and detachment from adjacent cells.[72] At the subcellular level, disruption of the Golgi complex and an accumulation of vesicles have been reported.[73] At the cellular level, AZA1, -2, and two other semi-synthetic analogues of AZA2 all induced gross morphological changes.[74] AZA1 is a potent cytotoxin towards primary cerebellar granular cells (CGCs),[75] neocortical cells,[76] and spinal cord neurons.[77] In CGCs, AZA-induced cytotoxicity was related to the activation of the c-Jun-N-terminal kinase (JNK),[78,79] whereby AZA1 exposure resulted in decreased neuronal volume that was protected by pre-incubation of the neurons with a JNK inhibitor (SP 600125), a chloride channel blocker (4,4-diisothiocyanatostilbene-2,2-disulfonic

acid; DIDS), and a Na^+-K^+-ATPase blocker (amiloride).[78,80] The effects of AZA1 and -2 on cytotoxicity (and other cellular indices) appear to be irreversible.[72,74,77,81] Experiments using human breast cancer cells and mouse fibroblasts exposed to AZA1 have also demonstrated that the reductions in cellular proliferation and density are not unlike the actions elicited by YTX, raising the possibility of similar mechanisms of action for these two phycotoxin classes.[82]

1.6. Objectives

One of the limiting issues in the analysis of compounds by LC-MS/MS is matrix effects. Matrix effects were observed for both the AZA and OA group toxins using instrumentation employed at the Marine Institute. Such interferences can affect the accuracy of results being produced hence there was a strong need to try and overcome these issues. The initial study (Chapter 2) was performed to assess the impact of such interferences on two LC-MS/MS instruments and implement methods to surmount them where present.

Prior to this study only AZA1–5 were isolated, characterised and assessed for toxicity. However, more than 30 AZAs had been identified[14] with little knowledge of what impact these additional analogues have on human health. Studies (Chapters 3−6) performed as part of this thesis set out to try and improve on previously reported methods used to isolate AZAs from shellfish in terms of efficiency and recoveries. With the discovery of the producing organism *A. spinosum* in 2009,[15] further isolation method development was envisaged from bulk culture extracts. Isolation of as many of the known and novel AZA analogues as possible was intended to enable full characterisation, the preparation of reference materials and further toxicological studies. Up to this point the mode of action of AZAs was unknown, hence the availability of sufficient amounts of purified toxin was essential to allow such studies to proceed. Furthermore with the change in

legislation from use of the MBA to LC-MS/MS for the detection of these toxins, the sustained supply of CRMs for the regulated toxins was imperative.

Additional questions remained about the effects of cooking on AZAs in shellfish. This was of concern due to processed shellfish being rejected by importing countries despite being under the regulatory limit when tested prior to processing. Heat induced decarboxylation of AZA17, -19, 21 and -23 to AZA3, -6, -4 and 9 respectively had already been reported,[17] however, the significance of these transformations had yet to be fully explored and further work in this area is detailed in Chapter 6.

1.7. References

(1) BIM 2012, BIM annual aquaculture survey. **2013**.

(2) Maguire, J. Applied simulations and integrated modelling for the understanding of toxic and harmful algal blooms. *EU Project ASIMUTH* **2011**, 1–8.

(3) Nijjar, M. S.; Nijjar, S. S. Ecobiology, clinical symptoms and mode of action of domoic acid, an amnesic shellfish toxin. In *Seafood and Freshwater Toxins: pharmacology, physiology and detection, Botana, L. M (Ed)*; Marcel Dekker: New York, USA, **2000**; pp. 325–358.

(4) Perl, T. M.; Bedard, L. M.; Kosatsky, T. M. D.; Hockin, J. C.; Todd, E. C. D.; Remis, R. S. An outbreak of toxic encephalopathy caused by eating mussels contaminated with domoic acid. *New England J. Med.* **1990**, *322*, 1775–1780.

(5) HABs, database http://www.marine.ie/home/publicationsdata/data/Habs+Search+Database/HabsSearch.htm. Accessed 14 May 2014.

(6) Doble, A. Pharmacology of domoic acid. In *Seafood and Freshwater Toxins: pharmacology, physiology and detection, Botana, L. M (Ed)*; **2000**; pp. 359–379.

(7) Oshima, Y.; Bolch, C. J.; Hallegraeff, G. M. Toxin composition of resting cysts of *Alexandrium tamarense* (Dinophyceae). *Toxicon* **1992**, *30*, 1539–1544.

(8) Oshima, Y.; Blackburn, S.; Hallegraeff, G. M. Comparative study on paralytic shellfish toxin profiles of the dinoflagellate *Gymnodinium catenatum* from three different countries. *Mar. Biol.* **1993**, *116*, 471–476.

(9) Anon. Report of the Joint FAO/IOC/WHO ad hoc Expert Consultation on Biotoxins in Molluscan Bivalves. *Food and Agriculture Organization* **2004**.

(10) Satake, M.; Ofuji, K.; Naoki, H.; James, K. J.; Furey, A.; McMahon, T.; Silke, J.; Yasumoto, T. Azaspiracid, a new marine toxin having unique spiro ring assemblies, isolated from Irish mussels, *Mytilus edulis*. *J. Am. Chem. Soc.* **1998**, *120*, 9967–9968.

(11) Satake, M.; Ofuji, K.; James, K. J.; Furey, A.; Yasumoto, T. New toxic event caused by Irish mussels. In *Harmful Algae*; Reguera, B.; Blanco, J.; Fernandez, M. L.; Wyatt, T., Eds.; Xunta de Galicia and Intergovernmental Oceanographic Commission of UNESCO: Santiago de Compostela, Spain, **1998**; pp. 468–469.

(12) Ofuji, K.; Satake, M.; McMahon, T.; Silke, J.; James, K. J.; Naoki, H.; Oshima, Y.; Yasumoto, T. Two analogs of azaspiracid isolated from mussels, *Mytilus edulis*, involved in human intoxications in Ireland. *Nat. Toxins* **1999**, *7*, 99–102.

(13) Ofuji, K.; Satake, M.; McMahon, T.; James, K. J.; Naoki, H.; Oshima, Y.; Yasumoto, T. Structures of azaspiracid analogs, azaspiracid-4 and azaspiracid-5, causative toxins of azaspiracid poisoning in Europe. *Biosci. Biotechnol. Biochem.* **2001**, *65*, 740–742.

(14) Rehmann, N.; Hess, P.; Quilliam, M. A. Discovery of new analogs of the marine biotoxin azaspiracid in blue mussels (*Mytilus edulis*) by ultra-performance liquid chromatography/tandem mass spectrometry. *Rapid Commun. Mass Spectrom.* **2008**, *22*, 549–558.

(15) Tillmann, U.; Elbrächter, M.; Krock, B.; John, U.; Cembella, A. D. *Azadinium spinosum* gen. et sp. nov. (Dinophyceae) identified as a primary producer of azaspiracid toxins. *Eur. J. Phycol.* **2009**, *44*, 63–79.

(16) Krock, B.; Tillmann, U.; John, U.; Cembella, A. D. Characterization of azaspiracids in plankton size-fractions and isolation of an azaspiracid-producing dinoflagellate from the North Sea. *Harmful Algae* **2009**, *8*, 254–263.

(17) McCarron, P.; Kilcoyne, J.; Miles, C. O.; Hess, P. Formation of azaspiracids-3, -4, -6, and -9 via decarboxylation of carboxyazaspiracid metabolites from shellfish. *J. Agric. Food Chem.* **2009**, *57*, 160–169.

(18) Twiner, M. J.; Rehmann, N.; Hess, P.; Doucette, G. J. Azaspiracid shellfish poisoning: a review on the chemistry, ecology, and toxicology with an emphasis on human health impacts. *Mar. Drugs* **2008**, *6*, 39–72.

(19) Aune, T.; Yndestad, M. Diarrhetic shellfish poisoning. In *Algal toxins in seafood and drinking water*; Academic Press: London, **1993**; pp. 87–104.

(20) Yasumoto, T.; Oshima, Y.; Sugawara, W.; Fukuyo, Y.; Oguri, H.; Igarashi, T.; Fujita, N. Identification of dinophysis fortii as the causative organism of diarrhetic shellfish poisoning. *Bull. Jpn. Soc. Sc. Fish.* **1980**, *46*, 1405 – 1411.

(21) Lembeye, G.; Yasumoto, T.; Zhao, J.; Fernandez, R. DSP outbreak in Chilean Fiords. In *Toxic Phytoplankton Blooms in the Sea*; Smayda, T. J. and S., Ed.; Elsevier: Newport R.I., USA, **1993**; pp. 525–529.

(22) Krogh, P.; Edler, L.; Graneli, E.; Nyman, U. Outbreak of diarrhetic shellfish poisoning on the West coast of Sweden. In *Toxic Dinoflagellates*; Anderson, D. M.; White, D. W.; Baden, D. G., Eds.; Elsevier: New York, **1985**; pp. 501–503.

(23) Yasumoto, T.; Murata, M.; Lee, J. S.; Torigoe, K. Polyether toxins produced by dinoflagellates. In *Mycotoxins and Phycotoxins '88*; Natori, S., Ed.; Elsevier: Amsterdam, **1989**; pp. 375 – 382.

(24) Hu, T. M.; Marr, J.; deFreitas, A. S. W.; Quilliam, M. A.; Walter, J. A.; Wright, J. L. C.; Pleasance, S. New diol esters isolated from cultures of the dinoflagellates Prorocentrum lima and Prorocentrum concavum. *J. Nat. Prod.* **1992**, *55*, 1631–1637.

(25) Marr, J. C.; Jackson, A. E.; McLachlan, J. L. Occurrence of Prorocentrum lima, a DSP toxin-producing species from the Atlantic coast of Canada. *J. Appl. Phycol.* **1992**, *4*, 17–24.

(26) Draisci, R.; Lucentini, L.; Giannetti, L.; Boria, P.; Poletti, R. First report of pectenotoxin-2 (PTX-2) in algae (*Dinophysis fortii*) related to seafood poisoning in Europe. *Toxicon* **1996**, *34*, 923–935.

(27) Lee, J. S.; Igarashi, T.; Fraga, S.; Dahl, E.; Hovgaard, P.; Yasumoto, T. Determination of diarrhetic shellfish toxins in various dinoflagellate species. *J. Appl. Phycol.* **1989**, *1*, 147–152.

(28) MacKenzie, L.; Holland, P.; McNabb, P.; Beuzenberg, V.; Selwood, A.; Suzuki, T. Complex toxin profiles in phytoplankton and Greenshell mussels (Perna canaliculus), revealed by LC-MS/MS analysis. *Toxicon* **2002**, *40*, 1321–1330.

(29) Miles, C. O.; Wilkins, A. L.; Samdal, I. A.; Sandvik, M.; Petersen, D.; Quilliam, M. A.; Naustvoll, L. J.; Rundberget, T.; Torgersen, T.; Hovgaard, P.; Jensen, D. J.; Cooney, J. M. A novel pectenotoxin, PTX-12, in *Dinophysis* spp and shellfish from Norway. *Chem. Res. Toxicol.* **2004**, *17*, 1423–1433.

(30) Vale, P.; Sampayo, A. M. Pectenotoxin-2 seco acid, 7-*epi*-pectenotoxin-2 seco acid and pectenotoxin-2 in shellfish and plankton from Portugal. *Toxicon* **2002**, *40*, 979–987.

(31) Yasumoto, T.; Murata, M.; Oshima, Y.; Matsumoto, G. K.; Clardy, J. Diarrhetic shellfish poisoning. In *Seafood Toxins*; Ragelis, E. P., Ed.; American Chemical Society, Symposium Series No. 262.: Washington, DC, **1984**; pp. 207–214.

(32) Miles, C. O.; Wilkins, A. L.; Munday, R.; Dines, M. H.; Hawkes, A. D.; Briggs, L. R.; Sandvik, M.; Jensen, D. J.; Cooney, J. M.; Holland, P. T. Isolation of pectenotoxin-2 from *Dinophysis acuta* and its conversion to pectenotoxin-2 seco acid, and preliminary assessment of their acute toxicities. *Toxicon* **2004**, *43*, 1–9.

(33) Murata, M.; Kumagai, M.; Lee, J. S.; Yasumoto, T. Isolation and structure of yessotoxin, a novel polyether compound implicated in diarrhetic shellfish poisoning. *Tetrahedron Lett.* **1987**, *28*, 5869–5872.

(34) Satake, M.; MacKenzie, L.; Yasumoto, T. Identification of *Protoceratium reticulatum* as the biogenetic origin of yessotoxin. *Nat. Toxins* **1997**, *5*, 164–167.

(35) Draisci, R.; Ferreti, E.; Palleschi, L.; Marchiafava, C.; Polleti, R.; Milandri, A.; Ceredi, A.; Pompei, M. High levels of yessotoxin in mussels and presence of yessotoxin and homoyessotoxin in dinoflagellates of the Adriatic Sea. *Toxicon* **1999**, *37*, 1187–1193.

(36) Rhodes, L.; McNabb, P.; De Salas, M.; Briggs, L.; Beuzenberg, V.; Gladstone, M. Yessotoxin production by *Gonyaulax spinifera*. *Harmful Algae* **2006**, *5*, 148–155.

(37) Aune, T.; Sørby, R.; Yasumoto, T.; Ramstad, H.; Landsverk, T. Comparison of oral and intraperitoneal toxicity of yessotoxin towards mice. *Toxicon* **2002**, *40*, 77–82.

(38) Tubaro, A.; Sosa, S.; Carbonatto, M.; Altinier, G.; Vita, F.; Melato, M.; Satake, M.; Yasumoto, T. Oral and intraperitoneal acute toxicity studies of yessotoxin and homoyessotoxins in mice. *Toxicon* **2003**, *41*, 783–792.

(39) Aasen, J. A. B.; Espenes, A.; Miles, C. O.; Samdal, I. A.; Hess, P.; Aune, T. Combined oral toxicity of azaspiracid-1 and yessotoxin in female NMRI mice. *Toxicon* **2011**, *57*, 909–917.

(40) Anon Commission Regulation (EU) No 786/2013 amending Annex III to Regulation (EC) No 853/2004 of the European Parliament and of the Council as regards the permitted limits of yessotoxins in live bivalve molluscs **2013**.

(41) Anonymous Commission Decision 225/2002/EEC, laying down detailed rules for the implementation of Council Directive 91/492/EEC as regards the maximum levels and the methods of analysis of certain marine biotoxins in bivalve molluscs, echinoderms, tunicates and marine gastropods (16.3.2002). Off. J. Europ. Commun. **2002**, L75, 62-64.

(42) Hess, P.; McCarron, P.; Rehmann, N.; Kilcoyne, J.; McMahon, T.; Ryan, G.; Ryan, M.; Twiner, M. J.; Doucette, G. J.; Satake, M.; Ito, E.; Yasumoto, T. Isolation and purification of azaspiracids from naturally contaminated materials, and evaluation of their toxicological effects—final project report ASTOX (ST/02/02). *Marine Institute—Marine Environment & Health Series—No. 28, ISSN: 1649-0053. http://www.marine.ie/NR/rdonlyres/2B06863D-3366-47CD-9ABB-B3302629FE46/0/ASTOX.pdf.* **2007**.

(43) Perez, R.; Rehmann, N.; Crain, S.; LeBlanc, P.; Craft, C.; MacKinnon, S.; Reeves, K.; Burton, I.; Walter, J. A.; Hess, P.; Quilliam, M. A.; Melanson, J. The preparation of certified calibration solutions for azaspiracid-1, -2, and -3, potent marine biotoxins found in shellfish. *Anal. Bioanal. Chem.* **2010**, *398*, 2243–2252.

(44) McCarron, P.; Giddings, S. D.; Reeves, K.; Quilliam, M. A. CRM-AZA-Mus-200603 CRMP Technical report **2011**.

(45) McCarron, P.; Emteborg, H.; Nulty, C.; Rundberget, T.; Loader, J. I.; Teipel, K.; Miles, C.; Quilliam, M. A.; Hess, P. A mussel tissue certified reference material for multiple phycotoxins. Part 1: design and preparation. *Anal. Bioanal. Chem.* **2011**, *400*, 821–833.

(46) Anon Commission Regulation (EU) No 15/2011 of 10th January 2011 amending Regulation (EC) No 2074/2005 as regards recognised testing methods for detecting marine biotoxins in live bivalve molluscs. L6/3-6. **2011**.

(47) Quilliam, M. A.; Hess, P.; Dell'Aversano, C. Recent developments in the analysis of phycotoxins by liquid chromatography-mass spectrometry. *IUPAC* **2001**, 383–391.

(48) Fux, E.; McMillan, D.; Bire, R.; Hess, P. Development of an ultra-performance liquid chromatography–mass spectrometry method for the detection of lipophilic marine toxins. *Journal of Chromatography A* **2007**, *1157*, 273–280.

(49) Gerssen, A.; Mulder, P. J.; McElhinney, M. A.; De Boer, J. Liquid chromatography–tandem mass spectrometry method for the detection of marine lipophilic toxins under alkaline conditions. *J. Chromatogr. A* **2009**, *1216*, 1421–1430.

(50) Blay, P.; Hui, J. P. M.; Chang, J.; Melanson, J. Screening for multiple classes of marine biotoxins by liquid chromatography–high-resolution mass spectrometry. *Anal. Bioanal. Chem.* **2011**, *400*, 577–585.

(51) Gerssen, A.; Mulder, P. P. J.; De Boer, J. Screening of lipophilic marine toxins in shellfish and algae: Development of a library using liquid chromatography coupled to orbitrap mass spectrometry. *Anal. Chim. Acta* **2011**, *685*, 176–185.

(52) Hu, T.; Curtis, J. M.; Walter, J. A.; Wright, J. L. Identification of DTX-4, a new water-soluble phosphatase inhibitor from the toxic dinoflagellate, Prorocentrum lima. *J. Chem. Soc. Chem. Commun.* **1995**, 597–599.

(53) Selwood, A.; Miles, C. O.; Wilkins, A. L.; Van Ginkel, R.; Munday, R.; Rise, F.; McNabb, P. Isolation, structural determination and acute toxicity of pinnatoxins E, F and G. *J. Agric. Food Chem.* **2010**, *58*, 6532–6542.

(54) Forsyth, C. J.; Sabes, S. F.; Urbanek, R. A. An efficient total synthesis of okadaic acid. *J. Am. Chem. Soc.* **1997**, *119*, 8381–8382.

(55) Nicolaou, K. C.; Li, Y. W.; Uesaka, N.; Koftis, T. V.; Vyskocil, S.; Ling, T. T.; Govindasamy, M.; Qian, W.; Bernal, F.; Chen, D. Y. K. Total synthesis of the proposed azaspiracid-1 structure, part 1: construction of the enantiomerically pure C1-C20, C21-C27, and C28-C40 fragments. *Angew. Chem. Int. Edit.* **2003**, *42*, 3643–3648.

(56) Nicolaou, K. C.; Chen, D. Y. K.; Li, Y. W.; Qian, W. Y.; Ling, T. T.; Vyskocil, S.; Koftis, T. V.; Govindasamy, M.; Uesaka, N. Total synthesis of the proposed azaspiracid-1 structure, part 2: coupling of the C1-C20, C21-C27, and C28-C40 fragments and completion of the synthesis. *Angew. Chem. Int. Edit.* **2003**, *42*, 3649–3653.

(57) Nicolaou, K. C.; Frederick, M. O.; Petrovic, G.; Cole, K. P.; Loizidou, E. Z. Total synthesis and confirmation of the revised structures of azaspiracid-2 and azaspiracid-3. *Angew. Chem. Int. Edit.* **2006**, *45*, 2609–2615.

(58) McMahon, T.; Silke, J. Re-occurence of winter toxicity. *Harmful algae News* **1998**, *17*, 12.

(59) EFSA. Opinion of the scientific panel on contaminants in the food chain on a request from the European Commission on marine biotoxins in shellfish – azaspiracids. *The EFSA Journal* **2008**, 1–52.

(60) Ito, E.; Satake, M.; Ofuji, K.; Kurita, N.; McMahon, T.; James, K.; Yasumoto, T. Multiple organ damage caused by a new toxin azaspiracid, isolated from mussels produced in Ireland. *Toxicon* **2000**, *38*, 917–930.

(61) Aasen, J. A. B.; Espenes, A.; Hess, P.; Aune, T. Sub-lethal dosing of azaspiracid-1 in female NMRI mice. *Toxicon* **2010**, *56*, 1419–1425.

(62) Aune, T.; Espenes, A.; Aasen, J. A. B.; Quilliam, M. A.; Hess, P.; Larsen, S. Study of possible combined toxic effects of azaspiracid-1 and okadaic acid in mice via the oral route. *Toxicon* **2012**, *60*, 895–906.

(63) Ito, E.; Frederick, M. O.; Koftis, T. V.; Tang, W.; Petrovic, G.; Ling, T.; Nicolaou, K. C. Structure toxicity relationships of synthetic azaspiracid-1 and analogs in mice. *Harmful Algae* **2006**, *5*, 586–591.

(64) Aune, T.; Espenes, A.; Aasen, J. A. B.; Quilliam, M. A.; Hess, P.; Larsen, S. Study of possible combined toxic effects of azaspiracid-1 and okadaic acid in mice via the oral route. *Toxicon* **2012**, *60*, 895–906.

(65) Ito, E.; Satake, M.; Ofuji, K.; Higashi, M.; Harigaya, K.; McMahon, T.; Yasumoto, T. Chronic effects in mice caused by the oral administration of sublethal doses of azaspiracid, a new marine toxin isolated from mussels. *Toxicon* **2002**, *40*, 193–203.

(66) Flanagan, A. F. Detection and biochemical studies on the novel algal toxin, azaspiracid. *PhD thesis, National University of Ireland* **2002**.

(67) Flanagan, A. F.; Kane, M.; Donlon, J.; Palmer, R. Azaspiracid, detection of a newly discovered phycotoxin *in vitro*. *J. Shell. Res.* **1999**, *18*, 716.

(68) Flanagan, A. F.; Callanan, K. R.; Donlon, J.; Palmer, R.; Forde, A.; Kane, M. A cytotoxicity assay for the detection and differentiation of two families of shellfish toxins. *Toxicon* **2001**, *39*, 1021–1027.

(69) Twiner, M. J.; Hess, P.; Bottein Dechraoui, M. Y.; McMahon, T.; Samons, M. S.; Satake, M.; Yasumoto, T.; Ramsdell, J. S.; Doucette, G. J. Cytotoxic and cytoskeletal effects of azaspiracid-1 on mammalian cell lines. *Toxicon* **2005**, *45*, 891–900.

(70) Twiner, M. J.; El-Ladki, R.; Kilcoyne, J.; Doucette, G. J. Comparative effects of the marine algal toxins azaspiracid- 1, -2, and -3 on Jurkat T lymphocyte cells. *Chem. Res. Toxicol.* **2012**, *25*, 747–754.

(71) Ueoka, R.; Ito, A.; Izumikawa, M.; Maeda, S.; Takagi, M.; Shin-ya, K.; Yoshida, M.; Van Soest, R. W. M.; Matsunaga, S. Isolation of azaspiracid-2 from a marine sponge *Echinoclathria*sp. as a potent cytotoxin. *Toxicon* **2009**, *53*, 680–684.

(72) Vilariño, N.; Nicolaou, K.; Frederick, M. O.; Cagide, E.; Ares, I. R.; Louzao, M. C. Cell growth inhibition and actin cytoskeleton disorganization induced by azaspiracid-1 structure-activity studies. *Chem. Res. Toxicol.* **2006**, *19*, 1459–1466.

(73) Kellmann, R.; Schaffner, C.; Grønset, T. A.; Satake, M.; Ziegler, M.; Fladmark, K. E. Proteomic response of human neuroblastoma cells to azaspiracid-1. *Proteomics* **2009**, *72*, 695–707.

(74) Vilariño, N.; Nicolaou, K. C.; Frederick, M. O.; Cagide, E.; Alfonso, C.; Alonso, E.; Vieytes, M. R.; Botana, L. M. Azaspiracid substituent at C1 is relevant to *in vitro* toxicity. *Chem. Res. Toxicol.* **2008**, *21*, 1823–1831.

(75) Vale, C.; Nicolaou, K. C.; Frederick, M. O.; Gomez-Limia, B.; Alfonso, A.; Vieytes, M. R.; Botana, L. M. Effects of azaspiracid-1, a potent cytotoxic agent, on primary neuronal cultures. A structure-activity relationship study. *J. Med. Chem.* **2007**, *50*, 356–363.

(76) Cao, Z.; Lepage, K. T.; Frederick, M. O.; Nicolaou, K. C.; Murray, T. F. Involvement of caspase activation in azaspiracid-induced neurotoxicity in neocortical neurons. *Toxicol. Sci.* **2010**, *114*, 323–334.

(77) Kulagina, N. V.; Twiner, M. J.; Hess, P.; McMahon, T.; Satake, M.; Yasumoto, T.; Ramsdell, J. S.; Doucette, G. J.; Ma, W.; O'Shaughnessy, T. J. Azaspiracid-1 inhibits bioelectrical activity of spinal cord neuronal networks. *Toxicon* **2006**, *47*, 766–773.

(78) Vale, C.; Gomez-Limia, B.; Nicolaou, K. C.; Frederick, M. O.; Vieytes, M. R.; Botana, L. M. The c-Jun-N-terminal kinase is involved in the neurotoxic effect of azaspiracid-1. *Cell Physiol. Biochem.* **2007**, *20*, 957–966.

(79) Vale, C.; Wandscheer, C.; Nicolaou, K. C.; Frederick, M. O.; Alfonso, C.; Vieytes, M. R. Cytotoxic effect of azaspiracid-2 and azaspiracid-2-methyl ester in cultured neurons: Involvement of the c-Jun N-terminal kinase. *J. Neurosci. Res.* **2008**, *86*, 2952–2962.

(80) Vale, C.; Nicolaou, K. C.; Frederick, M. O.; Vieytes, M. R.; Botana, L. M. Cell volume decrease as a link between azaspiracid-induced cytotoxicity and c-Jun-N-terminal kinase activation in cultured neurons. *Toxicol. Sci.* **2010**, *113*, 158–168.

(81) Vilariño, N.; Nicolaou, K. C.; Frederick, M. O.; Vieytes, M. R.; Botana, L. M. Irreversible cytoskeletal disarrangement is independent of caspase activation during *in vitro* azaspiracid toxicity in human neuroblastoma cells. *Biochem. Pharmacol.* **2007**, *74*, 327–335.

(82) Ronzitti, G.; Hess, P.; Rehmann, N.; Rossini, G. P. Azaspiracid-1 alters the E-cadherin pool in epithelial cells. *Toxicol. Sci.* **2007**, *95*, 427–435.

CHAPTER 2 – STRATEGIES FOR THE ELIMINATION OF MATRIX EFFECTS IN THE LC-MS/MS ANALYSIS OF OKADAIC ACID AND AZASPIRACID-1 IN MOLLUSCAN SHELLFISH

Kilcoyne, J. and Fux, E., 2010. Strategies for the elimination of matrix effects in the liquid chromatography tandem mass spectrometry analysis of the lipophilic toxins okadaic acid and azaspiracid-1 in molluscan shellfish. *Journal of Chromatography A*, 1217, 7123–7130.

2.1. Abstract

Considerable efforts are being made worldwide to replace *in vivo* assays with instrumental methods of analysis for the monitoring of marine biotoxins in shellfish. Analysis of these compounds by the preferred technique of liquid chromatography tandem mass spectrometry (LC-MS/MS) is challenged by matrix effects associated with the shellfish tissues. In methods validation, assessment of matrix interferences is imperative to ensure the validity and accuracy of results being produced.

Matrix interferences for the analysis of okadaic acid (OA) and azaspiracid 1 (AZA1) were assessed using acidic methods on electrospray triple stage quadrupole (TSQ) and hybrid quadrupole time of flight (QToF) instruments by the use of matrix matched standards for different tissue types. Using an acidic method no matrix interference and suppression was observed on the TSQ for OA and AZA1 respectively, whilst the opposite was observed on the QToF; matrix enhancement for OA and no matrix interference for AZA1. The suppression of AZAs on the TSQ was found to be due to interfering compounds being carried over from previous injections. The degree of suppression is very much dependent on the tissue type ranging from 15–70%. Several strategies were evaluated to eliminate these interferences, including the partitioning of the extract with hexane, optimisation of the chromatographic method and the use of on-line SPE.

Hexane clean up did not have any impact on matrix effects. The use of an alkaline method and a modified acidic method eliminated matrix suppression for AZA1 on the TSQ instrument while an on-line SPE method proved to be effective for the elimination of matrix enhancement of OA on the QToF.

2.2. Introduction

Diarrhetic shellfish poisoning (DSP) is a human illness caused by the consumption of shellfish contaminated with the lipophilic marine biotoxins okadaic acid (OA) and dinophysistoxins (DTX). DSP toxins are produced by marine dinoflagellate species of the genus *Dinophysis* and *Prorocentrum*, and are accumulated in filter-feeding molluscan shellfish. The DSP syndrome was first reported in Japan in 1978, and the occurrence of DSP toxins is now a worldwide issue with frequent *Dinophysis* outbreaks documented in Europe, Asia, South and North America over the past 20 years.[1–4] DSP symptoms include nausea, vomiting, gastrointestinal disturbances, and stomach pain.[5]

In 1995, the presence in shellfish of another lipophilic marine toxin, azaspiracid (AZA), was responsible for diarrhetic illnesses in several individuals who consumed shellfish harvested in Ireland.[6] The AZA group now includes more than 24 analogues that are either produced by phytoplankton, products of biotransformation in shellfish or by-products of toxin storage.[7] However, only AZA1, -2 and -3 are regulated by the European Union.[8] AZAs have been found in shellfish from several European countries, Morocco, Eastern Canada, Japan and more recently in shellfish from Chile.[9–13] The symptoms of azaspiracid shellfish poisoning (AZP) are similar to that of DSP, and include nausea, vomiting, diarrheoa, and stomach cramps.

The EU has set maximum levels of AZP and DSP toxins in shellfish destined for human consumption. These are 160 µg OA equivalents/kg from the OA group (sum of OA, DTX) and including pectenotoxin (PTX) and 160 µg AZA equivalents/kg from the AZA group (sum of AZA1, -2 and -3).[14] Until recently the mouse (or rat) bioassay (MBA) was the EU reference method for the detection of OA group and AZA toxins in shellfish. A study has shown that the detection limit of the MBA is adequate for the current regulatory limit of AZAs,[15] however, sensitivity is an issue at the lower levels.[16,17] Furthermore, additional concerns relating to accuracy and ethics prompted substantial efforts to replace it with instrumental methods.

The MBA was replaced by LC-MS/MS as the reference method for the detection of marine biotoxins in shellfish in 2014.[18] LC-MS/MS is considered the technique of choice as it offers improved sensitivity, selectivity and accuracy as well as being faster and automated. However, quantitation using LC-MS/MS in biological matrices is often challenging because of matrix effects which alter the accuracy and the precision of the method. Matrix effects are believed to be caused by endogenous compounds co-eluting with the analyte and competing for ionisation in the electrospray (ESI) source.[19,20]

A number of different approaches have been taken to eliminate or to correct for matrix effects in LC-MS/MS analyses including sample clean up, standard addition, matrix matched standards, internal standards or changes in chromatographic conditions such as the pH of the mobile phase or the nature of stationary phase.

Sample clean-up can be performed using liquid-liquid extraction (LLE) or solid phase extraction (SPE) which is available with a variety of stationary phases (normal and reverse phase, ion exchange and immunoaffinity material with antibodies specific to the analyte). SPE also has the benefit of pre-concentrating samples which can be useful when dealing with low levels of toxins. Two recent reports have shown this technique to be effective in raising

sensitivity as well as eliminating sample impurities,[21,22] however, its effectiveness in overcoming matrix effects was not clearly demonstrated in these studies. Dilution of extracts has also been reported to reduce matrix interferences,[15,23] yet such an approach compromises the sensitivity of the method.

In addition to sample clean up, various approaches have been used to correct for matrix effects. Quantitation using matrix matched standards entails the production of a calibration curve in solutions with the exact same composition as the samples by extracting blank material or by reconstructing the matrix artificially and spiking the analyte at different concentrations. Although this approach is perfectly acceptable when the sample matrix is identical in all samples being analysed its application for the monitoring of marine toxins in shellfish is limited. Indeed, the production of matrix matched standards in all shellfish varieties (up to 10 different varieties) that are typically encountered in monitoring laboratories is impractical. Furthermore, the production of a calibration curve in extracts of a given variety, does not imply that the matrix composition of another extract of the same variety but from a different location and/or harvested at a different time of the year will be identical since environmental factors and food source will influence the composition of the shellfish tissues e.g., lipid content.

The standard addition method eliminates the need for the availability of a blank matrix and only requires the analyte to be available as a calibration solution of sufficient concentration. This method has been used to deal with matrix suppression in the analysis of scallops for diarrhetic shellfish toxins.[24] Although the method is very powerful and widely accepted, its use in monitoring laboratories remains limited for a number of reasons, primarily due to increased sample preparation and analysis time.

The use of internal standards is a very efficient approach to ensure that satisfactory accuracy is obtained through the different steps of the analytical method. Unfortunately, the total or

partial synthesis of the isotopically labelled compound is required and currently no such compounds are available for the DSP and AZA toxins to our knowledge.

Elimination or reduction of matrix effects to an acceptable level can also be achieved through modifications of the chromatographic conditions to change the selectivity towards the interfering compounds and/or the analyte.

We examined matrix effects associated with shellfish tissues on two LC-MS/MS instruments; a QToF and a TSQ, using ESI sources and identical LC conditions. Matrix interferences were assessed using matrix matched standards for six different tissue types; *M. edulis, C. gigas, O. edulis, E. siliqua, P. maximus* meat, *P. maximus* gonad and where interferences are observed we describe efforts made to overcome them. The performances of the methods employed were also evaluated in terms of sensitivity, accuracy and precision.

2.3. Experimental section

CH_3CN, MeOH and hexane were purchased as pestican grade solvents from Labscan (Dublin, Ireland). Formic acid, ammonium formate and ammonium hydroxide were obtained from Sigma Aldrich (Steinheim, Germany). H_2O was obtained from a reverse-osmosis purification system (Barnstead, Dublin, Ireland). OA and AZA1 certified reference materials (CRM) were obtained from the NRC (Halifax, Canada).

2.3.1. LC-MS/MS

Two LC-MS/MS systems were used; a Micromass triple stage quadrupole (TSQ) Ultima coupled to a Waters 2695 HPLC and a Micromass time-of-flight (QToF) Ultima coupled to a Waters 2795 HPLC. Both systems were equipped with a z spray ESI source. The TSQ was operated in selected reaction monitoring (SRM) mode and the following transitions were monitored: OA, *m/z* 803.5>255.5 and 803.5>803.5 in negative ionisation mode; AZA1 *m/z*

842.5>654.4 and 842.5>672.4, AZA2 856.5>654.4 and 856.5>672.4, AZA3 828.5>640.4 and 828.5>658.4 in positive ionisation mode. The cone voltages were set at 70 V and 60 V in negative and positive modes respectively and the collision voltage was set at 40 V in both modes. Cone and desolvation gas flows were set at 100 and 800 L/h respectively while the source and desolvation temperatures were set at 150 °C and 350 °C respectively.

The QToF was operated in fragment ion scan (FIS) mode monitoring for the same precursor ions as those reported for the TSQ. The cone voltages were set at 80 V and 40 V in negative and positive modes, respectively. The collision energy was set at 30 V in negative mode and 50 V in positive mode. Cone and desolvation gas flows were set at 100 and 750 L/h respectively while the source and desolvation temperatures were set at 140 °C and 350 °C respectively. Quantitation was performed by summing the ions of *m/z* 824.5, 672.5, 654.5 and 362.5 for AZA1 (and the equivalent fragment ions for AZA2 and -3) and the ions of *m/z* 803.5 and 255.1 for OA.

2.3.2. Acidic gradient method

A gradient elution method was set with an acidic binary mobile phase, with phase A (100% aqueous) and phase B (95% aqueous CH_3CN), each containing 2 mM ammonium formate and 50 mM formic acid following the method of Quilliam *et al.*, 2001.[25] The gradient elution started with 30% B, increased to 90% B over 8 min, held for 2.5 min, decreased to 30% B in 0.5 min and held for 4 min to equilibrate the system before the next injection. The chromatographic separation was achieved using a Hypersil BDS C8 column; 50 x 2.1 mm, 3 µm with a guard column of the same stationary phase 10 x 2.1 mm, 3 µm (Thermo Scientific, Runcorn, UK). The flow rate was set at 0.25 mL/min and the injection volume at 5 µL. The column and sample temperatures were set at 25 °C and 6 °C, respectively.

We assessed matrix effects for several shellfish tissues over a number of months. The spike samples and *M. edulis* matrix matched standards were run in triplicate against MeOH standards (seven levels) using in-house validated and accredited methods of analysis for the monitoring of lipophilic toxins.

A matrix-matched standard curve was prepared with *M. edulis* in order to compare response factors over the range of concentrations representative of naturally contaminated shellfish. The accuracy was calculated as a percentage of difference between the slopes obtained in MeOH and in the *M. edulis* extracts. The accuracies reported for all other shellfish varieties were calculated from spiked samples at a single concentration. Within each batch all samples were analysed by triplicate injection.

2.3.3. Acidic gradient method with a 100% B flush

A modified gradient method with acidic mobile phase was also evaluated. The gradient started with 30% B at 0.25 mL/min, increased to 90% B over 8 min, held for 5 min, increased to 100% B at 0.4 mL/min, held for 5 min and set back to 30% B at 0.25 mL/min which was held for 4 min to equilibrate the system.

2.3.4. Alkaline method

The alkaline method followed that of Gerssen *et al.*, 2009;[26] a binary mobile phase was used, with phase A (100% aqueous) and phase B (90% aqueous CH_3CN), each containing 6.7 mM ammonium hydroxide. Separation was achieved using a Waters X bridge, C18 column (150 x 3 mm, 5 µm). The flow rate was set at 0.25 mL/min and the injection volume was set at 5 µL. The column and sample temperatures were set at 25 °C and 6 °C respectively. A gradient elution was employed, starting with 10% B which was held for 1 min and increased linearly

to 90% over 9 min. The mobile phase was held at 90% B for 3 min and returned to 10% B in 2 min. The system was then allowed to equilibrate for 4 min.

2.3.5. On-line SPE method

For the on-line SPE method a binary mobile phase was used, with phase A (100% aqueous) and phase B (95% aqueous CH_3CN), each containing 2 mM ammonium formate and 50 mM formic acid. The loading column was an Oasis HLB, 5 µm, 2.1 x 20 mm column and HPLC separation was achieved using a Hypersil BDS C8 column; 50 x 2.1, 3 µm; guard column, 10 x 2.1 mm, 3 µm (Thermo Scientific, Runcorn, UK). The flow rate was set at 0.2 mL/min and the injection volume was 10 µL. The column and sample temperatures were set at 25 °C and 6 °C respectively. The sample was initially injected onto the loading column with 20% B for 2 min after which time the switch valve directed the flow onto the analytical column and the flow was reduced to 0.02 mL/min. After 3 seconds the flow was increased to 0.075 mL/min and the % B was increased from 20% to 30% over 27 seconds. The % B was then increased further to 100% over 10 min, held for 18 min, then decreased to 30% B over 0.5 min and held for 9 min. The system was then equilibrated for 3 min at 20% B and a flow rate of 0.2 mL/min. The switching valve was set to direct the flow to waste after 23 min.

2.3.6. Partitioning of shellfish extract with hexane

A laboratory reference material (LRM) prepared with *M. edulis* tissue and contaminated with both OA group and AZA toxins was extracted using the extraction described below (preparation of matrix matched standards). A set volume (5 mL) of the filtered extract was partitioned with 15 mL of hexane. The sample was shaken vigorously for 1 min and the layers were allowed to settle. The LRM extract (bottom layer) was then collected in a centrifuge tube and an aliquot transferred into a HPLC vial for analysis.

A set volume (1 mL) of the hexane layer was then pipetted into HPLC vials and dried down under nitrogen. Dried residues were re-solubilised with 200 µL of MeOH with vortex mixing for 30 s. The sample was transferred into an insert vial for analysis. Three MeOH standards were run directly after three injections of the non-partitioned LRM extract in addition to the partitioned LRM extract, followed by a four point calibration curve (all performed in triplicate).

2.3.7. Preparation of matrix matched standards

For each tissue type, uncontaminated raw samples tested as part of the routine monitoring programme in Ireland were selected from different harvesting dates and sites (around the coasts of Ireland). The extraction procedure described in this study has been used for several years in the shellfish toxins monitoring program in Ireland.[27] The shellfish were shucked, homogenised and aliquoted for extraction where 2 g of tissue was extracted by vortexing for 1 min with 9 mL of MeOH, centrifuged at 5,000 rpm for 5 min and the supernatant decanted into a 20 mL volumetric flask. The remaining pellet was further extracted using an Ultra turrax for 1 min with an additional 9 mL of MeOH, centrifuged at 5,000 rpm for 5 min and the supernatant decanted into the same 20 mL volumetric flask which was then brought to volume with MeOH. The standards were prepared in 25 mL volumetric flasks containing 20 mL of filtered (Whatmann, 0.2 µm, cellulose acetate filter) tissue extract. For the *M. edulis* matrix matched standards increasing volumes of standard stock solution were added to the flasks and the volume was brought to the mark with MeOH with toxin concentrations ranging from 2.5–280 ng/mL for OA and 0.8–92 ng/mL for AZA1.

Spiked tissue samples were prepared for the following tissues: *C. gigas, O. edulis, E. siliqua, P. maximus* meat and *P. maximus* gonad. For the spiked tissue samples 1 mL of stock standard solution was added to the flasks and the volume brought to the mark with MeOH

such that the final concentration was 10 ng/mL and 6 ng/mL for OA and AZA1 (equivalent to 125 µg/kg and 75 µg/kg in tissue) respectively.

For all the matrix matched standards a sample to solvent ratio (SSR) of 12.5 was obtained which reflects the routine monitoring extraction method.

2.3.8. Statistical analysis

Statistical calculations were carried out using Sigmastat 3.0. The significance test used to compare varieties and methods was the two-way analysis of variance Holm-Sidak test. Alpha was set at 0.05 (95% confidence) for all experiments.

2.4. Results and discussion

2.4.1. Assessment of matrix effects using the acidic gradient method

The average concentrations and standard deviations shown in Table 2.1 were calculated from five batches acquired over several months. The accuracy of AZA1 measurements on the TSQ in the different varieties of shellfish ranged from 64.2 to 83.1%. Signal suppression was consistently observed and was significantly different between the shellfish varieties ($p = 0.009$). When the same method was performed on the QToF the accuracy ranged from 97.1 to 104.6% without significant differences between varieties ($p = 0.467$).

The accuracy observed for OA using the acidic method also greatly varied between the two instruments (Table 2.1). Acceptable accuracies were achieved on the TSQ which ranged from 94.3 to 110.9%. The two-way ANOVA test revealed that the accuracy was statistically different between the shellfish varieties ($p<0.001$). The pairwise multiple comparison procedure results demonstrated that the accuracy obtained for OA in *O. edulis* (110.9%) and for *M. edulis* (108.0%) were not significantly different ($p = 0.343$) but were significantly

different when compared to the other shellfish varieties (p values ranging from <0.001 to 0.041). The accuracy obtained for OA analysis on the QToF with the acidic method was affected by signal enhancement and ranged from 114.6 to 130.9% with a significant difference between the shellfish varieties (p = 0.008).

Table 2.1. Accuracy and precision data (expressed as percentages) obtained on QToF and TSQ with the acidic method (average ± SD; n = no of injections, p = no of concentration points).

Analyte	Shellfish variety	Acidic			
		TSQ		QToF	
AZA1	*M. edulis* (p=7)	82.6 (n=18)	± 7.8	102.7 (n=15)	± 11.3
	C. gigas (p=1)	83.1 (n=13)	± 4.5	104.6 (n=21)	± 7.8
	O. edulis (p=1)	69.8 (n=13)	± 6.8	101.2 (n=18)	± 3.6
	E. siliqua (p=1)	73.5 (n=12)	± 7.3	101.1 (n=21)	± 5.4
	P. max meat (p=1)	79.3 (n=13)	± 13.6	103.3 (n=21)	± 5.5
	P. max gonad (p=1)	64.2 (n=13)	± 3.6	97.1 (n=21)	± 3.1
OA	*M. edulis* (p=7)	108.0 (n=18)	± 8.4	130.9 (n=18)	± 7.7
	C. gigas (p=1)	102.4 (n=13)	± 3.2	114.6 (n=18)	± 16.4
	O. edulis (p=1)	110.9 (n=13)	± 8.3	130.5 (n=18)	± 18.1
	E. siliqua (p=1)	94.3 (n=12)	± 6.7	119.3 (n=18)	± 12.7
	P. max meat (p=1)	98.3 (n=13)	± 3.5	119.7 (n=15)	± 23.3
	P. max gonad (p=1)	101.3 (n=13)	± 5.1	125.9 (n=18)	± 11.0

Comparison of the results between instruments show that the apparent recoveries observed on the QToF were always higher than on the TSQ regardless of the shellfish variety and the method used.

During analysis of AZA1 on the TSQ it was noted that the injection of a standard after the injection of a number of tissue extracts led to a lower response than when injected after a calibration curve. The degree of suppression was dependent on the type of tissue extract. This phenomenon is illustrated in Figure 2.1 which shows the response of three consecutive injections of an AZA1 standard (104 ng/mL) after three injections of three shellfish extracts prepared from five different varieties. A six point calibration curve was systematically run after the three injections of the AZA1 standard and used to calculate the concentrations reported in Figure 2.1. Depending on the tissue type the degree of suppression ranged from 15 to 70%. In this instance *P. maximus* gonad tissue appeared to be the worst offender while the clams (*T. philippinarium*) had the least effect. Injections of the AZA1 standard after the oyster, mussel and scallop extracts have shown that the first injections are equally affected by signal suppression while the third injection led to a significantly higher response.

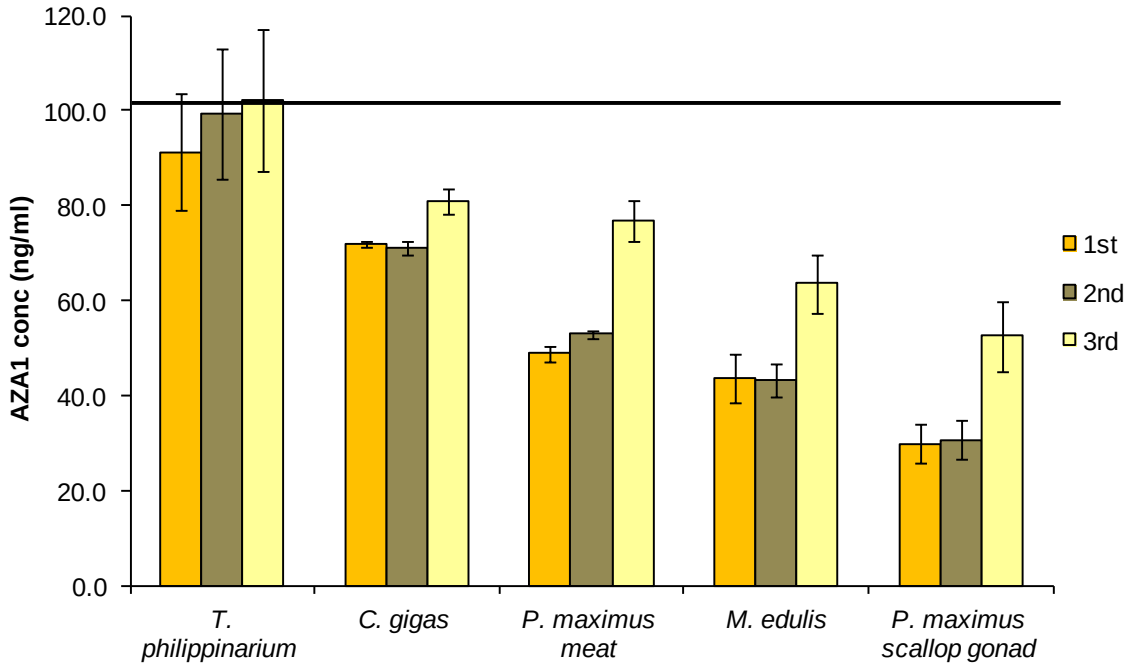

Figure 2.1. Concentration obtained for three consecutive injections of a standard of AZA1 (104 ng/mL shown as the bold line) on the TSQ using gradient elution following three injections of various shellfish tissue extracts. The error bars show the standard deviations obtained from the mean (n=3).

These results suggest that either later eluting compounds, or compounds lingering in the source are responsible for the signal suppression observed. This phenomenon is not observed for the analysis of OA on the QToF.

It was also noted that the results for the suppression obtained for the shellfish extracts in Figure 2.1 were dissimilar to those obtained in Table 2.1. This may be due to the fact that although some of the extracts used in the two separate experiments were from the same variety, they were harvested at different locations and times. This would suggest that the use of matrix matched standards from extracts other than the sample, can lead to erroneous results.

The within-day precision obtained with the acidic method for OA ranged from 1 to 10 % on both instruments while the between-day precision over at least five days was 8% on both the QToF and the TSQ (Table 2.2). The analysis of AZA1 using the acidic method on the QToF demonstrated excellent precision as the within-day precision ranged from 2 to 5% and a between-day precision of 11% (Table 2.2). The results obtained for AZA1 with the acidic method on the TSQ were not as good, with within-day precision ranging from 3 to 16%. The high variation on day five was due to a lower response of the first set of solutions that was injected compared to the second and the third replicate set (Table 2.2). A between-day precision of 8% was observed over five days.

Table 2.2. Within and between days precision obtained with the acidic method calculated on the percentage of difference in response factor between a set of spiked solutions of *M. edulis* extracts and MeOH. A set of seven solutions equivalent to 0.063 to 3.5 mg/kg for OA and 0.010 to 1.150 mg/kg for AZA1 was injected in triplicate on each day.

Days	n=3	OA QToF	OA TSQ	AZA QToF	AZA1 TSQ
1	Average	135.6	100.8	105.7	81.5
	Stdev	5.3	8.9	3.2	5.5
2	Average	132.0	108.1	86.0	82.0
	Stdev	7.2	4.1	2.8	7.8
3	Average	137.8	113.1	96.8	85.8
	Stdev	4.5	4.4	4.1	3.3
4	Average	129.5	100.6	108.5	86.3
	Stdev	9.9	7.4	4.9	4.4
5	Average	120.2	117.3	116.6	77.6
	Stdev	3.2	0.8	3.9	15.1
6	Average	130.5	-	-	-
	Stdev	3.9	-	-	-
Average		**130.9**	**108.0**	**102.7**	**82.6**
Stdev		**7.7**	**8.4**	**11.3**	**7.8**

2.4.2. Methods to address matrix effects

2.4.2.1. Partitioning with hexane

The LRM was extracted following the same procedure used for the other shellfish as described in the experimental section.

As part of our experiment we investigated the recoveries of OA and AZA1 (analysis of OA on TSQ and AZA1 on QToF) in the methanolic (and hexane) fraction after the hexane partitioning (data not shown). The recoveries were satisfactory for both compounds (> 95%). Hexane did not appear to have any effect on matrix suppression for the AZAs on the TSQ

with no significant differences being observed between the partitioned (hexane) LRM and the crude LRM (Figure 2.2). The suppression is still observed for the subsequent LRM and standard injections for both partitioned and non partitioned samples and reflects what was observed for the different tissue types (Figure 2.1).

Furthermore, the signal suppression effect observed in AZA1 standards after the injection of shellfish extracts presented in Figure 2.1 was also examined. The results from Figure 2.2 D show that the two injections of a methanolic standard of AZA1 (104 ng/mL) that followed three injections of the LRM were affected by signal suppression as the average concentrations were measured as 78.0 ± 5.6 and 79.4 ± 7.1 ng/mL for the first and second injections respectively. It is only on the third injection of the standard that the concentration measured (102.7 ± 4.1 ng/mL) returned within the expected theoretical concentration.

The effect of hexane partitioning on the signal enhancement effect observed for OA on the QToF instrument was also evaluated. Similarly to the above results, the hexane partitioning did not eliminate the matrix effects observed (data not shown).

These findings are in agreement with the results reported by Ito and Tsukada.[24] In this study the partitioning of scallop extracts with hexane and chloroform was evaluated for the reduction of signal suppression observed by LC-MS when the analysis of OA, DTX1, yessotoxin and pectenotoxin-6 was attempted. This clean-up procedure had no effect on the matrix effects observed. The LC-MS method from McNabb *et al*. (2005) also included a hexane partitioning step prior to injection but there is no information regarding the potential benefits of this clean-up step on matrix effects.[28] Although the partitioning step does not eliminate matrix effects, its application enables a higher degree of cleanliness in the source and in the system without detrimental effect on the accuracy.

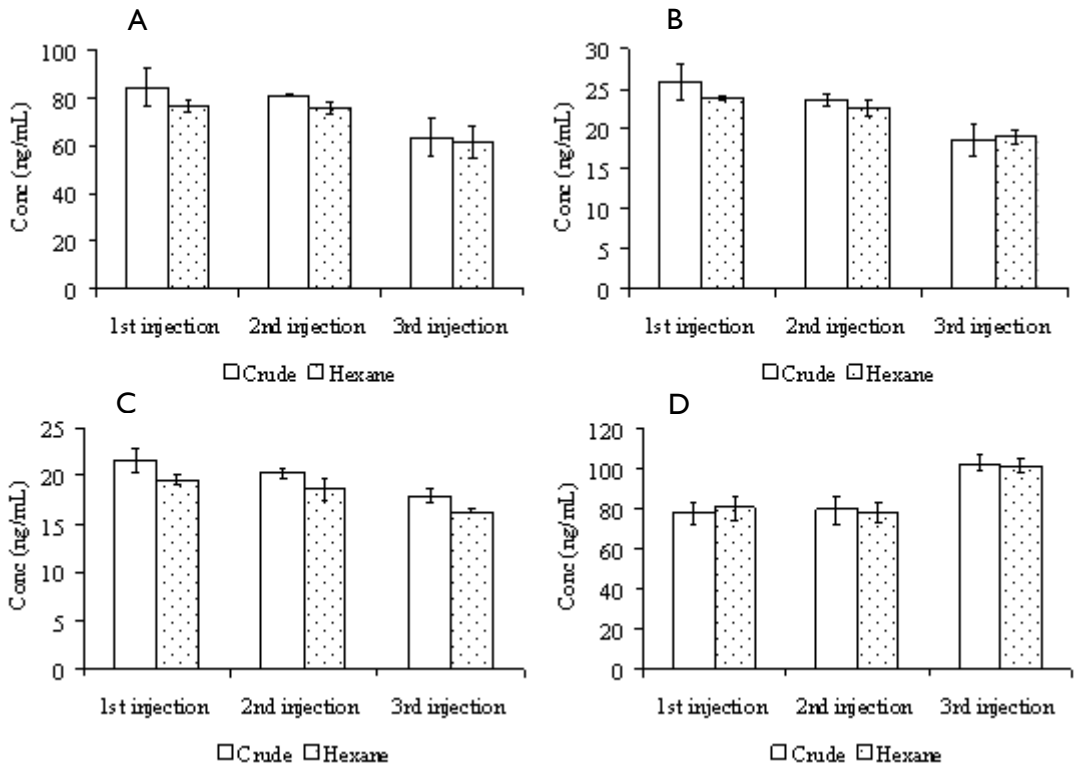

Figure 2.2. Average concentrations of AZAs (n=3) obtained by injection of three successive LRM extracts and three successive LRM extracts after hexane partitioning on the TSQ. Each series of three injections were separated by the injection of three successive standard solutions. A) Concentration of AZA1 in partitioned and non-partitioned LRM. B) Concentration of AZA2 in partitioned and non-partitioned LRM. C) Concentration of AZA3 in partitioned and non-partitioned LRM. D) Concentration of AZA1 standard (104 ng/mL) after the injection of three LRMs and three partitioned LRMs.

2.4.2.2. Alkaline method

Changing the selectivity of the method may help to overcome matrix interferences. The use of an alkaline method for the separation of lipophilic toxins was reported to increase the sensitivity for the OA group of toxins and enable better separation of the DSP (including PTX2) and AZA group of toxins. This separation allows analysis of both groups of toxins in the one run without having to alternate the mass spectrometer polarity.[26] An additional study

found that SPE on polymeric sorbents combined with an alkaline method can significantly reduce matrix interferences for both OA and AZA1.[22]

The alkaline method was run on both the QToF and TSQ instruments without any sample pre-treatment to determine any impact on matrix interferences. To assess the matrix effects MeOH standards were run with matrix matched standards in triplicate and the slopes compared (Table 2.3).

Excellent results were obtained when the analyses were performed on the TSQ using the alkaline method with accuracies of 90.9 to 108.1 % for AZA1 and 97.2 to 104.4 % for OA (Table 2.3). There was no statistically significant difference between the varieties ($p = 0.083$ and 0.278 for AZA1 and OA, respectively). Signal enhancement was systematically observed for both OA and AZA1 when the QToF was used with the alkaline method. For AZA1 the accuracy ranged from 107.7 to 135.5% with a significant difference observed between varieties ($p<0.01$) while the accuracy for OA ranged from 122.8 to 127.4 % without significant difference between varieties ($p = 0.928$).

By using the alkaline method the AZA1 suppression effect on the TSQ was overcome without any sample pre-treatment; analysis of three injections of a *P. maximus* gonad extract followed by three standard injections yielded 98% ± 1.1 recovery for the AZA1 (and OA) in the standard compared with 38% ± 12 recovery for AZA1 using the acidic method.

The precision of OA measurements using the alkaline method ranged from 0.4 to 11% on both instruments (Table 2.4). Between-day precision was 9.5 and 8.3% on the QToF and the TSQ, respectively. The precision obtained for AZA1 using the alkaline method was also acceptable with within-day precisions ranging from 2 to 14% on both instruments and between-day precisions of 9.2 and 16.6% on the QToF and TSQ, respectively.

The accuracies for OA and AZA1 using the acidic and the alkaline methods were reported in extracts of mussels (*M. edulis*), scallops (*P. maximus*) and oysters (C. *gigas*).[22] The crude

extracts spiked with OA (equivalent to 160 µg/kg) using a SSR of 10 showed that, with the acidic method and analysis of OA in the negative ESI mode, signal enhancement was observed in scallops and oysters (128.8 and 123.6%, respectively) while an acceptable accuracy was obtained in mussels (104.7%). The use of alkaline method led to excellent accuracies in crude extracts of mussels and in scallops (99.3 and 98.9%) while signal suppression was observed in oysters (79.6%). Therefore, a systematic decrease in the response (>20%) was observed when the alkaline method was used.

Table 2.3. Accuracy and precision data (%) obtained on QToF and TSQ with alkaline method (average ± SD; n = no of injections, p = no of concentration points).

Analyte	Shellfish variety	Alkaline			
		TSQ		QToF	
AZA1	*M. edulis* (p=7)	103.2 (n=12)	± 16.6	135.5 (n=12)	± 9.2
	C. gigas (p=1)	108.1 (n=9)	± 9.5	118.7 (n=12)	± 13.2
	O. edulis (p=1)	101.1 (n=9)	± 3.2	131.3 (n=12)	± 13.0
	E. siliqua (p=1)	90.9 (n=9)	± 4.5	107.7 (n=12)	± 11.2
	P. max meat (p=1)	102.1 (n=9)	± 4.3	107.9 (n=12)	± 7.3
	P. max gonad (p=1)	97.9 (n=9)	± 2.9	125.7 (n=12)	± 20.6
OA	*M. edulis* (p=7)	103.9 (n=12)	± 8.3	122.8 (n=15)	± 9.5
	C. gigas (p=1)	106.2 (n=9)	± 3.6	123.4 (n=12)	± 13.2
	O. edulis (p=1)	97.2 (n=9)	± 4.8	127.4 (n=12)	± 7.2
	E. siliqua (p=1)	99.5 (n=9)	± 3.2	126.0 (n=12)	± 15.9
	P. max meat (p=1)	101.6 (n=9)	± 8.0	124.3 (n=12)	± 17.8
	P. max gonad (p=1)	99.2 (n=9)	± 6.4	126.7 (n=12)	± 13.5

This trend was not observed in our study. In the past, signal enhancement (50%) was observed when the analysis of OA in crude extracts of mussels was performed on the same instrument and using the same acidic method.[23] Although the same variety of mussels were used (*M. edulis*), the flesh composition may have been different enough than in the present study to induce differences in the degree of matrix effects observed.

In the study by Gerssen *et al.*,[22] the crude extracts spiked with AZA1 (equivalent to 100 µg/kg) using a SSR of 10 showed that, with the acidic method, signal suppression was observed in mussel, scallops and oysters (accuracies of 84.3, 59.1 and 73.6%, respectively). The use of alkaline method systematically led to better accuracies (88.1, 89.0 and 83.5% in the crude extracts of mussels, scallops and oysters, respectively). The results we obtained on the TSQ (same instrument as in Gerssen *et al.*) are in agreement with these observations and the suppression effect observed for AZA1 using the acidic method was eliminated when the alkaline method was used. The suppression effect in the analysis of AZA1 has been reported for numerous shellfish varieties on different instruments with various chromatographic methods.[23,26,29,30] The results we obtained for AZA1 on the QToF with the acidic method are consistent with a previous study performed on this instrument[31] and within acceptable accuracies. However, signal enhancement was observed when the alkaline method was used.

Table 2.4. Within and between days precision obtained with the alkaline method calculated on the percentage of difference in response factor between a set of spiked solutions of *M. edulis* extracts and MeOH. A set of seven solutions equivalent to 0.063 to 3.5 mg/kg for OA and 0.010 to 1.150 mg/kg for AZA1 was injected in triplicate on each day.

Days	Replicates	OA QToF	OA TSQ	AZA QToF	AZA1 TSQ
1	Average	130.6	109.8	141.1	120.7
	Stdev	9.3	4.9	9.0	5.8
2	Average	114.5	111.8	134.9	114.2
	Stdev	4.9	3.2	13.7	9.1
3	Average	127.8	93.1	134.6	80.5
	Stdev	11.1	2.9	2.8	8.3
4	Average	115.2	107.6	131.6	95.5
	Stdev	7.5	0.4	10.7	9.8
5	Average	125.7	97.1	-	105.2
	Stdev	4.2	6.6	-	3.6
Average		**122.8**	**103.9**	**135.5**	**103.2**
Stdev		**9.5**	**8.3**	**9.2**	**16.6**

2.4.2.3. Modified acidic gradient method with 100% organic solvent flush

Standards and matrix matched standards were run in triplicate in each batch to assess the impact on matrix enhancement for OA on the QToF and matrix suppression for AZA on the TSQ. Four batches were run over a one-month period. The average and standard deviations (n=12) for the six shellfish varieties are shown in Table 2.5.

The introduction of the 100% CH_3CN flush for the analysis of AZA1 on the TSQ resulted in improved accuracies (Table 2.5) when compared to the results shown in Table 2.1. The suppression effect observed previously was eliminated and the accuracies ranged from 89.3 to 103.7%. Interestingly the highest bias was observed for *P. maximus* gonad which was also the case with the short acidic gradient method. The two-way ANOVA indicated that the differences in the mean values between shellfish varieties were significant ($p<0.001$). The

analysis of OA in the different shellfish varieties on the TSQ led to excellent accuracies, ranging from 98.2 to 105.8%. Although the analysis of OA using the short acidic gradient on the TSQ demonstrated acceptable accuracies, the method with the 100% CH_3CN flush provided more consistent results between varieties. After allowing for the effect of the days of analysis, the two-way ANOVA indicated that the difference between the mean values obtained for the different shellfish varieties was not significant ($p = 0.496$).

The signal enhancement observed in the analysis of OA with the QToF remained critical with the 'flushing' method. The accuracies ranged between 117.3 to 171.4%. A significant statistical difference was observed between varieties ($p<0.001$). Investigations showed that the pronounced enhancement effect was not related to the flushing step as the same results were obtained when using the shorter acidic method and with a new analytical column (data not shown).

Our results indicated that the suppression of AZA1 on the TSQ was caused either by late eluting compounds or due to compounds lingering in the source from previous injections. In order to determine which was the case, an experiment was performed using the acidic method which consisted of two injections of an *O. edulis* extract followed by the injection of an AZA1 standard in triplicate. The above procedure was then repeated with modifications. The flow going through the column was stopped after the injections of the *O. edulis* extract, the column was replaced with a union and the mobile phase B set at a flow rate of 0.4 mL/min for 5 min (as is the case with the acidic flush method). After 5 min the column was installed on the system and allowed to equilibrate for 3 min before the next injection of AZA1 standard. The experiment was repeated in triplicate.

As observed previously the AZA1 standard was suppressed by 17 ± 3% after two injections of the *O. edulis* extract using the acidic method. The suppression was still observed even after

the source was flushed (18 ± 5%) indicating that the interfering compounds were strongly retained on the column.

Table 2.5. Accuracy and precision data (expressed as percentages) obtained on QToF and TSQ (n=12) with the modified acidic gradient method with 100% organic solvent flush (average ± SD; p = no of concentration points).

Shellfish variety	AZA1		OA			
	TSQ		TSQ		QToF	
M. edulis (p=7)	103.7	± 7.7	100.7	± 10.3	162.4	± 11.6
C. gigas (p=1)	103.4	± 7.1	102.8	± 13.6	150.6	± 21.5
O. edulis (p=1)	94.8	± 8.8	105.8	± 12.1	164.4	± 13.1
E. siliqua (p=1)	94.9	± 6.8	100.4	± 9.3	134.9	± 11.8
P. max meat (p=1)	97.4	± 5.4	98.2	± 8.0	117.3	± 10.2
P. max gonad (p=1)	89.3	±10.8	100.3	± 11.2	171.4	± 15.2

2.4.2.4. On-line SPE

The use of two columns for the separation of compounds from complex mixtures such as shellfish provides another dimension to conventional liquid chromatography. This approach has been successfully used for both single laboratory and collaborative study validations for the determination of low level agricultural residues in soft drinks by LC-MS/MS.[32,33]

The performance of a combination of two columns was evaluated for OA analyses on the QToF using the acidic method. An Oasis HLB column was used as the initial column to trap OA from the matrix. The column was then back flushed onto the analytical column, the BDS Hypersil C8 for further separation. The approach was adapted from a method used for the analysis of phycotoxins in plankton cells.[34] The accuracy of the method was evaluated using the same approach as that for OA and AZA1 using the acidic and the alkaline methods. All solutions were injected in triplicate on five separate days over a five month period. Acceptable accuracies were obtained in all shellfish varieties which ranged from 86.5 to

102.6% (Table 2.6). Comparison of these results with those obtained using the acidic method on the QToF (Table 2.1) demonstrates that the use of a second column significantly reduced the matrix effects that were associated with OA analysis in shellfish varieties.

The between-day precision obtained using the column switching method was acceptable for all shellfish varieties with relative standard deviations ranging from 5.7 to 11.4% (Table 2.6).

The sensitivity of the column switching method was comparable to the acidic method on the same instrument with a limit of detection (LOD) equivalent to 16 µg/kg tissue (Table 2.7). Attempts to shorten the run time (from 43 min) by adjusting the gradient conditions and/or flow rates were unsuccessful.

Table 2.6. Accuracy (expressed as a percentage) of the column switching method on the QToF (acidic mobile phase) for OA in different shellfish varieties (average ± SD; n = no of injections, p = no of concentration points).

Shellfish variety	Average OA recovery ± SD (n=15)
M. edulis (p=7)	95.1 ± 11.4
C. gigas (p=1)	101.4 ± 10.2
O. edulis (p=1)	90.4 ± 5.7
E. siliqua (p=1)	86.5 ± 8.6
P. max meat (p=1)	93.5 ± 6.7
P. max gonad (p=1)	102.6 ± 10.9

2.4.3. Method performances

A fit for the purpose analytical method should meet the minimum performances for specific parameters set by international organizations.[35–37] The validation parameters include selectivity, accuracy, precision, range, sensitivity and ruggedness (the FDA and ICH guidelines also include the assessment of the stability of the analytes). When LC-MS/MS methods are used the selectivity of the method is generally excellent and the absence of

response in several blank samples is usually sufficient to demonstrate the specificity of a given method.

2.4.3.1. Sensitivity

The LOD observed for OA and AZA1 on both instruments and using the acidic and alkaline methods are shown in Table 2.7. The alkaline method allowed for a two-fold improvement in sensitivity compared to the acidic method. The LOD achieved for AZA1 was better with the acidic method than with the alkaline method by a factor of 1.7 on both instruments. The TSQ was 10 times more sensitive than the QToF for AZA1.

Table 2.7. LODs (signal to noise ≥ 3≤10) for AZA1 and OA on the TSQ and the QToF with the acidic and alkaline method determined in mussel extracts.

	Acidic (µg/kg)		Alkaline (µg/kg)	
	TSQ	QToF	TSQ	QToF
AZA1	0.3	3	0.5	5
OA	10	20	5	10

2.4.3.2. Accuracy

In the AOAC guidelines, acceptable accuracy is a function of the concentration and the purpose of the analysis. An accuracy of 75%–125% is considered acceptable for methods of quantitation at ppb levels, as in this study. The FDA guidelines[37] define an acceptable accuracy as being within 15% of the actual value except at the lower limit of quantitation (LOQ) at which 20% is acceptable. Therefore, the accuracy that we obtained for OA on the TSQ and for AZA on the QToF with the acidic method, as well as for both OA and AZA1 on the TSQ with the alkaline method, meet the requirements of the AOAC and the FDA guidelines.

2.4.3.3. Precision

According to the AOAC guidelines, repeatability is defined as the degree of agreement of results when conditions are maintained as constant as possible with the same analyst, reagents, equipment, and instruments performed within a short period of time. The repeatability varies with concentration and a theoretical calculated value can be obtained from the Horwitz equation (1) where c is the concentration of the analyte expressed as mass fraction.

(1) $RSDr = C^{-0.15}$

The HORRAT formula (equation 2) allows for the calculation of a ratio that should fall between 0.5 and 2 in order to consider the repeatability as satisfactory.

(2) $$HORRATr = \frac{RSDr\ (found)}{RSDr\ (calculated)}$$

Therefore, acceptable precisions for the extracts spiked with OA should have relative standard deviations ranging from 2.8 and 11.2 while acceptable precisions for AZA1 should range from 3.0 to 12.1. Almost all the standard deviations of the analyses carried out with both instruments were within the acceptable range. The FDA guidelines define acceptable precision as a RSD obtained from five measurements being less than 15% and less than 20% at the lower LOQ. Therefore, according to the FDA guidelines, acceptable precisions were obtained for OA and AZA1 using both acidic and alkaline methods for all shellfish varieties on the TSQ, except for *M. edulis,* using the alkaline method for which 16.6% RSD was observed.

We demonstrated that the within-day precision is greatly affected by a suppression effect for the AZAs. The injection of several shellfish extracts strongly suppressed the response in the samples analysed after the shellfish extracts. When the alkaline and modified acidic methods were evaluated this phenomenon was not observed.

2.5. Conclusions

We demonstrated the impact of matrix interference in the LC-MS/MS analysis of low-level toxins in molluscan shellfish, and strategies to overcome this. Contrasting results were obtained on two different LC-MS/MS instruments, using an acidic method, even with the same source type (ESI), using the same LC conditions (and samples) and the analyses performed by a single analyst. Significant differences were observed between shellfish varieties. Partitioning the sample with hexane proved unsuccessful in overcoming the interferences observed for OA on the QToF and AZAs on the TSQ.

Matrix suppression for AZA1 was overcome using an acidic method with an organic solvent flush and alternatively by an alkaline method. Matrix enhancement observed for OA on the QToF was eliminated only by an on-line SPE method.

In the author's lab the alkaline method is the method of choice for the TSQ while the acidic method (using on-line SPE for OA analysis) is the preferred procedure for the QToF.

Introduction of LC-MS/MS as the primary method for the regulatory monitoring of biotoxins in shellfish will be quite challenging, considering the variety of instrumentation and techniques available.

This study clearly demonstrates that different LC-MS/MS instruments can produce very dissimilar results due to matrix interferences and that it is necessary to initially evaluate matrix effects and where present implement procedures to eliminate and/or correct for them.

2.6. References

(1) Aune, T.; Yndestad, M. Algal toxins in seafood and drinking water. Academic Press, London, **1993**; pp 87.

(2) Yasumoto, T.; Oshima, Y.; Sugawara, W.; Fukuyo, Y.; Oguri, H.; Igarashi, T.; Fujita, N. Identification of dinophysis fortii as the causative organism of diarrhetic shellfish poisoning. *Bull. Jpn. Soc. Sc. Fish.* **1980**, *46*, 1405 – 1411.

(3) Lembeye, G.; Yasumoto, T.; Zhao, J.; Fernandez, R. DSP outbreak in Chilean Fiords. In: *Toxic Phytoplankton Blooms in the Sea*; Smayda, T. J. and S., Eds.; Elsevier: Newport R.I., USA, **1993**; pp. 525–529.

(4) Quilliam, M.; Gilgan, M.; Pleasance, S.; DeFreitas, A.; Douglas, D.; Frits, L.; Hu, T.; Marr, T.; Smyth, C.; Wright, J. *Can. Tech. Rep. Fish Aquat. Sci*., **1991**; *1799*, 18.

(5) Krogh, P.; Edler, L.; Graneli, E.; Nyman, U. Outbreak of diarrhetic shellfish poisoning on the West coast of Sweden. In: *Toxic Dinoflagellates*; Anderson, D. M.; White, D. W.; Baden, D. G., Eds.; Elsevier: New York, **1985**.

(6) McMahon, T.; Silke, J. Winter toxicity of unknown aetiology in mussels. *Harmful Algae News* **1996**, *14*.

(7) Rehmann, N.; Hess, P.; Quilliam, M. A. Discovery of new analogs of the marine biotoxin azaspiracid in blue mussels (*Mytilus edulis*) by ultra-performance liquid chromatography/tandem mass spectrometry. *Rapid Commun. Mass Spectrom.* **2008**, *22*, 549–558.

(8) Anon. Report of the Joint FAO/IOC/WHO ad hoc Expert Consultation on Biotoxins in Molluscan Bivalves. *Food and Agriculture Organization* **2004**.

(9) James, K. J.; Furey, A.; Lehane, M.; Ramstad, H.; Aune, T.; Hovgaard, P.; Morris, S.; Higman, W.; Satake, M.; Yasumoto, T. First evidence of an extensive northern

European distribution of azaspiracid poisoning (AZP) toxins in shellfish. *Toxicon* **2002**, *40*, 909–915.

(10) Taleb, H.; Vale, P.; Amanhir, R.; Benhadouch, A.; Sagou, R.; Chafik, A. First detection of azaspiracids in North West Africa. *J. Shell. Res.* **2006**, *25*, 1067–1071.

(11) Twiner, M. J.; Rehmann, N.; Hess, P.; Doucette, G. J. Azaspiracid shellfish poisoning: a review on the chemistry, ecology, and toxicology with an emphasis on human health impacts. *Mar. Drugs* **2008**, *6*, 39–72.

(12) Ueoka, R.; Ito, A.; Izumikawa, M.; Maeda, S.; Takagi, M.; Shin-ya, K.; Yoshida, M.; Van Soest, R. W. M.; Matsunaga, S. Isolation of azaspiracid-2 from a marine sponge *Echinoclathria sp.* as a potent cytotoxin. *Toxicon* **2009**, *53*, 680–684.

(13) Álvarez, G.; Uribe, E.; Ávalos, P.; Mariño, C.; Blanco, J. First identification of azaspiracid and spirolides in *Mesodesma donacium* and *Mulinia edulis* from Northern Chile. *Toxicon* **2009**, *55*, 638–641.

(14) Anonymous Commission Decision 225/2002/EEC, laying down detailed rules for the implementation of Council Directive 91/492/EEC as regards the maximum levels and the methods of analysis of certain marine biotoxins in bivalve molluscs, echinoderms, tunicates and marine gastropods (16.3.2002). *Off. J. Europ. Commun.* **2002**, L75, 62–64.

(15) Hess, P.; Butter, T.; Petersen, A.; Silke, J.; McMahon, T. Performance of the EU-harmonised mouse bioassay for lipophilic toxins for the detection of azaspiracids in naturally contaminated mussel (*Mytilus edulis*) hepatopancreas tissue homogenates characterised by liquid chromatography coupled to tandem mass spectrometry. *Toxicon* **2009**, *53*, 713–722.

(16) Hess, P. Requirements for screening and confirmatory methods for the detection and quantitation of marine biotoxins in end-product and official control. *Analytical and Bioanalytical Chemistrymm* **2010**, *397*, 1683–1694.

(17) EFSA. Influence of processing on the levels of lipophilic marine biotoxins in bivalve molluscs, statement of the panel on contaminants in the food chain (question No EFSA-Q-2009-00203), adopted on 25 March 2009. *The EFSA Journal* **2009**, *1016*, 1–10.

(18) Anon Commission Regulation (EU) No 15/2011 of 10th January 2011 amending Regulation (EC) No 2074/2005 as regards recognised testing methods for detecting marine biotoxins in live bivalve molluscs. L6/3-6. **2011**.

(19) Srinivas, N. Dodging matrix effects in liquid chromatography tandem mass spectrometric assays - compilation of key learnings and perspectives. *Biomed Chromatogr.* **2009**, *23*, 451–454.

(20) Jessome, L.; Volmer, D. Ion suppression: a major concern for mass spectrometry. *LCGC North America* **2006**, *24*, 498–510.

(21) These, A.; Scholz, J.; Preiss-Weigert, A. Sensitive method for the determination of lipophilic marine biotoxins in extracts of mussels and processed shellfish by high-performance liquid chromatography-tandem mass spectrometry based on enrichment by solid-phase extraction. *J. Chromatogr. A* **2009**, *1216*, 4529–4538.

(22) Gerssen, A.; McElhinney, M. A.; Mulder, P.; Bire, R.; Hess, P.; De Boer, J. Solid phase extraction for removal of matrix effects in lipophilic marine toxin analysis by liquid chromatography-tandem mass spectrometry. **2009**, 1213–1226.

(23) Fux, E.; Bire, R.; Rode, D.; Hess, P. Approaches to the evaluation of matrix effects in the liquid chromatography-mass spectrometry (LC-MS) analysis of three regulated

lipophilic toxin groups in mussel matrix (*Mytilus edulis*). *Food Addit. Contam.* **2008**, *25*.

(24) Ito, S.; Tsukada, K. Matrix Effect and Correction by Standard Addition in Quantitative Liquid Chromatography-Mass Spectrometric Analysis of Diarrhetic Shellfish Poisoning Toxins. *J. Chromatogr.* **2001**, *943*, 39–46.

(25) Quilliam, M. A.; Hess, P.; Dell'Aversano, C.; Koe, W.; Samson, R.; Van Egmond, H.; Gilbert, J.; Sabino, M. Proceedings of the Xth international IUPAC symposium on mycotoxins and phycotoxins, Sao Paulo, Brazil, May 22-25, 2000. In: *Mycotoxins and Phycotoxins in Perspective at the Turn of the Century, W.J. deKoe, R.A. Samson, H.P. van Egmond, J. Gilbert and M.Sabino (Eds.), Netherlands, W.J. deKoe* **2001**, 383–391.

(26) Gerssen, A.; Mulder, P. J.; McElhinney, M. A.; De Boer, J. Liquid chromatography–tandem mass spectrometry method for the detection of marine lipophilic toxins under alkaline conditions. *J. Chromatogr. A* **2009**, *1216*, 1421–1430.

(27) Hess, P.; Nguyen, L.; Aasen, J.; Keogh, M.; Kilcoyne, J.; McCarron, P.; Aune, T. Tissue distribution, effects of cooking and parameters affecting the extraction of azaspiracids from mussels, *Mytilus edulis*, prior to analysis by liquid chromatography coupled to mass spectrometry. *Toxicon* **2005**, *46*, 62–71.

(28) McNabb, P.; Selwood, A. I.; Holland, P. T. Multiresidue method for determination of algal toxins in shellfish: Single-laboratory validation and interlaboratory study. *AOAC Int.* **2005**, *88*, 761–772.

(29) Stobo, L. A.; Lacaze, J.; Scott, A. C.; Gallacher, S.; Smith, E. A.; Quilliam, M. A. Liquid chromatography with mass spectrometry - Detection of lipophilic shellfish toxins. *J. AOAC Int.* **2005**, *88*, 1371–1382.

(30) Fux, E.; McMillan, D.; Bire, R.; Hess, P. Development of an ultra-performance liquid chromatography-mass spectrometry method for the detection of lipophilic marine toxins. *J. Chromatogr. A* **2007**, *1157*, 273–280.

(31) McCarron, P.; Kilcoyne, J.; Miles, C. O.; Hess, P. Formation of azaspiracids-3, -4, -6, and -9 via decarboxylation of carboxyazaspiracid metabolites from shellfish. *J. Agric. Food Chem.* **2009**, *57*, 160–169.

(32) Paske, N.; Berry, B.; Schmitz, J.; Sullivan, D. Determination of low-level agricultural residues in soft drinks and sports drinks by gas chromatography with mass-selective detection: single-laboratory validation. *J. AOAC Int.* **2007**, *90*, 521–533.

(33) Miller, K. D.; Milne, P. Determination of low-level pesticide residues in soft drinks and sports drinks by liquid chromatography with tandem mass spectrometry: collaborative study. *J. AOAC Int.* **2008**, *91*, 202–236.

(34) Hardstaff, W. R.; Lewis, N.; Aasen, J. A. B.; Quilliam, M. A. Analysis of phycotoxins in planktonic cells. *Poster presentation, HABs, Copenhagen, Denmark* **2006**.

(35) ICH Tripartite guideline validation of analytical procedures, test and methodology. Available: www.ich.org. **2005**.

(36) IUPAC Harmonised guidelines for single laboratory validation. Available: www.iupac.org. **2002**.

(37) FDA Guidance for industry, bioanalytical method validation. Available: www.fda.gov/cder/guidance/index.htm. Accessed 2 April 2010.

CHAPTER 3 - IMPROVED ISOLATION PROCEDURE FOR AZASPIRACIDS FROM SHELLFISH, STRUCTURAL ELUCIDATION OF AZASPIRACID-6 AND STABILITY STUDIES

Kilcoyne, J., Keogh, A., Clancy, G., LeBlanc, P., Burton, I., Quilliam, M. A., Hess, P., and Miles, C. O. 2012. Improved isolation procedure for azaspiracids from shellfish, structural elucidation of azaspiracid-6, and stability studies, *Journal of Agriculture and Food Chemistry 60*, 2447–2455.

3.1. Abstract

Azaspiracids (AZAs) are a group of lipophilic polyether toxins produced by the small dinoflagellate *Azadinium spinosum*. They may accumulate in shellfish and can result in illnesses when consumed by humans. Research into analytical methods, chemistry, metabolism and toxicology of AZAs has been severely constrained by the scarcity of high-purity AZAs. Consequently, since their discovery in 1995, considerable efforts have been made to develop methods for isolation of AZAs in sufficient amounts and purities for toxicological studies, in addition to the preparation of standard reference materials. A 7-step procedure was improved for the isolation of AZA1–3, increasing recoveries two-fold compared to previous methods and leading to isolation of sufficiently purified AZA6 for structural determination by NMR spectroscopy. The procedure, which involved a series of partitioning and column chromatography steps, was performed on 500 g of *Mytilus edulis* hepatopancreas tissue containing ~ 14 mg of AZA1. Overall yields of AZA1 (52%), AZA2 (43%), AZA3 (43%) and AZA6 (38%) were good, and purities were confirmed by NMR spectroscopy. The structure of AZA6 was determined by 1- and 2-dimensional NMR spectroscopy and mass spectrometry. The stability of AZA6 relative to AZA1 was also

assessed in three solvents in a short-term study that demonstrated greatest stability in aqueous CH_3CN.

3.2. Introduction

Azaspiracids (AZAs) were discovered after 8 people in the Netherlands became ill in 1995 after consuming mussels harvested off the west coast of Ireland.[1] Contaminated mussels from this incident were sent to Tohoku University in Japan, where the primary causative agents (AZA1–3) were isolated and characterized.[2,3] The illness caused by the consumption of AZAs was named azaspiracid shellfish poisoning (AZP), and severe acute symptoms include nausea, vomiting, diarrhoea, and stomach cramps.[4] The AZA group now includes more than 20 analogues that are either produced by phytoplankton, through biotransformation in shellfish, or as by-products formed as a result of storage of the toxin.[5,6] However, only AZA1–3 are currently regulated by the European Union.[7] The other analogues had initially been found at lower concentrations and were therefore not deemed to be significant, but little is known about these additional analogues and to date only AZA1–5 have been isolated and fully characterized.

The Irish national biotoxin monitoring program was set up in 2001 and since that time the detection of AZAs in shellfish samples has resulted in significant shellfish farm closures.[8] AZAs have since been found in other European countries, Morocco, Eastern North America, Japan and more recently Chile.[9–13] The EU has set maximum levels of 160 μg/kg of toxins from the AZA group (defined as the sum of AZA1–3, corrected for their estimated toxic equivalence factors) for shellfish to be placed on the market.[7] Until recently, the mouse bioassay (MBA) was the EU reference method for the detection of marine biotoxins in shellfish. However, there were problems with this method in terms of sensitivity, accuracy,

false positives and ethics.[14] Although the current regulatory limit for AZAs may be detected by both MBA or LC-MS/MS methods, the MBA is not capable of detecting lower levels and the non-specific character of the assay has prevented its effective use in routine monitoring.[15,16] The MBA has now been replaced with liquid chromatography coupled to mass spectrometry (LC-MS/MS) as the reference method for the detection of lipophilic marine biotoxins in shellfish.[7]

Considerable efforts were made to try to identify the biological source of AZAs, and in 2002 James *et al.* reported *Protoperidinium crassipes* as the causative organism.[17] However, this species was not found to produce AZAs in culture (Tillmann and Krock, unpublished data). Furthermore, analysis of picked cells of *P. crassipes* in Norway showed no presence of AZAs.[18] As *P. crassipes* is a heterotrophic dinoflagellate; it is possible that it might feed on AZA-producing phytoplankton. In 2007, during an oceanographic survey in the North Sea, a small (5 µm in width) photosynthetic thecate dinoflagellate was identified (subsequently named *Azadinium spinosum*) that was abundant in water samples that also contained AZAs by LC-MS/MS. *A. spinosum* was subsequently found to produce AZA1 and AZA2 in culture.[19,20] It is believed that most of the other AZA analogues are produced as a result of metabolic processes in shellfish or as a result of storage.[6,21] This belief was corroborated by a study in which an Irish strain of *A. spinosum* was fed directly to shellfish resulting in the formation of the analogues AZA3, AZA6, AZA17 and AZA19.[22]

A number of toxicological studies have been performed showing AZAs to be teratogenic to fish,[23] damaging to the gastrointestinal tract in mice,[24,25] and potential lung-tumor promoters.[26] However, more detailed toxicological studies need to be performed on as many AZA analogues as is possible in order to establish more accurate regulatory limits and to identify all analogues that are relevant for public health protection. A recent study, investigating an increase in AZA3 concentration in shellfish tissue upon heating, showed that

AZA3 is produced as a result of decarboxylation of AZA17,[6] which in turn is a metabolic product of AZA1.[27] The same phenomenon was observed for AZA6 (i.e., decarboxylation of AZA19, which similarly appears to be a metabolic product of AZA2).[6] AZA2 was found to be the predominant toxin detected in Portugal, Morocco, Japan, and in scallops in Chile,[10,12,28,29] so it would not be surprising if the ratio of AZA6 to AZA3 was higher in samples from these countries than in profiles observed in European shellfish.

Isolation of AZAs has been reported previously,[3,30–33] however in three of these studies the purity was not assessed by NMR.[30–32] In this paper we describe the isolation of AZA1–3 and AZA6 from shellfish using a modified procedure with improved recoveries and purities. This enabled the confirmation, by NMR spectroscopy, of the structure for AZA6 (Figure 3.1) that had previously been proposed based on MS fragmentation studies and analogy with AZA3. We also assess the relative stabilities of AZA1 and AZA6 in three solvents.

3.3. Experimental section

3.3.1. Chemicals

All solvents (pestican grade) were purchased from Labscan (Dublin, Ireland). Sodium chloride (99+%), triethylamine (99%), ammonium acetate (97+%), ammonium formate (reagent grade), formic acid (>98%), and silica gel (10–40 µm, type H) were purchased from Sigma Aldrich (Steinheim, Germany). Sephadex LH-20 was from GE Healthcare (Uppsala, Sweden), LiChroprep RP C8 (25–40 µm) was from Merck (Darmstadt, Germany), Luna Phenyl-Hexyl (15 µm) was from Phenomenex (Cheshire, UK), and MeOH-d_3 (CD_3OH, 99.5%) was from Cambridge Isotope Laboratories (MA, USA). AZA1–3 certified reference materials (CRMs) were obtained from the NRC, Certified Reference Material Program (Halifax, NS, Canada).

3.3.2. Extraction and clean up efficiency from freeze dried and wet tissue

Three 10 g (W1) hepatopancreas samples were freeze-dried and extracted three times (Ultra turrax, IKA-Werke T25 at 11,000 rpm) for 1 min with EtOH (15 mL) in parallel with three wet samples. Extracts were centrifuged (3,950 x g) for 5 min and the supernatant decanted into 20 mL volumetric flasks which were brought to volume with EtOH. Prior to analysis by LC-MS/MS (method A) the samples were filtered (Whatman, 0.2 µm, cellulose acetate filter). The clean-up efficiency ((W1-W2)/W1 x 100) was assessed by combining the relevant extracts, evaporating the solvent *in vacuo* and determining the weight of the remaining residue (W2).

3.3.3. Isolation from shellfish

Cooked whole-mussel tissue (2.5 kg) from *M. edulis* collected in 2005 from Bruckless, Donegal, Ireland, was dissected to yield 500 g of hepatopancreas, which was homogenized with a Waring blender and freeze-dried (final weight 130 g). The freeze-dried hepatopancreas was extracted with EtOH (5 × 500 mL) using a Waring blender. The extracts were combined, evaporated *in vacuo*, and partitioned between EtOAc (150 mL) and aqueous NaCl (1 M, 50 mL). The EtOAc fraction was evaporated to dryness *in vacuo* and the oily residue was partitioned between hexane (200 mL) and MeOH–H_2O (9:1, 200 mL). The MeOH fraction was evaporated to dryness *in vacuo*, dissolved in EtOAc (20 mL), and ~ 4 g of silica gel was added. The sample was then carefully evaporated to dryness *in vacuo*, mixed to a fine powder and loaded onto a silica gel (55 g) column (19.5 × 5 cm). Vacuum assisted elution was performed successively with hexane, EtOAc, EtOAc–MeOH (9:1), (7:3), (1:1), and MeOH (300 mL of each, all containing 0.1% acetic acid except for hexane). The 7:3 EtOAc–MeOH fraction which FIA-MS/MS (method C) was shown to contain the AZAs, was evaporated *in vacuo*, loaded in MeOH onto a Sephadex LH-20 column (150 × 1.5 cm, packed in MeOH)

and eluted by gravity (~ 1 mL/min) with MeOH. The first 20 min of eluate was collected separately, with 3-min fractions collected thereafter. Fractions containing AZAs (fractions 8–15), as determined by FIA-MS/MS, were combined, evaporated to dryness *in vacuo*, and the sample loaded in CH_3CN–H_2O (6:4, plus 0.1% triethylamine) onto a column packed with Phenyl-Hexyl (19.9 × 2 cm). The sample was eluted with CH_3CN–H_2O (3:7, plus 0.1% triethylamine) at 4 mL/min, and 5 mL fractions were collected. Appropriate fractions were combined (AZA3, fractions 10–15; AZA6, fractions 16–23; AZA1, fractions 24–34 and AZA2, fractions 35–45) based on FIA-MS/MS analysis.

Final purification of AZA1 was achieved by semi-preparative LC (Agilent 1200) with photodiode array (PDA) detection (210 nm) using a Luna C8 (5 µm, 250 × 10 mm, Phenomenex) column eluted with CH_3CN–H_2O (1:1, plus 2 mM ammonium acetate) at 4 mL/min. The column temperature was 30 °C. AZA2, AZA3 and AZA6 were purified using the similar conditions as for AZA1, but with a narrower-bore column (Cosmosil C18, 5µm, 250 × 4.6 mm, Nacalai tesque) eluted with CH_3CN–H_2O (1:1, plus 2 mM ammonium acetate) at 1 mL/min. Purified AZAs were recovered by diluting the fractions with H_2O (to 20% CH_3CN), loading on to solid-phase extraction (SPE) cartridges (Oasis HLB, 200 mg), washing with MeOH–H_2O (1:9, 10 mL) to remove the buffer and eluting with MeOH–H_2O (9:1, 20 mL).

Purified samples were tested for phthalates (method E) which, if present, were removed by partitioning the sample in MeOH–H_2O (4:1, 20 mL) with 20 mL of hexane. Removal of solvent by evaporation *in vacuo* afforded purified AZAs as white solids.

3.3.4. Comparison of flash chromagraphy stationary phases

Two stationary phases (LiChroprep RP-8 and Luna Phenyl-Hexyl) were assessed for separation, clean-up and recovery efficiencies. Each stationary phase (packed in a 19.9 ×

2 cm column) was loaded with 200 µg of residue in $CH_3CN–H_2O$ (6:4, plus 0.1% triethylamine), which had been brought through the first 5 steps of the isolation procedure, and eluted with $CH_3CN–H_2O$ (3:7, plus 0.1% triethylamine) at 4 mL/min. Fractions containing AZAs, as determined by flow injection analysis with mass spectrometry detection (FIA–MS/MS, method C), were combined and analyzed by LC-MS/MS (method A).

3.3.5. Mass spectrometry

Two LC-MS/MS systems were used in positive ion mode, both of which were equipped with a z-spray ESI source.

Method A. Recoveries were determined by quantitative analysis of fractions on a Waters 2695 LC coupled to a Micromass triple-stage quadrupole (TSQ) Ultima operated in selected reaction monitoring (SRM) mode, with the following transitions: AZA1 *m/z* 842.5→654.4 and 842.5→672.4, AZA2 856.5→654.4 and 856.5→672.4, AZA3 828.5→640.4 and 828.5→658.4, AZA6 842.5→640.5 and 842.5→658.4. The cone voltage was 60 V and the collision voltage was 40 V, the cone and desolvation gas flows were set at 100 and 800 L/h, respectively, and the source temperature was 150 °C.

Binary gradient elution was used, with phase A consisting of H_2O and phase B of 95% CH_3CN in H_2O (both containing 2 mM ammonium formate and 50 mM formic acid) in a minor modification to the method of Quilliam *et al.*[34] Chromatography was performed with a Hypersil BDS C8 column (50 × 2.1 mm, 3 µm, with a 10 × 2.1 mm guard column of the same stationary phase) (Thermo Scientific). The gradient was from 30% B, to 90% B over 8 min at 0.25 mL/min, held for 5 min, then held at 100% B at 0.4 mL/min for 5 min, and returned to the initial conditions and held for 4 min to equilibrate the system. The injection volume was 5 µL and the column and sample temperatures were 25 °C and 6 °C, respectively.

Method B. Purity was initially assessed on a Micromass time-of-flight (QToF) Ultima coupled to a Waters 2795 LC by running MS scans (*m*/*z* 100–1000) using the same chromatographic conditions as above. Identification of other contaminant AZA analogues was also determined by performing product ion scans, where the precursor ions were selected and then fragmented, for all the known AZA analogues.

Method C. Qualitative analysis of fractions for AZAs was performed by FIA-MS/MS using a Micromass QToF Ultima coupled to a Waters 2795 LC. Samples (2 µL) were injected, using the 2795 autosampler, directly (no column) into the mass spectrometer monitoring for the precursor ions.

3.3.6. LC-PDA purity analysis

Method D. A concentrated sample (~500 µg/mL) was injected (1 µL) onto the analytical system (Shimadzu 10AVp) with photodiode array (PDA) detection (210 nm) using a Cosmosil C18 column, 5 µm, 250 × 4.6 mm eluted with CH_3CN–H_2O (1:1, plus 2 mM ammonium acetate) at 1 mL/min. The column temperature was 30 °C.

Method E. An additional method employed to detect any strongly retained compounds (e.g., phthalates) used an analytical LC system (Shimadzu LC 10AVp) with PDA detection at 210 nm. The sample collected after the SPE step was injected (5 µL) onto a Vydac C18, column (10 µm, 250 × 4.6 mm, Grace) and eluted with MeOH–H_2O (9:1) at 1 mL/min, maintaining the column temperature at 30 °C.

3.3.7. NMR spectroscopy

NMR-purity was assessed by ^{1}H NMR using a Bruker DRX-500 spectrometer. The structure of AZA6 was determined by analysis of ^{1}H, COSY, TOCSY, NOESY, ROESY, HSQC and HMBC spectra using a Bruker Avance III 700 spectrometer fitted with a 1.7 mm proton-

detect micro-cryoprobe. Approximately 50 µg of AZA6 were dissolved in 30 µL CD_3OH, and proton-detected spectra were acquired with pre-saturation of the OH peak. The TOCSY spectrum was recorded using an MLEV sequence with a 120 ms mixing time. The ROESY spectrum was acquired with a spin-lock pulse of 200 ms and a spin-lock field of approximately 3 kHz. Two HMBC spectra were recorded, optimized for long-range couplings of 8.33 Hz and 5.56 Hz (60 ms and 90 ms evolution times, respectively). All samples were tuned and matched to 50 Ω resistive impedance. Chemical shifts were referenced to internal CHD_2OH (3.31 ppm) or CD_3OH (49.15 ppm).

3.3.8. Stability studies

A side-fraction from the final step in the isolation procedure, containing both AZA6 and AZA1, was used to assess stability. Aliquots of the fraction were evaporated under a stream of N_2 and taken up in three solvents (MeOH, EtOH, and 4:1 $CH_3CN–H_2O$) and stored in flame-sealed ampoules (under nitrogen) at −18 °C, 4 °C and 40 °C for a 4-week period. Samples were ampouled in triplicate for each of the temperature and time points. The study was performed isochronously, and samples were analyzed simultaneously by LC-MS/MS (method A) with specimens stored at −80 °C used as the control.

3.3.9. Methylation with diazomethane

To identify whether the degradation products formed during the stability study were methyl esters or other methyl derivatives, AZA6 methyl-ester was synthesized. A purified sample (~ 60 ng) of AZA6 was added to the outside tube of an Aldrich diazomethane generator with System 45 connection, and 1 mL MeOH and 1.5 mL Et_2O were added. Diazomethane was generated in the inner tube of the apparatus and allowed to react *in situ* with the extract.

After reacting for 45 min at 0 °C with occasional swirling, the extract was transferred to a glass vial, evaporated to dryness under a stream of N_2, and the residue dissolved in MeOH (1 mL) for LC-MS/MS analysis (method B).

3.3.10. Cleavage with sodium periodate

Aliquots (50 µL) of 0.2 M solution of sodium periodate were added to 50 µL of purified AZA6 and AZA3 (~ 80 ng/mL in MeOH) in insert vials, vortex mixed for 20 s and analysed after ca. 2 h by LC-MS/MS (method B).

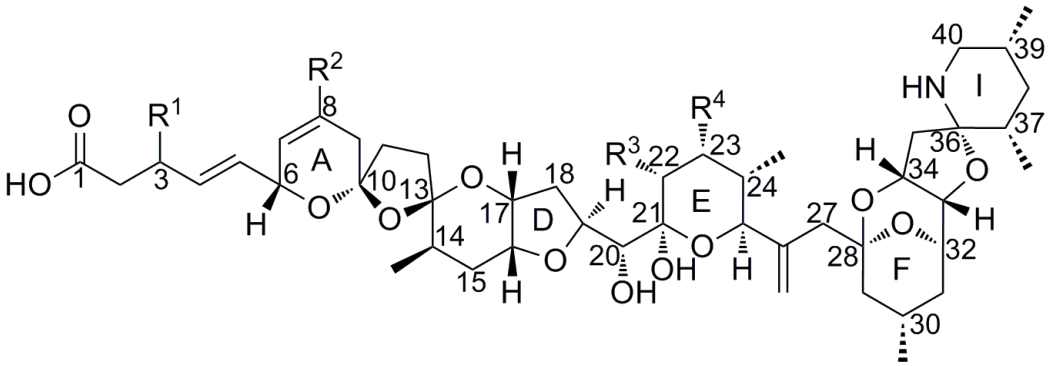

		R^1	R^2	R^3	R^4	$[M+H]^+$ *m/z*
1	Azaspiracid-1	H	H	CH_3	H	842.5
2	Azaspiracid-2	H	CH_3	CH_3	H	856.5
3	Azaspiracid-3	H	H	H	H	828.5
4	Azaspiracid-4	OH	H	H	H	844.5
5	Azaspiracid-5	H	H	H	OH	844.5
6	Azaspiracid-6	H	CH_3	H	H	842.5
7	Azaspiracid-7	OH	H	CH_3	H	858.5
8	Azaspiracid-8	H	H	CH_3	OH	858.5
9	Azaspiracid-9	OH	CH_3	H	H	858.5
10	Azaspiracid-10	H	CH_3	H	OH	858.5
11	Azaspiracid-11	OH	CH_3	CH_3	H	872.5
12	Azaspiracid-12	H	CH_3	CH_3	OH	872.5
13	Azaspiracid-13	OH	H	H	OH	860.5
14	Azaspiracid-14	OH	H	CH_3	OH	874.5
15	Azaspiracid-15	OH	CH_3	H	OH	874.5
16	Azaspiracid-16	OH	CH_3	CH_3	OH	888.5
17	Azaspiracid-17	H	H	CO_2H	H	872.5
18	Azaspiracid-19	H	CH_3	CO_2H	H	886.5
19	Azaspiracid-21	OH	H	CO_2H	H	888.5
20	Azaspiracid-23	OH	CH_3	CO_2H	H	902.5

Figure 3.1 Structures of azaspiracids with substitution points for analogues. Note that only AZA1–6 have their structures unambiguously established by NMR spectroscopy, while the remaining structures are tentative, based on MS fragmentations, biosynthetic and metabolic considerations, and analogy with known analogues.

3.4. Results and discussion

3.4.1. Extraction and partitioning

An exhaustive trial extraction was performed on 130 g of freeze-dried hepatopancreas sample resulting in a 95% clean up (Table 3.1). The use of EtOH as an extraction solvent for the purification of AZAs has previously been reported.[33] Small scale tests with MeOH and EtOH as extraction solvents showed that both solvents were equivalent in terms of extraction efficiency. EtOH was chosen as the extraction solvent primarily to minimize the formation of side products, which can be significant when MeOH is used as extractant.[5]

Freeze-drying of shellfish prior to extraction has been successfully employed previously in the isolation of pinnatoxins from Australian oysters.[35] This has many advantages, including avoiding the necessity of using H_2O miscible extraction solvents, complete control of extractant composition, and low H_2O content in the extract (thus avoiding difficulties during evaporation and potentially toxin stability problems). The effect of freeze-drying the mussel hepatopancreas prior to extraction of AZAs was therefore explored. Higher extraction efficiencies were achieved for the freeze-dried samples after the first and second extractions with 12% and 2% more AZAs being extracted respectively. No difference was observed in clean up efficiency (94.2% for both freeze-dried and wet tissues), but the extracts from the freeze-dried samples evaporated more quickly with little or no foaming in the subsequent vacuum-evaporation step. The two subsequent liquid–liquid partitioning steps resulted in only minor losses of toxin (~ 95% recovery) with an overall clean up efficiency of 67% (Table 3.1).

3.4.2. Silica gel

The sample was eluted from the silica gel column with step gradients of hexane, EtOAc, EtOAc–MeOH and MeOH. AZAs eluted in 7:3 EtOAc–MeOH, with only small losses of

toxin. The EtOAc–MeOH mixtures contained 0.1% acetic acid. Previous studies have shown that AZAs are unstable in acidic environments, but that shellfish tissue appears to have a protective effect.[36] As the sample at this stage of the isolation was still quite crude, and there appeared to be no degradation of the AZAs during small-scale trials, it was deemed to be safe to use acetic acid in the eluent at this point of the procedure. Attempts to replace the acetic acid with 0.1% triethylamine were unsuccessful, with the toxins eluting over three of the mobile-phase compositions, thereby reducing the clean-up efficiency significantly. Of all the steps in the procedure, silica gel chromatography (step 4) gave the greatest efficiency in terms of clean up (93%) and recovery (~ 95%) (Table 3.1).

3.4.3. Sephadex LH-20 chromatography

AZAs eluted together after ca. 64 min and were collected in 11 fractions. The clean-up efficiency of 66% was achieved with a recovery of 85%.

3.4.4. Phenyl-hexyl flash chromatography

Acidic mobile phases have previously been used for reverse-phase flash chromatographic purification,[33] but bring with them an inherent risk of acid-promoted degradation of AZAs during storage or evaporation. We found the use of triethylamine to be a safer alternative, with the toxins being stable whilst stored in the freezer as a dry sample (after evaporation of the mobile phase containing 0.1% triethylamine) for at least one month (data not shown).

Both the RP-8 and Phenyl-Hexyl stationary phases performed similarly in terms of clean-up efficiency and recovery however, with respect to resolution, the Phenyl-Hexyl proved to be much more efficient at separating the AZA analogues than the RP-8 stationary phase (Table 3.1). Separation of the AZA analogues at this stage in the procedure improved recoveries and purities in the final semi-preparative LC step (step 7), so the Phenyl-Hexyl stationary phase

was chosen as the stationary phase for flash chromatography. This step resulted in a clean-up of 64% (assessed after the RP-8 vs Phenyl-Hexyl experiment, see experimental section) and a recovery of ~ 90% (Table 3.1).

3.4.5. Preparative HPLC

An acidic mobile phase was used for semi-preparative LC purification in preliminary studies, but AZAs were very unstable when evaporated to dryness from the acidic eluent (unpublished information) confirming the results of Alfonso *et al.*[36] Therefore, a neutral mobile phase was chosen to prevent AZA degradation. Acceptable chromatography was obtained for AZA1 and AZA2 using the neutral mobile phase, but broad, fronting peaks were observed for AZA3 and AZA6. Similar chromatography for AZA3 was also observed using alkaline conditions on an analytical scale.[37] This is presumably related to the fact that both AZA3 and AZA6 lack a methyl group at the R^3 position (Figure 3.1, p 74) which somehow affects their chromatographic behavior. All fractions were collected based on UV detection at 210 nm to minimize contamination with non-AZA analytes.

Most (80%) of the AZA6 from the flash chromatography (step 6) was recovered in the AZA6 fraction, and 20% came from the AZA3 fraction. The recovery of AZA6 from the semi-preparative LC (61%) was slightly less than for the other AZA analogues (all ~ 85%), probably because co-eluting compounds necessitated significant heart cutting.

3.4.6. SPE recovery of AZAs from eluent

Fractions from the semi-preparative LC purification were diluted with H_2O and recovered on SPE cartridges in order to remove any buffer remaining in the sample, but also to reduce the H_2O content in, and volume of, the AZA fractions prior to evaporation, and as an additional final clean-up step to remove trace contaminants introduced via the LC eluents. This SPE

recovery resulted in very little loss of toxin, with recoveries of >95% being achieved, and greatly facilitated evaporation of the purified AZA-fractions to dryness.

3.4.7. Overall recoveries

7.3 mg of AZA1 was purified along with 1.6 mg of AZA2, 2.0 mg of AZA3 and 300 µg of AZA6. Overall recoveries (steps 1–7) were 52% for AZA1, 43% for AZA2 and -3, and 38% for AZA6, and represent a two-fold increase in recovery compared to previous isolations carried out as part of the ASTOX project.[33,38] Furthermore, the improved procedure is significantly easier to perform and less labor intensive.

Table 3.1. Batch summary table for purification of AZA1–3 and AZA6.

Step No	Step	AZA1 (mg)	AZA2 (mg)	AZA3 (mg)	AZA6 (mg)	Weight (g)
	Subsampling	14.1	4.0	4.8	0.78	505.0
1	1st crude extract	14.0	3.9	4.7	0.77	26.9
2	1st partitioning	13.3	3.7	4.4	0.73	23.9
3	2nd partitioning	12.6	3.5	4.2	0.69	8.9
4	Silica gel	11.9	3.3	4.0	0.65	0.6
5	LH20	10.1	2.8	3.4	0.55	0.2
6	Flash (phenyl-hexyl)*	9.2	2.5	2.4	0.49	-
7	Prep HPLC (C8/C18)	7.3	1.7	2.0	0.30	-
	% Recovery	52	43	43	38	
	% Purity	>95	>95	>95	>95	

3.4.8. Purity testing by MS, UV and NMR

The purity of the samples was first determined by mass spectrometry. An LC-MS scan was performed in the range *m*/*z* 100–1000, followed by LC-MS/MS analysis for all the known

AZA analogues as well as for any additional masses picked up in the MS scan (method B). The sample was also analyzed using the LC-PDA semi-preparative method (method D) to ensure that no additional peaks were observed in the UV trace. To determine whether strongly retained compounds, such as phthalates, were present in the sample, isocratic LC-PDA was performed (method E). Previous NMR analysis had shown the presence of a phthalate in some fractions which was detectable by LC-PDA (λ_{max} 205, 225 and 275 nm). This contaminant was conveniently removed by partitioning with hexane. Once samples were deemed to be sufficiently pure (LC-MS/MS and LC-PDA), they were prepared for NMR spectroscopy. The ^{1}H NMR spectra of AZA1–3 were compared to published NMR data and found to be essentially identical, and examination of the spectra indicated purities of >95%.

3.4.9. AZA6 structural elucidation by NMR

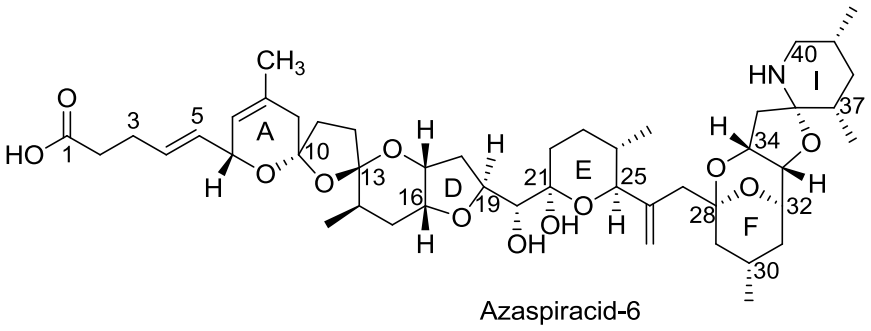

Azaspiracid-6

NMR data for AZA6 have not been published, and its proposed structure was based only on MS/MS fragmentation and on analogy with the structure of AZA3. AZA6 was therefore subjected to a more thorough series of 1- and 2D NMR experiments to verify its presumed structure. NMR analysis confirmed the previously postulated structure of AZA6, a methyl group at the R^2 position (C-8) and a methylene at C-22 (R^3 = H), see Figure 3.1 and Table 3.2. Structural elucidation of AZA6 was done using 1- and 2-dimensional homonuclear ^{1}H and heteronuclear ^{1}H{^{13}C} NMR spectroscopy to assign the ^{1}H and ^{13}C resonances, the chemical shifts of which were then compared with published data for AZA1–3.[2,3] One-

dimensional ^{1}H NMR and edited HSQC spectra showed that AZA6 had 6 methyl, 16 methylene, and 17 methine groups. Chemical shifts for eight quaternary carbons were ascertained from HMBC correlations (2.20,2.31/181.6, C-1; 5.71,5.32/72.29, C-6; 1.67,1.96/130.8, C-8; 1.93,0.91/106.9, C-10; 1.93,0.91/110.9, C-13; 2.13/98.1, C-21; 3.93/146.6, C-26; 2.14/97.6, C-28; and 0.83/95.6, C-36). Chemical shifts reported in Table 3.2 are from the HSQC (for ^{1}H and protonated ^{13}C atoms) and HMBC (for quaternary carbon atoms) spectra. Analysis of the COSY and TOCSY spectra led to the identification of 9 spin-systems based on protons and methyl groups attached to C-2–C-7; 8-CH_3; C-9; C-11–C-12; C-14–C-20; C-22–C-25; 26=CH_2; C-27; C-29–C-35; and C-37–C-40 (Figure 3.1). The following HMBC correlations defined the connections of the spin systems: C-6 to H-7; C-7 to 8- CH_3; C-8 to 8- CH_3 and H-9a,b; C-9 to 8- CH_3; C-10 to H-9; C-10 to H-11b; C-13 to H-12b; C-13 to H-14; C-13 to 14- CH_3; C-21 to H-22a,b; C-25 to 26=CH_2; 26=CH2 to H-27b; C-26 to H-27a,b; C-28 to H-27a,b; C-38 to 37-CH_3; and C-36 to H-40b. Periodate treatment of AZA6 yielded the same C-20–C-21-cleavage product as was obtained by treatment of AZA3, thereby establishing the presence of a 20,21-diol in AZA6 and a link between the C-14–C-20 and C-22–C-25 spin-systems.

The presence of a resonance at 1.67 ppm (8-Me) was consistent with the vinylic methyl group such as present in AZA2. The olefinic resonance at 5.32 ppm (H-7) showed more complex coupling than could be accounted for by its original assignment as H-9. When the ^{1}H spectrum was observed with resolution enhancement (Gaussian window function, LB = −2.0 Hz, GB = 0.25) the resonance at 5.32 ppm (8-Me) showed splitting into a multiplet ($J \approx$ 1.4 Hz) implying coupling to more than 3 protons. In addition there was a weak COSY correlation from 5.32 ppm (H-7) to 4.70 ppm (H-6) and an HMBC correlation from C-6 (72.3 ppm) to 5.32 ppm (H-7). This leads to the assignment of this vinylic proton resonance (5.32 ppm) to H-7 and it defines the double bond as between C-7 and C-8 in AZA6,

consistent with the structural revision of AZA1 by Nicolaou *et al.*[39] A detailed analysis of NMR data for AZA1 and AZA2 (C. O. Miles, A. L. Wilkins, F. Rise and J. Kilcoyne, unpublished) gave essentially identical results, so the original assignments[2,3] for AZA1–3 for C-7–C-9 and their attached protons and methyl groups are revised accordingly in Table 3.2.

Analysis of the TOCSY spectrum of AZA6 corresponding to the C-22 to C-25 spin system indicated that there was only one methyl group, and an additional methylene group, in ring-E compared to AZA1 and AZA2. This, along with COSY correlations, led to the conclusion that there is no methyl at C-22 of AZA6, analogous to AZA3.

ROESY NMR data confirmed that the relative stereochemistry of AZA6 was the same as that published for AZA1.[39] ROESY correlations were observed between H-30 and H-34, H-32 and H-33, and H-3 and H-34, consistent with the stereochemistry around rings F, G and H having H-32, H-33 and H-34 as equatorial, equatorial, and axial, respectively, with the 30-Me equatorial. In addition, ROESY correlations between the 37-Me and both H-33 and H-35a place the NH in ring-I on the β-face of ring-H. ROESY correlations between the 14-Me and both H-6 and H-11b support C-12 being axial to ring-C and the absence of a correlation between H-14 and H-16, were consistent with 14-Me being equatorial, and confirms the stereochemistry in this section of AZA6 as being that assigned to AZA1–3 by Nicolaou *et al.*[39–41] The ROESY correlation between H-16 and H-17, and H-16 and H18b, supports the cis-fusion of the 5-membered ring-D to ring-C. All the NMR data is thus consistent with the structure shown for AZA6 in Figure 3.1, as is the MS/MS fragmentation reported previously and used to propose the original tentative structure for this compound.[42] The periodate cleavage established that AZA6 had the same structure and relative stereochemistry as for AZA3 in the C-21–C-40 moiety. Furthermore, AZA6 is a metabolite produced by oxidative decarboxylation of the 22-Me group of AZA2 in shellfish,[6] so it must have the same absolute stereochemistry as AZA.

Table 3.2. NMR assignments for AZA6 (in CD_3OH) and AZA1–3 (in CD_3OD)[a,b].

	AZA-6			AZA-1			AZA-2			AZA-3		
	^{13}C	^{1}H		^{13}C	^{1}H		^{13}C	^{1}H		^{13}C	^{1}H	
1	181.6			180.3			177.8			177.8		
2	38.2	2.2	2.2	37.4	2.31	2.31	35.6	2.34	2.34	35.4	2.37	2.37
3	34.5	2.31	2.31	30.3	2.33	2.33	29.5	2.31	2.31	29.4	2.33	2.33
4	130.7	5.71		133.8	5.74		132.8	5.68		133	5.73	
5	133.2	5.39		131.8	5.46		132.1	5.42		132.4	5.47	
6	72.3	4.7		73.2	4.81		73.3	4.72		73.1	4.81	
7[c]	122.7	5.32		130.1	5.65		123.6	5.32		130	5.63	
8	130.8			124.1	5.76		132.8			124.2	5.75	
8-Me	22.64	1.67					23.8	1.67				
9[c]	40.05	1.94	2.39	36.5	2.15	2.49	41.1	1.97	2.42	36.5	2.13	2.48
10	106.9			107.9			108.3			108		
11	32.9	1.62	2.29	33.9	1.68	2.33	34	1.65	2.33	34	1.66	2.34
12	37.1	1.93	2.14	38.3	1.97	2.16	38.3	1.96	2.16	38.3	1.96	2.15
13	110.9			112.1			112.1			112.1		
14	30.5	1.98		31.7	2.02		31.7	2		31.7	2.02	
14-Me (41)	16.3	0.91		17.4	0.94		17.4	0.93		17.3	0.95	
15	32.3	1.71	1.79	33.4	1.77	1.85	33.4	1.73	1.83	33.4	1.75	1.84
16	77.5	3.89		79.1	3.89		79	3.87		79	3.91	
17	72.7	4.13		74.2	4.25		74.2	4.2		74	4.23	
18	38.1	1.98	2.04	37.8	2	2.01	37.7	1.98	1.98	38.2	1.98	1.98
19	79.3	4.39		79.9	4.44		79.9	4.42		80.3	4.43	
20	80.0	3.26		77.6	3.94		77.6	3.93		80.6	3.63	
21	98.1			101.1			101			98.7		
22	39.0	2.13	2.13	37.6	2.09		37.6	2.07		33.4	1.55	2.07
22-Me (42)				17.2	0.91		17.2	0.89				
23	29.0	1.56	1.56	38.9	1.44	1.44	39	1.43	1.43	30.1	1.61	1.61
24	39.0	1.3		43.1	1.35		43.1	1.33		42.3	1.28	
24-Me (43)	17.8	0.79		18.8	0.84		18.9	0.83		18.9	0.86	
25	80.1	3.93		80.4	4		80.4	3.97		80.7	4.08	
26	146.6			149.1			149.1			149.2		
26-CH2 (44)	115.5	5.1	5.19	117.2	5.18	5.36	118.1	5.17	5.35	118	5.18	5.35
27	48.1	2.14	2.33	50.4	2.26	2.43	50.1	2.24	2.42	50.2	2.26	2.43
28	97.6			99.5			99.5			99.5		
29	43.9	1.3	1.96	44.9	1.37	2.05	44.9	1.36	2.03	44.9	1.37	2.05
30	26.3	2.23		27.2	2.23		27.2	2.22		27.2	2.24	
30-Me (45)	23.5	0.9		24.3	0.96		24.1	0.93		24.3	0.96	
31	35.4	1.45	1.75	36.1	1.54	1.84	36.1	1.51	1.82	36.1	1.53	1.83
32	72.3	4.21		73.6	4.38		73.6	4.35		73.6	4.37	
33	78.9	3.68		82.3	4.08		82.4	4.06		82.4	4.07	
34	75.3	4.76		75.6	5.02		75.6	5		75.6	5.03	
35	42.8	1.86	2.36	42.5	2.5	2.64	42.4	2.49	2.62	42.3	2.54	2.64
36	95.6			97.4			97.4			97.4		
37	31.5	1.63		36.4	1.99		36.5	1.97		36.5	1.99	
37-Me (46)	15.8	0.83		16.2	0.98		16.2	0.97		16.2	0.98	
38	39.8	1.1	1.51	38.4	1.31	1.7	38.4	1.29	1.68	38.3	1.31	1.68
39	37.6	1.71		30.2	1.89		30.2	1.86		30.1	1.9	
39-Me (47)	19.2	0.82		19.3	0.95		19.3	0.94		19.3	0.95	
40	47.46	2.46	2.52	46.9	2.84	2.91	46.9	2.83	2.91	46.9	2.84	2.92

[a]Data from Satake *et al.*[3] [b]Data from Ofuji *et al.*[2] [c] Published assignments for positions 7 and 9 of AZA1–3[2,3] are interchanged as a consequence of the revised position of the olefin in ring A.[39]

3.4.10. AZA6 stability

The stability of AZA6 was compared with that of AZA1. Figure 3.2 shows that AZA6 is significantly less stable ($p<0.05$, Student's t-test) than AZA1 when stored in MeOH at 40 °C. These results parallel the observations of Perez *et al.*,[33] who showed that AZA3 was less stable than AZA1 under these conditions and confirms the results of McCarron *et al.*[43] showing that AZA6 exhibited similar instability to AZA3 in tissue CRM extracts. AZA6, like AZA3, but unlike AZA1 and AZA2, has no methyl group on the C-22 position. The mechanism responsible for this reduced stability is as yet unclear.

In this study the stability of AZA6 was determined in three solvents. Figure 3.2 shows that AZA6 is significantly more stable ($p<0.05$, Student's t-test) in 4:1 $CH_3CN–H_2O$ than in MeOH or EtOH. The appearance of additional LC-MS/MS peaks at *m/z* 856.5 and 870.5 after storage in MeOH and EtOH, respectively, indicated that these solvents were reacting with AZA6 to produce methyl and ethyl derivatives. The formation of AZA methyl esters after storage in MeOH has previously been reported, however, little evidence was provided to suggest these compounds were in fact methyl esters.[5] Methylation may occur at C-1 to produce the methyl ester or, alternatively, at C-21 to produce the methyl ketal. A purified sample of AZA6 was reacted with diazomethane to produce AZA6 methyl ester. The semi-synthetic methyl ester differed from the derivative observed during the stability study in both LC-MS/MS retention time and fragmentation pattern. The mass spectrum of the methyl ester showed a loss of 18 amu (*m/z* 838.5) from the parent ion, while the derivative showed a loss of 32 amu (*m/z* 824.5) from the parent ion, suggesting that the AZA6 is being methylated at the C-21 position to form a methyl ketal during storage in MeOH (Figure 3.3). The methyl ester of AZA6 also shows a different retention time to that of the methyl ketal, with the methyl ester being retained longer on the column. Furthermore, when the sample containing the methyl derivative was treated with sodium periodate, the compound remained intact

consistent with the proposition that the AZA6-derivative is methylated at the 21-position (i.e., AZA6 21-methyl ketal). These results support observations reported by Jauffrais *et al.*[44] which showed the formation of AZA1 and AZA2 methyl ketals in *A. spinosum* methanolic extracts.

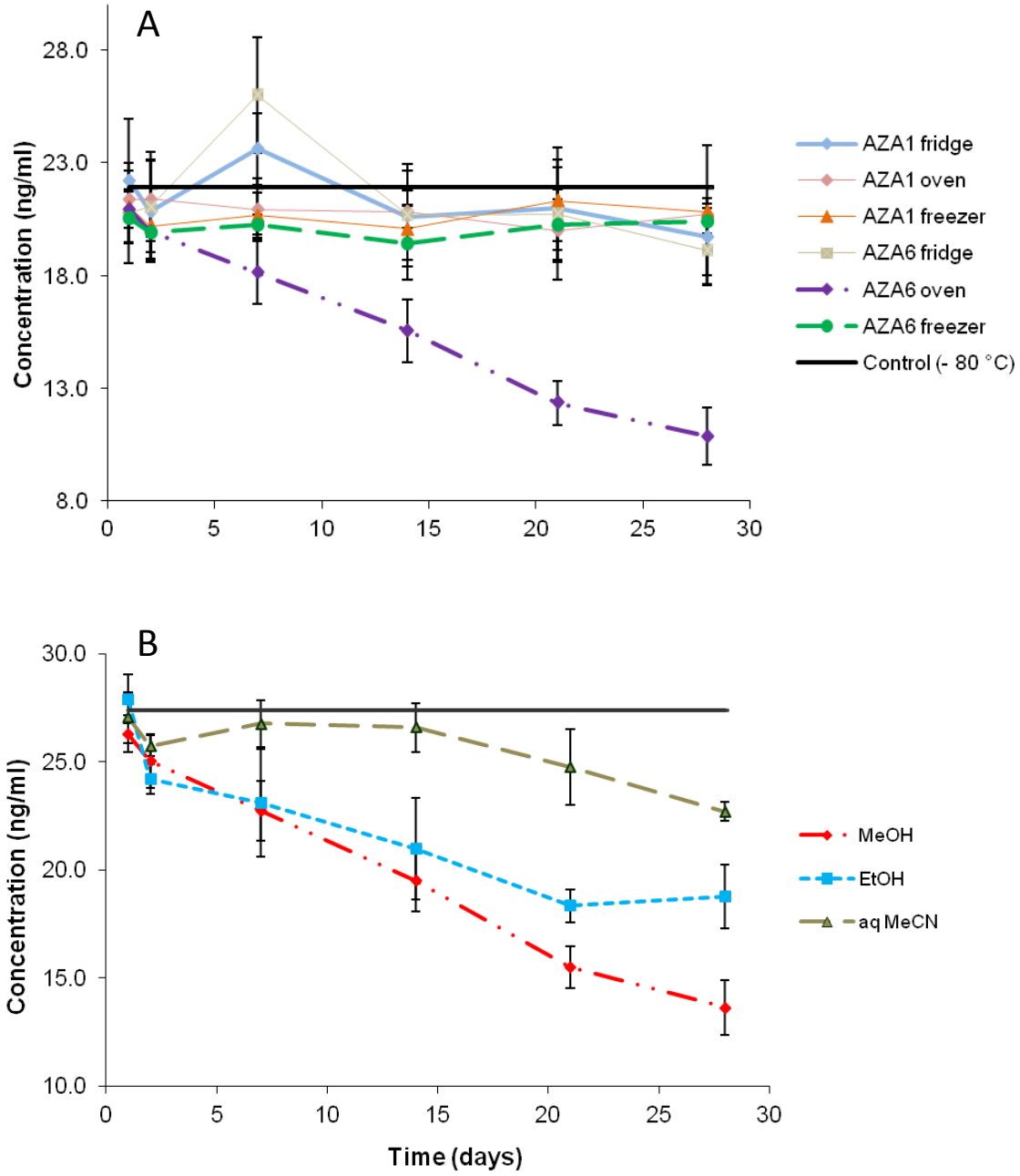

Figure 3.2. A) Stability of AZA1 and -6 stored in MeOH at −18 °C, 4 °C, and 40 °C and B) stability of AZA6 stored at 40 °C in MeOH, EtOH and 20% aqueous CH_3CN.

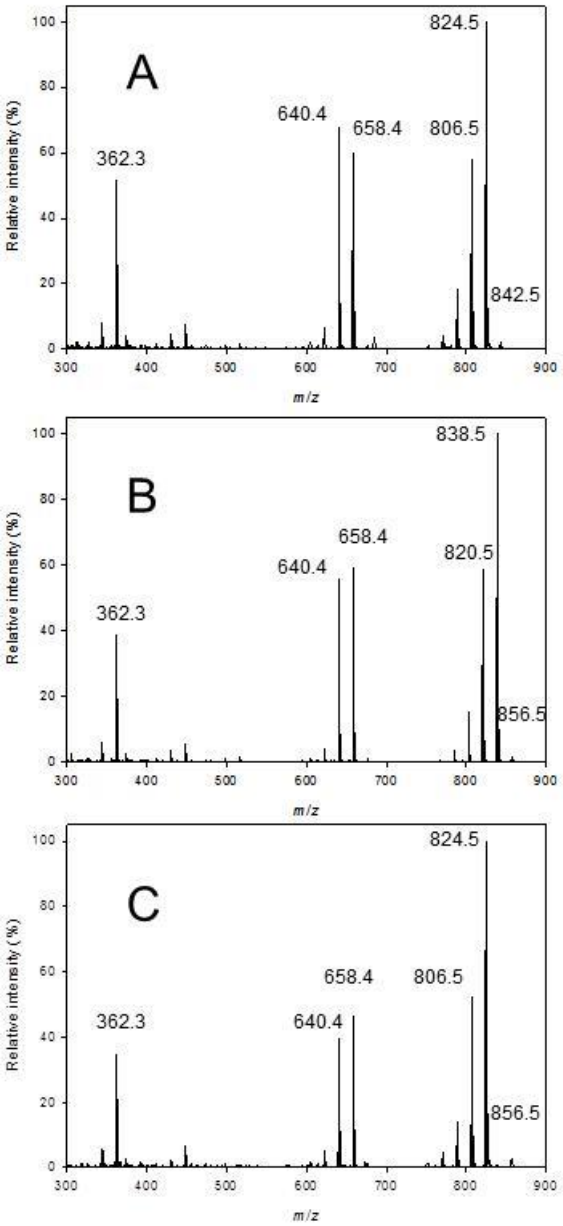

Figure 3.3. Mass spectra of a) AZA6, b) AZA6 methyl ester and c) AZA6 methyl ketal.

3.5. Conclusions

A method was optimized for the isolation of AZAs from highly contaminated *M. edulis* hepatopancreas. A seven-step procedure involving extraction, two partitioning, and four chromatography steps was employed. The method was adapted to limit degradation of sample by replacing acidic mobile phases with slightly basic and neutral mobile phases in two of the

chromatography steps. Improved separation of the AZAs during the penultimate step (flash chromatography; step 6) was achieved by using a Phenyl-Hexyl stationary phase, leading to a more efficient final clean up step by semi-preparative LC. Overall recoveries of ~40–50% were achieved for AZA1–3 and AZA6. Sufficient AZA6 was isolated for structural elucidation by NMR which confirmed the previously postulated[5] structure (Figure 3.1). A short-term stability study showed that AZA6 is significantly more stable in aqueous CH_3CN than in MeOH (the usual storage solvent) at 40 °C. The isolated AZAs are of sufficient purity for toxicological research and for the preparation of analytical standards.

3.6. References

(1) McMahon, T.; Silke, J. Winter toxicity of unknown aetiology in mussels. *Harmful Algae News* **1996**, *14*, 2.

(2) Ofuji, K.; Satake, M.; McMahon, T.; Silke, J.; James, K. J.; Naoki, H.; Oshima, Y.; Yasumoto, T. Two analogues of azaspiracid isolated from mussels, *Mytilus edulis*, involved in human intoxications in Ireland. ***Nat.*** *Toxins* **1999**, *7*, 99–102.

(3) Satake, M.; Ofuji, K.; Naoki, H.; James, K. J.; Furey, A.; McMahon, T.; Silke, J.; Yasumoto, T. Azaspiracid, a new marine toxin having unique spiro ring assemblies, isolated from Irish mussels, *Mytilus edulis*. *J. Am. Chem. Soc*. **1998**, *120*, 9967–9968.

(4) Satake, M.; Ofuji, K.; James, K. J.; Furey, A.; Yasumoto, T. New toxic event caused by Irish mussels. In: *Proc. 8th Int Conf Harmful Algae*; Reguera, B., Blanco, J., Fernandez, M.L., Wyatt, T., (eds.). Xunta de Galicia and Intergovernmental Oceanographic Commission of UNESCO: Vigo, Spain **1998**, 468–469.

(5) Rehmann, N.; Hess, P.; Quilliam, M. A. Discovery of new analogues of the marine biotoxin azaspiracid (AZA) in blue mussels (*Mytilus edulis*) tissue by ultra-performance liquid chromatography/tandem mass spectrometry. *Rapid Commun. Mass Spectrom*. **2008**, *16*, 2306–2316.

(6) McCarron, P.; Kilcoyne, J.; Miles, C. O.; Hess, P. Formation of azaspiracids-3, -4, -6, and -9 via decarboxylation of carboxyazaspiracid metabolites from shellfish. *J. Agric. Food Chem*. **2009**, *57*, 160–169.

(7) Anon. Commission Regulation (EU) No 15/2011 of 10th January 2011 amending Regulation (EC) No 2074/2005 as regards recognised testing methods for detecting marine biotoxins in live bivalve molluscs. L6/3–6, 2011.

http://eur-lex.europa.eu/LexUriServ/LexUriServ.do?uri=OJ:L:2011:006:0003:0006:EN:PDF.

(8) HABs database, http://www.marine.ie/home/publicationsdata/data/Habs+Search+Database/HabsSearch.htm.

(9) James, K. J.; Furey, A.; Lehane, M.; Ramstad, H.; Aune, T.; Hovgaard, P.; Morris, S.; Higman, W.; Satake, M.; Yasumoto, T. First evidence of an extensive northern European distribution of azaspiracid poisoning (AZP) toxins in shellfish. *Toxicon* **2002**, *40*, 909–915.

(10) Taleb, H. Vale, P.; Amanhir, R.; Benhadouch, A.; Sagou, R.; Chafik, A. First detection of azaspiracids in North West Africa. *J. Shellfish Res*. **2006**, *25*, 1067–1071.

(11) Twiner M.; Rehmann, N.; Hess, P.; Doucette, G. Azaspiracid shellfish poisoning: a review on the chemistry, ecology, and toxicology with an emphasis on human health impacts. *Mar. Drugs* **2008**, *6*, 39–72.

(12) Ueoka, R.; Ito, A.; Izumikawa, M.; Maeda, S.; Takagi, M.; Shin-ya, K.; Yoshida, M.; van Soest, R. W. M.; Matsunaga, S., Isolation of azaspiracid-2 from a marine sponge *Echinoclathria* sp. as a potent cytotoxin. *Toxicon* **2009**, *53*, 680–684.

(13) Álvarez, G.; Uribe, E.; Ávalos, P.; Mariño, C.; Blanco, J., First identification of azaspiracid and spirolides in *Mesodesma donacium* and *Mulinia edulis* from Northern Chile. *Toxicon* **2009**, *55*, 638–641.

(14) Hess, P. Requirements for screening and confirmatory methods for the detection and quantitation of marine biotoxins in end-product and official control. *Anal. Bioanal. Chem.* **2010**, *397*, 1683–1694.

(15) Hess, P.; Butter, T.; Petersen, A.; Silke, J.; McMahon, T. Performance of the EU-harmonised mouse bioassay for lipophilic toxins for the detection of azaspiracids in

naturally contaminated mussel (*Mytilus edulis*) hepatopancreas tissue homogenates characterised by liquid chromatography coupled to tandem mass spectrometry. *Toxicon* **2009**, *53*, 713–722.

(16) EFSA. Opinion of the scientific panel on contaminants in the food chain on a request from the European Commission on marine biotoxins in shellfish – azaspiracids. *EFSA J.* **2008**, 723, 1–52.

(17) James, K. J.; Moroney, C.; Roden, C.; Satake, M.; Yasumoto, T.; Lehane, M.; Furey, A. Ubiquitous 'benign' alga emerges as the cause of shellfish contamination responsible for the human toxic syndrome, azaspiracid poisoning. *Toxicon* **2003**, *41*, 145–151.

(18) Miles, C. O. Wilkins, A. L.; Samdal, I. A., Sandvik, M.; Petersen, D.; Quilliam, M. A.; Naustvoll, L. J.; Rundberget, T.; Torgersen, T.; Hovgaard, P.; Jensen, D. J.; Cooney, J. M. A novel pectenotoxin, PTX-12, in *Dinophysis spp*. and shellfish from Norway. *Chem. Res. Toxicol*. **2004,** *17*, 1423–1433.

(19) Krock, B.; Tillmann, U.; John, U.; Cembella, A. D. Characterization of azaspiracids in plankton size-fractions and isolation of an azaspiracid-producing dinoflagellate from the North Sea. *Harmful Algae* **2009**, *8*, 254–263.

(20) Tillmann, U.; Elbrächter, M.; Krock, B.; John, U.; Cembella, A. *Azadinium spinosum* gen. et sp. nov. (Dinophyceae) identified as a primary producer of azaspiracid toxins. *Eur. J. Phycol*. **2009,** *44*, 63–79.

(21) Rundberget, T.; Gustad, E.; Samdal, I. A.; Sandvik, M.; Miles, C. O. A convenient and cost-effective method for monitoring marine algal toxins with passive samplers. *Toxicon* **2009**, *53*, 543–550.

(22) Salas, R.; Tillmann, U.; John, U.; Kilcoyne, J.; Burson, A.; Cantwell, C.; Hess, P.; Jauffrais, T.; Silke, J. The role of *Azadinium spinosum* (Dinophyceae) in the

production of azaspiracid shellfish poisoning in mussels. *Harmful Algae* **2011**, *10*, 774–783.

(23) Colman, J. R.; Twiner, M. J.; Hess, P.; McMahon, T.; Satake, M.; Yasumoto, T.; Doucette, G. J.; Ramsdell, J. S. Teratogenic effects of azaspiracid-1 identified by microinjection of Japanese medaka (*Oryzias latipes*) embryos. *Toxicon* **2005,** 45, 881-890.

(24) Ito, E.; Satake, M.; Ofuji, K.; Higashi, M.; Harigaya, K.; McMahon, T.; Yasumoto, T. Chronic effects in mice caused by the oral administration of sublethal doses of azaspiracid, a new marine toxin isolated from mussels. *Toxicon* **2002**, *40*, 193–203.

(25) Aasen, J. A. B.; Espenes, A.; Hess, P.; Aune, T. Sub-lethal dosing of azaspiracid-1 in female NMRI mice. *Toxicon* **2010**, *56*, 1419–1425.

(26) Furey, A.; O'Doherty, S.; O'Callaghan, K.; Lehane, M.; James, K. Azaspiracid poisoning (AZP) toxins in shellfish: toxicological and health considerations. *Toxicon* **2010**, *56*, 173–190.

(27) O'Driscoll, D.; Skrabakova, Z.; O'Halloran, J.; Van Pelt, F.; James, K. Mussels increase xenobiotic (azaspiracid) toxicity using a unique bioconversion mechanism. *Environ. Sci. Technol*. **2011**, *45*, 3102–3108.

(28) Vale, P.; Bire, R.; Hess, P. Confirmation by LC–MS/MS of azaspiracids in shellfish from the Portuguese north-western coast. *Toxicon* **2008**, *51*, 1449–1456.

(29) López-Rivera, A.; O'Callaghan, K.; Moriarty, M.; O'Driscoll, D.; Hamilton, B.; Lehane, M.; James, K. J.; Furey, A. First evidence of azaspiracids (AZAs): a family of lipophilic polyether marine toxins in scallops (*Argopecten purpuratus*) and mussels (*Mytilus chilensis*) collected in two regions of Chile. *Toxicon* **2010**, *55*, 692–701.

(30) Moroney, C.; Lehane, M.; Braña-Magdalena, A.; Furey, A.; James, K. J. Comparison of solid-phase extraction methods for the determination of azaspiracids in shellfish

using liquid chromatography–electrospray mass spectrometry. *J. Chromatogr*. **2002**, *963*, 353–361.

(31) Alfonso, C.; Alfonso A.; Otero P.; Rodriguez, P.; Vieytes, M.; Elliot, C.; Higgins, C.; Botana, L. Purification of five azaspiracids from mussel samples contaminated with DSP toxins and azaspiracids. *J. Chromatogr. B* **2008**, *865*, 133–140.

(32) Ruppen Canas, I.; O'Callaghan, K.; Moroney, C.; Hamilton, B; James, K.; Furey, A. The development of a rapid method for the isolation of four azaspiracids for use as reference materials for quantitative LC–MS/MS methods. *Anal. Bioanal. Chem*. **2010**, *398*, 1477–1491.

(33) Perez, R.; Rehmann, N.; Crain, S.; LeBlanc, P.; Craft, C.; MacKinnon, S.; Reeves, K.; Burton, I.; Walter, J.; Hess, P.; Quilliam, M. A.; Melanson, J. The preparation of certified calibration solutions for azaspiracid-1, -2, and -3, potent marine biotoxins found in shellfish. *Anal. Bioanal. Chem*. **2010**, *398*, 2243–2252.

(34) Quilliam, M. A.; Hess, P.; Dell'Aversano, C. Recent developments in the analysis of phycotoxins by liquid chromatography-mass spectrometry. In: *Mycotoxins and Phycotoxins in Perspective at the Turn of the Millenium*; De Koe, W.J.; Sampson, R.A.; Van Egmond, H.P.; Gilbert J.; Sabino, M. (Eds.).; DeKoe W.J., Wageningen, The Netherlands **2001**, 383-391.

(35) Selwood, A.; Miles, C.O.; Wilkins, A.; Van Ginkel, R.; Munday, R.; Rise, F.; McNabb, P. Isolation, structural determination and acute toxicity of pinnatoxins E, F and G. *J. Agric. Food Chem.* **2010**, *58*, 6532–6542.

(36) Alfonso, C.; Rehmann, N.; Hess, P.; Alfonso, A.; Wandscheer, C.; Abuin, M.; Vale, C.; Paz, O.; Vieytes, M.; Botana, L. Evaluation of various pH and temperature conditions on the stability of azaspiracids and their importance in preparative isolation and toxicological studies. *Anal. Chem.* **2008**, *80*, 9672–9680.

(37) Gerssen, A.; Mulder, P. P. J.; McElhinney, M. A.; de Boer, J. Liquid chromatography–tandem mass spectrometry method for the detection of marine lipophilic toxins under alkaline conditions. *J. Chromatogr. A* **2009**, *1216*, 1421–1430.

(38) Hess, P.; McCarron, P.; Rehmann, N.; Kilcoyne, J.; McMahon, T.; Ryan, G.; Ryan, P. M.; Twiner, M. J.; Doucette, G. J.; Satake, M.; Ito, E.; Yasumoto, T. *Isolation and purification of azaspiracids from naturally contaminated materials, and evaluation of their toxicological effects*—final project report ASTOX (ST/02/02). Marine Institute—Marine Environment & Health Series—No. 28, ISSN: 1649-0053. **2007**. http://www.marine.ie/NR/rdonlyres/2B06863D-3366-47CD-9ABB-B3302629FE46/0/ASTOX.pdf. Accessed 27 April 2011.

(39) Nicolaou, K. C.; Frederick, M. O.; Petrovic, G.; Cole, K. P.; Loizidou, E. Z. Total synthesis and confirmation of the revised structures of azaspiracid-2 and azaspiracid-3. *Angew. Chem., Int. Ed*. **2006,** *45*, 2609–2615.

(40) Nicolaou, K. C.; Li, Y. W.; Uesaka, N.; Koftis, T. V.; Vyskocil, S.; Ling, T. T.; Govindasamy, M.; Qian, W.; Bernal, F.; Chen, D. Y. K. Total synthesis of the proposed azaspiracid-1 structure, part 1: Construction of the enantiomerically pure C1–C20, C21–C27, and C28–C40 fragments. *Angew. Chem., Int. Ed*. **2003,** *42*, 3643–3648.

(41) Nicolaou, K. C.; Chen, D. Y. K.; Li, Y. W.; Qian, W. Y.; Ling, T. T.; Vyskocil, S.; Koftis, T. V.; Govindasamy, M.; Uesaka, N. Total synthesis of the proposed azaspiracid-1 structure, part 2: Coupling of the C1–C20, C21–C27, and C28–C40 fragments and completion of the synthesis. *Angew. Chem., Int. Ed.* **2003,** *42*, 3649–3653.

(42) James, K. J.; Diaz Sierra, M.; Lehane, M.; Braña Magdalena, A.; Furey, A. Detection of five new hydroxyl analogues of azaspiracids in shellfish using multiple tandem mass spectrometry. *Toxicon* **2003**, *41*, 277–283.

(43) McCarron, P.; Emteborg, H.; Giddings, S.D.; Wright, E.; Quilliam, M.A. A mussel tissue certified reference material for multiple phycotoxins. Part 3: homogeneity and stability. *Anal. Bioanal. Chem.* **2011,** *400*, 847–858.

(44) Jauffrais, T.; Herrenknecht, C.; Séchet, V.; Sibat, M.; Tillmann, U.; Krock, B.; Kilcoyne, J.; Miles, C. O.; McCarron, P.; Amzil, Z.; Hess, P. Quantitative analysis of azaspiracids in *Azadinium spinosum* cultures, with a focus on azaspiracid methyl-esters as extraction artefacts. *Anal. Bioanal. Chem.* **2012,** *403*, 833–846.

CHAPTER 4 - EPIMERS OF AZASPIRACIDS: ISOLATION, STRUCTURAL ELUCIDATION, RELATIVE LC-MS RESPONSE, AND *IN VITRO* TOXICITY OF 37-*EPI*-AZASPIRACID-1

Kilcoyne, J.; McCarron, P.; Twiner, M. J.; Nulty, C.; Wilkins, A. L.; Rise, F.; Quilliam, M. A.; Miles, C. O. 2014. Epimers of azaspiracids: isolation, structural elucidation, relative LC-MS response, and *in vitro* toxicity of 37-*epi*-azaspiracid-1. *Chemical Research in Toxicology*, *27*, 587–600.

4.1. Abstract

Since azaspiracid-1 (AZA1) was identified in 1998, the number of AZA analogues has increased to over 30. The development of an LC-MS method using a neutral mobile phase led to the discovery of isomers of AZA1, AZA2 and AZA3, present at ~ 2–16% of the parent analogues in phytoplankton and shellfish samples. Under acidic mobile phase conditions, isomers and their parents are not separated. Stability studies showed that these isomers were spontaneous epimerization products whose formation is accelerated with the application of heat.

An AZA1 isomer was isolated from contaminated shellfish and identified as 37-*epi*-AZA1 by nuclear magnetic resonance (NMR) spectroscopy and chemical analyses. Similar analysis indicated that the isomers of AZA2 and AZA3 corresponded to 37-*epi*-AZA2 and 37-*epi*-AZA3, respectively. The 37-epimers were found to exist in equilibrium with the parent compounds in solution. 37-*epi*-AZA1 was quantitated by NMR and relative molar response studies were performed to determine potential differences in LC-MS response of AZA1 and 37-*epi*-AZA1.

Toxicological effects were determined using Jurkat T lymphocyte cells as an *in vitro* cell model. Cytotoxicity experiments employing a metabolically-based dye (i.e., MTS) indicated

that 37-*epi*-AZA1 elicited a lethal response that was both concentration- and time-dependent, with EC_{50} values in the sub-nanomolar range. Based on EC_{50} comparisons, 37-*epi*-AZA1 was 5.1-fold more potent than AZA1. This data suggests the presence of these epimers in seafood products should be considered in the analysis of AZAs for regulatory purposes.

4.2. Introduction

Azaspiracids (AZAs) are marine biotoxins (Figure 4.1) that originate from the phytoplankton *Azadinium*[1] and *Amphidoma*[2] spp. and that can accumulate in shellfish. The consumption of AZA-contaminated shellfish can lead to a human poisoning called azaspiracid shellfish poisoining.[3] *A. spinosum* has been shown to produce AZA1 and AZA2,[4] while many of the other analogues are produced as a result of metabolism within the shellfish.[5,6] The number of known AZA analogues in this group has increased considerably[7] since they were first discovered in 1998.[3] However, only AZA1, AZA2 and AZA3 are regulated by the EU.[8] To date, only AZA1–6 have been isolated and fully characterized.[3,9–11]

AZAs have been responsible for seven confirmed shellfish poisoning events.[12] Symptoms generally include gastrointestinal illness, such as nausea, vomiting, severe diarrhoea, and stomach cramps.[13] In animals, they can elicit similar diarrhetic effects[14] with severe intestinal pathology[15] but extracts given via intraperitoneal injection exhibited "neurotoxin-like" symptoms characterized by sluggishness, respiratory difficulties, spasms, progressive paralysis, and death within 20–90 minutes.[16,17] In feeding studies, the AZAs have been shown to be absorbed and systemically distributed with some microscopic pathology associated with the small intestine.[18–20] *In vitro*, the AZAs are also highly cytotoxic to various cell types, with cell death via apoptosis[21] occurring in low nanomolar concentrations.[22–25] Structure–activity relationship studies have shown that there are distinct differences in the potencies of the AZA analogues. AZA2 is the most potent, followed by AZA3, AZA1, and then the hydroxylated

AZA4 and AZA5.[9,16,26] The only target conclusively demonstrated for the AZAs has been the hERG potassium channel.[27]

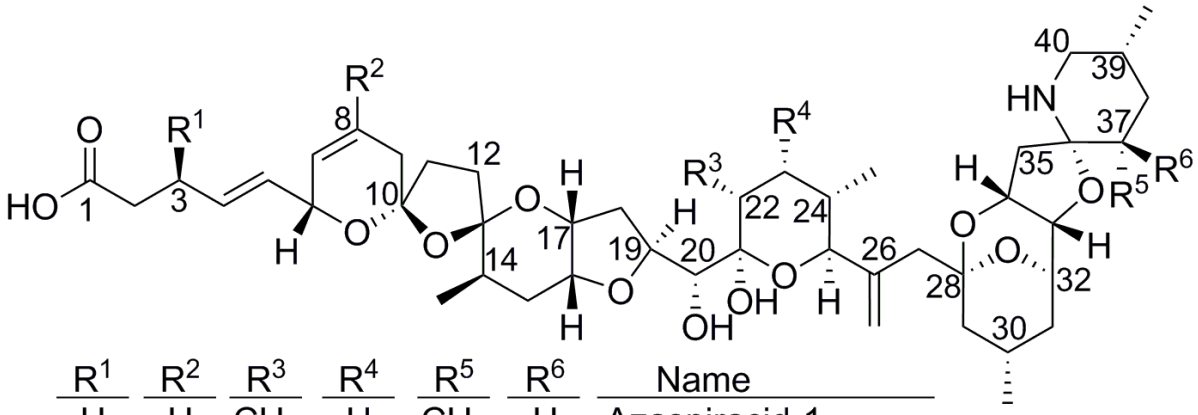

R^1	R^2	R^3	R^4	R^5	R^6	Name
H	H	CH_3	H	CH_3	H	Azaspiracid-1
H	H	CH_3	H	H	CH_3	37-*epi*-Azaspiracid-1
H	CH_3	CH_3	H	CH_3	H	Azaspiracid-2
H	CH_3	CH_3	H	H	CH_3	37-*epi*-Azaspiracid-2
H	H	H	H	CH_3	H	Azaspiracid-3
H	H	H	H	H	CH_3	37-*epi*-Azaspiracid-3
OH	H	H	H	CH_3	H	Azaspiracid-4
H	H	H	OH	CH_3	H	Azaspiracid-5
H	CH_3	H	H	CH_3	H	Azaspiracid-6
H	CH_3	H	H	H	CH_3	37-*epi*-Azaspiracid-6

Figure 4.1. Structures of AZA1−3, -6 and their 37-epimers, and AZA4 and -5.

Liquid chromatography–mass spectrometry (LC-MS) is the reference method for the analysis of lipophilic marine biotoxins in shellfish.[8] Considerable efforts were made to produce certified reference materials (CRMs) for AZAs,[28–31] which are now available.[32,33] The availability of CRMs is necessary to ensure accuracy of analytical results. A number of LC-MS methods for the analysis of AZAs have been published employing acidic[34–36] and basic[37] mobile phases. More recently, an LC-MS method for lipophilic toxin analysis was reported that used a neutral mobile phase.[38] This method revealed the presence of unidentified isomers of AZA1, AZA2 and AZA3 in tissue and calibrant CRMs. These isomers were resolved using a neutral eluent but co-eluted with the parent toxin in an acidic eluent.[33] The proportion of

these isomers for AZA1–3 in the tissue CRM ranged from 2–16% of their parent analogues. This finding is significant due to the potential of these isomers to interfere with the accuracy of analytical results. Although these isomers are not typically resolved using acidic and basic[37] methods, they may lead to discrepancies in analytical results depending on the amount present and their relative response factors. Isomers of AZAs have been reported previously but these were produced as a result of acid-catalyzed degradation of the main analogues, and the isomers were resolved from the parent compounds by LC using acidic eluents.[7,39]

In this paper we identify a group of epimerized AZA analogues found naturally in shellfish and phytoplankton, and report on their origin, stability, toxicity and relative response factors in LC-MS analysis. The potential consequences of AZA-epimerization for shellfish consumers are also briefly discussed.

4.3. Experimental section

4.3.1. Chemicals

All solvents (pestican grade) were purchased from Labscan (Dublin, Ireland) and Caledon (Georgetown, ON, Canada). Distilled H_2O was further purified using a Barnstead nanopure diamond UV purification system (Thermo Scientific, Iowa, USA). Sodium chloride (99+%), triethylamine (99%), ammonium acetate (97+%), ammonium formate (reagent grade), formic acid (>98%), and silica gel (10–40 µm, type H), were purchased from Sigma–Aldrich (Steinheim, Germany). Sodium chloride (99+%) and sodium periodate were purchased from Sigma Aldrich (St Louis, USA). Sephadex LH-20 was from GE Healthcare (Uppsala, Sweden), LiChroprep RP C8 (25–40 µm) was from Merck (Darmstadt, Germany), Luna phenyl-hexyl (15 µm) was from Phenomenex (Cheshire, UK), CD_3OH (99.5 atom-% D) was from Cambridge Isotope Laboratories (MA, USA), and CD_3OD and CD_3OH (100.0 and 99.8

atom-% D, respectively) were from Sigma–Aldrich (Steinheim, Germany). AZA CRMs were obtained from the National Research Council of Canada (Halifax, NS, Canada).

4.3.2. Culture toxin extraction

A sample (10 mL) of a culture of the Irish strain of *A. spinosum*[5] was transferred into a 15 mL centrifuge tube and centrifuged at 4,500 g for 5 min. The supernatant was decanted and the pellet was extracted with 1 mL of MeOH by vortex mixing for 1 min followed by centrifugation for 5 min at 10,500 *g*. The extract was filtered through a glass Pasteur pipette plugged with cotton wool into an HPLC vial, for LC-MS analysis (method A).

4.3.3. Analysis of raw shellfish tissues

AZA-contaminated raw shellfish samples, tested as part of the routine monitoring programme in Ireland, were selected for analysis of epimers. The shellfish were shucked and homogenised using a Warring blender before extraction. Tissue samples (2 g) were extracted by vortex mixing for 1 min with 9 mL of MeOH, centrifuged at (3,950 *g*) for 5 min, and the supernatant decanted into a 25 mL volumetric flask. The remaining pellet was further extracted using an Ultra turrax homogenizer (IKA-Werke T25 at 11,000 rpm) for 1 min with an additional 9 mL of MeOH, centrifuged at (3,950 *g*) for 5 min, and the supernatant decanted into the same 25 mL volumetric flask which was brought to volume with MeOH. The extracts were analysed by LC-MS (method A).

4.3.4. Heat treatment of raw AZA-contaminated shellfish and extracts

The extracts from above were transferred into centrifuge tubes and placed in a H_2O bath (Grant Ltd, Cambridge, UK) at 90 °C for 10 min, removed, allowed to cool and transferred into HPLC vials for LC-MS analysis (method A). Aliquots (6 × 2 g) of whole tissue

homogenate were weighed into centrifuge tubes, three of which were capped and placed in a H_2O bath at 90 °C for 10 min, removed, allowed to cool and extracted (using the above extraction method) in parallel with the three unheated samples. The extracts were analyzed by LC-MS (method B).

4.3.5. Stability studies

Dilutions of fractions collected from the final step in the isolation of AZAs,[11] containing AZA1–3 and their epimers, were dissolved in CH_3CN–H_2O (8:2) or in CH_3CN–H_2O (8:2) to which 0.1% v/v formic acid or triethylamine had been added. Aliquots of the solutions were transferred to amber ampoules, flame-sealed under nitrogen, and stored at −18 °C, 20 °C and 40 °C for up to 7 days. The study was performed using a reverse isochronous strategy[40] and samples were analyzed under reproducibility conditions by LC-MS (method A) with samples stored at −80 °C used as the control. An analogous study was performed in parallel using MeOH (instead of CH_3CN–H_2O) as solvent.

4.3.6. Isolation of 37-*epi*-AZA1 from shellfish

The isolation method employed is described in detail elsewhere.[11] Final separation of AZA1 from its epimer was achieved by semi-preparative HPLC (Shimadzu 10AVp) with photodiode array (PDA) detection at 210 nm using a Luna C8 column (5 µm, 250 × 10 mm) eluted with CH_3CN–H_2O (11:9, plus 2 mM ammonium acetate) at 4 mL/min with a column temperature of 30 °C. AZA2, AZA3 and their 37-epimers were purified using the same system as for AZA1, but with a narrower-bore column (Cosmosil C18, 5 µm, 250 × 4.6 mm) eluted with CH_3CN–H_2O (1:1, plus 2 mM ammonium acetate) at 1 mL/min. Purified AZAs were recovered by diluting the fractions with H_2O (to 20% CH_3CN), loading on to solid-phase extraction (SPE) cartridges (Oasis HLB, 200 mg), washing with MeOH–H_2O (1:9,

10 mL) to remove the buffer, and eluting with MeOH–H_2O (9:1, 20 mL). However, the epimers were not sufficiently pure at this stage and there was some conversion (~ 8%) of the epimers back to the parent compound during the SPE step. Samples were therefore passed through semi preparative HPLC a second time, the CH_3CN was removed on a rotary evaporator at 20 °C, the AZAs extracted from the buffer with an equal volume of EtOAc, and the solvent was removed on a rotary evaporator at 20 °C to give the epimers as colorless solids.

4.3.7. Periodate cleavage

Dilutions of fractions collected from the final step in the isolation procedure, containing both parent analogue and its epimer, were dissolved in MeOH. To 100 µL of sample was added 50 µL of 0.2 M sodium periodate solution, and the reaction analyzed immediately by LC-MS (method A) and again at intervals over a 2 h period, but including traces at *m/z* 448.4 (for the AZA1 and AZA2 oxidation product) and at *m/z* 434.4 (for the AZA3 oxidation product). As a control, the sodium periodate solution was replaced by H_2O.

4.3.8. Incorporation of deuterium from CH_3OD

An aliquot (0.5 mL) from the final step in the isolation procedure, containing both AZA1 and 37-*epi*-AZA1, was evaporated under nitrogen, taken up in 0.5 mL CH_3OD, stored at 40 °C, and aliquots analyzed periodically over 10 days by LC-MS (method A) for *m/z* 842.5, *m/z* 843.5 and *m/z* 844.5 to monitor deuterium incorporation. An aliquot (0.2 mL) of the partially deuterated sample was evaporated under nitrogen, dissolved in MeOH (40 µL) and added to 1 M phosphate buffered saline (PBS) (160 µL). The sample was stored at 40 °C and analyzed periodically over 4 days by LC-MS (method A) for *m/z* 842.5, *m/z* 843.5 and *m/z* 844.5 to monitor loss of deuterium.

4.3.9. LC-MS analysis

Method A. A Micromass Ultima time-of-flight (QToF) mass spectrometer equipped with a z-spray ESI source and coupled to a Waters 2795 LC was used for this method. Separation was performed on a 5 µm, 150 × 2 mm Luna C18 (2) column (Phenomenex, UK) operated at 30 °C, injecting 5 µL samples. A binary mobile phase of H_2O (A) and CH_3CN–H_2O (95:5) (B), each containing 5 mM ammonium acetate (pH 6.8), was used isocratically (A:B, 35:65) at a flow rate of 0.35 mL/min. The QToF was operated in product ion scan mode, where the precursor ions selected were: *m/z* 842.5 (AZA1 and AZA6); 856.5 (AZA2); and 828.5 (AZA3), in positive ionization mode. The cone voltage was 40 V and the collision voltage was 50 V, the cone and desolvation gas flows were set at 100 and 750 L/h, respectively, and the source temperature was 150 °C.

Method B. An Agilent 1200 LC system (Agilent Inc., Palo Alta, CA, USA) connected to an API4000 QTRAP mass spectrometer (AB Sciex, Concord, ON, Canada) equipped with a Turbospray ionization source was used for this method. Separation was performed on a 2.5 µm, 2.1 × 50 mm, Luna C18 (2) HST column (Phenomenex, Torrance, CA, USA) operated at 15 °C, injecting 1–5 µL samples. A binary mobile phase of H_2O (A) and CH_3CN–H_2O (95:5) (B), each containing 5 mM ammonium acetate (pH 6.8), was used, with a gradient from 25 to 100% B over 5 min at 0.35 mL/min and held at 100% B for 2 min before re-equilibration for the next run. The MS was operated in positive ion selected reaction monitoring (SRM) mode for the following transitions: *m/z* 842.5→672.5 (AZA1); *m/z* 856.5→672.5 (AZA2); *m/z* 828.5→658.5 (AZA3) and *m/z* 842.5→658.5 (AZA6) with collision energy 70 V. Typical parameters were electrospray voltage 5500 V, source temperature 400 °C, and declustering potential 70 V.

Method C. For the relative molar response study on AZA1 and 37-*epi*-AZA1, samples were analysed using a number of LC-MS/MS methods. Analyses were performed on an Agilent

1200 LC system (Agilent Inc., Palo Alta, CA, USA) connected to an API4000 QTRAP mass spectrometer (AB Sciex, Concord, ON, Canada) equipped with a Turbospray ionization source. The MS was operated in positive ion mode and SRM for the following transitions: *m/z* 842.5→824.5/806.5/672.4/654.4/462.3/362.3 (AZA1 and 37-*epi*-AZA1), with collision energies of 45 to 70 V. For selected ion monitoring (SIM) experiments, *m/z* 842.5 ($[M+H]^+$) was analyzed.

Method C(i) Gradient elution with a neutral mobile phase was run as described for method B.

Method C(ii) Isocratic elution with a neutral mobile phase was run on the same Luna column using 60% B at 0.3 mL/min.

Method C(iii) Gradient elution with acidic mobile phase was run on the same Luna column but eluting with H_2O (A) and CH_3CN–H_2O (95:5) (B), each containing 50 mM formic acid and 2 mM ammonium formate. Linear gradient elution was run from 25 to 100% B over 5 min at 0.3 mL/min and held at 100% B for 2 min, before re-equilibration for the next run.

Method C(iv) Isocratic elution with the acidic mobile phase was run on the same Luna column using 55% B at 0.3 mL/min.

High resolution MS/MS spectra. Aliquots (~ 5 µL) of AZA1 and -2 after NMR analysis in CD_3OH and CD_3OD, respectively, were diluted with 500 µL MeOH to remove rapidly exchangeable OD- and ND-groups, evaporated to dryness under N_2, and dissolved in 1 mL CH_3CN for analysis. High resolution MS/MS spectra of the $[MH+1]^+$ ions (*m/z* 843.5 and 857.5, respectively) of AZA1 and -2 during infusion of the solutions into a Q Exactive mass spectrometer (Thermo Scientific) using ESI in positive ion mode with mass-selection width set to *m/z* 0.4 and scan range *m/z* 150–900. The normalized collision energy was 30 V, resolution was set to 140 K, with capillary temperature 320 °C, S-lens RF level 50, spray voltage 3.8 kV, and sheath gas and auxiliary gas at 45 and 10 units respectively.

4.3.10. NMR spectroscopy

Structural Elucidation. Structural determinations were performed by analysis of ^{1}H, COSY, TOCSY, SELTOCSY, NOESY, ROESY, SELROESY, ^{13}C, DEPT135, HSQC and HMBC spectra using Bruker Avance I or Avance II 600 MHz spectrometers equipped with a TCI cryoprobe and Z-gradient coils. Samples of AZA1 (1 mg), 37-*epi*-AZA1 (0.1 mg) and AZA2 (1 mg) were dissolved in ~ 0.5 mL CD_3OD or CD_3OH at 30 °C, and chemical shifts were referenced to internal CHD_2OD or CHD_2OH (both 3.31 ppm), or CD_3OD or CD_3OH (49.0 ppm). Single- or double-frequency pre-saturation of solvent resonances was performed using continuous wave and/or excitation sculpting as required.

Quantitative NMR (qNMR). Quantitation of AZA1 and 37-*epi*-AZA1 by NMR was performed on a Bruker Avance II 600 spectrometer using a BBI probe (5 mm) and operating at room temperature. Purified samples dissolved in CD_3OH were measured against external standards of caffeine dissolved in H_2O (4.10 mM) as described previously for AZA CRMs[32] using techniques described previously by Burton *et al*.[41]

4.3.11. Toxicology

Cell Culturing. Non-adherent human Jurkat E6-1 T lymphocyte cells (American Type Culture Collection TIB-152; Manassas, VA, USA) were grown as described by Twiner *et al*.[22,26] Briefly, cells were grown in RPMI medium (cat. #11875-093, Invitrogen, CA, USA) supplemented with 10% (v/v) fetal bovine serum (FBS; cat. #26140, Invitrogen, CA, USA) and maintained in a humidified incubator (Sanyo 18AIC-UV) with 5% CO_2 in air at 37 °C. Cells were subcultured with fresh medium at an inoculum ratio of 1:4 every 3 to 4 days by transferring 2.5 mL of cells to 7.5 mL of fresh supplemented medium in 75 cm^3 screw cap culture flasks.

Cytotoxicity assay. The effect of AZA1 and 37-*epi*-AZA1 on viability of Jurkat T lymphocyte

cells was determined. Jurkat T lymphocytes were selected based on initial *in vivo* observations,[15] cell sensitivity following extensive *in vitro* cytotoxicity screening experiments,[22] and for comparative purposes to other AZA analogues for which potencies have been determined using this assay.[26,29] The Jurkat T lymphocyte cell line was grown as described above and cells were seeded in 100 μL of the supplemented medium at 35,000 cells per well in black, sterile, 96-well culture plates for 24 h to allow for recovery and settling. The AZA analogues were added at various concentrations for 24, 48, and 72 h of continuous exposure prior to assessment of cytotoxicity. The final concentrations of AZA1 ranged from 9.5×10^{-8} to 5×10^{-12} M, and the final concentrations of 37-*epi*-AZA1 ranged from 7.6×10^{-7} to 5×10^{-12} M. Parallel controls of equivalent amounts of MeOH/PBS were used to normalize the viability data for each treatment. Following exposure of the cells to the AZA analogues for the specified period of time, cellular viability/cytotoxicity was assessed using the MTS (3-(4,5-dimethylthiazol-2-yl)-5-(3-carboxymethoxyphenyl)-2-(4-sulfophenyl)-2H-tetrazolium) assay (Promega Biosciences, San Luis Obispo, CA, USA; cat. no. G5421). Each well received 10 μL of the MTS solution, the cells were incubated for 4 h at 37 °C, and absorbance at 485 nm was measured (FluoStar microplate reader, BMG Lab Technologies). Data are presented as means ± standard error of three separate experiments (n=3). In addition, each cytotoxicity experiment was performed using duplicate wells. Cytotoxicity data were blank-corrected and normalized to the control (% viability) and plotted using GraphPad Prism (ver. 5.0c, San Diego, USA).

*Collection of Samples for Metabolites***.** Samples were taken throughout the course of the toxicology experiments to determine AZA analogue stability and/or metabolite composition. In parallel with the cytotoxicity experiments outlined above, these experiments were conducted using AZA1 and 37-*epi*-AZA1 with initial concentrations in each well of 94.8 and 767 nM, respectively. Samples were taken directly from the 96-well plates containing T

lymphocyte cells at 0, 24, 48, and 72 h following the addition of the AZAs. The experiments were conducted in triplicate and also repeated in the absence of cells. At the given time, the entire volume (100 µL) of the well contents were transferred to a glass vial and then immediately frozen at −70 °C. Direct analysis of the samples was performed by LC-MS (method B).

4.4. Results and discussion

4.4.1. Observation and formation

The AZA isomers were first observed during the development of analytical methods for the measurement of a mussel tissue matrix CRM for AZAs. When LC conditions were switched from using an acidic mobile phase to a neutral one, additional isomeric peaks were resolved (Figure 4.2). Analysis of a fresh *A. spinosum* culture showed no detectable AZA1 and AZA2 isomers, while extracts of raw shellfish (*M. edulis* and *C. gigas*) contaminated with AZAs (0.08–4.8 µg/g) showed the presence of only minor amounts (< 2%). However, when the extracts were heated to 90 °C for 10 min, the concentration of isomers increased to 6–15% of the parent compounds (Figure 4.3).

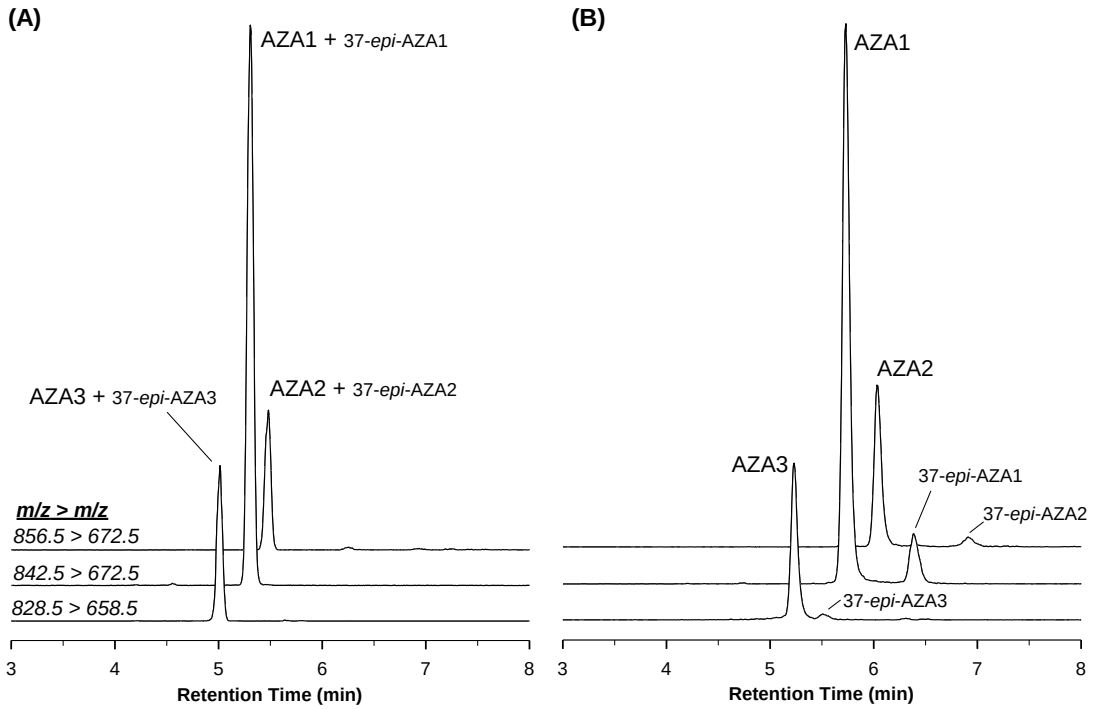

Figure 4.2. LC-MS analysis of CRM-AZA-Mus[33] with (A) acidic pH and (B) neutral pH mobile phases, showing co-elution and resolution of the 37-*epi*-AZAs, respectively.

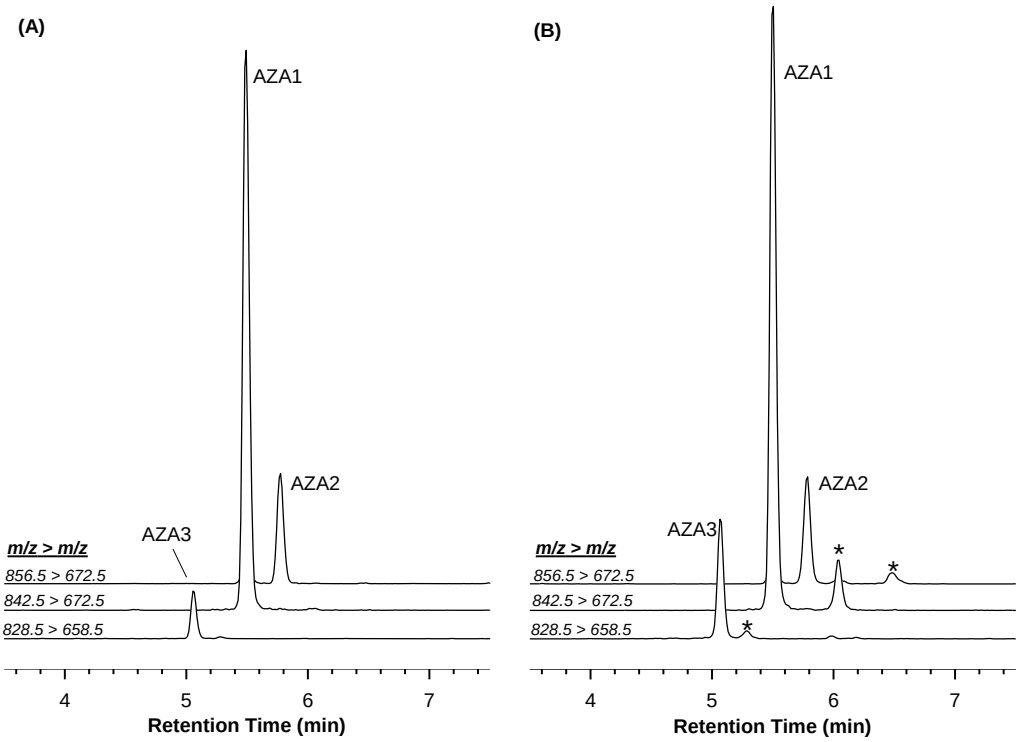

Figure 4.3. LC-MS/MS analysis of raw (A) and cooked (B) mussel samples using method B. 37-epimers are marked with *. The increase in AZA3 after cooking is due to heat induced decarboxylation of AZA17.[6]

These results strongly suggested that the isomers are heat-promoted conversion products and further highlights the fact that the chemical profile of these toxins in shellfish can change significantly during cooking. Previous studies have shown that levels of certain AZAs (e.g., AZA3) increased dramatically upon cooking as a result of other AZA analogues undergoing decarboxylation.[6]

4.4.2. Stability

Short-term stability studies were performed for the isomers of AZA1–3 using dilutions of fractions collected from the isolation step for AZAs,[11] at −18 °C, ~ 20 °C and 40 °C in two solvents and under weakly acidic and basic conditions over a 7 day period. The results showed that the isomers were stable at freezer and room temperatures, while at higher temperatures (40 °C) they converted back to the parent analogues (Figure 4.4). Greatest stability is observed under weakly basic conditions while the weakly acidic conditions increased instability. The isomers were significantly more stable in aqueous CH_3CN than in MeOH, with the rate of conversion being twice as fast in MeOH (Figure 4.4). Isomerization of AZA2 was observed during NMR analysis in CD_3OD, but appeared to cease upon addition of 0.1% v/v d_5-pyridine.

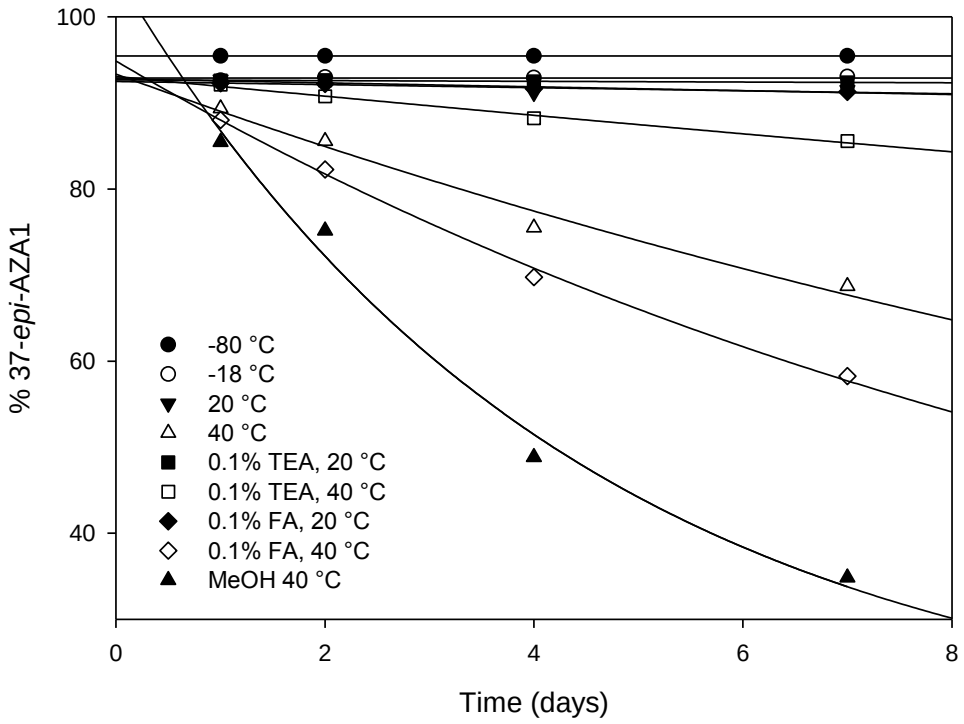

Figure 4.4. Stability of 37-*epi*-AZA1 in aqueous CH_3CN, in aqueous CH_3CN containing 0.1% TEA, in aqueous CH_3CN containing 0.1% FA at -18 °C, ~ +20 °C and at +40 °C and in MeOH at 40 °C, with −80 °C being used as a control. Lines show data fitted to exponential decay to 16% epimer at equilibrium.

The stability data indicated that equilibrium is reached at ~ 16% isomer (Table 4.1). Conversion of the isomer to the parent analogue was faster for AZA3 relative to AZA1 and AZA2 (Table 4.1). In the presence of MeOH, methyl ketals[11] were also formed at the higher temperatures, particularly so for AZA3 and under the acidic conditions.

Table 4.1. Half-life (days)[a] for 37-*epi*-AZA1, AZA2 and AZA3 in aqueous CH_3CN at 40 °C.

Treatment	37-*epi*-AZA1	37-*epi*-AZA2	37-*epi*-AZA3
0.1% Formic acid	7.5	7.0	2.1
Neutral	11	11	4.5
0.1 % TEA	38	32	28

[a]From LC-MS data fitted to exponential decay curve with 16% epimer at equilibrium, using SigmaPlot 12.0.

The stability studies provided valuable information with respect to handling of the samples. The fact that the isomers were relatively stable at room temperature over a number of days meant that there was no conversion whilst performing the semi preparative HPLC step. Procedures that are normally performed at higher temperatures (evaporation of solvents and NMR spectroscopy) could be performed at lower temperatures to deal with this instability. Thus, evaporation steps were carried out at ≤ 20 °C and qNMR was performed at 20 °C.

Previous studies on AZAs showed that the stability of AZA1 and AZA6 was significantly improved when stored in $CH_3CN–H_2O$ (8:2) when compared to MeOH.[11] Experiments performed in this study confirm these findings. Not only was there faster conversion of isomers to the parent analogues in MeOH, but the formation of methyl ketals[11] was observed in MeOH and was promoted under the acidic conditions.

4.4.3. Purification

AZAs were isolated from mussels to obtain sufficient quantities for the preparation of reference materials and for toxicological studies.[11] During the semi-preparative HPLC purification (7th step) of the isolation procedure, peaks eluting close to the main AZA1–3 peaks were collected separately, and through LC-MS analysis shown to be mixtures of the parent analogue and its isomer. A purified sample of the AZA1 isomer was obtained by performing an additional HPLC separation step. Analysis of the isomer fraction collected immediately after the semi preparative step showed that < 1% of the parent analogue was present. However, after the sample was passed through the SPE cartridge to remove the buffer, significant conversion to the parent compound had occurred (~ 8%). The use of other SPE stationary phases (C18 and C8) also had the same effect. Evaporation of the organic solvent from the sample at ≤ 20 °C and subsequent extraction of the sample with EtOAc proved to be effective at maintaining the stability of the isomer with no conversion being

observed. Sufficient AZA1 isomer (~ 150 µg) with adequate purity (containing ≤ 1.5% AZA1) was isolated for analysis by NMR (both structural and quantitative). Small amounts of the AZA2 and AZA3 isomers were also isolated but not in sufficient quantities for NMR analyses. Nevertheless, sufficient levels of isomers were present in stored NMR samples of AZAs 1–3 to permit partial NMR signal assignments.

Previous AZA purification procedures employed an acidic mobile phase in the final purification step.[29,32] Therefore, any isomer present would have been collected as part of the parent analogue peak. The procedure used in the present study employed a neutral mobile phase, which enabled the isomers to be resolved from the parent analogue peaks and permitted their purification. In addition to the AZA1–3 isomers, a fraction containing the equivalent isomer of AZA6 was also collected which suggests these isomers exist for all the known AZA analogues.

4.4.4. Structure determination

LC-MS. The only clear differences in the LC-MS spectra between the parent analogue and its isomer were changes to the ratio of the H_2O loss, retro Diels–Alder (RDA) (*m*/*z* 672/654) and the relative intensity of the *m*/*z* 462 fragment ions (Figure 4.5).

Periodate cleavage. Periodate cleaves the diol moiety of AZAs at C-20/21 to produce a lactone.[6,7,11] In MeOH, AZA1 and its isomer were both cleaved by periodate at essentially the same rate, giving products with the same mass but having different retention times. This shows that the isomer cannot simply be the 21-*epi*-AZA1, because C-21 is oxidized to a carbonyl group during cleavage and could not therefore give rise to isomeric oxidation products. Rather, the isomer of AZA1 must result from structural modification in C-22–C-40.

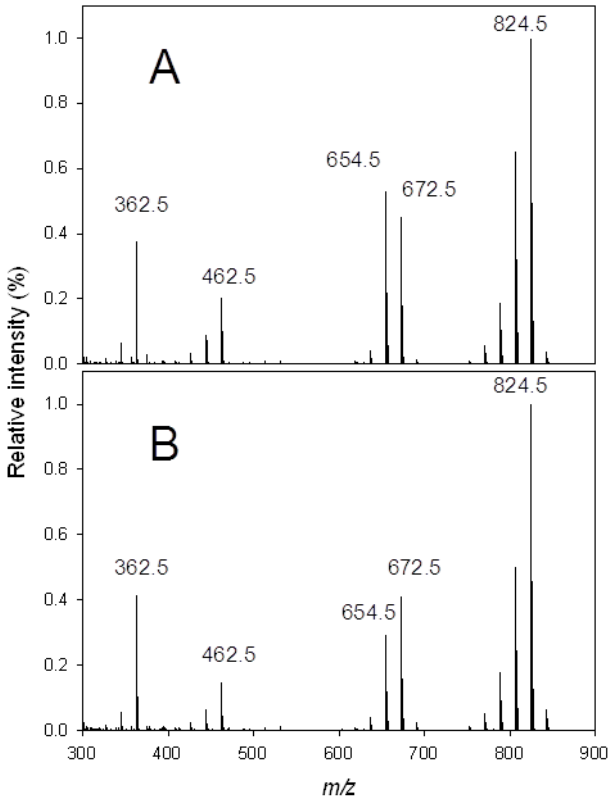

Figure 4.5. Mass spectra of A) AZA1 and B) 37-*epi*-AZA1 (method A), showing different ratios for the *m/z* 654/672 ions.

NMR spectroscopy. The structure determination of AZAs and their isomers is complicated by the known, but hitherto poorly defined, pH dependency of the majority of the proton and carbon atoms of the penultimate six membered nitrogen-containing ring and the five membered furanosyl ring attached to it.[11] For example, Ofuji *et al*.[9] have reported shifts of 2.83 ppm and 2.91 ppm for the H-40 methylene resonances of AZA2 in CD_3OD, whereas we observed chemical shifts ranging between 2.54 and 2.80 ppm for these protons in the NMR spectra of two samples of AZA2 (Table 4.2) and in the spectra of other AZAs examined in our laboratory. The NMR spectral data originally reported for AZA1–5[3,9,10] were obtained from CD_3OD containing 0.5% v/v CD_3CO_2D in order to sharpen some of the resonances in the region around the amino group (M. Satake, University of Tokyo, Japan, personal communication). However, given that we found the isomerization of AZAs in MeOH to be catalyzed by dilute acetic acid, structural NMR analysis of the AZA-isomers in this CD_3OD

containing CD_3CO_2D was not considered appropriate. We therefore used CD_3OD without added acid, although as a consequence of this some of the chemical shifts varied significantly from sample-to-sample, presumably because the degree of protonation of the amino group varied slightly from isolation-to-isolation.

A further complication in the structural analysis of AZAs is that the chemical shift of H-20 is also sensitive to the extent to which the terminal ring nitrogen atom is protonated. We have observed shifts for this proton in the range 3.55 to 3.86 ppm in specimens of AZA1 and AZA2, and some other AZAs examined in our laboratory whereas Ofuji *et al*.[9,10] have reported shifts in the vicinity of 3.94 ppm for the mildly acidified solutions of AZAs that they examined. Notwithstanding the varying H-20 chemical shifts, an identical series of ROESY correlations, indicative of a common C-20 stereochemistry, was observed between H-20 and the nearby H-18a, H-19, H-22 and 22-CH_3 protons.

The sensitivity of H-20 chemical shifts to the varying extent of *N*-protonation can be interpreted as indicating the preferred solution conformation of AZAs as one in which the proton (or protons) attached to the terminal ring *N*-atom are positioned towards the central C-20 atom. Detailed analyses of 1D-SELROESY and 2D-ROESY data verified this proposal. In particular, irrespective of the chemical shift of the H-20 signal and of protons attached to carbon atoms in the C-31−C-40 portion of AZAs (which vary from specimen to specimen), moderate to strong inter-ring ROESY correlations were observed from H-40_{eq} to H-19, and to the pro-*Z* 26=CH_2 proton, together with ROESY correlations arising from suitably oriented terminal-ring protons. These correlations are consistent with a preferred solution of AZAs amino group and H-40 protons orientated towards H-19. The known pH sensitivity of some of the protons in close proximity to the terminal ring *N*-atom, and remote from it (H-20), can now be rationalized, since variations in the degree of protonation of the nitrogen atom will also influence the chemical shift of the H-20 proton. The resulting steric hindrance of the

amino group in this conformation may also explain its observed lack of reactivity towards alkylation and acylation.[42]

Because LC-MS studies had shown that AZAs underwent slow isomerization in MeOH, preliminary NMR investigations of the isomers were able to be performed on samples in deutero-MeOH containing both the parent analogue and its isomer (Table 4.3). This has the advantage that chemical shifts for both the parent AZA and its isomer can be directly compared, despite the sensitivity of some of the chemical shifts towards pH. However, signals from the parent compound were often greater than 20-fold more intense than those of the isomer, and many of these signals overlapped signals from the isomer, making structural analysis challenging and only partial assignment of isomer resonances was possible via analysis of 1D and 2D NMR spectra. The stability data obtained during this work eventually allowed isolation of the isomer of AZA1 in sufficient amounts (~ 150 μg) and purity (> 95%) for structure elucidation by NMR spectroscopy.

The chemical shifts established for the ring-A–D carbons and protons for the AZA1 and AZA2 isomers were essentially identical to those which we determined for AZA1 or AZA2, respectively, in CD_3OD, CD_3OH or d_6-DMSO, and in accordance with those reported by Ofuji *et al*.[9] However, the assignments for resonances from the 7- and 9- positions were reversed[11] due to the revision of the position of the ring-A double bond from the 8(9)-position to the 7(8)-position as established by synthesis.[43–45] In addition, the original assignments for the 11- and 12-positions[9] were reversed based on HMBC correlations observed for the methylene protons of AZA2 that resonate at 2.33 and 2.16 ppm. HSQC data showed that those protons were attached to the methylene carbons resonating at 33.2 and 37.4 ppm, respectively. In the HMBC spectrum of AZA2, the proton signal at 2.33 ppm exhibited an HMBC correlation to the C-14 methine carbon signal, which resonated at 31.0 ppm, while the proton signal at 2.16 ppm exhibited an HMBC correlation to the C-9 methylene carbon at

40.4 ppm (mistakenly assigned as the C-7 resonance by Ofuji *et al*.[9] due to the incorrect position of the ring-A double bond). These correlations are consistent with methylene proton signals at 2.33 ppm and 2.16 ppm showing ^{3}J correlations to C-14 (31.0 ppm) and C-9 (40.3 ppm), respectively, rather than ^{4}J correlations (rarely seen in HMBC spectra). Thus, these HMBC correlations indicated that the proton signal at 2.33 ppm is from H-12, and that the signal at 2.16 ppm is from H-11, and consequently that their carbon signals at 33.2 and 37.4 ppm arise from C-12 and C-11, respectively. The equivalent HMBC correlations were also observed for AZA1 and its isomer, indicating that this re-assignment applies to other AZAs. Other than for the reversal of the Ofuji *et al*.'s assignments for the 11- and 12-methylene groups, proton and carbon chemical shifts, ^{1}H coupling constants observed in ^{1}H NMR or SELTOCSY experiments, together with TOCSY and ROESY correlations observed for the isomers of AZA1 and AZA2 (where resolved from those of AZA2), were consistent with ring-A–D portions the structures of the isomers being the same as that reported for AZA1 and AZA2, respectively.

Knowledge of both the pH dependency of some of the chemical shifts and the preferred solution confirmation of AZAs, as revealed by inter ring ROESY correlations, facilitated the structure determination of the AZA1 isomer. In particular, the AZA1 isomer exhibited a series of ROESY correlations (e.g. H-20 (3.50 ppm) to H-19 (4.45 ppm), H-16 (3.91 ppm), H-22 (2.30 ppm), H-18a (2.07 ppm), and 22-Me (0.82 ppm); and H-40$_{eq}$ (2.62 ppm) to the pro-*Z* 26=CH_2 proton (5.28 ppm), H-19 (4.43 ppm) and 39-Me (0.88 ppm)) similar to those observed for AZA1 and AZA2. However there were ROESY correlations shown by other terminal ring protons, most notably between the 37-Me (1.06 ppm) and H-39 (1.84 ppm), H-38a (1.44 ppm) and H-35a/b (2.11 ppm)) which were consistent with axial orientation of the 37-Me group in the AZA1 isomer rather than the equatorial orientation in AZA1 and all other known AZAs (Figure 4.1).

Table 4.2. NMR assignments for AZA2 and 37-*epi*-AZA2 from a partially epimerized sample in CD_3OD.

	AZA2		37-*epi*-AZA2	
Atom	^{13}C	^{1}H	^{13}C	^{1}H
1	181.3		n.r.	
2	38.3	2.24, 2.24	n.r.	n.r.
3	30.3	2.32, 2.32	n.r.	n.r.
4	133.5	5.73	n.r.	n.r.
5	131.2	5.41	n.r.	n.r.
6	72.7	4.72	n.r.	n.r.
7	123.1	5.34	n.r.	n.r.
8	131.0		n.r.	
9	40.4	1.98, 2.43	n.r.	n.r.
10	107.5		n.r.	
11	37.4	1.97, 2.16	n.r.	n.r.
12	33.2	1.66, 2.33	n.r.	n.r.
13	111.3		n.r.	
14	31.0	2.01	n.r.	2.01
15	32.6	1.74, 1.84	n.r.	1.75, 1.82
16	78.2	3.89	78.1	3.91
17	73.3	4.20	73.0	4.17
18	37.4	2.01, 2.01	n.r.	2.00, 2.06
19	79.2	4.43	n.r.	4.43
20	77.0	3.82	77.0	3.50
21	100.1		99.8	
22	36.6	2.13	35.9	2.30
23	38.5	1.43, 1.43	n.r.	1.41, 1.41
24	42.2	1.36	n.r.	1.35
25	79.7	3.97	79.8	3.88
26	148.2		148.1	
27	49.5	2.23, 2.41	49.2	2.14, 2.37
28	98.5		n.r.	
29	44.3	1.35, 2.03	44.1	1.32, 2.00
30	26.5	2.24	n.r.	2.26
31	35.5	1.51, 1.82	n.r.	1.50, 1.78
32	72.8	4.33	72.7	4.24
33	81.0	3.97	79.0	3.81
34	75.0	4.95	75.4	4.82
35	42.1	2.34[a], 2.56		n.r., 2.13
36	96.5		96.6	
37	36.2	1.93	37.3	n.r.
38	38.3	1.26, 1.65	38.9	1.45, 1.73
39	30.1	1.82	n.r.	1.84
40	46.5	2.75, 2.80	47.9	2.62, 2.67
8-Me	23.0	1.69	n.r.	n.r.
14-Me	16.7	0.94	n.r.	0.94
22-Me	16.4	0.91	16.5	0.90
24-Me	18.1	0.83	18.1	0.82
26=CH2	116.6	5.16, 5.33	115.7	5.13, 5.28
30-Me	23.6	0.95	23.9	0.94
37-Me	15.6	0.95	15.9	1.06
39-Me	18.8	0.93	19.3	0.88

[a]Exchanges deuterium. n.r., not resolved from AZA2 signals.

Table 4.3. NMR assignments for AZA1 and 37-*epi*-AZA1.

	AZA1 in CD_3OD		AZA1 in CD_3OH		AZA1 in CD_3OD + 0.5% CD_3CO_2D[a]		AZA1 in d_6-DMSO		37-*epi*-AZA1 in CD_3OD	
Atom	^{13}C	^{1}H	^{13}C	^{1}H	^{13}C	^{1}H	^{13}C	^{1}H	^{13}C	^{1}H
1	181.2		180.6		180.3		n.r.	n.r.	181.3	
2	38.1	2.25, 2.25	37.6	2.25, 2.25	37.4	2.31, 2.31	n.r.	n.r.	38.4	2.25, 2.25
3	30.2	2.33, 2.33	29.9	2.33, 2.33	30.3	2.33, 2.33	27.3	2.21	30.3	2.33, 2.33
4	133.7	5.75	133.4	5.74	133.8	5.74	128.1	5.63	133.7	5.75
5	130.7	5.44	130.6	5.43	131.8	5.46	129.5	5.39	130.7	5.44
6	72.5	4.79	72.3	4.78	73.2	4.81	70.2	4.71	72.5	4.80
7	129.4	5.63	129.3	5.63	130.1	5.65	122.4	5.61	129.4	5.64
8	123.2	5.73	123.1	5.72	124.1	5.76	122.4	5.71	123.3	5.73
9	35.7	2.12, 2.46	35.6	2.12, 2.47	36.5	2.15, 2.49	34.4	2.03, 2.43	35.8	2.12, 2.48
10	107.2		107.1		107.9		105.0		107.3	
11	37.5	1.97, 2.14	37.4	1.95, 2.13	38.3	1.97, 2.16	36.2	1.89, 2.02	37.6	1.95, 2.14
12	33.2	1.66, 2.33	33.1	1.65, 2.32	33.9	1.68, 2.33	31.9	1.54, 2.19	33.3	1.65, 2.33
13	111.3		111.2		112.1		109.2		111.4	
14	31.0	2.02	80.8	2.01	31.7	2.02	29.3	1.89	31.1	2.03
15	32.6	1.76, 1.85	32.5	1.75, 1.84	33.4	1.77, 1.85	31.3	1.60, 1.71	32.7	1.76, 1.83
16	78.2	3.88	78.1	3.88	79.1	3.89	75.6	3.84	78.1	3.91
17	73.3	4.23	73.2	4.22	74.2	4.25	71.1	4.05	73.0	4.20
18	37.3	1.99, 2.01	37.1	1.95, 1.99	37.8	2.00, 2.01	37.7	1.86, 1.98	39.0	2.00, 2.07
19	79.2	4.43	79.1	4.42	79.9	4.44	77.7	4.26	79.2	4.43
20	76.9	3.86	76.8	3.88	77.6	3.94	74.8	3.25	77.0	3.50
21	100.2		100.2		101.1		97.8		99.9	
22	36.6	2.12	36.6	2.09	37.6	2.09	34.3	2.17	35.9	2.30
23	38.3	1.43, 1.43	38.1	1.42, 1.42	38.9	1.44, 1.44	37.3	1.31, 1.31	38.6	1.42, 1.42
24	42.3	1.35	42.1	1.34	43.1	1.35	40.4	1.22	42.2	1.36
25	79.6	3.98	79.5	3.97	80.4	4.00	77.5	3.81	79.9	3.87
26	148.3		148.2		149.1		146.7		148.1	
27	49.5	2.24, 2.42	49.6	2.23, 2.41	50.4	2.26, 2.43	47.5	2.04, 2.25	49.0	2.14, 2.37
28	98.6		98.5		99.5		95.9		98.3	
29	44.3	1.36, 2.03	44.1	1.35, 2.03	44.9	1.37, 2.05	43.4	1.20, 1.9	44.6	1.32, 2.00
30	26.4	2.23	26.3	2.22	27.2	2.23	24.8	2.17	26.7	2.26
31	35.4	1.52, 1.83	35.2	1.51, 1.82	36.1	1.54, 1.84	34.3	1.33, 1.71	35.5	1.50, 1.78
32	72.8	4.35	72.7	4.34	73.6	4.38	70.8	4.13	72.2	4.24
33	81.2	4.01	81.2	4.02	82.3	4.08	76.9	3.61	78.8	3.81
34	74.9	4.98	74.8	4.98	75.6	5.02	73.7	4.68	75.4	4.83

35	41.9	2.41, 2.59	47.7	2.43, 2.59	42.5	2.50[c]	41.7	1.76, 2.21	45.1	2.11[b]
36	96.6		96.5		97.4		93.9		96.8	
37	36.0	1.95	35.8		36.4	1.99	36.4	1.58	39.1	1.78
38	38.0	1.28, 1.67	37.8	1.28, 1.66	38.4	1.31, 1.70	38.8	1.00, 1.45	36.8	1.45, 1.73
39	29.8	1.85	29.6	1.85	30.2	1.89	30.4	1.53	25.0	1.84
40	46.4	2.79, 2.84	46.3	2.79, 2.86	46.9	2.84, 2.91	46.3	2.33, 2.38	47.8	2.62, 2.67
14-Me	16.6	0.95	16.5	0.94	17.4	0.95	15.9	0.86	16.7	0.95
22-Me	16.4	0.91	16.3	0.90	17.2	0.91	16.3	0.789	16.6	0.90
24-Me	18.1	0.84	17.9	0.83	18.8	0.84	17.5	0.738	18.1	0.82
26=CH2	116.8	5.16, 5.34	116.8	5.16, 5.33	117.2	5.18, 5.36	113.4	4.96, 5.11	115.5	5.13, 5.28
30-Me	23.5	0.95	23.4	0.95	24.3	0.96	23.3	0.84	23.9	0.94
37-Me	15.5	0.96	15.4	0.96	16.2	0.98	15.7	0.75	15.8	1.06
39-Me	18.6	0.94	18.4	0.94	19.3	0.95	19.0	0.76	19.3	0.88

[a]NMR data from Satake *et al*.[3]; solvent composition, personal communication from M. Satake.
[b]One of the H-35 signals not identified due to exchange.
n.r., not resolved from AZA1 signals.

This deduction was supported by the occurrence of the C-39 methine carbon signal of the AZA1 isomer at 25.0 ppm compared to 29.8 ppm in AZA1 (Table 4.3). The upfield shift observed for C39 is reminiscent of that exhibited by C-37 of DTX2 (21.0 ppm), which possesses an axial 35-methyl group relative to that of C-37 in DTX1 (27.5 ppm) which possesses an equatorial 35-methyl group.[46]

Confirmation of 37-epimerization (Figure 4.6), and the identification of the axial and equatorial H-38 and H-40 methylene protons of the epimer of AZA1 (and AZA2), was obtained via analyses of the coupling constants exhibited by the H-38 and H-40 methylene protons, revealed in contour plots and slices extracted from 2D-HSQC and TOSCY spectra, the resolution of which for protons in 6-membered rings was sufficient to resolve large $^{2}J_{gem}$ and $^{3}J_{ax–ax}$ couplings (~ 10–12 Hz) but not the smaller $^{3}J_{ax–eq}$ or $^{3}J_{eq–eq}$ couplings (typically 3–4 Hz or less). In a 1D-SELTOCSY spectrum of epimerized AZA1 obtained at the resonance frequency of the 37-Me of 37-*epi*-AZA1 (1.06 ppm) (Figure 4.1), H-38_{ax} appeared as a well-defined triplet of doublets due to $^{2}J_{H\text{-}38ax–H\text{-}38eq}$ and $^{3}J_{H\text{-}38ax–H\text{-}39ax}$ couplings of 10–12 Hz. In contrast, H-38_{ax} appeared as a quartet-like signal in the 2D-HSQC, TOCSY and 1D-SELTOCSY spectra of AZA1 and AZA2 due to $^{2}J_{H\text{-}38ax–H\text{-}38eq}$, $^{3}J_{H\text{-}38ax–H\text{-}39ax}$ and $^{3}J_{H\text{-}38ax–H\text{-}37ax}$ couplings of ~ 10–12 Hz. The H-38_{eq} signal of each the compounds appeared as a doublet since only the large $^{2}J_{H\text{-}38ax–H\text{-}38eq}$ coupling of ~ 10–12 Hz and not smaller $^{3}J_{ax–eq}$ or $^{3}J_{eq–eq}$ couplings were resolved in HSQC or TOCSY slices (Figure 4.1). Similar observations were made for epimerized samples of AZA2 (Table 4.2) as well as for all other AZAs studied (unpublished observations).

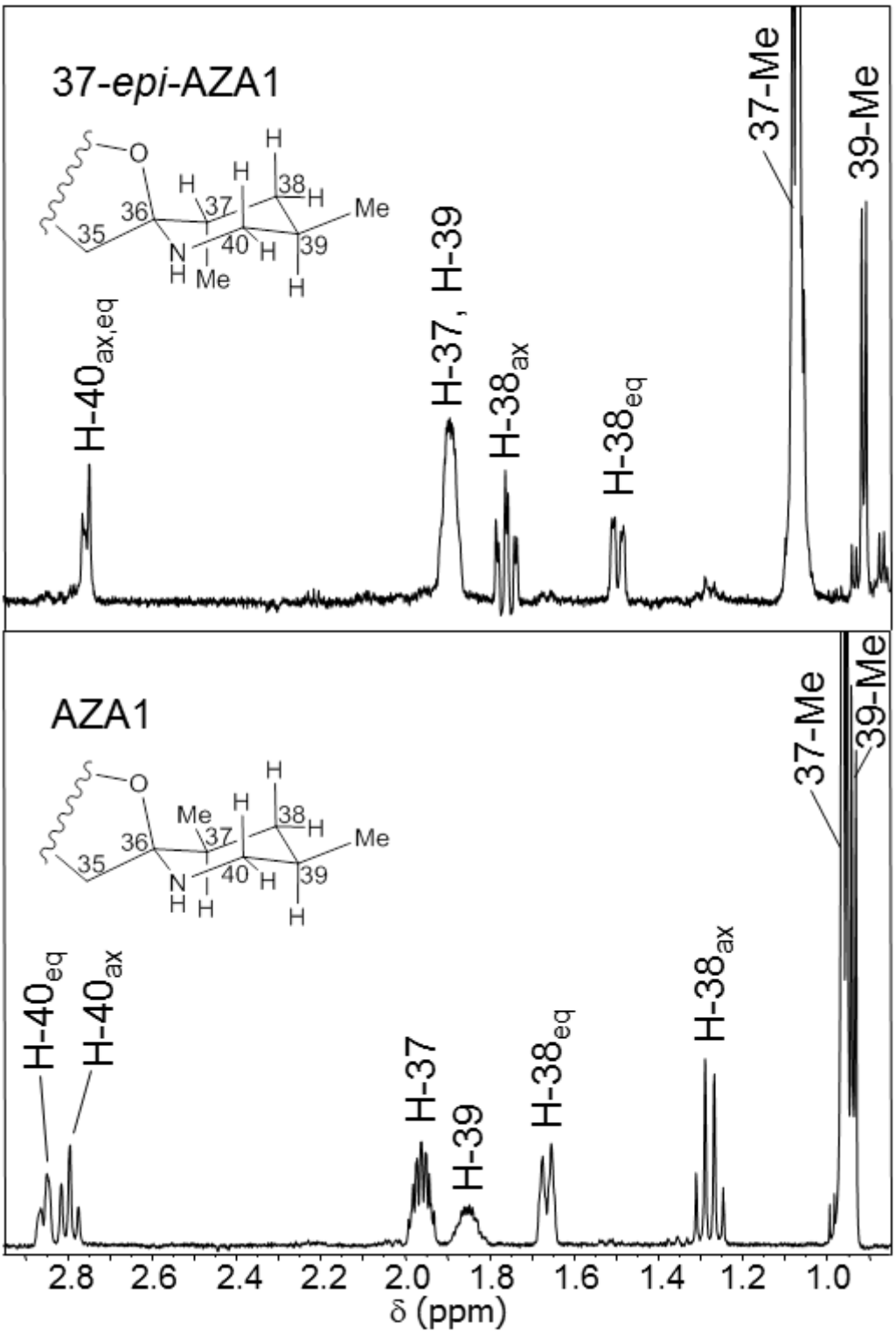

Figure 4.6. Top, 1D SELTOCSY NMR spectrum of 37-*epi*-AZA1 determined at the resonance frequency of its axial 37-methyl group (1.06 ppm); Bottom, 1D-SELTOCSY NMR spectrum of AZA1 at the frequency of its equatorial 37-methyl group (0.96 ppm). Both spectra were acquired from the same specimen of partially epimerized AZA1 in CD_3OH.

The axially and equatorially oriented H-40 protons of AZAs were identified similarly, since in the 2D-HSQC and TOCSY spectra H-40$_{ax}$ appeared as a triplet-like signal due to well resolved $^{2}J_{\text{H-40ax–H-40eq}}$ and $^{3}J_{\text{H-40ax–H-39ax}}$ couplings while the H-40$_{eq}$ appeared as a doublet signal due to resolution in HSQC spectra of only the larger $^{2}J_{\text{H-40ax–H-40eq}}$ coupling and not the smaller $^{3}J_{\text{H-40eq–H-39ax}}$ coupling (Figure 4.1). These observations were supported by NoE correlations observed in the ROESY and SELROESY spectra of AZA1, 37-*epi*-AZA1 (Figure 4.7), and in a mixed sample of AZA2 and its epimer (data not shown).

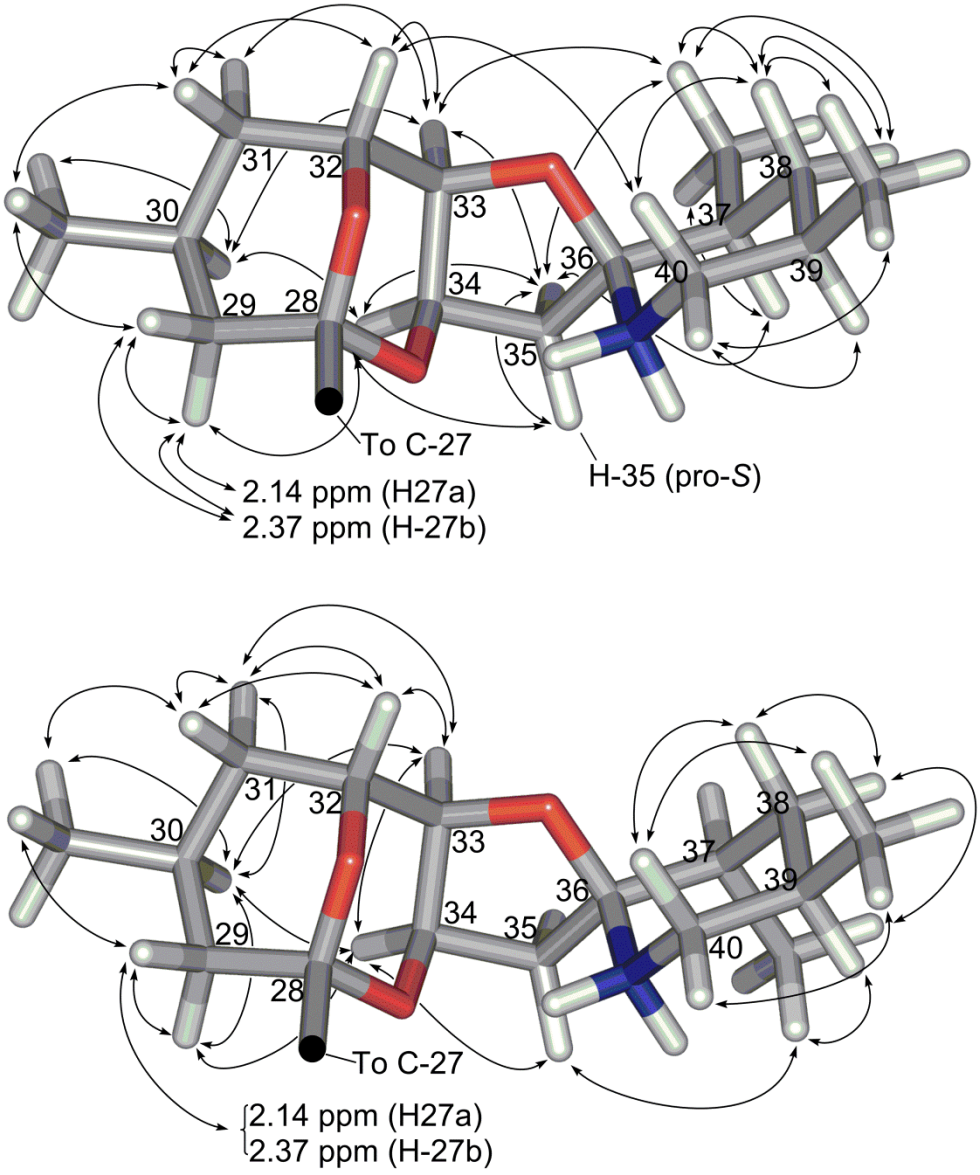

Figure 4.7. NoE correlations observed for the F–I rings of AZA1 (top) and 37-*epi*-AZA1 (bottom) in ROESY and SELROESY spectra from CD_3OH and/or CD_3OD.

It was apparent from the inter-ring ROESY correlations that the H-40_{eq} protons in AZA1 and 37-*epi*-AZA1 exhibited to H-19 to the pro-*Z* 26=CH_2, that the C-36 configuration of 37-*epi*-AZA1 was as in AZA1 since the foregoing pair of ROESY correlations would not have been observed for 37-*epi*-AZA1 had it also been epimerized at C-36.

The analyses of stereochemically definitive H-38 and H-40 coupling constants was enhanced by the acquisition of NMR spectral data for AZA1 and 37-*epi*-AZA1 in CD_3OH, including ^1H, 2D-COSY, TOCSY, ROESY and HSQC data, with pre-saturation of the protonated CD_3OH/HOD signals. This appreciably sharpened the H-40 methylene protons of the respective compounds by preventing the NH proton (or the protonated variant of it) from exchanging deuterium with the solvent and the consequent line broadening effect due to $^3J_{D–C–C–H}$ coupling(s) between the N–D (or N–D_2^+) and H-40 methylene protons. Essentially identical ^1H (to within 0.01 ppm) and ^{13}C shifts (to within 0.1 ppm) were obtained in CD_3OD and CD_3OH. On the other hand, a significant difference (and in some cases beneficial resolution of overlapped methylene proton signals) was observed when d_6-DMSO was substituted for CD_3OD or CD_3OH (Table 4.3).

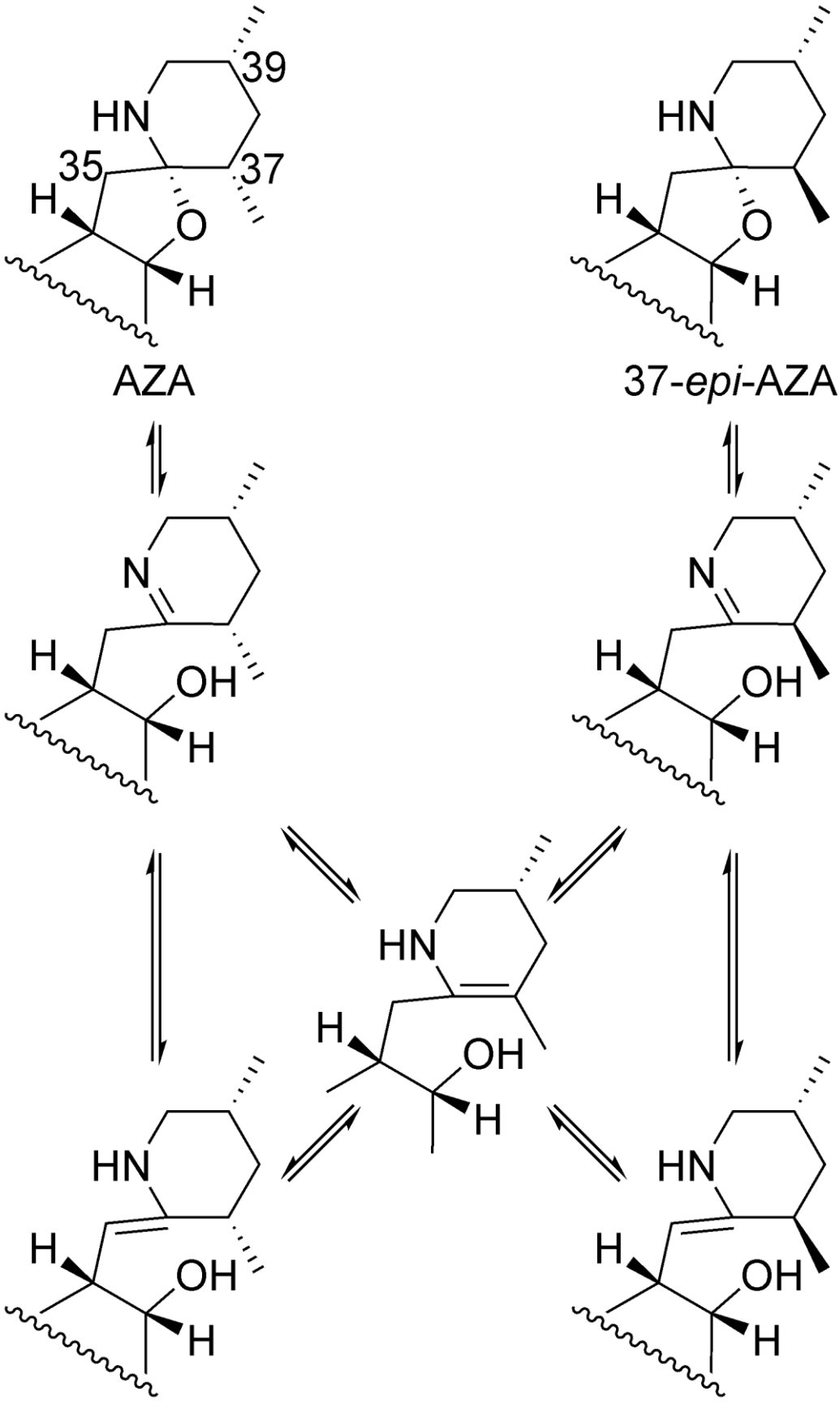

Scheme 1. Possible mechanism for 37-epimerisation of AZAs.

Epimerization at C-37 presumably proceeds as shown in Scheme 1. Consistent with this was the observation that deuterium was rapidly incorporated at C-37 of the epimer formed during isomerisation of AZA1 and AZA2 in CD_3OD, together with a slower incorporation of deuterium at the pro-*S* position at C-35 (2.34 ppm in AZA2). Examination of AZA2 after NMR in CD_3OD using high resolution MS/MS of the *m*/*z* 857.5 ion confirmed the presence of deuterium (as well as ^{13}C) in the C-33–C-40 fragment.

To verify this finding, a sample containing 37-*epi*-AZA1 and AZA1 was stored in CH_3OD at 40 °C and analyzed periodically by LC-MS. The incorporation of deuterium was observed via the appearance of fragment peaks with extra mass. Intensity changes observed in HSQC spectra indicated rapid uptake of a first deuterium and a somewhat slower incorporation of a second at H-37 and H-35_S, respectively, with a very slow (possibly due to steric effects) incorporation of a third deuterium at H-35_R.

After 10 days of storage in CH_3OD, the deuterated sample was evaporated, taken up in PBS (with 20% MeOH), and stored at 40 °C to assess the rate of deuterium loss from the structure in this medium. Deuterium was washed out fairly rapidly, with ~ 60% of the original deuterium remaining after 4 days. In addition, it was observed that the AZA epimer converted back to AZA1 at a much faster rate in the PBS solution after 24 h (80% conversion) than in MeOH (14% conversion). These findings are significant as they could enable the production of stable isotope-labelled internal standards that could be used to compensate for matrix effects and increase the accuracy of LC-MS quantitation. Furthermore, it might be possible to produce tritium-labelled AZAs for biochemical investigations.

4.4.5. Relative molar response study

37-*epi*-AZA1 that had been isolated and purified for structural elucidation was quantitated by qNMR. The molar response of the epimer was assessed against purified AZA1[11] that had also been quantitated by qNMR. Accurate working standards were then prepared by diluting the qNMR stock solutions in high purity degassed MeOH. The concentrations of the working solutions were 1.3 µM for AZA1, and 1.2 µM for 37-*epi*-AZA1. The anthryldiazomethane (ADAM) derivatization method for LC-FLD of AZAs[42] was applied to the AZA1 and 37-*epi*-AZA1 standards to provide supporting information for the qNMR data. However, due to instability of 37-*epi*-AZA1, a significant proportion of it converted back to AZA1 under the derivatization conditions and the ADAM results for the epimer would therefore not be reliable quantitatively.

A number of mass spectrometric experiments were carried out (LC-MS method C) in order to determine the molar response of 37-*epi*-AZA1 relative to AZA1. The results are summarized in Table 4.4. Although the proportion of epimer present in samples is approximately 2–16%, and may be considered relatively low, it is still important to understand any potential differences in response in the MS detection of the epimers when compared to the parent AZA analogues. When establishing the relative molar responses of different compounds in LC-MS the mobile phase composition can influence the ionization efficiency, therefore it is important to test under isocratic conditions if possible. Differences can also arise due to the MS detection mode. While SIM detection depends only on the ionization efficiency of the compounds in the ESI source, and the transport of the ions through to the quadrupole, detection in SRM can also be affected by differences in the fragmentation of compounds. Therefore, to establish baseline response factors initial analyses were done using isocratic elution with detection in SIM mode. SRM is more commonly used in routine/regulatory LC-

MS/MS analysis of lipophilic toxins, therefore the standards were also analysed in SRM mode.

Table 4.4. Relative molar response factors (with standard deviation of the last significant figure in parenthesis) of 37-*epi*-AZA1 in relation to AZA1 (AZA1(area/concentration)/37-*epi*-AZA1(area/concentration))[a].

	Neutral		Acidic	
MS mode (ion/transition)	Gradient[b]	Isocratic[c]	Gradient[d]	Isocratic[e]
SIM (842.5)		0.94 (3)		0.93 (3)
SRM (842→824)	0.912 (4)	0.883 (3)	0.860 (4)	0.882 (4)
SRM (842→806)	1.016 (7)	0.995 (5)	0.977 (5)	0.971 (3)
SRM (842→672)	0.968 (3)	0.920 (3)	0.913 (5)	0.912 (5)
SRM (842→654)	0.588 (4)	0.580 (2)	0.554 (3)	0.554 (1)
SRM (842→462)	0.801 (4)	0.763 (3)	0.745 (4)	0.746 (2)
SRM (842→362)	1.106 (6)	1.105 (4)	1.091 (7)	1.097 (2)

[a]Determined by SIM and SRM LC-MS experiments using gradient and isocratic LC elution with neutral and acidic mobile phases. Propagated standard deviations (of the last significant figure) from LC-MS/MS analyses are shown in parentheses. [b]Method C(i). [c]Method C(ii). [d]Method C(iii). [e]Method C(iv).

In most cases the response factor of the 37-*epi*-AZA1 was not considerably different from that of AZA1. The isocratic elution SIM data obtained for AZA1 and 37-*epi*-AZA1 was consistent between acidic and neutral pH mobile phases and the results suggest that 37-*epi*-AZA1 has a slightly lower response than AZA1 when analysed under these conditions (0.94 relative to AZA1). In all SRM transitions *m/z* 842.5 was selected in Q1, and following fragmentation a variety of ions were selected in Q3. The data shows that the SRM transition selected for analysis of 37-*epi*-AZA1 could have a significant impact on quantitation when using an AZA1 standard (Table 4.4). Although the initial collision induced H_2O losses (*m/z* 824 and 806) are not ideal transitions for confirmatory purposes, due to the higher probability of interferences

from isobaric compounds, they both show response factors for 37-*epi*-AZA1 within 10% of those observed when using the same transitions for AZA1. The *m/z* 672 fragment that results from RDA cleavage of the A-ring also gave a similar response factor. However, the subsequent H_2O loss from this RDA fragment (*m/z* 654) gave a much lower response for 37-*epi*-AZA1 relative to AZA1 (~ 0.57). This difference correlates to one of the major differences observed in the product ion spectrum of both compounds (Figure 4.5). The intensity of the *m/z* 654 ion is much reduced in the product ion spectrum of 37-*epi*-AZA1, which is probably due to this H_2O loss occurring near C-21, Figure 4.5. Therefore, the 842→654 transition is not ideal for quantitation of AZA1 and 37-*epi*-AZA1 under conditions where they are not resolved. A lower response factor was also observed when using *m/z* 462 as the Q3 ion in SRM (0.76 relative to AZA1), which correlates with the reduced intensity of this ion in the product ion spectrum of 37-*epi*-AZA1 (Figure 4.5). The *m/z* 362 ion is frequently used as a confirmatory transition in SRM analysis of regulated AZAs and a slightly higher response factor was observed when using this as the Q3 ion in SRM analysis of 37-*epi*-AZA1. With an acidic mobile phase (pH 2.3) the use of gradient or isocratic elution had no impact on the relative response of 37-*epi*-AZA1. This is because AZA1 and 37-*epi*-AZA1 co-elute at this pH, and are being ionized in the ESI source at the same mobile phase strength. However, it can be seen that on average the relative molar response of 37-*epi*-AZA1 relative to AZA1 was slightly higher when using neutral mobile phase compared to acidic. This is because 37-*epi*-AZA1 is resolved from AZA1 at the neutral pH, eluting later. The increased organic content of the mobile phase when 37-*epi*-AZA1 elutes conceivably causes the slightly higher response observed.

4.4.6. Toxicology

Of all the functional assays developed for AZAs, the Jurkat T lymphocyte cell assay was found to be the most sensitive,[29] and was therefore chosen to assess the toxicity of 37-*epi*-AZA1. In this assay, cells initially respond to AZAs by a reduction in membrane integrity, organelle protrusion concurrent with flattening of cells, the retraction of their pseudopodia or lamellipodia, followed by protracted cell lysis.[22]

In a manner not unlike many other AZA analogues 37-*epi*-AZA1 was cytotoxic to Jurkat T lymphocyte cells in a time- and concentration-dependent manner (Figure 4.8). The 37-*epi*-AZA1 was shown to be 5.1-fold more potent than the parent AZA1 (Table 4.5) making it comparable in potency (*in vitro*) to AZA2 and AZA3 (8.3- and 4.5-fold more potent than AZA1, respectively).[26] However, this work has shown the epimer to be highly unstable, rapidly converting back to its parent analogue at temperatures > 20 °C, and since all of the cytotoxicity experiments were run for a protracted period of time (up to 72 h) at 37 °C, it was anticipated that there could be significant conversion of the epimer back to AZA1. As such, samples were taken frequently throughout the course of the study and subsequently analysed by LC-MS to assess for these (or other) structural changes.

Table 4.5. Calculated EC_{50} values (nM) with 95% confidence intervals (CI) and relative potencies (Rel. Pot.) for AZA analogues based on T lymphocyte cytotoxicity.

AZA analogue	24 h		48 h		72 h		Mean EC_{50}	Rel. Pot.
	EC_{50}	95% CI	EC_{50}	95% CI	EC_{50}	95% CI		
AZA1	1.0	0.2–4.9	1.1	0.5–2.5	1.3	0.6–3.0	1.1	1.0
37-*epi*-AZA1	0.2	0.05–0.4	0.3	0.1–0.5	0.2	0.1–0.5	0.2	5.1

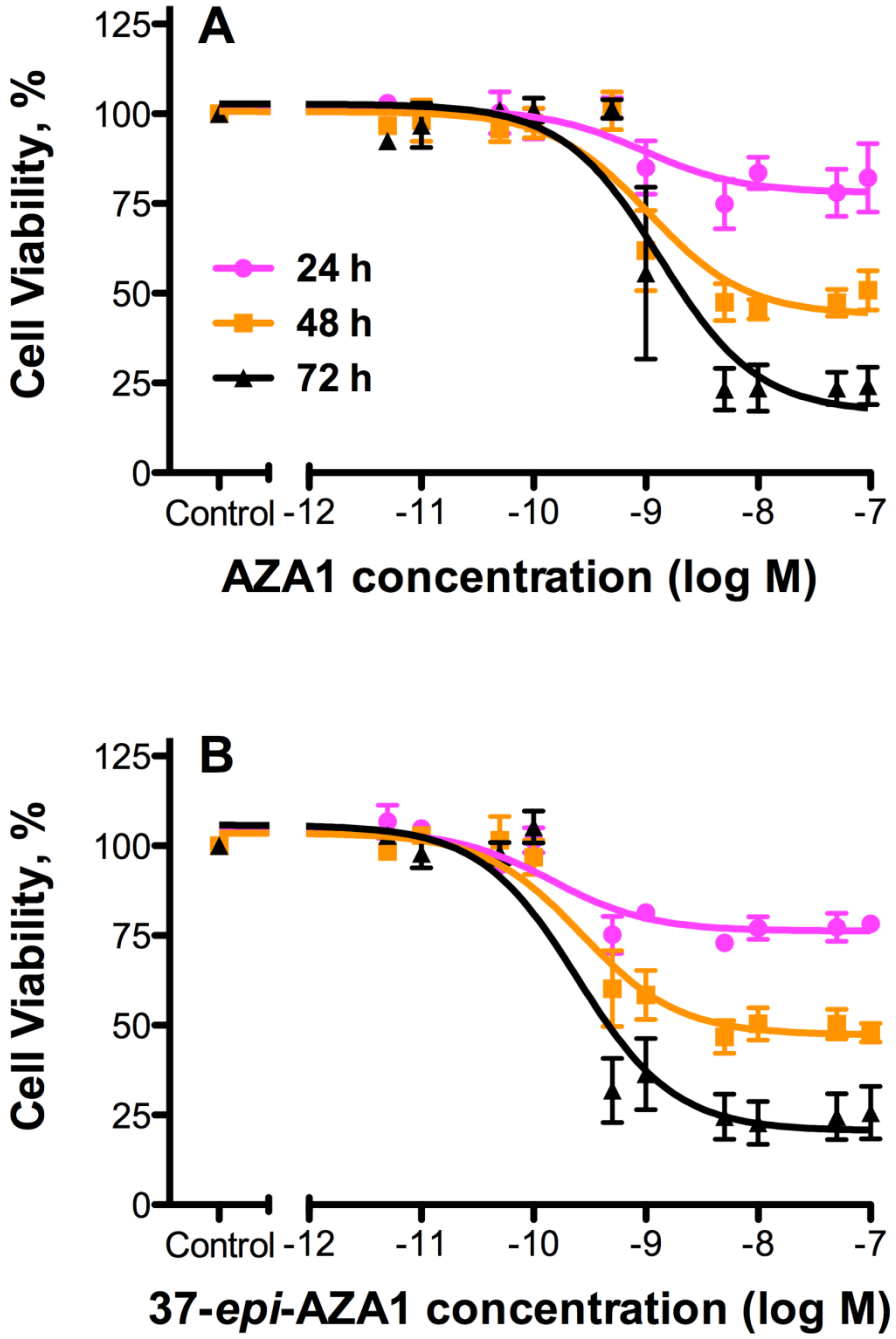

Figure 4.8. Effect of AZA1 and 37-*epi*-AZA1 on T lymphocyte cell viability. Jurkat T cells were exposed to various concentrations of A) AZA1 and B) 37-*epi*-AZA1 for 24, 48, or 72 h and viability was assessed using the MTS assay. All data (mean ± SE; n = 3) were normalized to the control (10% MeOH vehicle). Non-linear, three-parameter dose–response (variable slope) analysis was performed and EC_{50} values were calculated (Table 4.5).

The analysis showed that the samples taken immediately after injection (i.e., t = 0 h) consisted of 94% 37-*epi*-AZA1 and 6% AZA1. After 24 h, considerable conversion of the epimer to AZA1 had taken place (73% AZA1), with nearly full equilibration between 48 and 72 h (~ 12% isomer). Similar conversion rates were observed in the stability study in which the deuterated AZA epimer mix was stored in a MeOH:PBS solution at 40 °C. In parallel, analysis of the AZA1 sample at t = 0 showed that 3% of the isomer was present while after 24 h the amount increased to 11% with apparent equilibration being achieved after 48 h at 12% (Table 4.5). Assuming the total AZAs remain constant over the course of the experiment, we have shown that there was little to no metabolism or irreversible binding (e.g., to protein or plastic) of the AZAs (Table 4.6).

Table 4.6. Proportions of 37-*epi*-AZA1 and AZA1 following exposure to the Jurkat T lymphocyte cell assay (37 °C) and in the absence of cells in aqueous CH_3CN at 40 °C (n=3).

	Jurkat T lymphocyte cells (37-*epi*-AZA1)		Jurkat T lymphocyte cells (AZA1)		Aqueous CH_3CN	
Time	% 37-*epi*-AZA1	% AZA1	% 37-*epi*-AZA1	% AZA1	% 37-*epi*-AZA1	% AZA1
0	94 ± 1	6 ± 1	4 ± 1	96 ± 1	96 ± 1	4 ± 1
24	27 ± 5	73 ± 1	11 ± 1	89 ± 1	89 ± 1	11 ± 1
48	14 ± 2	86 ± 1	12 ± 1	88 ± 1	86 ± 1	14 ± 1
72	12 ± 1	88 ± 1	12 ± 1	88 ± 1	76 ± 1	24 ± 1

The conversion of 37-*epi*-AZA1 to the parent compound at 24 h (~ 75% AZA1) was surprising given the significantly higher potency determined for the epimer. However, previous experiments using this assay[13] and other *in vitro* methods by various investigators[25,47,48] indicate that the toxic effects of AZAs are immediately elicited and

irreversible, which could explain the increased potency of the 37-*epi*-AZA1 despite its instability under the conditions tested. Although these laboratory findings suggest that the epimeric forms of AZA may present more of a toxicological hazard than the parent molecules and may be important from a monitoring perspective, we do not yet know the stability and/or contribution of these analogues *in situ*, nor whether a similar structure–activity relationship applies *in vivo*.

4.5. Conclusions

37-Epimers of AZA1–3 and AZA6 were detected in tissue CRMs using a neutral mobile phase with LC-MS detection. The proportion of the epimers ranged from 2–16%, with proportions increasing following the application of heat. Stability studies showed that the epimers convert at higher temperatures back to the parent analogue and that equilibrium in solution is reached at ~ 16%. Sufficient amounts of 37-*epi*-AZA1 were isolated to enable full structural elucidation by NMR showing it to differ from AZA1 in the orientation of the methyl group at the C-37 position. Although only 37-*epi*-AZA1 was fully characterized it is highly likely that the epimers of AZA2, AZA3 and AZA6 have the same stereochemistry. Work currently being undertaken suggests that these epimers exist for all AZAs. Relative molar response factor studies by LC-MS revealed no major difference in response factors between the two compounds when analysed by SIM or SRM when the typical transitions are used (842→824, 842→672 and 842→362), but a significant difference was observed for the 842→654 transition and this is therefore not recommended for quantitative analysis of AZAs. 37-*epi*-AZA1 was 5.1 times more cytotoxic to Jurkat T lymphocyte cells than AZA1. Consequently, full equilibration (to 16% 37-*epi*-AZA1) of a sample containing AZA1 could be expected to increase the sample's toxicity in this assay by ~ 1.7-fold, assuming that the epimer has

the same toxicological mechanism of action as AZA1. Furthermore, the observation that the rate of epimerization is increased in weakly acidic solutions may be of relevance to toxicity via oral exposure. This and previous[6] studies thus highlight the importance of assessing toxin profiles in cooked shellfish (typically shellfish are cooked before consumption) due to toxin conversions, as well as the need for further toxicological studies (*in vitro* and *in vivo*) to be performed on the conversion products such as these AZA-epimers.

4.6. References

(1) Tillmann, U., Elbrächter, M., Krock, B., John, U., and Cembella, A. D. (2009) *Azadinium spinosum* gen. et sp. nov. (Dinophyceae) identified as a primary producer of azaspiracid toxins. *Eur. J. Phycol. 44*, 63–79.

(2) Krock, B., Tillmann, U., Voß, D., Koch, B. P., Salas, R., Witt, M., Potvin, É., and Jeong, H. J. (2012) New azaspiracids in *Amphidomataceae* (Dinophyceae). *Toxicon 60*, 830–839.

(3) Satake, M., Ofuji, K., Naoki, H., James, K. J., Furey, A., McMahon, T., Silke, J., and Yasumoto, T. (1998) Azaspiracid, a new marine toxin having unique spiro ring assemblies, isolated from Irish mussels, *Mytilus edulis*. *J. Am. Chem. Soc. 120*, 9967–9968.

(4) Krock, B., Tillmann, U., John, U., and Cembella, A. D. (2009) Characterization of azaspiracids in plankton size-fractions and isolation of an azaspiracid-producing dinoflagellate from the North Sea. *Harmful Algae 8*, 254–263.

(5) Salas, R., Tillmann, U., John, U., Kilcoyne, J., Burson, A., Cantwell, C., Hess, P., Jauffrais, T., and Silke, J. (2011) The role of *Azadinium spinosum* (Dinophyceae) in the production of azaspiracid shellfish poisoning in mussels. *Harmful Algae 10*, 774–783.

(6) McCarron, P., Kilcoyne, J., Miles, C. O., and Hess, P. (2009) Formation of azaspiracids-3, -4, -6, and -9 via decarboxylation of carboxyazaspiracid metabolites from shellfish. *J. Agric. Food Chem. 57*, 160–169.

(7) Rehmann, N., Hess, P., and Quilliam, M. A. (2008) Discovery of new analogs of the marine biotoxin azaspiracid in blue mussels (*Mytilus edulis*) by ultra-

performance liquid chromatography/tandem mass spectrometry. *Rapid Commun. Mass Spectrom. 22*, 549–558.

(8) Anon. (2011) Commission Regulation (EU) No 15/2011 of 10th January 2011 amending Regulation (EC) No 2074/2005 as regards recognised testing methods for detecting marine biotoxins in live bivalve molluscs. L6/3-6. http://eurlex.europa.eu/LexUriServ/LexUriServ.do?uri=OJ:L:2011:006:0003:0006:EN:PDF

(9) Ofuji, K., Satake, M., McMahon, T., Silke, J., James, K. J., Naoki, H., Oshima, Y., and Yasumoto, T. (1999) Two analogues of azaspiracid isolated from mussels, *Mytilus edulis*, involved in human intoxications in Ireland. *Nat. Toxins 7*, 99–102.

(10) Ofuji, K., Satake, M., McMahon, T., James, K. J., Naoki, H., Oshima, Y., and Yasumoto, T. (2001) Structures of azaspiracid analogs, azaspiracid-4 and azaspiracid-5, causative toxins of azaspiracid poisoning in Europe. *Biosci. Biotechnol. Biochem. 65*, 740–742.

(11) Kilcoyne, J., Keogh, A., Clancy, G., LeBlanc, P., Burton, I., Quilliam, M. A., Hess, P., and Miles, C. O. (2012) Improved isolation procedure for azaspiracids from shellfish, structural elucidation of azaspiracid-6, and stability studies. *J. Agric. Food Chem. 60*, 2447–2455.

(12) Twiner, M. J., Hess, P., and Doucette, G. (2014) Azaspiracids: toxicology, pharmacology, and risk assessment, in *Seafood and Freshwater Toxins, 3rd Edition* (Botana, L. M., Ed.) in press, CRC Press, Boca Raton, FL.

(13) Twiner, M. J., Rehmann, N., Hess, P., and Doucette, G. J. (2008) Azaspiracid shellfish poisoning: a review on the chemistry, ecology, and toxicology with an emphasis on human health impacts. *Mar. Drugs 6*, 39–72.

(14) McMahon, T., and Silke, J. (1996) Winter toxicity of unknown aetiology in mussels. *Harmful Algae News 14*.

(15) Ito, E., Satake, M., Ofuji, K., Kurita, N., McMahon, T., James, K., and Yasumoto, T. (2000) Multiple organ damage caused by a new toxin azaspiracid, isolated from mussels produced in Ireland. *Toxicon 38*, 917–930.

(16) Satake, M., Ofuji, K., James, K. J., Furey, A., and Yasumoto, T. (1998) New toxic event caused by Irish mussels, in *Harmful Algae* (Reguera, B., Blanco, J., Fernandez, M. L., Wyatt, T., Eds.) pp 468–469, Xunta de Galicia and Intergovernmental Oceanographic Commission of UNESCO, Santiago de Compostela, Spain.

(17) McMahon, T., and Silke, J. (1998) Re-occurence of winter toxicity. *Harmful algae News 17*, 12.

(18) Aasen, J. A. B., Espenes, A., Hess, P., and Aune, T. (2010) Sub-lethal dosing of azaspiracid-1 in female NMRI mice. *Toxicon 56*, 1419–1425.

(19) Aasen, J. A. B., Espenes, A., Miles, C. O., Samdal, I. A., Hess, P., and Aune, T. (2011) Combined oral toxicity of azaspiracid-1 and yessotoxin in female NMRI mice. *Toxicon 57*, 909–917.

(20) Aune, T., Espenes, A., Aasen, J. A. B., Quilliam, M. A., Hess, P., and Larsen, S. (2012) Study of possible combined toxic effects of azaspiracid-1 and okadaic acid in mice via the oral route. *Toxicon 60*, 895–906.

(21) Twiner, M. J., Hanagriff, J. C., Butler, S., Madhkoor, A. K., and Doucette, G. J. (2012) Induction of apoptosis pathways in several cell lines following exposure to the marine algal toxin azaspiracid-1. *Chem. Res. Toxicol. 25*, 1493–1501.

(22) Twiner, M. J., Hess, P., Bottein Dechraoui, M. Y., McMahon, T., Samons, M. S., Satake, M., Yasumoto, T., Ramsdell, J. S., and Doucette, G. J. (2005) Cytotoxic

and cytoskeletal effects of azaspiracid-1 on mammalian cell lines. *Toxicon 45*, 891–900.

(23) Twiner, M. J., Ryan, J. C., Morey, J. S., Smith, K. J., Hammad, S. M., Van Dolah, F. M., Hess, P., McMahon, T., Satake, M., Yasumoto, T., and Doucette, G. J. (2008) Transcriptional profiling and inhibition of cholesterol biosynthesis in human T lymphocyte cells by the marine toxin azaspiracid. *Genomics 91*, 289–300.

(24) Vale, C., Nicolaou, K. C., Frederick, M. O., Gomez-Limia, B., Alfonso, A., Vieytes, M. R., and Botana, L. M. (2007) Effects of azaspiracid-1, a potent cytotoxic agent, on primary neuronal cultures. A structure-activity relationship study. *J. Med. Chem. 50*, 356–363.

(25) Kulagina, N. V., Twiner, M. J., Hess, P., McMahon, T., Satake, M., Yasumoto, T., Ramsdell, J. S., Doucette, G. J., Ma, W., and O'Shaughnessy, T. J. (2006) Azaspiracid-1 inhibits bioelectrical activity of spinal cord neuronal networks. *Toxicon 47*, 766–773.

(26) Twiner, M. J., El-Ladki, R., Kilcoyne, J., and Doucette, G. J. (2012) Comparative effects of the marine algal toxins azaspiracid- 1, -2, and -3 on Jurkat T lymphocyte cells. *Chem. Res. Toxicol. 25*, 747–754.

(27) Twiner, M. J., Doucette, G. J., Rasky, A., Huang, P. X., Roth, B. L., and Sanguinetti, M. C. (2012) The marine algal toxin azaspiracid is an open state blocker of hERG potassium channels. *Chem. Res. Toxicol. 25*, 1975–1984.

(28) Quilliam, M. A.; Reeves, K.; MacKinnon, S.; Craft, C.; Whyte, H.; Walter, J.; Stobo, L.; Gallacher, S. (2006) Preparation of reference materials for azaspiracids, in *Proceedings of the 5th International Conference of Molluscan Shellfish Safety* (Deegan, B., Butler, C., Cusack, C., Henshilwood, K., Hess, P.,

Keaveney, S., McMahon, T., O'Cinneide, M., and Silke, J., Eds.) pp 111–115, Marine Institute, Galway, Ireland.

(29) Hess, P., McCarron, P., Rehmann, N., McMahon, T., Ryan, G., Ryan, M., Twiner, M. J., Doucette, G. J., Satake, M., Ito, E., and Yasumoto, T. (2007) Isolation and purification of azaspiracids from naturally contaminated materials, and evaluation of their toxicological effects—final project report ASTOX (ST/02/02). *Marine Institute—Marine Environment & Health Series—No. 28, ISSN: 1649-0053. http://www.marine.ie/NR/rdonlyres/2B06863D-3366-47CD-9ABB-B3302629FE46/0/ASTOX.pdf.*

(30) McCarron, P., Emteborg, H., and Hess, P. (2007) Freeze-drying for the stabilisation of shellfish toxins in mussel tissue (*Mytilus edulis*) RMs. *Anal. Bioanal. Chem. 387*, 2475–86.

(31) McCarron, P., Kotterman, M., De Boer, J., Rehmann, N., and Hess, P. (2007) Feasibility of irradiation as a stabilisation technique in the preparation of tissue RMs for a range of shellfish toxins. *Anal. Bioanal. Chem. 387*, 2487–93.

(32) Perez, R., Rehmann, N., Crain, S., LeBlanc, P., Craft, C., MacKinnon, S., Reeves, K., Burton, I., Walter, J. A., Hess, P., Quilliam, M. A., and Melanson, J. (2010) The preparation of certified calibration solutions for azaspiracid-1, -2, and -3, potent marine biotoxins found in shellfish. *Anal. Bioanal. Chem. 398*, 2243–2252.

(33) McCarron, P., Giddings, S. D., Reeves, K., and Quilliam, M. A. (2011) CRM-AZA-Mus-200603 CRMP Technical report, in *CRMP Technical Report CRM-AZA-Mus-200603*, 2011.

(34) Quilliam, M. A., Hess, P., Dell'Aversano, C., Koe, W., Samson, R., Van Egmond, H., Gilbert, J., and Sabino, M. (2001) Mycotoxins and phycotoxins in

perspective at the turn of the century, in *Proceedings of the Xth international IUPAC symposium on mycotoxins and phycotoxins* (deKoe, W. J., Samson, R. A., van Egmond, H. P., Gilbert, J., and Sabino, M., Eds.) pp383–391, deKoe, W. J., The Netherlands.

(35) McNabb, P., Selwood, A. I., and Holland, P. T. (2005) Multiresidue method for determination of algal toxins in shellfish: single-laboratory validation and interlaboratory study. *AOAC Int. 88*, 761–772.

(36) Kilcoyne, J., and Fux, E. (2010) Strategies for the elimination of matrix effects in the liquid chromatography tandem mass spectrometry analysis of the lipophilic toxins okadaic acid and azaspiracid-1 in molluscan shellfish. *J. Chromatogr. A 1217*, 7123–7130.

(37) Gerssen, A., Mulder, P. J., McElhinney, M. A., and De Boer, J. (2009) Liquid chromatography–tandem mass spectrometry method for the detection of marine lipophilic toxins under alkaline conditions. *J. Chromatogr. A 1216*, 1421–1430.

(38) McCarron, P., Giddings, S. D., and Quilliam, M. A. (2011) A mussel tissue certified reference material for multiple phycotoxins. Part 2: liquid chromatography–mass spectrometry, sample extraction and quantitation procedures. *Anal. Bioanal. Chem. 400*, 835–846.

(39) Alfonso, C., Rehmann, N., Hess, P., Alfonso, A., Wandscheer, C., Abuin, M., Vale, C., Otero, P., Vieytes, M., and Botana, L. M. (2008) Evaluation of various pH and temperature conditions on the stability of azaspiracids and their importance in preparative isolation and toxicological studies. *Anal. Chem. 80*, 9672–9680.

(40) Lamberty, A., Schimmel, H., and Pauwels, J. (1998) The study of the stability of reference materials by isochronous measurements. *J. Anal. Chem. 360*, 359–361.

(41) Burton, I., Quilliam, M. A., and Walter, J. A. (2005) Quantitative ^{1}H NMR with external standards: use in preparation of calibration solutions for algal toxins and other natural products. *Anal. Chem. 77*, 3123–3131.

(42) McCarron, P., Giddings, S. D., Miles, C. O., and Quilliam, M. A. (2011) Derivatization of azaspiracid biotoxins for analysis by liquid chromatography with fluorescence detection. *J. Chromatogr. A 1218*, 8089–8096.

(43) Nicolaou, K. C., Li, Y. W., Uesaka, N., Koftis, T. V., Vyskocil, S., Ling, T. T., Govindasamy, M., Qian, W., Bernal, F., and Chen, D. Y. K. (2003) Total synthesis of the proposed azaspiracid-1 structure, part 1: construction of the enantiomerically pure C1-C20, C21-C27, and C28-C40 fragments. *Angew. Chem. Int. Edit. 42*, 3643–3648.

(44) Nicolaou, K. C., Chen, D. Y. K., Li, Y. W., Qian, W. Y., Ling, T. T., Vyskocil, S., Koftis, T. V., Govindasamy, M., and Uesaka, N. (2003) Total synthesis of the proposed azaspiracid-1 structure, part 2: coupling of the C1-C20, C21-C27, and C28-C40 fragments and completion of the synthesis. *Angew. Chem. Int. Edit. 42*, 3649–3653.

(45) Nicolaou, K. C., Frederick, M. O., Petrovic, G., Cole, K. P., and Loizidou, E. Z. (2006) Total synthesis and confirmation of the revised structures of azaspiracid-2 and azaspiracid-3. *Angew. Chem. Int. Edit. 45*, 2609–2615.

(46) Larsen, K., Petersen, D., Wilkins, A. L., Samdal, I. A., Sandvik, M., Rundberget, T., Goldstone, D., Arcus, V., Hovgaard, P., Rise, F., Rehmann, N., Hess, P., and Miles, C. O. (2007) Clarification of the C-35 stereochemistries of dinophysistoxin-1 and dinophysistoxin-2, and its consequences for binding to protein phosphatase. *Chem. Res. Toxicol. 20*, 868–875.

(47) Vilariño, N., Nicolaou, K., Frederick, M. O., Cagide, E., Ares, I. R., and Louzao, M. C. (2006) Cell growth inhibition and actin cytoskeleton disorganization induced by azaspiracid-1 structure-activity studies. *Chem. Res. Toxicol. 19,* 1459–1466.

(48) Vilariño, N., Nicolaou, K. C., Frederick, M. O., Vieytes, M. R., and Botana, L. M. (2007) Irreversible cytoskeletal disarrangement is independent of caspase activation during *in vitro* azaspiracid toxicity in human neuroblastoma cells. *Biochem. Pharmacol. 74*, 327–335.

CHAPTER 5 – ISOLATION, STRUCTURE ELUCIDATION, RELATIVE LC-MS RESPONSE, AND *IN VITRO* TOXICITY OF AZASPIRACIDS FROM THE DINOFLAGELLATE *AZADINIUM SPINOSUM*.

Kilcoyne, J., Nulty, C., Jauffrais, T., McCarron, P., Herve, F., Foley, B., Rise, F., Crain, S., Wilkins, A. L., Twiner, M., Hess, P., Miles, C. O. 2014. Isolation, structure elucidation, relative LC-MS response, and *in vitro* toxicity of azaspiracids from the dinoflagellate *Azadinium spinosum*. *Journal of Natural Products*, 2014, 77, 2465–2474.

5.1. Abstract

We identified three new azaspiracids (AZAs) with molecular weights of 715, 815 and 829 Da (AZA33 (**3**), AZA34 (**4**) and AZA35, respectively) in mussels, seawater and *Azadinium spinosum* culture. Approximately 700 µg of **3** and 250 µg of **4** were isolated from a bulk culture of *A. spinosum* and their structures determined by MS and NMR spectroscopy. These compounds differ significantly at the carboxyl end of the molecule from known AZA analogues, and therefore provide valuable information on structure–activity relationships. Initial toxicological assessment was performed using an *in vitro* model system based on Jurkat T lymphocyte cytotoxicity, and the potencies of **3** and **4** were found to be 0.22- and 5.5-fold that of AZA1 (**1**), respectively. Thus, major changes in the carboxyl end of **1** resulted in significant changes in toxicity. In mussel extracts, **3** was detected at low levels, whereas **4** and AZA35 were detected only at extremely low levels or not at all. The structures of **3** and **4** are consistent with AZAs being biosynthetically assembled from the amino end.

5.2. Introduction

Numerous azaspiracid (AZA) analogues have been identified in shellfish,[1,2] however, only AZA1 (**1**), AZA2 (**2**) and AZA3 are currently regulated by the European Union.[3] Compounds **1** and **2** are produced by the dinoflagellate *Azadinium spinosum*,[4] while the majority of the other reported analogues are due to shellfish metabolism.[5–7]

A number of toxicological studies have shown AZAs to be teratogenic in fish,[8] damaging to the gastrointestinal tract in mice,[9,10] and potential lung tumour promoters.[11] A recent *in vitro* study on **1**, **2** and AZA3 confirmed the high potency of AZAs and suggested multiple molecular targets for these compounds which are differentially affected by the various AZA analogues.[12,13] However, further toxicological studies need to be performed on as many AZA analogues as possible to establish more accurate regulatory limits and to identify all analogues that are relevant for public health protection.

The isolation and structure elucidation of **1**, **2**, AZA3–6[14–17] and 37-*epi*-AZA1[18] from shellfish have been reported. Purification of these compounds is necessary: 1) to enable the preparation of certified reference materials (CRMs), which are essential for the successful implementation of monitoring programs; 2) for use in toxicology studies, so that regulators can implement appropriate closure limits, and; 3) for structure elucidation by NMR, enabling a better understanding of the chemistry involved. Isolation of AZAs from shellfish is a labour intensive procedure requiring up to eight steps involving extraction, partitioning and column chromatography.[17,19] Such compounds are ideally isolated from cultures of the producing organisms due to the initial extract being significantly cleaner than from shellfish, and therefore requiring fewer purification steps.[20–22] Isolation of AZAs from a marine sponge[23] and cultures of *A. spinosum*[24] have been reported.

More recently, the presence of unidentified AZAs in the dinoflagellates *Amphidoma languida* (with molecular weights of 815 and 829 Da) and *Azadinium poporum* (with molecular weights of 845 and 857 Da) were reported.[25] All of the AZAs identified previously give a characteristic LC-MS/MS fragment at *m/z* 362, whereas these compounds gave an *m/z* 348 fragment, suggesting the lack of a methyl or methylene group in rings E–I (Figure 5.1). AZAs were also detected in isolates of *A. poporum* from Chinese coastal waters.[26] Although one strain did not produce detectable AZAs, three other strains produced exclusively **2**.[26] Furthermore, AZAs (with molecular weights of 827, 857 and 829 Da) were present in a newly discovered strain *Azadinium dexteroporum*, all of which produced the characteristic *m/z* 362 LC-MS/MS fragments.[27]

Here we report the identification of three new AZAs – AZA33 (**3**), AZA34 (**4**) and AZA35 from a bulk culture of *A. spinosum*, two of which were isolated in sufficient quantities for structure elucidation by NMR spectroscopy. We additionally report on their stability, toxicity and relative response factors in LC-MS/MS analysis, and assess their relevance in terms of human health protection.

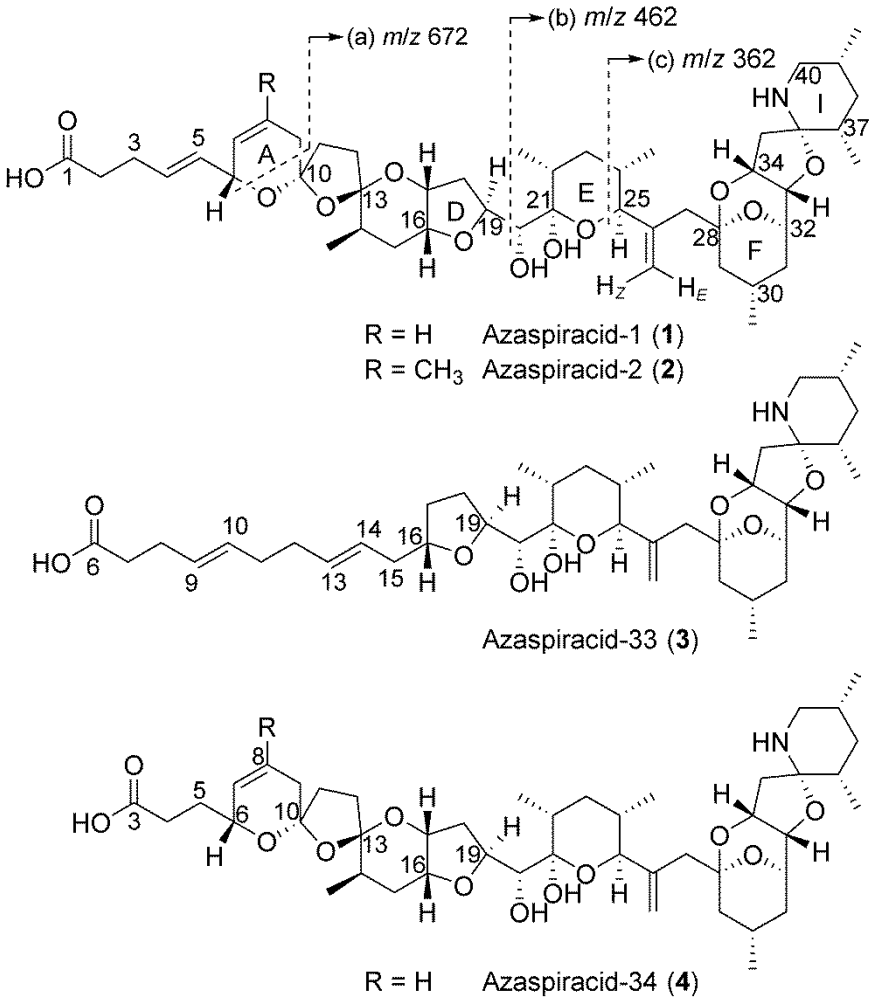

Figure 5.1. Structures of AZA1 (**1**), AZA2 (**2**), AZA33 (**3**) and AZA34 (**4**) including atom numbering. Note that atom numbering for **3** and **4** starts at C-6 and C-3, respectively, so that structurally related atoms in **3** (C-16–C-40) and **4** (C-6–C-40) retain the same atom numbering as their corresponding atoms in **1** in Table 5.2. Also shown are the major MS/MS fragmentation pathways for **1** and **2**. Compounds **3, 4** and AZA35 showed fragmentations (b) and (c), whereas **4** and AZA35 also exhibited the RDA fragmentation pathway (a) but **3** did not (Figure 5.2).

5.3. Experimental section

5.3.1. General experimental procedures

NMR experiments for structure elucidation were run using Bruker Avance I and Avance II 600 MHz spectrometers equipped with TCI cryoprobes and Z-gradient coils, at 30 °C and a Bruker DRX-500 spectrometer was used for qNMR.

Mass spectrometric studies were performed using a Waters 2695 LC coupled to a Micromass triple-stage quadrupole (TSQ) Ultima, a Waters 2795 LC coupled to a Micromass quadrupole time of flight (QToF) Ultima and an Agilent 1200 LC system connected to an API4000 QTRAP mass spectrometer equipped with a Turbospray ionization source.

5.3.2. Biological material

A. spinosum strains were collected from the West coast of Ireland (SM2[6]) and the North Sea (3D9[36]). *Mytilus edulis* samples contaminated with AZAs were obtained from shellfish harvesting sites along the West coast of Ireland. SPATT extracts generated in studies carried out by Fux *et al*.[28,37] were used for analysis. The SPATTs were deployed along the Northwest (Bruckless, Donegal) and Southwest coasts of Ireland (Bantry Bay) at different depths (0, 5 and 10 m) during an AZA toxic event.

5.3.3. Culture extraction

Samples (10 mL) of cultures of an Irish strain (SM2[6]) and a North Sea strain (3D9[36]) of *A. spinosum* were loaded onto solid-phase extraction (SPE) cartridges (Oasis HLB, 100 mg), washed with MeOH/H_2O (1:9, 5 mL), and eluted with MeOH (3 mL). The eluate was evaporated under a stream of nitrogen, taken up in 250 µL MeOH, and analysed by LC-MS/MS (method A).

5.3.4. Shellfish extraction

Samples were prepared as described in Kilcoyne *et al.*[18] The extracts were analysed by LC-MS/MS (method A).

5.3.5. Isolation and purification

Initial isolation steps were performed from bulk cultures of the 3D9 strain of *A. spinosum* as described by Jauffrais *et al.*[24] HP-20 resin extracts were combined, evaporated *in vacuo*, and partitioned between EtOAc (150 mL) and aqueous NaCl (1 M, 50 mL). The EtOAc fraction was evaporated to dryness *in vacuo*, the residue dissolved in EtOAc (20 mL), and 4 g of silica gel added. The sample was then carefully evaporated to dryness *in vacuo*, mixed to a fine powder, and loaded onto a silica gel (6 g) column (with dimensions of 3 × 5 cm). Vacuum-assisted elution was performed successively with hexane, EtOAc, EtOAc/MeOH (9:1, 7:3, and 1:1), and MeOH (30 mL of each, all containing 0.1% acetic acid except for hexane). The 7:3 EtOAc/MeOH fraction, which flow-injection analysis (FIA)-MS/MS (method B) showed to contain the AZAs, was evaporated *in vacuo*, and the sample loaded in CH_3CN/H_2O (6:4, plus 0.1% triethylamine) onto a column packed with Phenyl-Hexyl (19.9 × 2 cm). The sample was eluted with CH_3CN/H_2O (7:13, plus 0.1% triethylamine) at 4 mL/min, and 5 mL fractions were collected. Appropriate fractions were combined (**4** and **1**, fractions 15–18; and **2** and **3**, fractions 19–25) based on FIA-MS/MS analysis (method B).

Final purification of **3** and **4** was achieved by semi-preparative LC (Agilent 1200) with photodiode array (PDA) detection (210 nm) using a Cosmosil C18, 5µm, 250 × 4.6 mm, Nacalai tesque column at 30 °C eluted with CH_3CN/H_2O (13:7, plus 2 mM ammonium acetate) at 1 mL/min. Purified **3** and **4** were recovered by evaporation to ~ 20% CH_3CN, loading onto SPE cartridges (Oasis HLB, 200 mg), washing with $MeOH/H_2O$ (1:9,

10 mL) to remove the buffer, and eluting step-wise with MeOH/H_2O (4:6, 6:4, 8:2, 10:0, 20 mL each) with > 95% of **3** and **4** recovered in the 8:2 MeOH/H_2O. Removal of solvent by evaporation *in vacuo* afforded purified **3** and **4** as white solids (700 µg and 250 µg respectively).

AZA33 (**3**). white, amorphous solid; ^{1}H and ^{13}C data (CD_3OD, 600 MHz), see Table 5.1; HRESIMS *m/z* 716.4759 $[M+H]^+$ (calcd for $C_{41}H_{66}NO_9$, 716.4738).

AZA34 (**4**). white, amorphous solid; ^{1}H and ^{13}C data (CD_3OD, 600 MHz), see Table 5.1; HRESIMS *m/z* 816.4900 $[M+H]^+$ (calcd for $C_{45}H_{70}NO_{12}$, 816.4898).

5.3.6. LC-MS experiments

Method A. Recoveries were determined by quantitative analysis of fractions on a Waters 2695 LC coupled to a Micromass TSQ Ultima operated in SRM mode for the following transitions: *m/z* 842.5→824.5/362.3 (**1**); *m/z* 856.5→838.5/362.3 (**2**); *m/z* 716.5→698.5/362.3 (**3**); *m/z* 816.5→798.5/362.3 (**4**); and *m/z* 830.5→812.5/362.5 (AZA35). The cone voltage was 60 V, collision energy was 50 V, the cone and desolvation gas flows were set at 100 and 800 L/h, respectively, and the source temperature was 150 °C.

Binary gradient elution was used, with mobile phase A consisting of H_2O and mobile phase B of 95% CH_3CN in H_2O (both containing 2 mM ammonium formate and 50 mM formic acid). Chromatography was performed with a Hypersil BDS C8 column (50 × 2.1 mm, 3 µm, with a 10 × 2.1 mm guard column of the same stationary phase) (Thermo Scientific). The gradient was from 30–90% B over 8 min at 0.25 mL/min, held for 5 min, then held at 100% B at 0.4 mL/min for 5 min, returned to the initial conditions and held for 4 min to equilibrate the system. The injection volume was 5 µL and the column and sample temperatures were 25 °C and 6 °C, respectively.

Method B. Qualitative analysis of fractions for AZAs was performed by FIA-MS/MS using a Micromass QToF Ultima coupled to a Waters 2795 LC. Samples (2 µL) were injected directly (no column) into the mass spectrometer, monitoring for the precursor ions.

Method C. Purity was assessed on a Micromass QToF Ultima coupled to a Waters 2795 LC by running MS scans (*m*/*z* 100–1000) using the same chromatographic conditions as method B. Structure analysis of AZA analogues was performed via product ion scans, where the precursor ions were selected and then fragmented, for all the known AZA analogues.

Method D. Accurate mass measurements were performed on a Waters Acquity UPLC coupled to a Xevo G2-S QToF operated in MS^e mode, scanning from 100−1200 *m/z* and using leucine enkephalin as the reference compound. The cone voltage was 40 V, collision energy was 50 V, the cone and desolvation gas flows were set at 100 and 1000 L/h, respectively, and the source temperature was 120 °C.

Chromatography was performed with an Acquity UPLC BEH C18 (50 × 2.1 mm, 1.7 µm) column (Waters), using the same mobile phase described in method A. The gradient was from 30–90% B over 2 min at 0.4 mL/min, held for 2 min, and returned to the initial conditions and held for 1 min to equilibrate the system. The injection volume was 5 µL and the column and sample temperatures were 25 °C and 6 °C, respectively.

Method E. The samples were analysed using a neutral eluent to enable the separation of 37-epimers[18] of **3** and **4**. Separation was performed using a 2.5 µm, 2.1 × 50 mm, Luna C18(2) HST column (Phenomenex) and the mobile phase was H_2O (A) and CH_3CN/H_2O (95:5) (B), each containing 5 mM ammonium acetate (pH 6.8).

Method F. For the relative molar response study, accurate AZA working standards (1.3 µM for **1**, 1.6 µM for **3**, and 1.3 µM for **4**) were prepared by diluting purified AZAs

in high purity degassed MeOH and quantitating by qNMR. Samples were analysed using gradient and isocratic LC-MS/MS methods with acidic eluents (method A). Analysis was performed on an Agilent 1200 LC system with the same Luna column described in method E, eluted at 0.3 mL/min, connected to an API4000 QTRAP mass spectrometer (AB Sciex) equipped with a Turbospray ionization source. The MS was operated in positive ion mode and SRM transitions were as follows: *m/z* 842.5→824.5/672.5/462.3/362.3 (**1**); *m/z* 716.5→698.5/462.3/362.3 (**3**) and *m/z* 816.5→798.5/672.5/362.3 (**4**). For SIM experiments, *m/z* 842.5, 716.5 and 816.5 ($[M+H]^+$) were analysed. Typical parameters were 5500 V electrospray voltage, 400 °C source temperature, 70 V declustering potential and collision energies of 45 to 70 V (where applicable). The injection volume was 1–5 µL and the column and sample temperatures were 25 °C and 6 °C, respectively. *Method F(i)*. Gradient elution used a linear gradient from 25–100% B over 5 min and held at 100% B for 2 min before re-equilibration for the next run. *Method F(ii)*. Used isocratic elution with 60% B.

5.3.7. Stability studies

Purified samples of **1**, **3** and **4** were combined and aliquots (in MeOH) were stored in flame-sealed ampoules (under nitrogen) at −18 °C, +20 °C and +40 °C for up to 7 days. The study was performed isochronously,[38] and samples were analyzed simultaneously by LC-MS/MS (method A) with specimens stored at −80 °C used as controls.

5.3.8. Periodate cleavage

Aliquots (100 µL) of purified and diluted samples (~ 100 ng/mL) of **1**, **3** and **4** were oxidised by adding 50 µL of 0.2 M $NaIO_4$. The samples were analysed immediately by

LC-MS/MS (method C) but with an additional trace for the oxidised AZA product (*m/z* 448.3).

5.3.9. Methylation with diazomethane

To determine whether a carboxylic acid group was present, purified **3** and **4** (~ 60 ng) samples were reacted with diazomethane. The samples were added to the outside tube of an Aldrich diazomethane generator with System 45 connection, and 1 mL MeOH and 1.5 mL Et_2O were added. Diazomethane was generated in the inner tube of the apparatus and allowed to react *in situ* with the extract. After reacting for 45 min at 0 °C with occasional swirling, the extracts were transferred to a glass vial, evaporated to dryness under a stream of N_2, and residues dissolved in MeOH (1 mL) for LC-MS/MS (method C).

5.3.10. NMR experiments

Structural determinations were performed by analysis of ^{1}H, COSY, TOCSY, SELTOCSY, NOESY, ROESY, SELROESY, ^{13}C, DEPT135, HSQC and HMBC spectra. Samples of **1** (1 mg), **3** (0.1 mg) and **4** (0.1 mg) were dissolved in ~ 0.5 mL CD_3OD and chemical shifts were referenced to internal CHD_2OD (3.31 ppm), or CD_3OD (49.0 ppm). Single- or double-frequency pre-saturation of solvent resonances was performed using continuous wave and/or excitation sculpting as required.

Quantitation of pure **3** and **4** was performed on aliquots in CD_3OH. The sample was run against external standards of caffeine in H_2O (4.01 mM) as described previously.[39]

5.3.11. Toxins and other materials

All solvents (pesticide analysis grade) were from Labscan and Caledon. Distilled H_2O was further purified using a Barnstead nanopure diamond UV purification system (Thermo Scientific). Sodium chloride (99+%), triethylamine (99%), ammonium acetate (97+%), ammonium formate (reagent grade), formic acid (>98%), silica gel (10–40 µm, type H), sodium periodate and CD_3OD (100.0 atom-% D) were from Sigma–Aldrich. Sephadex LH-20 was from GE Healthcare, LiChroprep RP C8 (25–40 µm) was from Merck, Luna Phenyl-Hexyl (15 µm) was from Phenomenex, CD_3OH (99.5 atom-% D) for qNMR was from Cambridge Isotope Laboratories. AZA CRMs were obtained from the National Research Council of Canada.

5.3.12. Toxicology

Cell Culturing. Human Jurkat E6-1 T lymphocyte cells (American Type Culture Collection TIB-152) were grown as described by Twiner et al.[40] Briefly, cells were grown in RPMI-1640 medium (cat. #11875-093, Invitrogen) supplemented with 10% (v/v) fetal bovine serum (FBS; cat. #26140, Invitrogen) and maintained in a humidified incubator (Sanyo 18AIC-UV) with 5% CO_2 in air at 37 °C. Cells were subcultured with fresh medium at an inoculum ratio of 1:4 every 3 to 4 days by transferring 2.5 mL of cells to 7.5 mL of fresh supplemented medium in 75 cm^3 screw cap culture flasks.

Cytotoxicity Assay. The effect of the AZA analogues on the viability of Jurkat T lymphocyte cells was determined. Exponentially growing cells were seeded in 100 µL of the supplemented medium at a density of 30,000 cells per well in black, sterile, 96-well culture plates for 12–18 h to allow for recovery and settling. AZA analogues were added at various concentrations and assessed for cytotoxicity after 24, 48, or 72 h of exposure. Parallel controls of equivalent amounts of PBS/MeOH were used to

normalize the viability data for each treatment. Cellular viability/cytotoxicity was assessed using the MTS (3-(4,5-dimethylthiazol-2-yl)-5-(3-carboxymethoxyphenyl)-2-(4-sulfophenyl)-2H-tetrazolium) assay (Promega Biosciences, cat. no. G5421). Like other tetrazolium-based assays, MTS in the presence of an electron coupling reagent (phenazine methosulfate; PMS) measures cellular viability by determining the activity of mitochondrial dehydrogenases.[41] As a substrate for dehydrogenases, MTS becomes reduced into a soluble, purple dye that can be quantitated colorimetrically to determine the relative level of cellular viability/cytotoxicity per well. Following exposure of the cells to the AZA analogues for the specified time, each well received 10 µL of a PMS/MTS (1:20) solution (final concentrations of 7.9 and 158.5 µg/mL, respectively). Cells were incubated for 4 h, after which absorbance readings at 485 nm were obtained using a FluoStar microplate reader (BMG Lab Technologies). Data are presented as means ± SE of three separate experiments (n=3). In addition, each cytotoxicity experiment was performed using duplicate wells. Cytotoxicity data were blank-corrected and normalized to the control (% viability). EC_{50} and 95% confidence intervals were calculated using three-parameter, variable slope, non-linear regression analysis (GraphPad Prism, ver. 5.0c).

5.4. Results and discussion

5.4.1. Analysis

In 2009, preliminary analysis (data not shown) of SPATT (Solid Phase Adsorption Toxin Tracking) disks deployed at Bruckless, Ireland, in 2005[28] during a major AZA event (where levels in mussels reached ~ 9 µg/g AZA equivalents[29]), showed the presence of numerous candidate AZAs, including new analogues with *m/z* 716.4745, 816.4909, and 830.5069. Subsequent analysis of extracts from a culture of *A. spinosum* by LC-MS/MS showed the presence of three new AZAs showing accurate masses of *m/z* 716.4759 (**3**), 816.4900 (**4**) and 830.5046 (AZA35). Compound **3** was also subsequently detected in an *A. spinosum* (SHETF6) extract collected from the Shetland Islands by Tillmann et al.[30] The three compounds all had fragmentations characteristic of AZAs (Figure 5.2). The ratios of **2** and **3**, relative to **1** were both 0.3 in cells of *A. spinosum* cultures (SM2 and 3D9 strains). Compounds **4** and AZA35 were much less abundant with ratios of 0.15, and 0.02 relative to **1**, respectively, found in the culture medium of the 3D9 strain (Figure 5.3).

Analysis of shellfish samples contaminated with **1**, **2** and AZA3 (0.08–8.0 µg/g AZA equivalents), tested as part of the routine biotoxin monitoring programme at the Marine Institute, were also analysed for **3**, **4** and AZA35. Compound **3** was detected in all samples tested, **4** was only detected (<0.04 µg/g) in samples with > 4.0 µg/g AZA equivalents, while AZA35 was not detected in any of the samples. The levels of **3**, relative to **1** and **2**, in the SPATTs and shellfish were significantly lower than in the cultures (SM2 and 3D9 strains) (Figure 5.3), suggesting that **3** might be chemically transformed in seawater and shellfish.

After tangential flow filtration of a bulk culture of *A. spinosum* into retentate and permeate,[24] **4** and AZA35 were detected only in the permeate (Figures 5.3 and 5.4).

Similarly, higher levels of **4** were detected in the SPATT extracts relative to the *A. spinosum* culture extracts suggesting that these compounds may be extracellular, perhaps being produced within the cell and excreted. Alternatively, they may simply be released after cellular lysis or mechanical stress on the cellular membranes during pumping and filtration. In any case, shellfish have been shown to be capable of absorbing AZAs from both the algal cells and the dissolved phase.[31]

Epimers of **1**, **2**, AZA3 and AZA6 at C-37 have previously been reported using LC-MS with a neutral eluent.[18,32] LC-MS analysis of *A. spinosum* extracts and purified samples of **3** and **4** using a neutral eluent showed the presence of additional peaks (ranging from ~ 5−12% relative to the parent peak) which were not observed using an acidic eluent. The spectra of these peaks differed from those of the parent compounds only in their fragment ion ratios, as was observed for 37-*epi*-AZA1.[18] It is likely that these peaks correspond to the 37-epimers of **3** and **4.**

Compounds **3** (700 µg) and **4** (150 µg) were isolated from the culture extract of *A. spinosum* (3D9) used for the isolation of **1** and **2** that has been described previously.[24] The stabilities of **3** and **4** were compared with that of **1** over a period of 7 days at −18 °C, +20 °C and +40 °C in MeOH. Both compounds exhibited similar stability to **1**; each being stable at the freezer and room temperatures over 7 days with minor degradation (< 5%) after 7 days of storage at 40 °C.

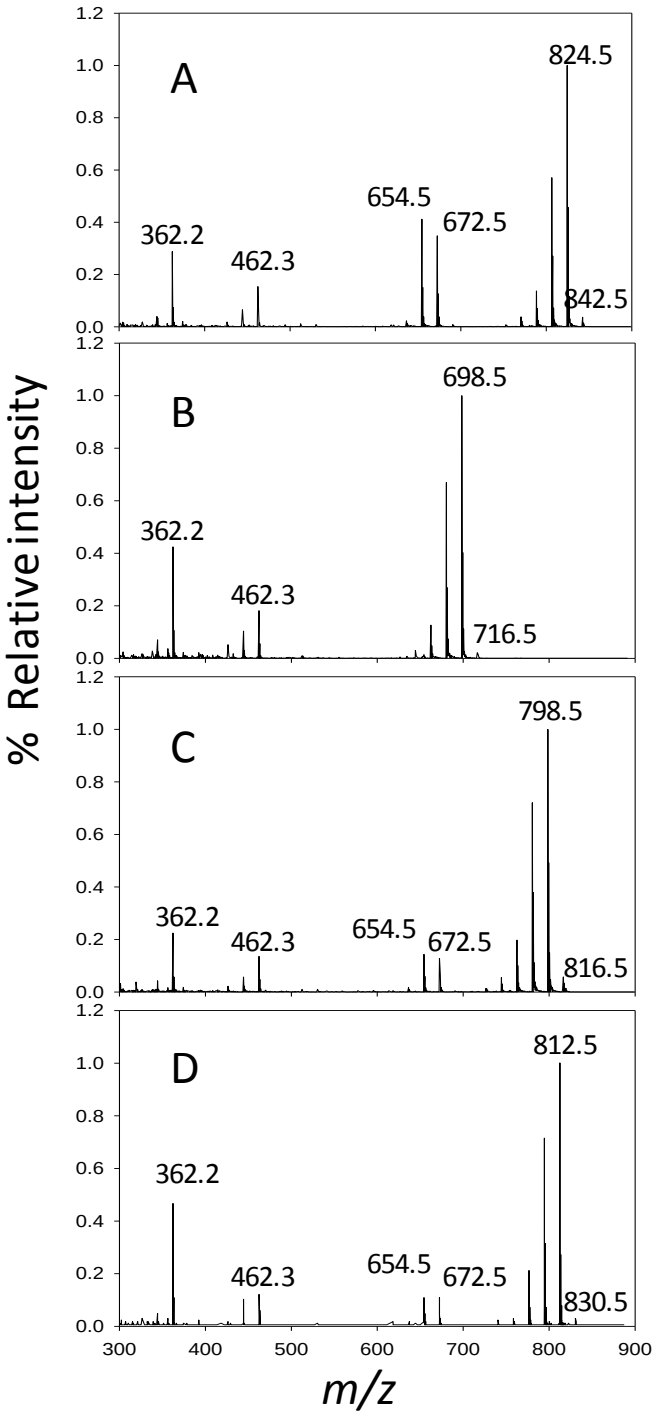

Figure 5.2. Mass spectra of A) AZA1 (**1**), B) AZA33 (**3**), C) AZA34 (**4**) and D) AZA35 at a collision energy of 50 V.

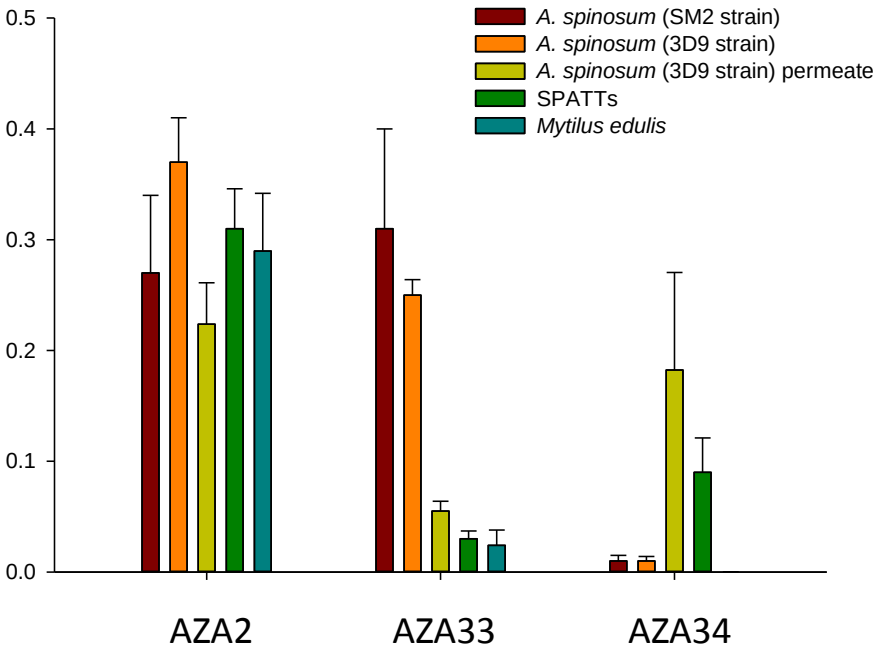

Figure 5.3. Ratios of AZA2 (**2**), -33 (**3**) and -34 (**4**) relative to AZA1 (**1**) detected by LC-MS/MS in *A. spinosum* SM2 (n=10), *A. spinosum* 3D9 (n=36), *A. spinosum* permeate (n=3), SPATTs (n=7) and shellfish (*Mytilus edulis*, n=20).

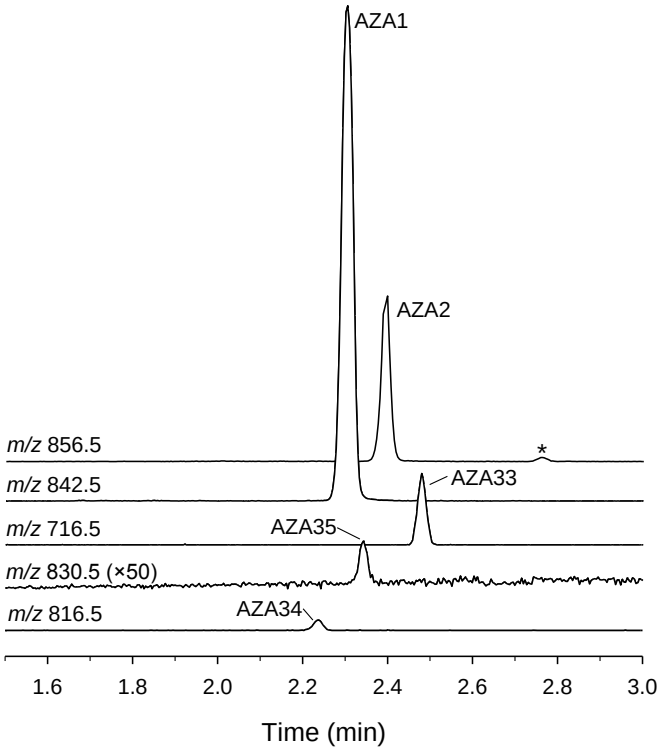

Figure 5.4. LC-MS chromatogram (method D) of a HP-20 resin permeate extract from a bulk culture of *A. spinosum* showing peaks for AZA34 (**4**), AZA1 (**1**), AZA35, AZA2 (**2**) and AZA33 (**3**). Peak marked with * corresponds to AZA1 methyl ester.[42]

5.4.2. Structure determination

LC-MS. High Resolution MS data were consistent with **3**, **4** and AZA35 possessing the molecular formulae shown in Table 5.1, indicating that **3**, **4** and AZA35 possess six, two, and one fewer carbon atoms than **1**, respectively.

The mass spectrum of **3** (Figure 5.2) showed typical AZA-type H_2O loss fragments (*m/z* 698 and 680). Additionally, fragments at *m/z* 362 and 462 suggested that the amino end (i.e., C-21–C-40 and substituents) of **1** was also present in **3**. No retro Diels–Alder (RDA) fragment was present, however, suggesting that the A/B/C ring-system of **3** differed from that of **1**. Thus, the carboxyl end of **3** (i.e., C-1−C-19) differed from that of **1** by the absence of $C_6H_6O_3$ and by the presence of four instead of seven rings/double bonds.

Compound **4** also displayed H_2O loss fragments (*m/z* 798 and 780), but also showed an RDA fragment at *m/z* 672, in addition to fragments at *m/z* 362 and 462 that are characteristic of the C-21–C-40 moiety of **1** (Figure 5.2). The MS data therefore suggested that the structure of **4** was very similar to that of **1**, including an intact A-ring, and that **4** differed from **1** by loss of C_2H_4 from the side chain attached to the A-ring.

The mass spectrometric data for AZA35 (Figure 5.2 and Table 5.1) are consistent with an additional CH_2 group in the structure of **4** between C-3 and C-9, possibly in the form of a methyl group at C-8 (as in **2**). NMR data will be required to confirm this proposal.

LC-MS analysis showed that treatment of **3** and **4** with periodate yielded the same C-20–C-21-cleavage product (*m/z* 448) as was obtained by treatment of **1**. This establishes not only the presence of a 20,21-diol in both **3** and **4**, but confirms that the same C-21–C-40 moiety that is present in **1** is also present in **3** and **4**.

Purified **3** and **4** were treated with diazomethane. LC-MS/MS analysis confirmed conversion to the corresponding methyl esters, thus establishing the presence of a carboxyl group in the side-chain attached at C-16 or C-6, respectively, of **3** and **4**.

Table 5.1. Exact masses of $[M+H]^+$ ions and calculated molecular formulae for AZA1 (**1**), -2 (**2**), -33 (**3**), -34 (**4**) and -35 in an *A. spinosum* (3D9) HP-20 permeate extract.

AZA	Molecular Formula ($[M+H]^+$)	Measured *m/z* $[M+H]^+$	Rings + double bonds	Δ (ppm)
AZA1 (**1**)	$C_{47}H_{72}NO_{12}$	842.5052	13	0.4
AZA2 (**2**)	$C_{48}H_{74}NO_{12}$	856.5195	13	−1.2
AZA33 (**3**)	$C_{41}H_{66}NO_9$	716.4759	10	3.8
AZA34 (**4**)	$C_{45}H_{70}NO_{12}$	816.4900	12	0.9
AZA35	$C_{46}H_{72}NO_{12}$	830.5046	12	-0.4

*NMR spectroscopy—AZA33 (**3**).*

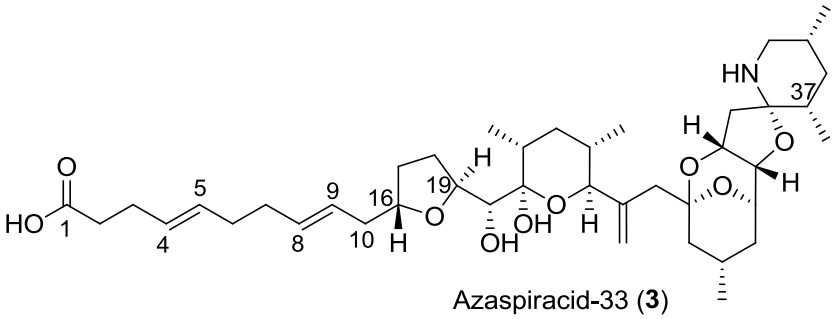

Azaspiracid-33 (**3**)

Detailed analysis of ^1H, ^{13}C, DEPT135, COSY, TOCSY, SELTOCSY, HSQC and HMBC spectra of **3** showed the presence of the pentacyclic C-20−C-40 ring system, present in all other known AZAs, consistent with results of the periodate cleavage experiment. During NMR analysis of both **3** and **4**, a series of minor peaks (~ 3–10%) were also observed which were attributable to the corresponding 37-epimers, due to susceptibility of AZAs to epimerization in MeOH under neutral and weakly acidic

conditions.[18] The presence of these epimers is noted, but is not discussed further as these minor peaks did not interfere with NMR analysis of the parent compounds.

AZAs are characterized by a distinctive doublet-of-triplet-like signal, akin to a quartet, at 4.41−4.43 ppm (H-19). The corresponding signal of **3** appeared at 4.08 ppm (dt, J = 8.2, 6.7 Hz). This indicated modification in **3** of the normal AZA structure in the vicinity of C-19, with the retention of three adjacent coupled protons (H-18 and H-20). Correlations in the COSY spectrum confirmed that the H-19 signal (4.08 ppm) was coupled to H-20 (3.34 ppm) and a pair of methylene proton signals (H-18a/b) at 1.95 and 2.00 ppm. In the TOCSY spectrum, H-19 showed additional correlations to a pair of methylene protons centered at 1.92 and 1.55 ppm (H-17), and an oxygenated methine signal at 3.907 ppm (H-16), the chemical shift of which differed marginally from that of the H-25 (3.911 ppm). In the HSQC spectrum, the foregoing protons showed correlations to carbons at 30.5 (C-18), 30.9 (C-17) and 81.5 ppm (C-16). These observations are consistent with the attachment to C-20 (77.4 ppm), via C-19 (80.3 ppm), of a tetrahydrofuran ring (two methylene carbons at 30.5 (C-18) and 30.9 ppm (C-17) and an oxygenated methine carbon at 81.5 ppm (C-16)), as in all other known AZAs.[33] The structure of this tetrahydrofuran ring differs, however, from known AZAs in that it possesses two methylene carbons, indicating that it is not *cis*-fused to a six-membered pyran ring as is the case for all other AZAs. It follows that the remaining $C_{10}H_{15}O_2$ portion of **3** (not accounted for by the proposed C-16 to C-40 substructure ($C_{31}H_{50}NO_7$)) must be attached to the oxygenated C-16 atom at 81.5 ppm. Moreover, it follows from the $C_{10}H_{15}O_2$ formulation, that the residue attached to C-16 must possess a total of three rings and/or double bonds. The presence in this residue of a carboxyl group (also consistent with the diazomethane reactivity), two olefinic double bonds, and five methylene carbons was indicated by the occurrence of signals at 181.9 ppm

(COOH), 127.8, 130.8, 131.5 and 133.4 ppm (2 × CH=CH groups), and at 30.9, 33.9, 34.1, 39.7 and 40.5 ppm (5 × CH_2 groups), precluding the presence of rings in C-6–C-15.

Notwithstanding the appreciable overlap of the four olefinic proton signals (5.40–5.53 ppm, Figure 5.5C), the resolution of the COSY spectrum was such that the connectivities depicted in Figure 5.1 could be established, and were supported by TOCSY and SELTOCSY spectra run with a range of mixing times. The resonances of the ^{13}C atoms to which these protons were attached were established by correlations observed in the HSQC spectrum.

H-16 (3.907 ppm) showed COSY correlations to the H-17 methylene protons (1.55 and 1.92 ppm) and to the pair of diastereotopic side chain protons at 2.17 and 2.24 ppm (H-15). These protons show a COSY correlation to the least shifted of the four olefinic protons at 5.43 ppm (H-14). In the HSQC spectrum, this proton exhibited a correlation to the olefinic carbon signal at 127.8 ppm (C-14). In the HMBC spectrum, H-16 (3.907 ppm) showed a correlation to the olefinic C-14 carbon (127.8 ppm), and the protons at 5.43 (H-14) and 2.17 (H-15) also showed correlations to 133.4 ppm (C-13). C-13 in turn showed an HSQC correlation to a methine signal at 5.50 ppm (H-13). These observations defined the location of the first of the two double bonds in the 10-carbon side chain attached to C-16.

The two pairs of methylene protons at 2.03 ppm (4H, br s, H-11 and H-12) were not overlapped in the ^{1}H NMR spectrum by other signals, and showed COSY correlations only to the olefinic proton signals centered at 5.45 (H-10) and 5.50 ppm (H-13). In the HMBC spectrum, the protons at 2.04 ppm showed correlations to the four olefinic carbons (127.8, 130.8, 131.5 and 133.4 ppm) and adjacent partner methylene carbons (33.9 and 34.1 ppm, C-11 and C-12). The resolution of the processed HMBC spectrum

was such that while the four olefinic carbon correlations were resolved, the methylene carbon resonances, which differed by 0.2 ppm, were not. The foregoing COSY and HMBC observations demonstrated that the methylene carbons (C-11and C-12) with superimposed proton signals at 2.03 ppm must be located between the C-9(10) and C-13(14) double bonds.

The remaining pair of methylene carbons at 30.9 and 39.7 ppm, which showed HSQC correlations to pairs of protons at 2.26 (2H) and 2.18 (2H) ppm, respectively, and a terminal carboxyl group (181.9 ppm), must be attached to C-9. Consistent with this, the olefinic proton signal at 5.48 (H-9) ppm showed a COSY correlation to 2.26 ppm (H-8a/b), while HMBC correlations were observed between the proton signal at 2.18 ppm (H-7a/b) and the carboxyl carbon (C-6, 181.9 ppm) and a methylene carbon (C-8, 30.9 ppm).

Homonuclear decoupling experiments were also consistent with the attachment to C-16 of a 10 carbon side-chain (Figure 5.1). In particular, homonuclear decoupling at 2.04 ppm under standard conditions collapsed the lines attributable to the H-10 and H-13 olefinic protons (5.45 ppm and 5.50 ppm, respectively) to 15.3 Hz doublets (Figure 5.5B). These couplings demonstrate that the 9(10)- and 13(14)-double bonds are both *trans*-substituted. Similarly, homonuclear decoupling at 2.21 ppm (between the frequencies of the H-7 and H-8 methylene protons) using a higher power level that was also effective at decoupling the nearby H-15 methylene protons (at 2.17 and 2.24 ppm), resulted in the H-9 (5.48 ppm) and H-14 (5.43 ppm) olefinic protons appearing as well-defined 15.3 Hz doublets (Figure 5.5A). Under these conditions, the H-10 (5.45 ppm) and H-13 (5.50 ppm) olefinic protons appeared as doublets (J = 15.3 Hz) of poorly resolved, residually coupled, triplets ($J_{residual}$ ~ 1–2 Hz) due to incomplete decoupling of the adjacent H-11 and H-12 methylene protons at 2.04 ppm.

The H-19 (4.08 ppm) proton of **3** exhibited ROESY correlations that paralleled those which we have previously observed for **1**,[18] including moderate intensity inter-ring correlations to the equatorial H-40 proton (2.46 ppm) and the more shifted of the two olefinic 26-methylene protons (H-26_Z, 5.27 ppm). H-19 (4.08 pm) also showed ROESY correlations to H-22 (2.37 ppm) and the 22-methyl group (0.89 ppm), as did H-20 (3.34 ppm). H-16 (3.907 ppm) showed ROESY correlations to the adjacent H-15 methylene protons (2.17 and 2.24 ppm) of the 10-carbon side-chain, and to one of the H-17 protons (1.92 ppm), together with a low intensity (0.15%) ROESY correlation to the more distant H-19 proton (4.08 ppm) as also seen in ROESY spectra of **1** and **2**. These observations showed that the C-16, C-19 and C-20 configurations of **1** and **3** are essentially identical, that the dispositions of their C-16–C-20 tetrahydrofuran ring and 20-CHOH groups are similar, and that the inter-ring spatial relationships between the C-19, C-26 and C-40 regions of **3** are comparable to those of **1**. These observations are consistent with the relative configuration proposed for the C-16–C-19 region of **3** (Figure 5.1).

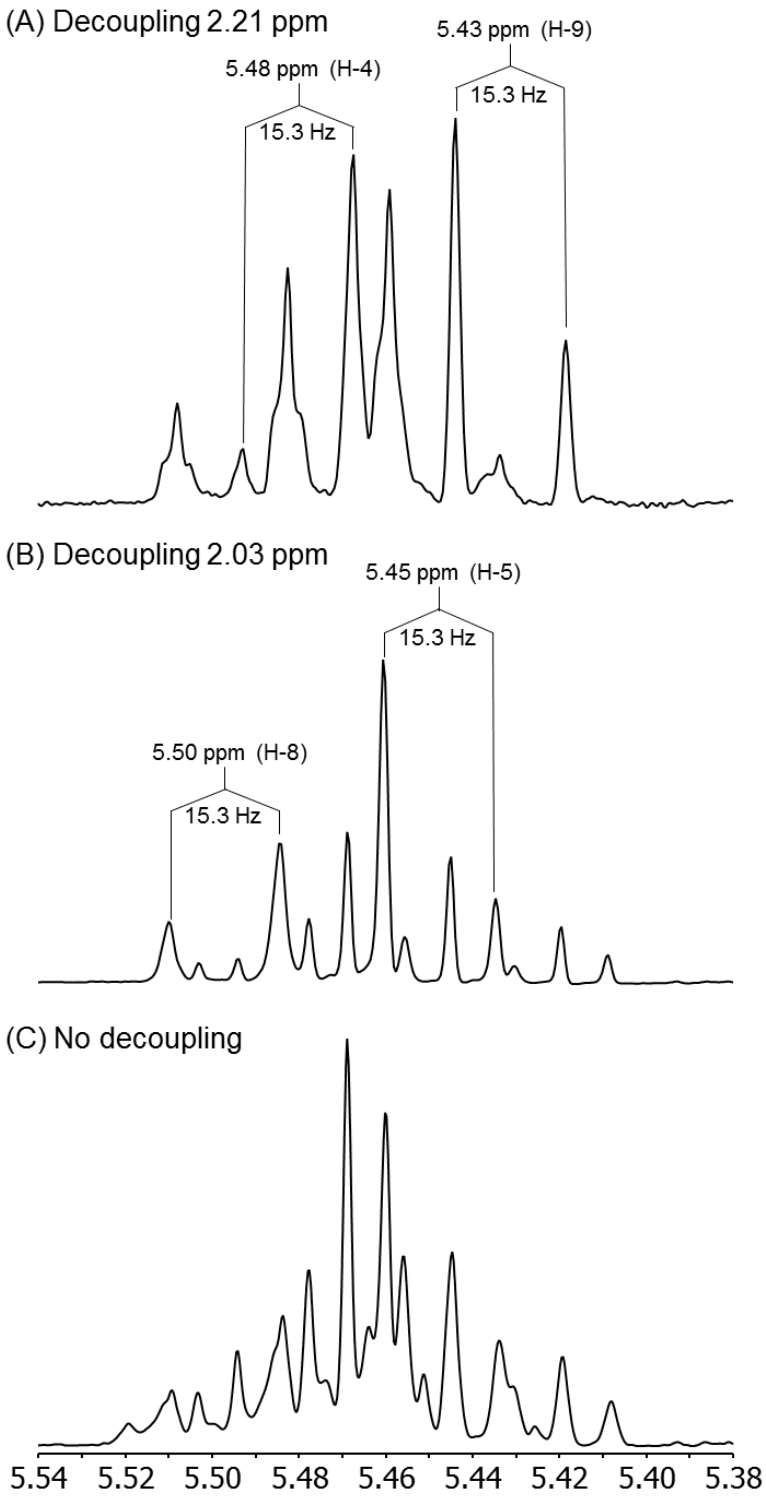

Figure 5.5. ^{1}H NMR spectra of AZA33 (**3**) from 5.38–5.54 ppm, showing the side-chain olefinic protons (H-4, H-5, H-8 and H-9), with: (A) high-power decoupling at 2.21 ppm (decoupling ~ 2.16–2.26 ppm (H-2, H-3, and H-10)); (B) low power decoupling at 2.04 ppm (decoupling H-6 and H-7), and; (C) no decoupling.

*NMR spectroscopy—AZA34 (**4**).*

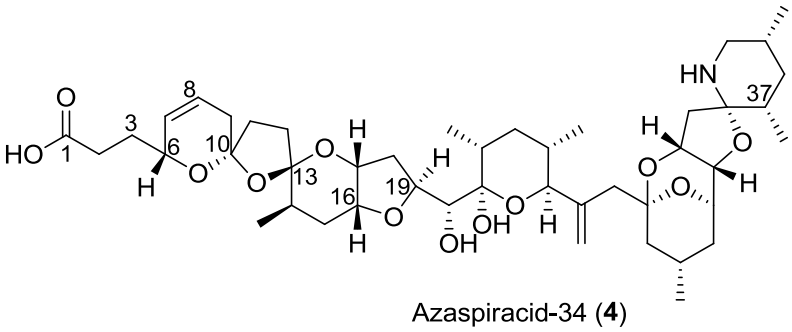

Azaspiracid-34 (**4**)

In full accord with the mass spectrometric and periodate cleavage results discussed above, detailed analysis of ^{1}H, ^{13}C, DEPT135, COSY, TOCSY, SELTOCSY, HSQC and HMBC spectra showed that **4** possessed an intact C-6−C-40 ring system and that the 5-carbon ring-A-side-chain present at C-6 in all other reported AZAs had been replaced by a 3-carbon $–CH_2-CH_2-COOH$ side chain. The ^{1}H chemical shifts of the modified side chain methylene groups were elucidated via correlations in COSY and TOCSY spectra. H-6 (4.41 ppm), which was coincident with the H-19 signal, exhibited COSY correlations to the H-5a/b methylene protons (1.76 and 1.85 ppm). These correlations were readily differentiated from those which H-19 exhibited to H-18a/b (2.02 ppm), H-20 (3.55 ppm), and H-17 (4.19 ppm). The TOCSY spectrum at the frequency of H-6 (4.41 ppm) and at the frequencies of other protons associated with the mutually coupled H-4a/b–H-5a/b–H-6–H-7–H-8–H-9a/b spin systems included correlations to 2.21 and 2.31 ppm, attributable to the H-4a/b protons. The H-4 and H-5 methylene protons showed HSQC correlations to resonances at 34.7 and 33.2 ppm (C-4 and C-5, respectively), while the protons at 2.21 and 2.31 (H-4a/b) showed HMBC correlations to 181.9 (C-3), 70.5 (C-6) and 33.2 ppm (C-5).

The chemical shifts of carbons and protons associated with the C-6–C-40 portion of **4** were similar, but not in all cases identical, to those of **1** (Table 5.2) and several other AZAs.[14–17] It is apparent from an analysis of published NMR data that the chemical

shifts of atoms in the vicinity of the 40-NH group and the C-20 portions of AZA are dependent on the pH of the examined NMR solutions.[17,18] The presence of acetic acid (or deuteroacetic acid) in NMR solutions significantly increases the chemical shifts of the 40-methylene protons (reported chemical shifts for these protons are in the range 2.5–2.9 ppm), presumably due to protonation of the NH group, and that this in turn influences the chemical shifts of some of the other more remote protons (most notably H-20; reported chemical shifts are in the range 3.5−3.9 ppm) that are in close proximity to H-19.[18] However, because addition of weak acid promotes epimerization at C-37, addition of d_5-pyridine may be a better option for pH control during NMR analysis of AZAs.[18]

The NMR spectra of all AZAs examined in our laboratory,[18] including **3** and **4**, have exhibited moderate intensity inter-ring ROESY correlations between the equatorial H-40 methylene proton and both H-19 and the more shifted of the two protons of the exomethylene group located at C-26. Compound **4**, in both 2D-ROESY and a series of 1D-SELROESY NMR experiments, exhibited an equivalent series of ROESY correlations to that observed for **1**, including a moderate intensity ROESY correlation between H-6 (4.41 ppm) and the 14-methyl group (0.95 ppm) which showed its C-6 configuration to be identical to that of **1**. H-6 (4.41 ppm) also showed ROESY correlations to the H-5a/b protons (1.76 and 1.85 ppm). The foregoing ROESY correlations were readily distinguishable from those which the superimposed H-19 signal showed to H-20 (3.55 ppm), H-18a/b (2.02 ppm), H-22 (2.24 ppm), the 22-methyl group (0.89 ppm) and one of the olefinic methylene protons attached to C-26 (5.26 ppm), because none of the correlations exhibited by the H-6 and H-19 signals overlapped and no nearby atoms possessed similar chemical shifts.

The NMR data provided definitive proof of the structures, showing that **3** consists of a *trans,trans*-4,8-decadienoic acid unit attached via its C-10 (i.e., C-15 of **3**) to the C-16 of an AZA tetrahydrofuran D-ring. Compound **4** differed from **1** only by having a shorter three carbon side chain without the double bond.

Many polyether toxins from dinoflagellates, such as okadaic acid and yessotoxin, are generated by cyclisation of a long carbon chain assembled primarily from acetate units via polyketide synthase enzyme clusters.[34] Examination of their structures suggest that this is also likely for AZAs, with the polyether structure of **1** being assembled from a 40-carbon chain. If this is indeed the case, it would appear that **4** is assembled from a 38-carbon chain and **3** from a 35-carbon chain. The production of **4** is consistent with a failure to incorporate one acetate unit, into the growing carbon chain during polyether biosynthesis. The fact that **3** has an odd numbered chain length may be due to oxidative cleavage of a C-5/C-6 double bond in a 40 carbon chain precursor. Furthermore, the structures of **3** and **4** suggest that AZAs may be assembled and cyclized from the amino-end, because in both of these compounds the C-19–C-40 substructure, including the relative configuration and all substituents, has been successfully assembled in an identical manner to **1** and **2** in *A. spinosum*'s AZA-synthase.

Table 5.2. NMR assignments (^{1}H 600 MHz, ^{13}C 150 MHz) for AZA1 (**1**), -33 (**3**) and -34 (**4**) in CD_3OD.

Position	**1**[a]		**3**		**4**	
	^{13}C	^{1}H	^{13}C	^{1}H	^{13}C	^{1}H
1	181.2					
2	38.1	2.25, 2.25				
3	30.2	2.33, 2.33			181.9	
4	133.7	5.75			34.7	2.21, 2.31
5	130.7	5.44			33.2	1.76, 1.85
6	72.5	4.79	181.9		70.5	4.41
7	129.4	5.63	39.7	2.18, 2.18	130.1	5.70
8	123.2	5.73	30.9	2.26, 2.26	123.3	5.72
9	35.7	2.12, 2.46	131.5	5.48[b]	37.6	2.11, 2.46
10	107.2		130.8	5.45[c]	107.1	
11	37.5	1.97, 2.14	34.1[d]	2.03, 2.03	37.6	1.94, 2.12
12	33.2	1.66, 2.33	33.9[d]	2.03, 2.03	33.0	1.64, 2.32
13	111.3		133.4	5.50[c]	111.0	
14	31.0	2.02	127.8	5.43[b]	30.9	2.01
15	32.6	1.76, 1.85	40.5	2.17, 2.24	32.6	1.75, 1.81
16	78.2	3.88	81.5	3.907	78.1	3.89
17	73.3	4.23	30.9	1.55, 1.92	73.1	4.19
18	37.3	1.99, 2.01	30.5	1.95, 2.00	38.3	2.02, 2.02
19	79.2	4.43	80.3	4.08	79.2	4.41
20	76.9	3.86	77.4	3.34	77.2	3.55
21	100.2		100.0		99.5	
22	36.6	2.12	35.7	2.37	36.3	2.24
23	38.3	1.43, 1.43	39.0	1.39, 1.39	38.3	1.41, 1.41
24	42.3	1.35	42.2	1.36	42.0	1.35
25	79.6	3.98	79.5	3.911	79.8	3.93
26	148.3		148.0		148.2	
27	49.5	2.24, 2.42	49.6	2.15, 2.34	49.4	2.16, 2.35
28	98.6		98.0		97.9	
29	44.3	1.36, 2.03	44.7	1.30, 1.98	44.7	1.31, 1.98
30	26.4	2.23	26.7	2.25	26.4	2.24
31	35.4	1.52, 1.83	35.6	1.47, 1.77	35.6	1.48, 1.78
32	72.8	4.35	72.7	4.24	72.8	4.26
33	81.2	4.01	79.4	3.74	79.6	3.77
34	74.9	4.98	75.4	4.81	75.5	4.82
35	41.9	2.41, 2.59	43.0	1.88, 2.39	43.1	2.00, 2.43
36	96.6		95.8		95.8	
37	36.0	1.95	37.7	1.76	37.3	1.76
38	38.0	1.28, 1.67	39.9	1.14, 1.54	39.8	1.17, 1.55
39	29.8	1.85	31.0	1.69	31.2	1.68
40	46.4	2.79, 2.84[e]	47.4	2.53, 2.46[e]	47.7	2.55, 2.55
14-Me	16.6	0.95			16.6	0.95
22-Me	16.4	0.91	16.9	0.89	16.3	0.89
24-Me	18.1	0.84	18.1	0.81	18.0	0.82
26=CH_2	116.8	5.16, 5.34[f]	115.4	5.07, 5.27[f]	115.6	5.10, 5.26[f]
30-Me	23.5	0.95	23.7	0.93	23.6	0.93
37-Me	15.5	0.96	16.1	0.86	16.0	0.88
39-Me	18.6	0.94	19.5	0.85	19.2	0.86

[a]From Kilcoyne et al.[18]
[b]Decoupled by homonuclear decoupling at 2.21 ppm (Figure 5.5A).
[c]Decoupled by homonuclear decoupling at 2.04 ppm (Figure 5.5B).
[d]Assignments interchangeable.
[e]H_{axial}, $H_{equatorial}$
[f]H_E, H_Z

5.4.3. Relative molar response

Compounds **3** and **4** were quantitated by quantitative NMR (qNMR), and their molar responses in various LC-MS methods were assessed against purified **1**, that had also been quantitated by qNMR. A number of LC-MS analyses were performed employing an acidic (isocratic and gradient) mobile phase in both SIM (selected ion monitoring) and SRM (selected reaction monitoring) modes.

LC-MS data obtained in SIM mode suggested that **3** and **4** had very similar responses to **1** when analysed under the various conditions (Table 5.3). In SRM mode, differences in response factors were observed. The response using the H_2O loss fragment for **3** was similar to that for **1**, while a higher response factor was obtained for **4**. The RDA fragment for **4** gave a lower response factor than for **1**, as did the *m*/*z* 462 fragment for **3**. The *m*/*z* 362 transitions for both **3** and **4** were slightly lower than that for **1** (Table 5.3). These results suggest that, in the absence of standards, **3** and **4** would be more accurately quantitated against **1** in SIM mode.

Table 5.3. Relative molar response factors (propagated standard deviation of the last significant figure in parentheses) of AZA33 (**3**) and AZA34 (**4**) in relation to AZA1 (**1**) (**1**(area/concentration)/(**3** or **4**(area/concentration)))[a].

MS mode (ion/transition)	**3**		**4**	
	Gradient[b]	Isocratic[c]	Gradient[b]	Isocratic[c]
SIM $[M+H]^+$	1.03 (2)	0.97 (3)	1.01 (3)	1.05 (3)
SRM ($[M+H]^+ - H_2O$)	1.03 (11)	1.05 (3)	1.22 (9)	1.17 (7)
SRM ($[M+H]^+ \rightarrow 672$)	-	-	0.41 (2)	0.39 (2)
SRM ($[M+H]^+ \rightarrow 462$)	0.77 (5)	0.80 (5)	-	-
SRM ($[M+H]^+ \rightarrow 362$)	0.91 (6)	0.90 (4)	0.90 (7)	0.87 (4)

[a]Determined by SIM and SRM LC-MS experiments using gradient and isocratic LC elution with an acidic mobile phase. [b]Method F(i). [c]Method F(ii).

5.4.4. Toxicity

Compounds **3** and **4** were cytotoxic to Jurkat T lymphocyte cells in a time- and concentration-dependent manner (Figure 5.6), and were 0.22- and 5.5-fold as potent as **1**, respectively (Table 5.4).

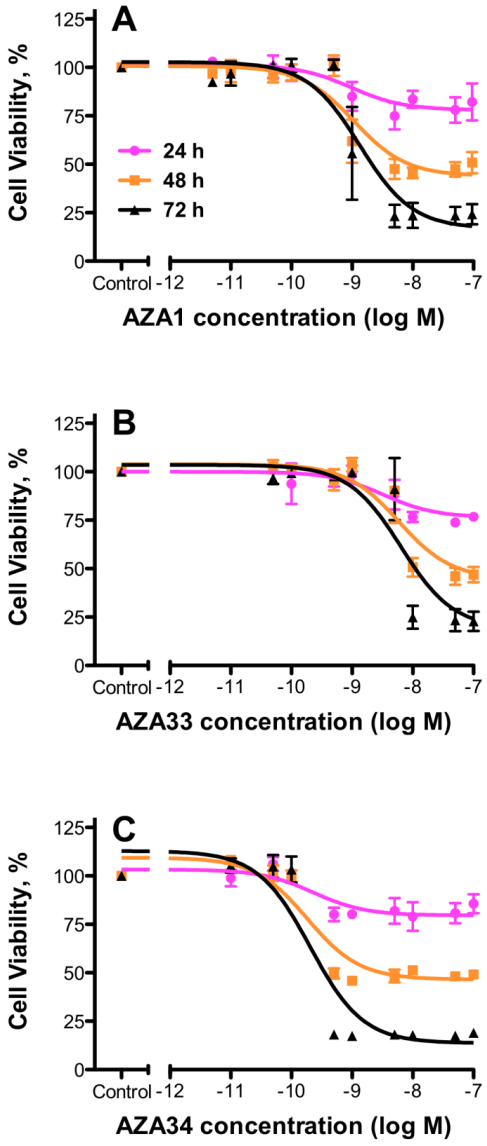

Figure 5.6. Effect of AZA analogues on T lymphocyte cell viability. Jurkat T cells were exposed to various concentrations of (A) AZA1 (**1**), (B) AZA33 (**3**), and (C) AZA34 (**4**) for 24, 48, or 72 h and viability was assessed using the MTS assay. All data (mean ± SE; n=3) were normalized to the control (10% MeOH vehicle). Non-linear, three parameter dose–response (variable slope) analysis was performed and EC_{50} values calculated (Table 5.4).

Although these compounds were present in minor amounts relative to **1** and **2** in French and Irish shellfish, their major significance lies in their structural differences and their usefulness in establishing structure–activity relationships. Analogue **3** is similar to **1** but without the A/B/C ring structure, while **4** differs from **1** only by the shorter side chain and absence of the 4,5- alkene. In the absence of the A/B/C ring structure, relative cytotoxic potency was reduced ~ 5-fold (relative to **1**) (Table 5.4), suggesting that although this fragment of the AZA molecule influences toxicity, it is not the primary toxicophore or epitope necessary for AZAs to bind to and affect their target(s). On the other hand, the shorter side chain and absence of the 4,5-alkene in **4** enhanced cytotoxic potency by > 5 fold (Table 5.4). This increase in potency may be due to greater interaction of the molecular target(s) with the negatively charged carboxylic acid due to the altered configuration. Although **1**, **2** and AZA3 have been shown to induce apoptosis[13] and selectively inhibit hERG potassium channels,[35] the effects of **3** and **4** on these pathways have not yet been characterized. The results presented here suggest that it may be possible to link a reporter molecule in the vicinity of the carboxyl moiety of AZAs and still retain sufficient binding affinity to probe the AZAs' molecular target.

Table 5.4. Calculated EC_{50} values (nM) with 95% confidence intervals (CI) and relative potencies (Rel. Pot.) for AZA analogues based on T lymphocyte cytotoxicity.

AZA	24 h		48 h		72 h		Mean	Rel.
	EC_{50}	95% CI	EC_{50}	95% CI	EC_{50}	95% CI	EC_{50}	Pot.
1	0.96	0.19–4.9	1.10	0.46–2.5	1.3	0.59–3.0	1.1	1.0
3	3.3	0.79–13	5.9	2.4–15	6.4	2.8–15	5.2	0.22
4	0.23	0.042–1.2	0.18	0.098–0.34	0.20	0.11–0.38	0.20	5.5

5.5. Conclusions

Three new AZAs were identified in seawater (SPATT) samples and in cultured *A. spinosum*, two of which (**3** and **4**) were present in sufficient amounts for purification. Structures were determined by LC-MS/MS and NMR spectroscopy. Compound **3** was found to have major structural differences compared to **1**, while **4** only differed by a shorter side chain and the lack of an alkene group at the C-4–C-5 position. The fact that **4** was more abundant in natural seawater samples and in culture medium raises questions regards its biological and ecological roles. Analysis of these AZAs using a neutral mobile phase indicates that 37-epimers also exist for these compounds.

Cytotoxicity was assessed employing Jurkat T lymphocyte cells, and potencies relative to **1** for **3** and **4** were found to be 0.22 and 5.5, respectively. Both **3** and **4** were present in Irish mussels at very low levels and are not considered of relevance to human health. However, with the notable differences in structure and potency, these analogues further our knowledge of AZA structure–activity relationships.

5.6. References

(1) Rehmann, N., Hess, P., and Quilliam, M. A. *Rapid Commun. Mass Spectrom.* **2008**, *22*, 549–558.

(2) Twiner, M. J., Rehmann, N., Hess, P., and Doucette, G. J. *Mar. Drugs* **2008**, *6*, 39–72.

(3) Anon. (2011) Commission Regulation (EU) No 15/2011 of 10th January 2011 amending Regulation (EC) No 2074/2005 as regards recognised testing methods for detecting marine biotoxins in live bivalve molluscs. L6/3-6.

(4) Krock, B., Tillmann, U., John, U., and Cembella, A. D. *Harmful Algae* **2009**, *8*, 254–263.

(5) McCarron, P., Kilcoyne, J., Miles, C. O., and Hess, P. *J. Agric. Food Chem.* **2009**, *57*, 160–169.

(6) Salas, R., Tillmann, U., John, U., Kilcoyne, J., Burson, A., Cantwell, C., Hess, P., Jauffrais, T., and Silke, J. *Harmful Algae* **2011**, *10*, 774–783.

(7) Jauffrais, T., Contreras, A., Herrenknecht, C., Truquet, P., Séchet, V., Tillmann, U., and Hess, P. *Aquat. Toxicol.* **2012**, *124–125*, 179–187.

(8) Colman, J. R., Twiner, M. J., Hess, P., McMahon, T., Satake, M., Yasumoto, T., Doucette, G. J., and Ramsdell, J. S. *Toxicon* **2005**, *45*, 881–890.

(9) Ito, E., Satake, M., Ofuji, K., Higashi, M., Harigaya, K., McMahon, T., and Yasumoto, T. *Toxicon* **2002**, *40*, 193–203.

(10) Aasen, J. A. B., Espenes, A., Hess, P., and Aune, T. *Toxicon* **2010**, *56*, 1419–1425.

(11) Furey, A., O'Doherty, S., O'Callaghan, K., Lehane, M., and James, K. J. *Toxicon* **2010**, *56*, 173–190.

(12) Twiner, M. J., El-Ladki, R., Kilcoyne, J., and Doucette, G. J. *Chem. Res. Toxicol.* **2012**, *25*, 747–754.

(13) Twiner, M. J., Hanagriff, J. C., Butler, S., Madhkoor, A. K., and Doucette, G. J. *Chem. Res. Toxicol.* **2012**, *25*, 1493–1501.

(14) Satake, M., Ofuji, K., Naoki, H., James, K. J., Furey, A., McMahon, T., Silke, J., and Yasumoto, T. *J. Am. Chem. Soc.* **1998**, *120*, 9967–9968.

(15) Ofuji, K., Satake, M., McMahon, T., Silke, J., James, K. J., Naoki, H., Oshima, Y., and Yasumoto, T. *Nat. Toxins* **1999**, *7*, 99–102.

(16) Ofuji, K., Satake, M., McMahon, T., James, K. J., Naoki, H., Oshima, Y., and Yasumoto, T. *Biosci. Biotechnol. Biochem.* **2001**, *65*, 740–742.

(17) Kilcoyne, J., Keogh, A., Clancy, G., LeBlanc, P., Burton, I., Quilliam, M. A., Hess, P., and Miles, C. O. *J. Agric. Food Chem.* **2012**, *60*, 2447–2455.

(18) Kilcoyne, J., McCarron, P., Twiner, M. J., Nulty, C., Wilkins, A. L., Rise, F., Quilliam, M. A., and Miles, C. O. *Chem. Res. Toxicol.* **2014**, *27*, 587–600.

(19) Perez, R., Rehmann, N., Crain, S., LeBlanc, P., Craft, C., MacKinnon, S., Reeves, K., Burton, I., Walter, J. A., Hess, P., Quilliam, M. A., and Melanson, J. *Anal. Bioanal. Chem.* **2010**, *398*, 2243–2252.

(20) Laycock, M., Thibault, P., Ayer, S., and Walter, J. *Nat. Toxins* **1994**, *2*, 175–183.

(21) Miles, C. O., Wilkins, A. L., Munday, R., Dines, M. H., Hawkes, A. D., Briggs, L. R., Sandvik, M., Jensen, D. J., Cooney, J. M., and Holland, P. T. *Toxicon* **2004**, *43*, 1–9.

(22) Abraham, A., Plakas, S. M., Wang, Z., Jester, E., El Said, K. R., Granade, H. R., Henry, M. S., Blum, P. C., Pierce, R. H., and Dickey, R. W. *Toxicon* **2006**, *48*, 104–115.

(23) Ueoka, R., Ito, A., Izumikawa, M., Maeda, S., Takagi, M., Shin-ya, K., Yoshida, M., Van Soest, R. W. M., and Matsunaga, S. *Toxicon* **2009**, *53*, 680–684.

(24) Jauffrais, T., Kilcoyne, J., Séchet, V., Herrenknecht, C., Truquet, P., Hervé, F., Bérard, J. B., Nulty, C., Taylor, S., Tillmann, U., Miles, C. O., and Hess, P. *Mar. Drugs* **2012**, *10*, 1360–1382.

(25) Krock, B., Tillmann, U., Voß, D., Koch, B. P., Salas, R., Witt, M., Potvin, É., and Jeong, H. J. *Toxicon* **2012**, *60*, 830–839.

(26) Gu, H., Luo, Z., Krock, B., Witt, M., and Tillmann, U. *Harmful Algae* **2013**, *21–22*, 64–75.

(27) Percopo, I., Siano, R., Rossi, R., Soprano, V., Sarno, D., and Zingone, A. *J. phycol.* **2013**, *49*, 950–966.

(28) Fux, E., Marcaillou, C., Mondeguer, F., Bire, R., and Hess, P. *Harmful Algae* **2008**, *7*, 574–583.

(29) HABs, database. http://www.marine.ie/home/publicationsdata/data/Habs+Search+Database/HabsSearch.htm. Accessed 14 May 2014.

(30) Tillmann, U., Soehner, S., Nézan, E., and Krock, B. *Harmful Algae* **2012**, *20*, 142–155.

(31) Jauffrais, T., Kilcoyne, J., Herrenknecht, C., Truquet, P., Séchet, V., Miles, C. O., and Hess, P. *Toxicon* **2013**, *65*, 81–89.

(32) McCarron, P., Giddings, S. D., and Quilliam, M. A. *Anal. Bioanal. Chem.* **2011**, *400*, 835–846.

(33) Hess, P., McCarron, P., Krock, J., Kilcoyne, J., and Miles, C. O. (2014) Azaspiracids: chemistry, biosynthesis, metabolism and detection, in *Seafood and*

Freshwater Toxins (Botana, L. M. , Ed.) 3rd ed., pp 799–821, CRC Press, Boca Raton, FL.

(34) Kellmann, R., Stüken, A., Orr, R. J., Svendsen, H. M., and Jakobsen, K. S. *Mar. Drugs* **2010**, *8*, 1011–1048.

(35) Twiner, M. J., Doucette, G. J., Rasky, A., Huang, P. X., Roth, B. L., and Sanguinetti, M. C. *Chem. Res. Toxicol.* **2012**, *25*, 1975–1984.

(36) Tillmann, U., Elbrächter, M., Krock, B., John, U., and Cembella, A. D. *Eur. J. Phycol.* **2009**, *44*, 63–79.

(37) Fux, E., Bire, R., and Hess, P. *Harmful Algae* **2009**, *8*, 523–537.

(38) Lamberty, A., Schimmel, H., and Pauwels, J. *J. Anal. Chem.* **1998**, *360*, 359–361.

(39) Burton, I., Quilliam, M. A., and Walter, J. A. *Anal. Chem.* **2005**, *77*, 3123–3131.

(40) Twiner, M. J., Hess, P., Bottein Dechraoui, M. Y., McMahon, T., Samons, M. S., Satake, M., Yasumoto, T., Ramsdell, J. S., and Doucette, G. J. *Toxicon* **2005**, *45*, 891–900.

(41) Mosmann, T. *J. Immuno. Methods* **1983**, *65*, 55–63.

(42) Jauffrais, T., Herrenknecht, C., Sechet, V., Sibat, M., Tillmann, U., Krock, B., Kilcoyne, J., Miles, C. O., McCarron, P., Amzil, Z., and Hess, P. *Anal. Bioanal. Chem* **2012**, *403*, 833–846.

CHAPTER 6 – STRUCTURE ELUCIDATION, RELATIVE LC-MS RESPONSE, *IN VITRO* TOXICITY OF AZASPIRACIDS 7−10 ISOLATED FROM MUSSELS (*MYTILUS EDULIS*) AND PROPORTIONS IN SHELLFISH.

Kilcoyne, J., Twiner, M., McCarron, P., Crain, S., Giddings, S. D., Foley, B., Rise, F., Hess, P., Wilkins, A. L., Miles, C. O. Structure elucidation, relative LC-MS response and *in vitro* toxicity of azaspiracids isolated from mussels (*Mytilus edulis*). *Journal of Agriculture and Food Chemistry*, 2015, DOI: 10.1021/acs.jafc.5b01320.

Kilcoyne, J., McCarron, Hess, P., Miles, C. O. Effects of heating on proportions of azaspiracids 1–10 in mussels (*Mytilus edulis*) and identification of novel carboxylated analogues. *Manuscript in preparation.*

6.1. Abstract

Azaspiracids (AZAs) 7–10 (**7**−**10**) were isolated from shellfish and their structures, previously proposed based only on LC-MS/MS data, were confirmed by NMR spectroscopy. Samples of AZA4–6 (**4**−**6**) and **7**−**10** accurately quantitated by qNMR, were used for a relative molar response study, assaying cytotoxicity with Jurkat T lymphocyte cells and assessing proportions in naturally contaminated mussels.

LC-MS/MS molar response studies performed using isocratic and gradient elution, in both SIM and SRM modes, showed that responses for the analogues ranged from 0.3 to 1.2 relative to AZA1 (**1**). All AZA analogues tested were cytotoxic to Jurkat T lymphocyte cells in a time- and concentration-dependent manner. However, there were distinct differences in their EC_{50} values, with cytotoxicity potencies being AZA6 > AZA8 > AZA1 > AZA4 ≈ AZA5 ≈ AZA9 > AZA10. This provides valuable

information on structure–activity relationships. Analysis of heat-treated shellfish naturally contaminated with AZAs revealed high levels of **3** and **6** in some samples that were otherwise below the limit of quantitation before cooking. Relative to **1**, the average (n=40) levels of **4** (range 0–27%), **5** (range 1–21%) and **8** (range 1–27%) were each ~ 5%, while **7**, **9** and **10** (range 0–8%) were each under 1.5%.

6.2. Introduction

The consumption of shellfish contaminated with azaspiracids (AZAs) leads to the syndrome azaspiracid poisoning (AZP).[1] Poisoning incidents associated with this toxin group have been reported.[2,3] In all cases, the source of the implicated shellfish was Ireland where the levels and number of AZA occurrences have been most problematic.[4] AZAs have been reported to produce "neurotoxin-like" symptoms via intraperitoneal injection in mice, with death in 20–90 min.[5] Oral administration was found to produce clinical disease that was dose- and time-dependent, in addition to damaging the intestinal organs.[6–9] AZA1 (**1)** is a K^+ channel blocker,[10] and is highly cytotoxic to multiple cell types which undergo atypical apoptosis after exposure.[11]

AZAs were first identified in the late 1990s and since then more than 30 analogues have been identified in shellfish,[12] phytoplankton,[13–15] crabs[16] and a marine sponge.[17] Only **1**, AZA2 (**2**) and AZA3 (**3**) are currently regulated in raw shellfish.[18] Compounds **1**,[19] **2**, **3**,[20] AZA4 (**4)**, AZA5 (**5)**[21] and AZA6 (**6**)[22] have been isolated and their structures elucidated through a combination of NMR spectroscopy and chemical reactions. More recently, 37-*epi*-**1** that was isolated from shellfish extracts, was found to differ structurally from **1** in respect of the orientation of the methyl group at C-37, and to be 5-fold more toxic than **1** using the Jurkat T lymphocyte cell assay.[23]

LC-MS analysis revealed the presence of hitherto unknown AZAs in the dinoflagellates *Amphidoma languida,*[14] *Azadinium poporum*[24] and *Azadinium spinosum.*[15] The AZAs identified in *A. spinosum,* subsequently named AZA33 and -34, were found to be the same structurally at the amine end of the molecule (C-21–40) compared to **1**, producing the characteristic *m/z* 362 fragment during LC-MS/MS analysis.[15] AZAs from *A. poporum* (AZA36 and -37), on the other hand, appear to differ by the lack of a methyl or methylene group in the I-ring, resulting in an equivalent fragment with *m/z* 348.[9] The AZAs (with molecular masses of 815 and 829 Da) detected in the *A. languida* also displayed fragment ions with *m/z* 348, suggesting that these compounds also may lack a methyl group in the I-ring.[14]

Here we describe the isolation of **4**, **5**, AZA7 (**7**), AZA8 (**8**), AZA9 (**9**) and AZA10 (**10**) (Figure 6.1) from shellfish, with confirmation by NMR of the structures previously postulated based on LC-MS/MS. Relative molar response studies using mass spectrometry were performed following the preparation of reference standards which were quantitated using quantitative NMR (qNMR). The toxicity of **4**–**10** was assessed using the Jurkat T Lymphocyte cell assay and the results used to discern structure–activity relationships (SARs). The relevance of these toxins for human health protection in terms of toxicity and proportions detected in mussels was also evaluated.

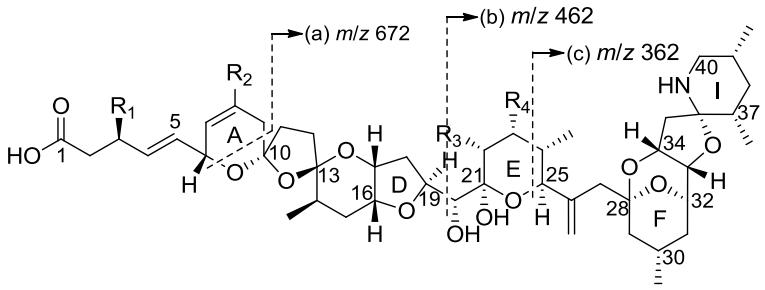

	R_1 (C-3)	R_2 (C-8)	R_3 (C-22)	R_4 (C-23)	$[M+H]^+$ *m/z*	Origin	Status
AZA1 (**1**)	H	H	CH_3	H	842.5	*A. spinosum*	phycotoxin
AZA2 (**2**)	H	CH_3	CH_3	H	856.5	*A. spinosum*	phycotoxin
AZA3 (**3**)	H	H	H	H	828.5	shellfish	metabolite
AZA4 (**4**)	OH	H	H	H	844.5	shellfish	metabolite
AZA5 (**5**)	H	H	H	OH	844.5	shellfish	metabolite
AZA6 (**6**)	H	CH_3	H	H	842.5	shellfish	metabolite
AZA7 (**7**)	OH	H	CH_3	H	858.5	shellfish	metabolite
AZA8 (**8**)	H	H	CH_3	OH	858.5	shellfish	metabolite
AZA9 (**9**)	OH	CH_3	H	H	858.5	shellfish	metabolite
AZA10 (**10**)	H	CH_3	H	OH	858.5	shellfish	metabolite

Figure 6.1. Structures of **1**–**10**, their protonated masses and origin. The *m/z* values of the fragments are for **1**; corresponding fragments were observed for **2**–**10**.

6.3. Experimental section

6.3.1. General experimental procedures

NMR experiments for structure elucidation were run using Bruker Avance I and Avance II 600 MHz spectrometers equipped with TCI cryoprobes and Z-gradient coils, at 30 °C and a Bruker DRX-500 spectrometer using a TXI probe and Z-gradient coils at 20 ^{o}C was used for qNMR.

Mass spectrometric studies were performed using a Waters 2695 LC coupled to a Micromass triple-stage quadrupole (TSQ) Ultima, a Waters 2795 LC coupled to a

Micromass quadrupole time of flight (QToF) Ultima and an Agilent 1200 LC system connected to a SCIEX API4000 QTRAP mass spectrometer equipped with a Turbospray ionization source.

6.3.2. Biological material

Mytilus edulis samples contaminated with AZAs were obtained from shellfish harvesting sites along the West coast of Ireland. The samples selected for analysis (n=40) were from different locations and harvested in different years.

6.3.3. Isolation and purification

The isolation procedure has been previously described by Kilcoyne et al.[22] Final purification of AZAs was achieved by semi-preparative LC (Agilent 1200) with photodiode array (PDA) detection (210 nm) using a Cosmosil C18 column, 5 µm, 250 × 4.6 mm, Nacalai tesque) eluted with CH_3CN/H_2O (1:1, plus 2 mM ammonium acetate) at 1 mL/min. The column temperature was 30 °C. Due to the presence of co-eluting compounds two additional semi-preparative steps using CH_3CN/H_2O (0.8:1, plus 2 mM ammonium acetate) were required to attain sufficient purity for NMR. Purified AZAs were recovered by diluting the fractions with H_2O (to 20% CH_3CN), loading on to solid-phase extraction (SPE) cartridges (Oasis HLB, 200 mg), washing with $MeOH/H_2O$ (1:9, 10 mL) to remove the buffer, and eluting with $MeOH/H_2O$ (9:1, 20 mL). Removal of solvent by evaporation *in vacuo* afforded purified AZAs as white solids.

AZA7 (**7**). white, amorphous solid; ^{1}H and ^{13}C data (CD_3OD, 600 MHz), see Table 6.1; HRESIMS *m/z* 858.4990 $[M+H]^+$ (calcd for $C_{47}H_{71}NO_{13,}$ 858.5009).

AZA8 (**8**). white, amorphous solid; ^{1}H and ^{13}C data (CD_3OD, 600 MHz), see Table 6.1; HRESIMS *m/z* 858.5002 $[M+H]^+$ (calcd for $C_{47}H_{71}NO_{13,}$ 858.5009).

AZA9 (**9**). white, amorphous solid; ^{1}H and ^{13}C data (CD_3OD, 600 MHz), see Table 6.1; HRESIMS *m/z* 858.5007 $[M+H]^+$ (calcd for $C_{47}H_{71}NO_{13,}$ 858.5009).

AZA10 (**10**). white, amorphous solid; ^{1}H and ^{13}C data (CD_3OD, 600 MHz), see Table 6.1; HRESIMS *m/z* 858.5012 $[M+H]^+$ (calcd for $C_{47}H_{71}NO_{13,}$ 858.5009).

6.3.4. Analysis of raw and cooked shellfish tissues

AZA-contaminated raw samples, tested as part of the routine monitoring programme in Ireland, were selected for analysis. The shellfish were shucked and homogenised before extraction. Tissue samples were weighed (2 g) in duplicate into 50 mL centrifuge tubes with one set placed in a H_2O bath (Grant Ltd) and heated to 90 °C for 10 min, then allowed to cool. The samples were extracted by vortex mixing for 1 min with 9 mL of MeOH, centrifuged at 3,950 g (5 min), and the supernatants decanted into 25 mL volumetric flasks. The remaining pellet was further extracted using an Ultra turrax (IKA) for 1 min with an additional 9 mL of MeOH, centrifuged at 3,950 × g, 5 min, and the supernatants decanted into the same 25 mL volumetric flasks, which was then brought to volume with MeOH. The extracts were analysed by LC-MS/MS (method A). Certified standards of **1**–**3** and the reference standards prepared for **4**–**10** were used for quantitation.

6.3.5. Periodate cleavage

Dilutions (~ 100 ng/mL) of purified **7**−**10** in MeOH were used. To 100 µL of each sample was added 50 µL of 0.2 M sodium periodate solution, and the reactions analyzed immediately by LC-MS (method A) including traces at *m/z* 448.4 (for the **7** oxidation

product), *m/z* 464.4 (for the **8** oxidation product), *m/z* 434.4 (for the **9** oxidation product) and at *m/z* 450.4 (for the **10** oxidation product).

6.3.6. LC-MS experiments

Method A. Recoveries were determined by quantitative analysis of fractions on a Waters 2695 LC coupled to a Micromass triple-stage quadrupole (TSQ) Ultima operated in SRM mode for the following transitions: *m/z* 842.5→824.5/362.3 (**1** and **6**); *m/z* 856.5→838.5/362.3 (**2**); *m/z* 828.5→810.5/362.3 (**3**); *m/z* 844.5→826.5/362.3 (**4** and **5**) and *m/z* 858.5→ 840.5/362.3 (**7**–**10**). The cone voltage was 60 V, collision energy was 50 V, the cone and desolvation gas flows were set at 100 and 800 L/h, respectively, and the source temperature was 150 °C.

Binary gradient elution was used, with phase A consisting of H_2O and phase B of CH_3CN (95%) in H_2O (both containing 2 mM ammonium formate and 50 mM formic acid). Chromatography was performed with a Hypersil BDS C8 column (50 × 2.1 mm, 3 µm, with a 10 × 2.1 mm guard column of the same stationary phase) (Thermo Scientific). The gradient was from 30% B, to 90% B over 8 min at 0.25 mL/min, held for 5 min, then held at 100% B at 0.4 mL/min for 5 min, and returned to the initial conditions and held for 4 min to equilibrate the system. The injection volume was 5 µL and the column and sample temperatures were 25 °C and 6 °C, respectively.

Method B. Structure determination and purity was assessed on a Micromass time-of-flight (QToF) Ultima coupled to a Waters 2795 LC by running MS scans (*m/z* 100–1000) using the same chromatographic conditions as above. Identification of other contaminant AZA analogues was also determined by performing product ion scans, where the precursor ions were selected and then fragmented, for all the known AZA analogues.

Method C. Qualitative analysis of fractions for AZAs was performed by flow injection analysis (FIA)-MS/MS using a Micromass quadrupole time of flight (QToF) Ultima coupled to a Waters 2795 LC. Samples (2 µL) were injected directly (no column) into the mass spectrometer, monitoring for the precursor ions.

Method D. For a relative molar response study accurate working standards were prepared by diluting the qNMR stock solutions in high purity degassed MeOH. The concentrations of the working solutions were ~ 1 µM for all analogues. Analysis was performed on an Agilent 1200 LC system connected to an API4000 QTRAP mass spectrometer (AB Sciex) equipped with a Turbospray ionization source. The MS was operated in positive ion mode and SRM transitions were as follows: *m/z* 842.5→824.5/672.5/462.3/362.3 (**1**); *m/z* 844.5→826.5/658.5/362.3 (**4**); *m/z* 844.5→826.5/674.5/362.3 (**5**); *m/z* 842.5→824.5/658.5/362.3 (**6**); *m/z* 858.5→840.5/672.5/362.3 (**7**); *m/z* 858.5→840.5/688.5/362.3 (**8**); *m/z* 858.5→840.5/658.5/362.3 (**9**) and *m/z* 858.5→840.5/674.5/362.3 (**10**). For selected ion monitoring (SIM) experiments *m/z* 842.5 (**1** and **6**), 844.5 (**4** and **5**) and 858.5 (**7**–**10**) were analysed. Typical parameters were 5500 V electrospray voltage, 400 °C source temperature, 70 V declustering potential and collision energies of 45 to 70 V (where applicable). Method D (i) used gradient elution with the same acidic mobile phase as method A, separation being performed on a 2.5 µm, 2.1 × 50 mm, Luna C18(2) HST column (Phenomenex). The gradient was from 25 to 100% B over 5 min at 300 µL/min and held at 100% B for 2 min, before re-equilibration for the next run. The injection volume was 1–5 µL and the column and sample temperatures were 25 °C and 6 °C, respectively. Method D (ii) used isocratic elution with the acidic mobile phase on the same Luna column, with 60% B at 300 µL/min.

Method E. For separation of the 37-epimers[33] a neutral gradient elution was used. Separation was performed on the same Luna column used in method D, operated at 15 °C, injecting 1–5 µL samples. A binary mobile phase of H_2O (A) and CH_3CN (95%) in H_2O (B), each containing 5 mM ammonium acetate (pH 6.8), was used with a linear gradient from 25 to 100% B over 5 min at 350 µL/min and held at 100% B for 2 min, before re-equilibration for the next run.

Method F. Accurate mass measurements and quantitation were performed on a Waters Acquity UPLC coupled to a Xevo G2-S QToF operated in MS^e mode, scanning from 100−1200 *m/z* and using leucine enkephalin as the reference compound. The cone voltage was 40 V, collision energy was 50 V, the cone and desolvation gas flows were set at 100 and 1000 L/h, respectively, and the source temperature was 120 °C.

Chromatography was performed with an Acquity UPLC BEH C18 (50 × 2.1 mm, 1.7 µm) column (Waters), using the same mobile phase described in method A. The gradient was from 30–90% B over 2 min at 0.4 mL/min, held for 2 min, and returned to the initial conditions and held for 1 min to equilibrate the system. The injection volume was 2 µL and the column and sample temperatures were 25 °C and 6 °C, respectively.

6.3.7. NMR experiments

Structures were determined by analysis of ^1H, COSY, TOCSY, NOESY, ROESY, HSQC and HMBC, ^{13}C and DEPT135 NMR spectra. Samples of **4**–**10** (~ 0.1 mg) were dissolved in ~ 0.5 mL CD_3OD at 30 °C, and chemicals shifts were referenced to internal CHD_2OD (3.31 ppm) or CD_3OD (49.0 ppm). Single- or double-frequency pre-saturation of solvent resonances was performed using continuous wave and/or excitation sculpting, as required.

Quantitation of **1** and **4**–**10** was performed on aliquots of the purified compounds by dissolving in CD_3OH.[34] The samples were run against external standards of caffeine dissolved in H_2O (4.10 mM) as described previously for AZA certified reference materials.[35]

6.3.8. Toxins and other materials

All solvents (pesticide analysis grade) were from Labscan and Caledon. Distilled H_2O was further purified using a Barnstead nanopure diamond UV purification system (Thermo Scientific). Sodium chloride (99+%), triethylamine (99%), ammonium acetate (97+%), ammonium formate (reagent grade), formic acid (>98%), silica gel (10–40 µm, type H), sodium chloride (99+%), sodium periodate, Trace CERT caffeine and CD_3OD (100.0 atom-% D) were from Sigma–Aldrich. Sephadex LH-20 was from GE Healthcare, LiChroprep RP C8 (25–40 µm) was from Merck, Luna Phenyl-Hexyl (15 µm) was from Phenomenex, CD_3OH (99.5 atom-% D) for qNMR was from Cambridge Isotope Laboratories. AZA CRMs were obtained from the National Research Council of Canada.

6.3.9. Toxicology

Cell Culturing. Human Jurkat E6-1 T lymphocyte cells (American Type Culture Collection TIB-152) were grown as described by Twiner et al.[36] Briefly, cells were grown in RPMI medium (cat. #11875-093, Invitrogen) supplemented with 10% (v/v) fetal bovine serum (FBS; cat. #26140, Invitrogen) and maintained in a humidified incubator (Sanyo 18AIC-UV) with 5% CO_2 in air at 37 °C. Cells were subcultured with fresh medium at an inoculum ratio of 1:4 every 3 to 4 days by transferring 2.5 mL of cells to 7.5 mL of fresh supplemented medium in 75 cm^3 screw cap culture flasks.

Cytotoxicity Assay. To determine the effect of **1, 4**–**6** and **8**–**10** on cellular toxicity, Jurkat T lymphocyte cells were continuously exposed to toxins and viability determined. The non-adherent human cell line Jurkat T lymphocyte (ATCC cat. # TIB-152) was grown in RPMI medium supplemented with 10% (v/v) fetal bovine serum (FBS). Cells were maintained in humidified 5% CO_2 in air at 37 °C and subcultured with fresh medium at an inoculum ratio of 1:10 every 5 to 7 days by transferring 1 mL of cells to 9 mL of fresh supplemented medium in 75 cm^2 screw cap culture flasks. Cells were seeded in a volume of 100 μL of the supplemented medium at a density of 35,000 cells per well in black, sterile, 96-well culture plates for 24 h to allow for recovery and settling. Each AZA was added at a single concentration (10 nM) for 24, 48, or 72 h of continuous exposure prior to assessment of cytotoxicity. Parallel controls of equivalent amounts of MeOH/phosphate buffered saline were used to normalize the viability data for each treatment. Cellular viability/cytotoxicity was assessed using the 3-(4,5-dimethylthiazol-2-yl)-5-(3-carboxymethoxyphenyl)-2-(4-sulfophenyl)-2H-tetrazolium (MTS) assay (Promega Biosciences). Like other tetrazolium-based assays, MTS in the presence of an electron coupling reagent (phenazine methosulfate; PMS) measures cellular viability by determining the activity of mitochondrial dehydrogenase.[37] As a substrate for dehydrogenases, MTS becomes reduced into a soluble, purple dye that can be quantitated colourimetrically to determine the relative level of cellular viability/cytotoxicity per well. Following exposure of the cells to the AZA analogues for the specified period of time, each well received 10 μL of a PMS/MTS (1:20) solution. Cells were incubated for 4 h, after which absorbance readings at 485 nm were obtained using a FluoStar microplate reader (BMG Lab Technologies). Data are presented as means ± SE of three to five separate experiments (n=3–5). In addition, each cytotoxicity experiment was performed using duplicate wells.

Cytotoxicity data were blank-corrected and normalized to the control (% viability) and plotted using GraphPad Prism (ver. 5.0c).

6.4. Results and discussion

The isolation of **6** has previously been described.[22] Hydroxylated analogues **4**, **5** and **7**–**10** are less lipophilic than **1**–**3** and **6**, and therefore eluted earlier (Figure 6.5) and were more difficult to separate from the other contaminants in the sample. In the initial semi preparative step **4** and **5** and **7**–**10** were collected as two separate fractions. Individual analogues were separated in a second chromatographic step, while a third was required to achieve sufficient purity for NMR spectroscopy. The amounts purified ranged from ~ 100–200 µg. Each analogue also contained its corresponding 37-epimer (~ 2–15%) as recently reported.[23] Sufficient purity for the cytotoxicity assay was achieved for all AZAs except for **7** (purity ~ 63%), which was contaminated with **5** and another hitherto unreported AZA (~ 20%) with a molecular mass of 825 Da, which was also detected in the initial hepatopancreas extract. Compounds **4**, **5**, **6, 8** and **10** all had purities (including the 37-epimers) of > 95%, while **9** had a purity of 89%.

6.4.1. Structure determination

The AZAs isolated in this study showed typical AZA fragmentation patterns – a molecular ion, retro Diels Alder (RDA) and *m/z* 362 fragments, all of which appeared in clusters, indicative of several H_2O losses. Structure assignments for **4** and **5** have been published based on ^{1}H NMR, fast atom bombardment (FAB) MS[21] and high resolution MS/MS.[12] The data showed C-3 and C-23 hydroxylation for **4** and **5**, respectively. These analogues were suggested to be bioconversion products of **3**.[25]

Postulated structures for **7**–**10** have been published based solely on high resolution MS/MS. Compounds **7** and **9** were proposed to be hydroxylated at C-3.[12] C-3 hydroxy analogues show fragments within the molecular ion cluster indicative of a loss of CO_2 followed by several H_2O losses. The presence of a fragment peak at *m/z* 408 strongly

suggested hydroxylation at C-23 for **8** and **10**.[12] Analogues **7** and **8** are proposed to be bioconversion products of **1**, while **9** and **10** are believed to be bioconversion products of **2**.[25] The MS/MS data in this study supported the previously proposed structures.

LC-MS analysis showed that treatment of **7**−**10** with periodate yielded C-20–C-21-cleavage products at *m/z* 448.4 for 7 (same for **1** and **2**), *m/z* 464.4 for **8**, *m/z* 434.4 for **9** (same for **3** and **6**) and *m/z* 450.4 for **10** (same for **5**).

The analogues were subjected to a thorough series of 1- and 2D NMR experiments to verify their postulated structures. We also determined ^{13}C assignments for **4** and **5**, whose structures have previously been based only on ^{1}H NMR data together with oxidative cleavage of **4** and chiral synthesis of the resulting C-1 to C-4 cleavage product. This facilitated comparison of a full set of ^{13}C and ^{1}H NMR assignments for **7** and **8**–**10** (Table 6.1).

Structure elucidation was done using 1- and 2-dimensional homonuclear ^{1}H, ^{13}C and heteronuclear ^{1}H{^{13}C} NMR spectroscopy to assign the ^{1}H and ^{13}C resonances, the chemical shifts of which were then compared with the published ^{1}H and (for **1**–**3** and **6**) ^{13}C NMR data for **1**–**6**.[19–22] The majority of chemical shifts in Table 6.1 are taken from 1-dimensional NMR spectra but some chemical shifts were taken from 2-dimensional spectra where necessary due to weak or overlapping signals. All samples inevitably contained low percentages of the corresponding 37-epimer,[23] but this did not interfere with NMR analyses and is not discussed further. Other minor AZAs were sometimes present as contaminants in the samples but not at levels sufficient to prevent spectrometric analysis. ^{1}H NMR assignments for **4** and **5** closely paralleled those of Ofuji et al.,[21] apart from variations[23] attributable to the degree of protonation on the amino group. The ^{13}C and ^{1}H chemical shifts for the 22-positions of **4**, **5** and **9** were markedly different to those reported for **6** (39.0, and 2.13 (2H) ppm),[22] however

examination of the original data indicates that these signals resonate at 31.5 ppm and at 1.50 and 2.10 ppm. This is in accord with the published NMR data for **3**,[20] as well as that presented here for **4**, **5**, and **9**.

In accord with structures previously proposed on the basis of mass spectrometric data,[12] NMR spectrometric analysis demonstrated that **4**, **7** and **9** were 3-hydroxylated congeners of **3**, **1** and **6**, respectively (Figure 6.1). Although it is not possible to determine the configuration at C-3 from ROESY correlations and coupling constants, **4** has been shown to be 3*R*-hydroxyazaspiracid-3 by degradation reactions and synthesis of the degradation products.[21] Compounds **7** and **9** showed the same pattern of chemical shifts (Table 6.1), coupling constants and ROESY correlations as for **4**, strongly suggesting that all three congeners possess the same configuration at C-3. This is consistent with their biogenesis in mussels via enzymatic oxidations and decarboxylations of **1** and **2** produced by dinoflagellates.

NMR spectrometric analysis of **5**, **8** and **10** showed that these were 23β-hydroxylated congeners of **3**, **1** and **6**, respectively (Figure 6.1). The relative configuration of the E-rings of **5**, **8** and **10** were established from coupling constants (from ^{1}H and SELTOCSY spectra) and ROESY correlations (Figure 6.2). As **5**, **8** and **10** are produced in mussels by enzymatic oxidations and decarboxylations of **1** and **2** biosynthesized by dinoflagellates, it follows that their absolute configurations are as shown in Figure 6.1.

Examination of the assignments within Table 6.1, and comparison with NMR assignments for **1**–**3**[19,20] and **6**[22] obtained under the same conditions and calibrated identically, reveals diagnostic effects on chemical shifts arising from the hydroxylations and methylations of the azaspiracid skeleton. Hydroxylation at C-3 leads to not only to marked changes in the C-3 and H-3 resonances, but also to significant changes (≥

~1 ppm for ^{13}C, ≥ ~0.05 ppm for ^{1}H) to the nearby C-2, C-4, H-2, H-5 and H-six resonances. Similarly, hydroxylation at C-23 leads to consistent alterations in the chemical shifts of C-22–C-25 and H-22–H-25 as well as the appended 22- (if present) and 24-methyl groups in the E-ring. Addition of a methyl group at C-8 also results in characteristic changes to the C-7–C-9 and H-6–H-9 resonances. Similarly, the presence or absence of a 22-methyl has characteristic pronounced effects on the chemical shifts of C-22–C-24 and H-22 and H-23. The previously reported effect attributed to the state of ionization of the amino group[23] is evident in Table 6.1, leading to systematic changes to most of the resonances of rings F–I (C-35, C-37–C-40, H-29, H-31–H-40, and the 37- and 39-methyl groups). This effect is also observable on a number of remote resonances (H-18, H-19 and the olefinic methylene at C-26), consistent with molecular modelling and ROESY correlations indicating the F–I-ring-system to be folded over in such a way that the amino group is near H-19, so that **1**, **2**,[23] **4**, **5** and **7**–**10** all showed ROESY correlations between H-19 and H-40_{eq}. Knowledge of these consistent substituent effects on the AZA skeleton will be helpful during NMR structure analysis of other AZA congeners and metabolites.

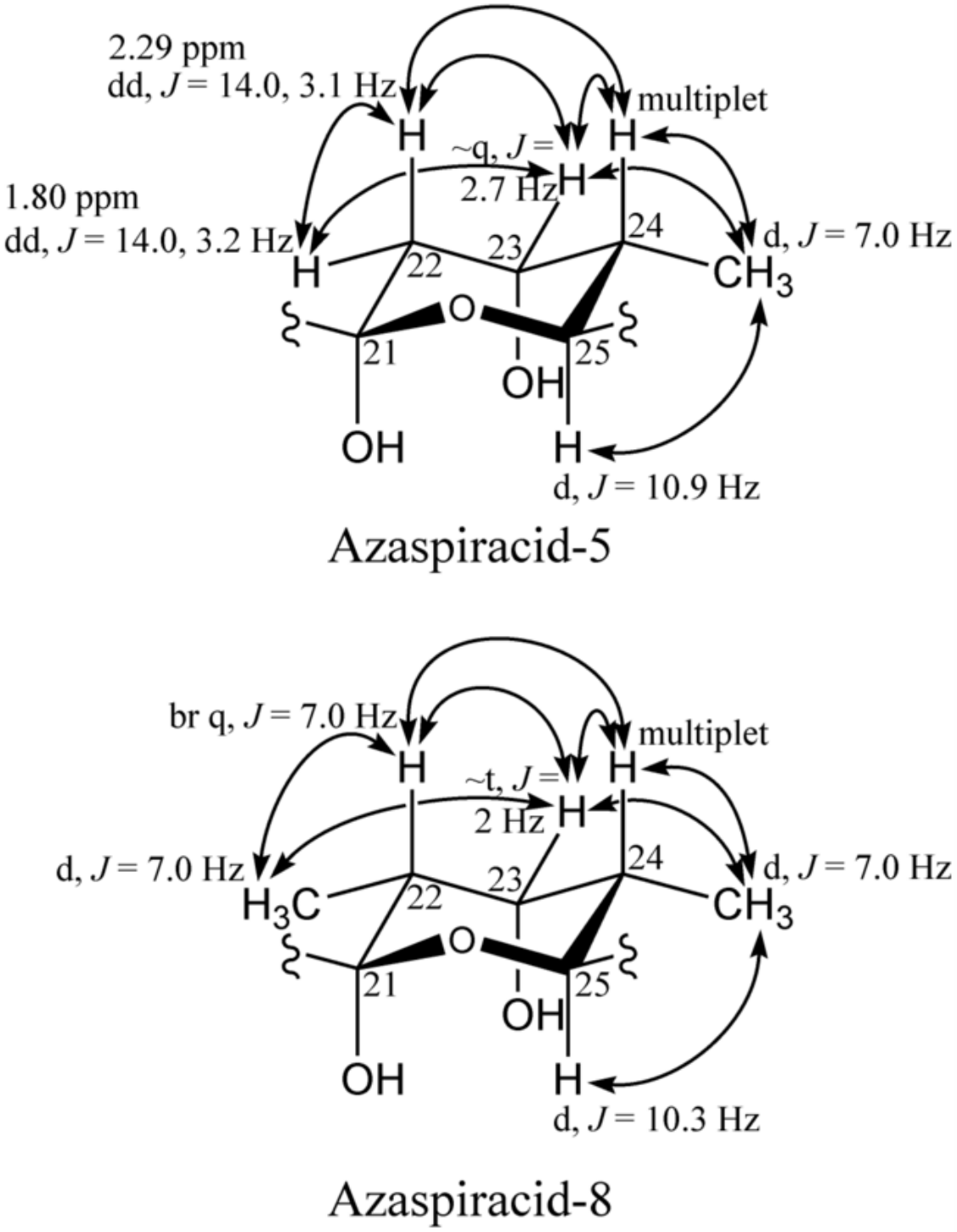

Figure 6.2. Structures for the E-rings of **5** (top) and **8** (bottom), showing dispositions of substituents. Observed ^{1}H-^{1}H coupling constants, and correlations (arrows) observed in the ROESY NMR spectra, are also shown.

Table 6.1. NMR Assignments for **4**, **5** and **7−10** in CD_3OH.

Position	**4**		**5**		**7**		**8**		**9**		**10**	
	^{13}C	^{1}H	^{13}C	^{1}H	^{13}C	^{1}H	^{13}C	^{1}H	^{13}C	^{1}H	^{13}C	^{1}H
1	179.9		181.7		179.7		181.6		179.9		181.5	
2	45.3	2.32, 2.36	38.5	2.23, 2.23	45.3	2.32, 2.36	38.5	2.23, 2.23	45.2	2.32, 2.36	38.6	2.22, 2.22
3	70.4	4.42	30.4	2.32, 2.32	70.5	4.43	30.4	2.33, 2.33	70.5	4.42	30.4	2.32, 2.32
4	135.0	5.77	133.9	5.75	135.0	5.77	133.9	5.75	134.7	5.75	133.6	5.72
5	130.5	5.67	130.6	5.43	130.5	5.68	130.6	5.43	131.0	5.65	131.0	5.40
6	71.8	4.86	72.5	4.79	71.8	4.86	72.5	4.79	72.0	4.79	72.7	4.72
7	129.0	5.67	129.4	5.64	129.0	5.66	129.5	5.64	122.6	5.37	123.1	5.34
8	123.4	5.74	123.2	5.73	123.4	5.74	123.2	5.72	131.2		131.0	
9	35.8	2.12, 2.48	35.7	2.11, 2.47	35.8	2.13, 2.48	35.7	2.12, 2.48	40.4	1.98, 2.42	40.4	1.96, 2.42
10	107.1		107.2		107.1		107.2		107.4		107.4	
11	33.2	1.65, 2.31	33.2	1.63, 2.32	33.2	1.65, 2.31	33.2	1.64, 2.33	33.3	1.64, 2.32	33.3	1.63, 2.32
12	37.6	1.96, 2.15	37.5	1.95, 2.13	37.6	1.96, 2.15	37.5	1.96, 2.13	37.5	1.97, 2.16	37.4	1.96, 2.15
13	111.3		111.3		111.3		111.3		111.2		111.2	
14	30.9	2.01	31.0	2.00	30.9	2.03	31.0	2.01	31.0	2.00	31.0	1.99
15	32.7	1.74, 1.83	32.6	1.75, 1.83	32.7	1.75, 1.83	32.6	1.76, 1.83	32.7	1.73, 1.82	32.6	1.73, 1.82
16	77.9	3.92	78.0	3.90	78.0	3.90	78.2	3.89	77.9	3.91	78.0	3.90
17	73.3	4.18	73.1	4.20	73.1	4.19	73.2	4.22	73.1	4.16	73.1	4.17
18	38.4	1.99, 2.06	38.2	2.00, 2.00	38.7	2.00, 2.04	37.9	2.00, 2.00	38.4	2.00, 2.06	38.2	2.01, 2.01
19	79.8	4.41	79.4	4.38	79.3	4.41	78.9	4.38	79.6	4.41	79.3	4.38
20	80.2	3.29	79.3	3.49	77.3	3.48	76.7	3.77	80.2	3.30	79.4	3.50
21	97.9		99.5		99.8		102.2		97.8		99.5	
22	31.9	1.51, 2.11	38.5	1.80, 2.29	36.1	2.28	40.0	2.18	31.9	1.51, 2.11	38.5	1.80, 2.28
23	29.4	1.58, 1.62	71.1	3.93	38.7	1.41, 1.41	76.5	3.60	29.4	1.58, 1.62	71.1	3.93
24	39.5	1.33	45.5*	1.48	42.0	1.36	46.7	1.49	39.5	1.33	44.5	1.48
25	80.6	3.96	74.1	4.35	79.7	3.92	73.6	4.33	80.5	3.96	74.1	4.36

26	147.2		147.6		148.0		148.0		147.1		147.5	
27	48.5	2.17, 2.36	48.9	2.23, 2.42	49.3	2.15, 2.35	49.3	2.24, 2.43	48.5	2.17, 2.36	48.9	2.23, 2.42
28	98.0		98.5		98.0		98.6		98.1		98.5	
29	44.3	1.33, 1.98	44.2	1.37, 2.05	44.8	1.30, 1.97	44.3	1.36, 2.06	44.4	1.33, 1.98	44.2	1.37, 2.05
30	26.7	2.24	26.5	2.25	26.7	2.24	26.4	2.24	26.7	2.25	26.5	2.25
31	35.8	1.48, 1.77	35.5	1.52, 1.82	35.9	1.47, 1.77	35.4	1.52, 1.83	35.8	1.48, 1.78	35.5	1.51, 1.81
32	72.7	4.24	72.8	4.33	72.9	4.23	72.9	4.35	72.7	4.24	72.8	4.33
33	79.3	3.72	79.3*	3.93	79.4	3.72	81.2	4.01	79.4	3.72	79.7	3.93
34	75.6	4.80	75.2	4.94	75.5	4.79	75.0	4.99	75.6	4.80	75.2	4.94
35	43.1	1.90, 2.38	42.2*	2.29, 2.52	43.0	1.90, 2.38	41.8	2.42, 2.56	43.1	1.90, 2.39	42.1	2.11, 2.52
36	95.9		96.4		96.0		96.5		95.9		96.4	
37	37.9	1.74	36.5*	1.88	37.7	1.74	36.0	1.93	37.9	1.75	36.5	1.88
38	40.0	1.14, 1.54	38.2*	1.24, 1.63	39.9	1.14, 1.53	38.0	1.27, 1.65	40.0	1.14, 1.54	38.6	1.24, 1.63
39	31.7	1.66	30.8*	1.83	31.8	1.65	29.6	1.88	31.7	1.66	30.3	1.83
40	47.8	2.51, 2.57	46.2*	2.74, 2.74	47.5	2.48, 2.52	46.3	2.77, 2.82	47.8	2.51, 2.57	46.3	2.74, 2.74
14-Me	16.7	0.938	16.6	0.941	16.7	0.942	16.6	0.944	16.7	0.927	16.6	0.930
22-Me					16.5	0.890	13.7	1.097				
24-Me	18.2	0.819	14.7	0.918	18.1	0.813	14.9	0.924	18.2	0.818	14.7	0.917
26=CH_2	116.1	5.14, 5.22	117.1	5.21, 5.35	115.3	5.09, 5.25	117.1	5.20, 5.39	116.1	5.14, 5.23	117.0	5.21, 5.35
30-Me	23.9	0.928	23.6	0.952	23.8	0.929	23.5	0.958	23.9	0.929	23.7	0.951
37-Me	16.1	0.860	15.7	0.929	16.1	0.855	15.5	0.952	16.1	0.860	15.7	0.927
39-Me	19.5	0.855	18.9	0.921	19.4	0.850	18.7	0.940	19.5	0.862	18.9	0.922
8-Me									23.0	1.70	23.0	1.69

6.4.2. Relative molar response

For the AZAs studied, differences in response factors were less significant in selected ion monitoring (SIM) mode under isocratic conditions (Table 6.2). In LC-MS/MS the mobile phase composition can influence the ionization efficiency; therefore analysis under isocratic conditions produces more accurate results. The response factor for **6** was very similar to that of **1**. Given that **6** differs from **1** only by the position of a methyl group, this is not surprising. All the hydroxylated AZAs gave lower response factors, with **7**, **9** and **10** being the lowest at ~ 0.5.

The data shows that the SRM transition selected for analysis of all the AZAs, including **6**, can significantly impact quantitation when using **1** as a calibration standard (Table 6.2). The H_2O loss transition for **6** was similar to that of **1**; however the RDA cleavage of the A-ring resulted in significantly higher response factors under both isocratic and gradient conditions. For all the other AZAs, the differences in SRM mode were even greater. The results suggest that, in the absence of standards for the hydroxylated analogues, quantitation will be most accurate in SIM mode under isocratic conditions. Even so, the concentration of hydroxylated AZAs may be significantly underestimated when AZA1 alone is used as the only analytical standard (Table 6.2).

Table 6.2. Relative (to **1**) molar responses of **4–10** by LC-MS/MS under acidic conditions.

AZA	SIM		SRM isocratic			SRM gradient		
	isocratic	gradient	H_2O loss	RDA	362	H_2O loss	RDA	362
4	0.88	0.75	0.80	0.81	0.86	0.96	0.96	1.03
5	0.77	0.70	0.55	0.47	0.47	0.61	0.54	0.53
6	0.95	0.93	1.06	1.21	1.17	1.05	1.21	1.13
7	0.45	0.40	0.37	0.33	0.37	0.40	0.37	0.40
8	0.84	0.81	0.58	0.41	0.47	0.59	0.47	0.51
9	0.53	0.49	0.45	0.48	0.61	0.50	0.53	0.68
10	0.49	0.48	0.34	0.33	0.35	0.34	0.35	0.36

6.4.3. Toxicology

All available AZA analogues tested were cytotoxic to Jurkat T lymphocyte cells in a time- and concentration-dependent manner (Figure 6.3). However, there were distinct differences in the relative potencies of each analogue as revealed by their EC_{50} values (Table 6.3). The range of EC_{50} values for the eight analogues tested in this study were 0.1 to 3.07 nM, a 31-fold range. Based on the EC_{50} values, the relative potencies were: **2**[27] > **6** > **8** ≈ **3**[27] > **1** > **4** ≈ **5** ≈ **9** >**10**. Impurities in **7** prevented it from being subjected to the Jurkat cell assay.

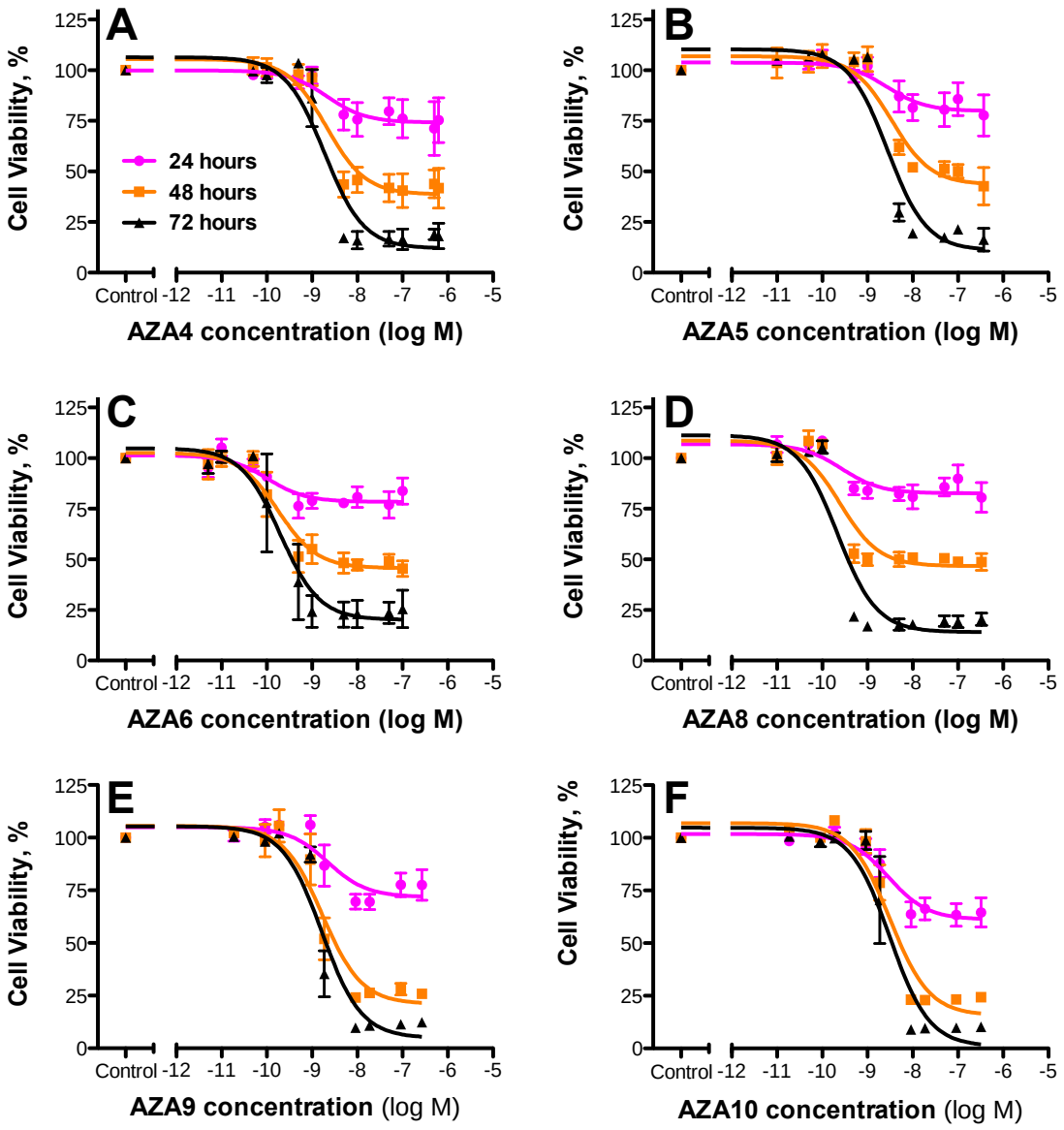

Figure 6.3. Effect of various AZA analogues on T lymphocyte cell viability. Jurkat T cells were exposed to various concentrations of (A) AZA4 (**4**), (B) AZA5 (**5**), (C) AZA6 (**6**), (D) AZA8 (**8**), (E) AZA9 (**9**), and (F) AZA10 (**10**) for 24, 48, or 72 h and viability was assessed using the MTS assay. All data (mean ± SE; n=3–5) were normalized to the control (10% MeOH vehicle). Non-linear, three parameter dose-response (variable slope) analysis was performed and EC_{50} values were calculated (Table 6.3).

In the present study, the AZAs tested represented differing sites of methylation, and hydroxylation. Collectively, SAR analysis using these data and published data for **2** and **3**[26] suggest that AZA potency was somewhat increased by methylation at C-8 and/or C-22 (i.e., **2**, **6**) whereas potency was reduced somewhat by hydroxylation at C-3 and/or C-23 (i.e., **4**, **5**) (Table 6.3, Figure 6.3). These findings allow us to speculate on the relative potencies of other analogues such as AZA12 (predicted to have relatively higher potency) and AZA13 (predicted to have relatively lower potency) based on their structures. Interestingly, reduced potencies of **4** and **5** relative to **1** in the Jurkat cell assay are the same as those determined by intraperitoneal injection in mice.[21] The utility of this *in vitro* cytotoxicity assay for relative analogue potencies (i.e., TEFs) are further corroborated by previous *in vitro* and *in vivo* studies whereby both techniques also clearly demonstrated increased potencies of **2** and **3** relative to **1**.[19,20,26] However, recent *in vivo* studies (mouse intraperitoneal and mouse oral) showed that **1** is more toxic than **2** (mouse intraperitoneal ≈ oral; TEF = 0.6−0.7) and **3** (mouse intraperitoneal = oral; TEF = 0.5).[9] Furthermore the toxicity of **6** was determined by mouse intraperitoneal for the first time and was found to be less toxic (TEF = 0.7) than **1**.[9] Although the reason for this discrepancy is unknown at this time, the highest credence should be acknowledged to oral *in vivo* studies. However, these experiments are logistically difficult to perform due to the high mass of toxins needed. Hence, further studies should be conducted to isolate more of the minor analogues to conclusively clarify their toxicological importance.

Table 6.3. Calculated EC_{50} values (nM) with 95% Confidence Intervals (CI) and relative potencies (Rel. Pot.) for AZA analogues based on T lymphocyte cytotoxicity.

AZA	24 h		48 h		72 h		Mean EC_{50}	Rel. Pot.
	EC_{50}	95% CI	EC_{50}	95% CI	EC_{50}	95% CI		
1	0.96	0.19–4.9	1.10	0.46–2.5	1.3	0.59–3.0	1.1	1.0
4	2.1	0.31–15	2.1	0.97–4.4	1.9	1.0–3.5	2.0	0.55
5	2.7	0.48–15	3.4	1.7–6.9	2.8	1.6–4.7	3.0	0.38
6	0.1	0.026–0.41	0.18	0.083–0.37	0.2	0.079–0.49	0.16	7.0
8	0.27	0.060–1.2	0.25	0.12–0.51	0.22	0.12–0.40	0.25	4.5
9	2.2	0.66–7.4	1.7	0.95–3.0	1.7	1.1–2.6	1.87	0.4
10	2.9	1.20–6.8	3.2	2.1–4.8	3.1	1.8–5.5	3.07	0.2

6.4.4. Analysis of cooked shellfish

Compounds **3**, **4**, **6** and **9** are produced by heat-induced decarboxylation of AZA17, -21, -19 and -23 respectively, and are not normally present in significant amounts in uncooked mussels.[27] As **5** and **10** are proposed to be direct bioconversion products of **3** and **6** respectively,[25] these compounds also would not be present in significant amounts in uncooked shellfish. The analysis of cooked shellfish most accurately reflects what is ingested by the consumer, and additional differences have been reported between the analysis of raw and cooked shellfish (*M. edulis*) in terms of concentration levels.[28] To determine the relative importance of **1**–**10**, raw shellfish contaminated with AZAs were heated to simulate cooking (with no water loss). LC-MS analysis with quantitative standards showed that **1**–**3** (regulated) and **6** (not regulated) were the predominant toxins in cooked mussels (Figure 6.4), however in some samples levels of **4** were higher than **6** (Table 6.5 and Figure 6.5). Levels of the metabolites were very variable, possibly due to differing rates of shellfish metabolism[25,29] and time of harvesting i.e., mussels harvested directly following an intense bloom will likely have higher levels of **1** and **2** than if they were harvested some time after the bloom (due to metabolism). The average

levels of the remaining analogues relative to **1** were low; **4**, **5** and **8** were each ~ 5%, while **7**, **9** and **10** were each under 1.5%, however there was huge variation and in some samples these analogues were present in significant amounts, particularly for **4**, **5** and **8**. (Figure 6.4 and Table 6.5).

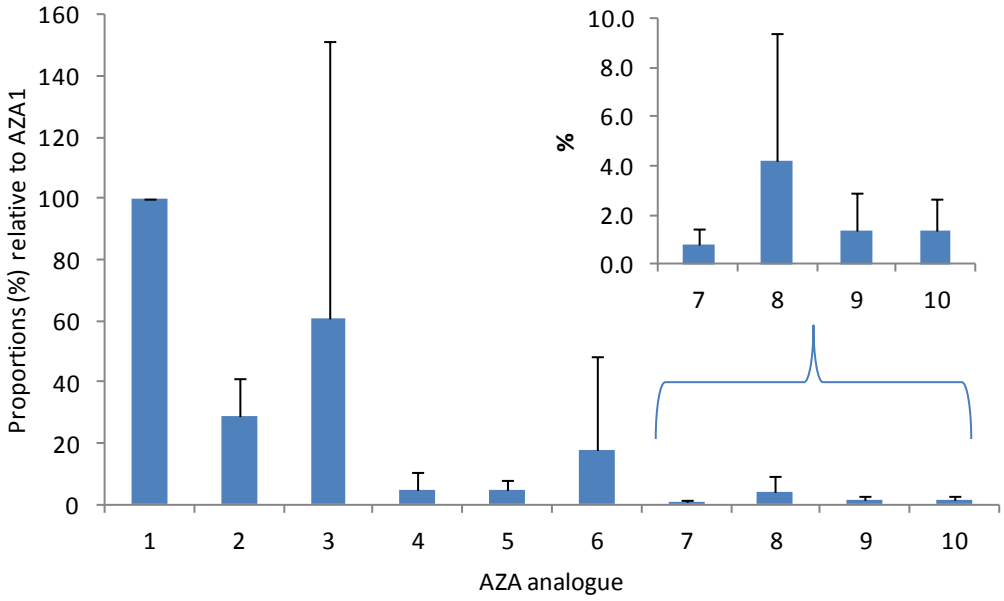

Figure 6.4. Proportions of **2**–**10** relative to **1** in cooked *M. edulis* (mean ± standard deviation; n=40), see Table 6.5.

The feeding study (of *M. edulis* with *A. spinosum*) performed by Jauffrais et al[25] showed that metabolism of **1** and **2** to AZA17 and -19, respectively is observed after 3 h with levels of these analogues increasing up to 2 days and then remaining constant up to the end of the experiment (4 days). Relative to **1** the proportions of AZA17 and -19 reached a maximum of 145% and 55% respectively while the analogues **4**, **5** and **7**–**10** accounted for ~ 58%. However, these studies were performed under laboratory conditions and the high levels of AZA accumulation observed in real life samples could not be replicated.

In this study levels of **5** and **10** increased significantly (Figures 6.5 and 6.6) after heat treatment suggesting that they are predominantly bioconversion products of AZA17 and -19 i.e., decarboxylation (at C-22) of hydroxylated (at C-23) AZA17 and -19. In the heating process enzymes responsible for hydroxylation would have been destroyed, hence it is unlikely that the observed increase in **5** and **10** levels were due to hydroxylation of **3** and **6** respectively.

Biotoxin monitoring programs operated under the EU regulatory framework must analyse raw shellfish, and typically very low levels of **3** and **6** (if monitored) are detected in such samples.[4] However, in the heat treated mussels, levels (relative to **1**) of **3** ranged widely from 11–501%, (Figure 6.4 and Table 6.4). Similarly levels (relative to **1**) of **6** ranged from 3–170% (Figures 6.4 and 6.5). In this study **6** was found to be 7-fold more potent than **1** while a mouse oral study found it to be only slightly less toxic than **1**.[9] These results highlight the degree to which AZA-toxicity can be underestimated in routine monitoring programs where raw mussels are tested, and suggest that **6** should be included in the regulation of these compounds. Previously, levels of AZA analogues other than **1**–**3** were reported to comprise less than 5%,[12] however this study indicates that the analogues **4**–**10** comprise on average 13% (ranging from 5% to 24%) of the total AZAs (**1**–**10**) in cooked shellfish. Different toxin profiles have been reported from other countries, where **2** is more predominant than **1**[17,30–32] and the shellfish from these locations are thereby more likely to contain higher levels of **6**, **10** and possibly **9**, and in such circumstances these analogues may have greater significance.

Many samples analysed as part of the Irish monitoring program which were below the regulatory limit (and subsequently marketed with no reports of human intoxications), would have been above the limit had the tissues been cooked prior to analysis (Table

6.4). This suggests that the current regulatory limit may be sufficiently low for the prevention of the acute illness associated with this toxin group.

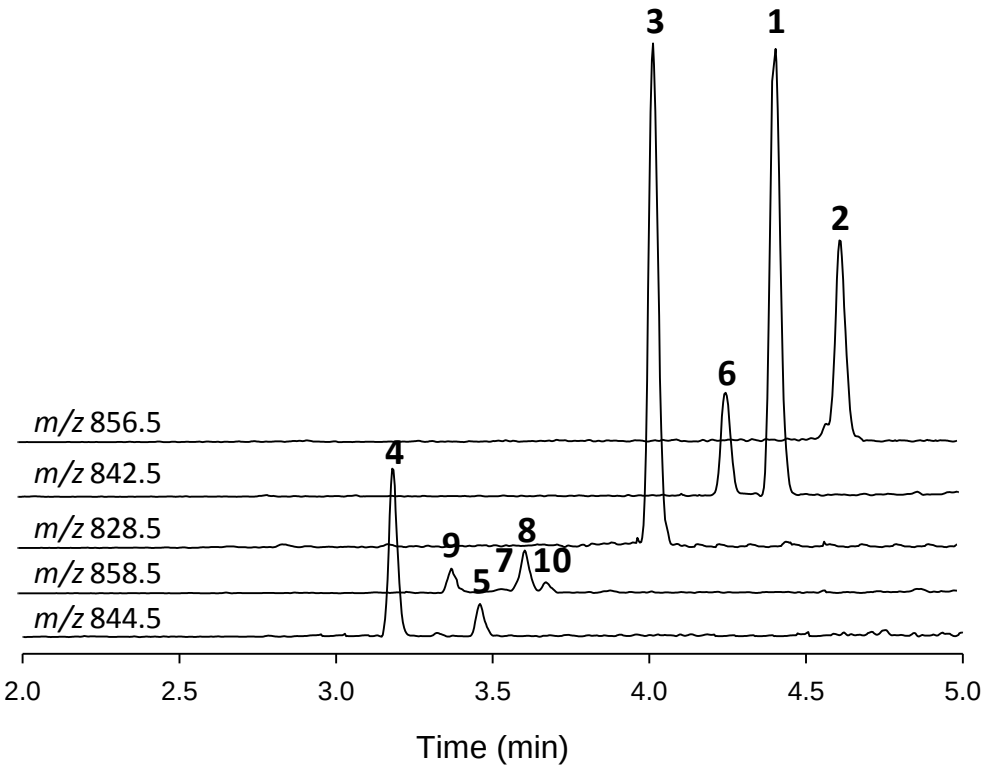

Figure 6.5. Analysis (method F) of a cooked *M. edulis* sample extract (from the Marine Institute biotoxin monitoring programme) showing peaks for AZA1–10.

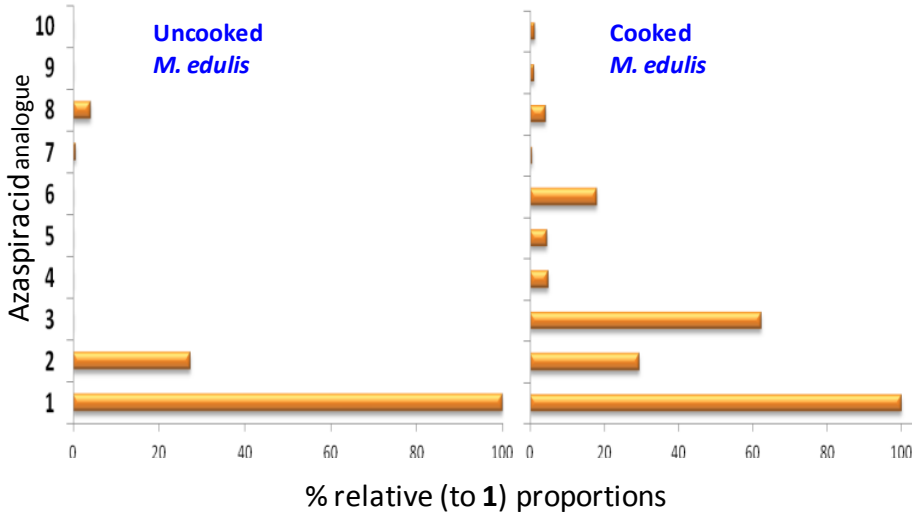

Figure 6.6. Proportions of **2**–**10** relative to **1** in uncooked and cooked *M. edulis* (n=40).

Table 6.4. Measured concentrations of **1**−**3** and **6** in Irish *M. edulis* samples before and after cooking.

Harvesting location (Irish Atlantic coast)	Harvesting date	Raw					Cooked					
		1 (µg/g)	**2** (µg/g)	**3** (µg/g)	**6** (µg/g)	***AZA equiv. (1−3) (µg/g)**	**1** (µg/g)	**2** (µg/g)	**3** (µg/g)	**6** (µg/g)	***AZA equiv. (1−3) (µg/g)**	**AZA equiv. including AZA6 (no TEF) (µg/g)**
West	26/09/2012	0.06	0.02	0.00	0.00	0.10	0.06	0.02	0.07	0.02	0.18	0.20
Southwest	27/09/2012	0.16	0.04	0.01	0.00	0.24	0.16	0.04	0.06	0.01	0.30	0.31
Southwest	27/09/2012	0.10	0.02	0.00	0.00	0.15	0.10	0.02	0.04	0.01	0.20	0.21
Northwest	27/09/2012	0.04	0.01	0.00	0.00	0.07	0.04	0.02	0.07	0.02	0.17	0.19
West	24/09/2012	0.22	0.05	0.01	0.00	0.33	0.20	0.05	0.12	0.03	0.48	0.51
West	24/09/2012	0.12	0.03	0.00	0.00	0.18	0.10	0.03	0.07	0.02	0.24	0.26
Southwest	24/09/2012	0.11	0.03	0.00	0.00	0.16	0.09	0.02	0.04	0.01	0.18	0.19
West	24/09/2012	0.03	0.01	0.01	0.00	0.07	0.03	0.02	0.14	0.04	0.25	0.29
Southwest	26/09/2012	0.08	0.02	0.00	0.00	0.12	0.08	0.02	0.03	0.00	0.16	0.17
West	24/09/2012	0.02	0.02	0.01	0.00	0.06	0.03	0.02	0.08	0.02	0.18	0.20

*AZA equivalents calculated following application of the toxic equivalent factor for **2** (1.8) and **3** (1.4) relative to **1**.
Red indicating areas where there is significant change.

Table 6.5. Proportions (%) of **2**–**10** relative to **1** (method F) in cooked *M. edulis* (n=40) harvested off the Atlantic coast of Ireland.

Harvesting location	Harvesting date	**2**	**3**	**4**	**5**	**6**	**7**	**8**	**9**	**10**	*AZA equiv. (µg/g)
West	10/12/2013	23.2	15.2	2.8	4.0	4.9	0.0	1.3	0.8	0.5	0.63
Southwest	09/12/2013	24.6	17.4	5.6	2.9	3.3	1.5	2.4	1.2	0.5	1.72
Southwest	09/12/2013	19.6	35.5	5.2	4.9	8.4	0.3	2.1	1.1	1.6	0.38
Southwest	09/12/2013	21.4	33.2	5.5	4.9	8.6	1.0	2.1	0.1	1.0	0.39
Northwest	09/12/2013	18.0	45.0	6.7	5.1	12.4	2.2	1.6	0.3	2.3	0.21
Northwest	24/10/2013	30.8	34.5	7.5	2.8	6.3	0.4	2.2	1.4	0.7	1.04
Southwest	23/10/2013	27.2	29.6	12.9	3.1	6.9	0.6	3.8	3.4	0.6	1.44
Southwest	23/10/2013	23.9	32.8	2.5	2.5	5.5	0.0	1.9	0.0	0.6	0.41
West	22/10/2013	27.2	22.1	2.4	2.8	6.1	0.0	2.1	0.2	0.0	0.19
Southwest	22/10/2013	21.9	26.5	6.6	2.6	5.9	0.5	3.6	1.5	0.8	0.32
Southwest	21/10/2013	29.2	34.9	12.2	2.9	6.7	0.8	5.3	3.1	1.1	1.10
Northwest	21/10/2013	27.8	29.7	6.0	1.9	5.8	0.8	2.3	1.3	0.5	0.91
Southwest	21/10/2013	23.8	27.1	6.1	2.1	6.0	0.5	2.6	1.9	0.7	0.94
West	21/10/2013	21.2	26.4	3.2	4.8	7.5	0.2	1.4	1.3	1.7	0.31
West	21/10/2013	22.9	14.1	2.0	2.2	4.0	0.3	1.3	0.1	1.0	0.52
Southwest	21/10/2013	25.2	16.6	1.0	1.3	2.9	0.0	1.2	0.0	0.8	0.54
Southwest	21/10/2013	26.3	41.2	5.4	3.5	9.5	1.0	4.2	0.6	1.4	0.37
Northwest	17/10/2013	29.2	34.1	7.6	2.5	6.0	0.4	2.6	2.1	0.6	0.85
Southwest	15/10/2013	28.6	46.4	13.5	3.7	8.7	0.4	5.3	3.3	1.1	0.89
[#]Southwest	15/10/2013	35.6	96.7	26.5	5.4	23.2	1.4	8.3	7.6	2.0	0.70
Northwest	14/10/2013	30.2	43.4	10.2	3.1	8.9	0.7	4.1	1.6	0.8	0.98
Southwest	14/10/2013	27.1	21.2	8.3	2.1	5.2	0.5	2.8	3.0	0.7	1.75
Southwest	13/10/2013	32.1	60.2	17.1	3.9	14.4	0.9	7.1	4.7	1.1	1.05
Southwest	01/11/2012	25.0	10.5	0.9	1.7	2.8	0.8	1.1	0.0	0.6	0.99
Southwest	27/09/2012	26.8	30.6	1.7	2.6	6.9	0.6	2.3	0.9	1.1	0.44
Southwest	27/09/2012	31.0	41.6	0.0	3.9	10.0	0.0	1.5	0.0	1.2	0.15
Northwest	27/09/2012	44.7	204.1	0.0	11.1	67.3	0.0	12.6	0.0	0.0	0.07
West	26/09/2012	33.9	114.4	2.2	6.7	30.3	1.6	0.9	0.0	6.9	0.10
Southwest	26/09/2012	23.3	37.3	0.4	3.7	10.9	0.4	1.9	0.7	2.5	0.12
Southwest	24/09/2012	22.2	36.8	0.6	3.2	11.9	3.0	1.6	0.0	2.4	0.20
West	24/09/2012	21.7	57.0	0.0	5.4	17.5	1.2	1.9	0.1	3.7	0.33
Southwest	24/09/2012	23.6	42.2	0.6	5.1	10.7	0.7	1.9	0.1	2.6	0.16
West	24/09/2012	32.4	78.4	2.4	8.1	19.1	0.0	3.3	0.0	0.0	0.18
West	24/09/2012	78.8	501.5	0.2	21.2	170.2	0.0	27.0	0.0	0.0	0.07
West	24/09/2012	70.3	330.7	0.0	9.8	103.1	0.0	19.5	1.7	0.0	0.06
Northwest	24/09/2012	49.7	127.1	0.5	12.4	55.6	0.0	13.0	0.9	0.0	0.06
West	27/08/2012	26.9	19.2	0.7	1.3	4.8	0.3	1.0	0.0	0.9	2.50
Southwest	22/09/2011	32.1	28.2	1.5	2.1	6.4	0.3	3.1	0.0	0.4	0.27
Southwest	17/11/2009	10.9	30.8	4.5	4.7	9.3	0.0	0.0	0.0	0.0	0.30
Southwest	22/07/2008	28.0	16.6	7.9	1.7	3.6	0.3	1.8	1.8	0.7	4.80
Avg %		29.4	62.3	4.9	4.5	18.0	0.6	4.1	1.1	1.2	
stdev		12.3	90.7	5.5	3.7	31.0	0.6	5.3	1.6	1.3	

* Values for raw shellfish, AZA equivalents calculated following application of the toxic equivalent factor for **2** (1.8) and **3** (1.4) relative to **1**.

[#]See Figure 6.5 for chromatogram.

6.5. Conclusions

Compounds **4**–**10** were purified from shellfish, with the structures of **7**–**10** being elucidated for the first time by NMR, which confirmed the previously postulated structures based on LC-MS/MS studies. qNMR was performed on all purified samples and subsequent LC-MS relative molar response factors and cytotoxicity were determined. Differences in the LC-MS molar responses relative to **1** were observed, particularly for the hydroxylated analogues (up to 3-fold). Greatest accuracy was achieved by analysis in SIM mode under isocratic conditions. Combining all the cytotoxicity data published to date for AZAs using the Jurkat T lymphocyte cell assay, the order of potencies are: **2** > **6** ≈ AZA34[15] ≈ 37-*epi*-**1**[23] > **8** ≈ **3** > **1** > **4** ≈ **9** > **5** ≈ **10** > AZA33.[15] Analysis of heat-treated mussels from Ireland that were naturally contaminated with AZAs revealed high levels of **3** and **6**. These compounds were not present at significant levels in the raw shellfish, highlighting the fact that AZA equivalent values for raw mussels grossly underestimate the toxicity of the AZAs present. Not only do these results suggest that tissues should be heat-treated prior to analysis, but also that **6** should be included in the regulations to more accurately reflect the toxin profile of to which shellfish consumers are exposed. Levels of analogues **4**, **5** and **7**–**10** were low in Irish mussels, and did not contribute significantly to overall toxicity, although the situation may be different for other shellfish varieties. However, in areas where **2** is the predominant AZA analogue, **6**, **9** and **10** will most likely have more relevance than in Irish mussels. This study further suggests that the current regulatory limit may be sufficiently low for protection of human health from acute AZA intoxication from Irish mussels.

6.6. References

(1) Twiner, M. J., Rehmann, N., Hess, P., and Doucette, G. J. *Mar. Drugs* **2008**, *6*, 39–72.

(2) Furey, A., O'Doherty, S., O'Callaghan, K., Lehane, M., and James, K. *Toxicon* **2010**, *56*, 173–190.

(3) Klontz, K. C., Abraham, A., Plakas, S. M., and Dickey, R. W. *Ann. Intern. Med.* **2009**, *150*, 361.

(4) HABs, database. http://www.marine.ie/home/publicationsdata/data/Habs+Search+Database/HabsSearch.htm. Accessed 14 May 2014.

(5) McMahon, T., and Silke, J. *Harmful Algae News* **1996**, *14*.

(6) Aune, A., Espenes, A., Aasen, J. A. B., Quilliam, M. A., Hess, P., and Larsen, S. *Toxicon* **2012**, *60*, 895–906.

(7) Ito, E., Satake, M., Ofuji, K., Higashi, M., Harigaya, K., McMahon, T., and Yasumoto, T. *Toxicon* **2002**, *40*, 193–203.

(8) Aasen, J. A. B., Espenes, A., Hess, P., and Aune, T. *Toxicon* **2010**, *56*, 1419–1425.

(9) Kilcoyne, J., Jauffrais, T., Twiner, M., Doucette, G., Aasen Bunæs, J. A., Sosa, S., Krock, B., Séchet, V., Nulty, C., Salas, R., Clarke, D., Geraghty, J., Duffy, C., Foley, B., John, U., Quilliam, M. A., McCarron, P., Miles, C. O., Silke, J., Cembella, A., Tillmann, U., and Hess, P. Marine Institute - Marine Research Sub-Programme (NDP 2007-2013) series, **2014** (http://oar.marine.ie/handle/10793/970).

(10) Twiner, M. J., Doucette, G. J., Rasky, A., Huang, P. X., Roth, B. L., and Sanguinetti, M. C. *Chem. Res. Toxicol.* **2012**, *25*, 1975–1984.

(11) Twiner, M. J., Hanagriff, J. C., Butler, S., Madhkoor, A. K., and Doucette, G. J. *Chem. Res. Toxicol.* **2012**, *25*, 1493–1501.

(12) Rehmann, N., Hess, P., and Quilliam, M. A. *Rapid Commun. Mass Spectrom.* **2008**, *22*, 549–558.

(13) Krock, B., Tillmann, U., John, U., and Cembella, A. D. *Harmful Algae* **2009**, *8*, 254–263.

(14) Krock, B., Tillmann, U., Voß, D., Koch, B. P., Salas, R., Witt, M., Potvin, É., and Jeong, H. J. *Toxicon* **2012**, *60*, 830–839.

(15) Kilcoyne, J., Nulty, C., Jauffrais, T., McCarron, P., Herve, F., Wilkins, A. L., Foley, B., Rise, F., Crain, S., Twiner, M. J., Hess, P., and Miles, C. O. *J. Nat. Prod*. **2014**, dx.doi.org/10.1021/np500555k.

(16) Torgersen, T., Bremnes, N. B., Rundberget, T., and Aune, T. *Toxicon* 2008, *51*, 93–101.

(17) Ueoka, R., Ito, A., Izumikawa, M., Maeda, S., Takagi, M., Shin-ya, K., Yoshida, M., Van Soest, R. W. M., and Matsunaga, S. *Toxicon* **2009**, *53*, 680–684.

(18) Anon. (2011) Commission Regulation (EU) No 15/2011 of 10th January 2011 amending Regulation (EC) No 2074/2005 as regards recognised testing methods for detecting marine biotoxins in live bivalve molluscs. L6/3-6.

(19) Satake, M., Ofuji, K., Naoki, H., James, K. J., Furey, A., McMahon, T., Silke, J., and Yasumoto, T. *J. Am. Chem. Soc.* **1998**, *120*, 9967–9968.

(20) Ofuji, K., Satake, M., McMahon, T., Silke, J., James, K. J., Naoki, H., Oshima, Y., and Yasumoto, T. *Nat. Toxins* **1999**, *7*, 99–102.

(21) Ofuji, K., Satake, M., McMahon, T., James, K. J., Naoki, H., Oshima, Y., and Yasumoto, T. *Biosci. Biotechnol. Biochem.* **2001**, *65*, 740–742.

(22) Kilcoyne, J., Keogh, A., Clancy, G., LeBlanc, P., Burton, I., Quilliam, M. A., Hess, P., and Miles, C. O. *J. Agric. Food Chem.* **2012**, *60*, 2447–2455.

(23) Kilcoyne, J., McCarron, P., Twiner, M. J., Nulty, C., Wilkins, A. L., Rise, F., Quilliam, M. A., and Miles, C. O. *Chem. Res. Toxicol.* **2014**, *27*, 587–600.

(24) Krock, B., Tillmann, U., Witt, M., and Gu, H. *Harmful Algae* **2014**, *36*, 22–28.

(25) Jauffrais, T., Marcaillou, C., Herrenknecht, C., Truquet, P., Séchet, V., Nicolau, E., Tillmann, U., and Hess, P. *Toxicon* **2012** *60*, 582–595.

(26) Twiner, M. J., El-Ladki, R., Kilcoyne, J., and Doucette, G. J. *Chem. Res. Toxicol.* **2012**, *25*, 747–754.

(27) McCarron, P., Kilcoyne, J., Miles, C. O., and Hess, P. *J. Agric. Food Chem.* **2009**, *57*, 160–169.

(28) Hess, P., Nguyen, L., Aasen, J., Keogh, M., Kilcoyne, J., McCarron, P., and Aune, T. *Toxicon* 2005, *46*, 62–71.

(29) Salas, R., Tillmann, U., John, U., Kilcoyne, J., Burson, A., Cantwell, C., Hess, P., Jauffrais, T., and Silke, J. *Harmful Algae* **2011**, *10*, 774–783.

(30) Taleb, H., Vale, P., Amanhir, R., Benhadouch, A., Sagou, R., and Chafik, A. *J. Shell. Res.* **2006**, *25*, 1067–1071.

(31) Vale, P., Bire, R., and Hess, P. *Toxicon* **2008**, *51*, 1449–1456.

(32) López-Rivera, A., O'Callaghan, K., Moriarty, M., O'Driscoll, D., Hamilton, B., Lehane, M., James, K. J., and Furey, A. *Toxicon* **2010**, *55*, 692–701.

(33) McCarron, P., Giddings, S. D., and Quilliam, M. A. *Anal. Bioanal. Chem.* 2011, *400*, 835–846.

(34) Burton, I., Quilliam, M. A., and Walter, J. A. *Anal. Chem.* **2005**, *77*, 3123–3131.

(35) Perez, R., Rehmann, N., Crain, S., LeBlanc, P., Craft, C., MacKinnon, S., Reeves, K., Burton, I., Walter, J. A., Hess, P., Quilliam, M. A., and Melanson, J. *Anal. Bioanal. Chem.* **2010**, *398*, 2243–2252.

(36) Twiner, M. J., Hess, P., Bottein Dechraoui, M.-Y., McMahon, T., Samons, M. S., Satake, M., Yasumoto, T., Ramsdell, J. S., and Doucette, G. J. *Toxicon* **2005**, *45*, 891–900.

(37) Mosmann, T. *J. Immuno. Methods* **1983**, *65*, 55–63.

CONCLUSIONS AND FUTURE WORK

7.1. Conclusions

Matrix effects were assessed on two LC-MS/MS instruments – a TSQ and a QToF. Matrix interferences were observed on both instruments but interestingly the type of interferences were quite different despite the fact that there were no differences in the type of source (ESI) nor in the methods of analysis (one theory is that matrix interferences occur in the source). Matrix suppression was observed for the AZAs on the TSQ (with the degree of suppression changing between shellfish varieties), while matrix enhancement was observed for OA on the QToF. The matrix suppression on the TSQ was overcome by changing the pH of the mobile phase from acidic (pH = 2.5) to alkaline (pH = 11) but also by extending the run time such that the column could be flushed with organic solvent to flush out any late eluting compounds. The matrix enhancement on the QToF was eliminated by the use of an on-line SPE method and by the use of matrix matched standards (since there was no significant difference in matrix effect between shellfish varieties). These methods were implemented in the routine monitoring programme at the MI to ensure accuracy of results being reported.

An isolation procedure from shellfish was adapted and improved such that recoveries increased ~ 2-fold. Using this procedure AZA6, 37-*epi*-AZA1 and AZA7−10 were isolated, subsequently characterised and assessed for toxicity for the first time. The previously proposed structure for AZA6−10, based on LC-MS/MS analysis, was confirmed by NMR.

A method was further developed for the isolation of AZAs from bulk cultures of *A. spinosum*. Using this method the novel AZAs, AZA33 and -34 were purified, characterised and assessed for toxicity.

Using the purified AZAs isolated as part of this PhD both *in vitro* and *in vivo* toxicity studies were performed (as part of the ASTOX 2 project) confirming AZA toxicity. The results from the oral and intraperitoneal mice studies correlated very well, contradicting previous reports and showing that AZA1 is more toxic than AZA2 (TEF = 0.6) and -3 (TEF = 0.5). An *in vivo* (mouse intraperitoneal) study was additionally performed for AZA6 and it was found to be slightly less toxic than AZA1 (TEF = 0.7). Additional studies looking at the combined effects of AZA1 with OA and YTX showed that there is no increased toxicity when these groups co-occur.

In vitro toxicity analysis was performed using the Jurkat T lymphocyte cell assay (Table 7.1) and demonstrated the following potencies: AZA2 > AZA6 > AZA34 ≈ 37-*epi*-AZA1 > AZA8 ≈ AZA3 > AZA1 > AZA4 ≈ AZA9 > AZA5 ≈ AZA10 > AZA33. The results indicate AZA potency is gained by methylation of C-8 and/or C-22 (AZA2, -6, -8) while AZA potency is reduced by C-3 and/or C-23 hydroxylation (AZA4, -5, -9, 10). AZA33 (AZA1 missing A/B/C rings) was less potent than AZA1 (~5-fold), whereas AZA34 (AZA1 missing C-4/C-5 alkene) was 5.5-fold more potent. Similarly, 37-*epi*-AZA1 was 5.1-fold more potent than AZA1.

In addition to the above mentioned analogues, AZA1–3 were also purified in sufficient quantities for the preparation of CRMs (to ensure a sustained supply). Bulk culturing of the producing organisms and improvements in isolation procedures have enabled more effective purification of a range of AZA analogues. In this study reference standards were prepared for 16 AZA analogues (Table 7.1) enabling the relevance of these analogues to be established, in terms of proportions and toxicity. Proportions were determined in AZA contaminated shellfish that were submitted to the biotoxin national monitoring programme. Previous studies showed that levels of AZA3, -4, -6 and -9 can increase when shellfish are cooked due to decarboxylation of AZA17, -21, -19 and -24

respectively. These results were confirmed in this study. Levels of AZA3 and -6 ranged widely probably due to the different rates of AZA1 and -2 metabolism (oxidation of methyl at C-22 to produce the carboxy analogues AZA17 and -19 respectively) in the mussels tested. However, in some samples the proportions of AZA3 and -6 were 3-fold those of AZA1 and -2 respectively. These results highlight the degree to which AZA equivalents are underestimated in routine monitoring programs where uncooked shellfish are tested, and suggest that AZA6 should be included in the AZA regulation. Levels of the 37-epimers were also found to be significant in terms of human health protection.

7.2. State of the art

Over the course of the ASTOX 2 project ten additional *Azadinium* and related species have been identified from samples taken from European (Ireland, Britain, Scandinavia, Iceland, Greenland, Italy), Asian (China, Korea) and South American (Argentina) waters. Some of these species are producers of novel AZAs, whilst others do not appear to produce any AZAs. Interestingly, different strains of the same species (*A. poporum*) were found to have very different toxin profiles, some producing novel AZAs, whilst others were found to produce either known AZAs or none at all. During the project a molecular probe was developed capable of detecting and distinguishing between *A. spinsoum*, *A. obesum* and *A. poporum*. These probes currently contribute to the monitoring programme at the Marine Institute, enabling effective detection and forecasting of blooms which otherwise are difficult to detect.

Feeding studies performed as part of the ASTOX 2 project with *A. spinosum* showed that mussels will feed directly on these organisms with no requirement for a vector

species. Mussels reached the regulatory limit after 5 days; however, the high concentrations observed in the wild could not be replicated under laboratory conditions. This may indicate: (i) that vectors are required to facilitate shellfish toxin accumulation (e.g., *Favella ehrenbergii* which has been shown to actively feed on *A. spinosum*); (ii) longer term feeding trials are required or (iii) other variables, as yet unknown, contribute to high uptake of toxins. The laboratory studies also showed that *A. spinosum* has a negative effect on shellfish in terms of mortality rates, feeding behaviour and physiology. Additionally, these studies showed that mussels take up AZAs from the dissolved phase and therefore the release of AZAs from decaying blooms may also have consequences for other species, not normally associated with these toxins.

Both calibrant and tissue CRMs are available for AZA1–3, which were produced as part of the ASTOX project. Replacement stocks have recently been prepared to keep with demand using the purified toxins produced as part of this thesis.

The heat-induced transformation of AZA17 and -19 into AZA3 and -6, respectively, was confirmed in the project. Using the RMs produced, the relevance of some of the minor and novel AZAs were determined, highlighting AZA6 as a potential significant contributor to overall toxicity. The other purified analogues for which RMs were prepared were found to be of less significance. The importance of other novel AZA analogues identified in the project, such as those which lack a methyl group in the amino ring, have yet to be established.

The *in vitro* and *in vivo* toxicity studies performed to date confirm AZA toxicity. Studies on mini pigs showed that these animals are less susceptible to AZAs than humans, and that AZAs cross the intestinal barrier and distribute throughout the body causing internal organ damage at cellular and tissue levels. The results from the oral and intraperitoneal mice studies carried out as part of the ASTOX 2 project correlated very

well, contradicting previous reports and showing that AZA1 is more toxic than AZA2 and -3. These results were reflected in the analysis of the mini pig blood samples that showed AZA1 is most rapidly taken up into the blood, followed by AZA2 and then -3. Studies looking at the combined effects of AZA1 with OA and YTX showed that there is no increased toxicity when these groups co-occur. The *in vitro* studies were effectively used to assess the toxicity of the minor analogues and demonstrated the following potencies: AZA2 > AZA6 > AZA34 ≈ 37-*epi*-AZA1 > AZA8 ≈ AZA3 > AZA1 > AZA4 ≈ AZA9 > AZA5 ≈ AZA10 > AZA33 ≈ AZA36 > AZA37 > AZA26.

The mode of action of AZAs has remained elusive for some time. Recent studies by Twiner *et al* have shown that AZAs are potassium channel blockers, however the concentrations required to induce such effects are 2-fold those required to cause cytotoxicity and therefore this is not considered to be the primary mode of action. Hence other modes of action need to be explored and it is likely that the various analogues may exhibit unique modes of action and/or receptors.

7.3. Future work

Although much has been learned about this toxin group in recent years thanks to projects such as ASTOX and ASTOX 2, there still remains many unanswered questions and ongoing research. Future work should focus on the following areas to protect the shellfish industry and allow relevant authorities to more accurately assess the impacts of these toxins on human health and the marine environment.

- There is a strong need for high quality CRMs as monitoring and research laboratories move away from animal based assays towards chemical methods of

analysis. Replacement stocks of the regulated AZAs are now available due to the work performed as part of this thesis; however, these stocks are limited and depending on demand may only last a few years. Stocks of RMs are additionally required for some of the unregulated AZA toxins (e.g., AZA6). This issue is fast becoming problematic not only due to the increasing intensity and distribution of these toxic blooms but also due to increasing detection of novel phytoplankton species producing novel toxins. Future work will include the isolation of these novel AZAs. The availability of RMs for as many of these analogues as is possible will enable effective monitoring, the development of rapid assay test kits, more in depth toxicological studies and determination of the mode of action.

- The development of early warning system for the aquaculture industry and monitoring laboratories is required to limit losses for the industry. Mapping of these species using gene probes at sea and development of *in situ* biosensors will assist in this process.
- An assessment of the relevance of the additional species/toxins to the shellfish industry and human health is required in terms of shellfish (and other species) populations and development, prevalence and accumulation in shellfish and toxic effects on humans.
- It is still not fully understood how mussels may become so highly contaminated in the field. ASTOX 2 studies have shown only limited accumulation occurs when mussels are fed *A. spinosum*. Additionally, the shellfish are adversely affected by this species. Knowledge of feed and environmental factors and what additional vectors could be involved would aid in developing mitigation strategies.

- More toxicological and epidemiological data is required. AZAs are suspected carcinogens; therefore more long term exposure studies need to be performed. The primary mode of action needs to be determined to enable the development of an effective antidote.
- There is the potential for some of the *Azadinium* and related species to be producers of novel compounds with therapeutic effects, potentially with effects antagonistic to those by AZAs. Full knowledge of their molecular targets may lead to these compounds having a positive impact.
- It is important to know how AZAs behave when consumed i.e., only accounting for less than 30% of what had been administered following mouse and pig studies. Studies performed to date have not identified any AZA metabolites in these animals. Such knowledge will reveal how organisms process and eliminate AZAs following exposure, with the potential for interspecies extrapolation (including humans) and may lead to an understanding of the molecular mechanisms involved.

Table 7.1. List of AZA analogues purified and characterized, their protonated masses, origin and toxicity.

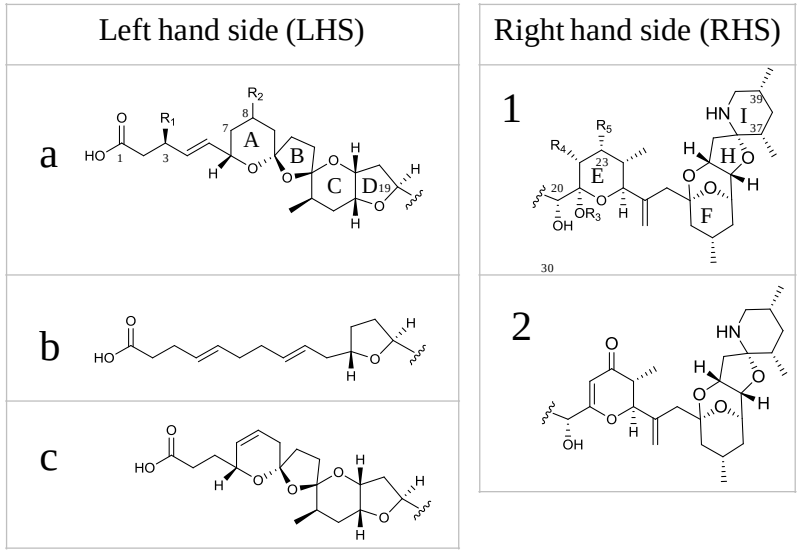

	Type§	R_1	7,8	R_2	R_3	R_4	R_5	R_6	$[M+H]^+$	Origin	Status	Toxicity (Jurkat) EC_{50}
AZA1	a1	H	Δ	H	H	CH_3	H	CH_3	842.5	*A. spinosum*	phycotoxin	1.1
37-*epi*-AZA1	a1	H	Δ	H	H	CH_3	H	CH_3	842.5	*A. spinosum*	artefact	0.2
AZA2	a1	H	Δ	CH_3	H	CH_3	H	CH_3	856.5	*A. spinosum*	phycotoxin	0.3
AZA3	a1	H	Δ	H	H	H	H	CH_3	828.5	shellfish	metabolite	0.6
AZA4	a1	OH	Δ	H	H	H	H	CH_3	844.5	shellfish	metabolite	2.0
AZA5	a1	H	Δ	H	H	H	OH	CH_3	844.5	shellfish	metabolite	3.0
AZA6	a1	H	Δ	CH_3	H	H	H	CH_3	842.5	shellfish	metabolite	0.2
AZA7	a1	OH	Δ	H	H	CH_3	H	CH_3	858.5	shellfish	metabolite	-
AZA8	a1	H	Δ	H	H	CH_3	OH	CH_3	858.5	shellfish	metabolite	0.3
AZA9	a1	OH	Δ	CH_3	H	H	H	CH_3	858.5	shellfish	metabolite	1.9
AZA10	a1	H	Δ	CH_3	H	H	OH	CH_3	858.5	shellfish	metabolite	3.1
AZA26	a2	H	Δ	H	-	-	-	-	824.5	shellfish	metabolite	36.6
AZA33	b1	-	Δ	-	H	CH_3	H	CH_3	716.5	*A. spinosum*	phycotoxin	5.2
AZA34	c1	-	Δ	-	H	CH_3	H	CH_3	816.5	*A. spinosum*	phycotoxin	0.2

§ The type refers to variations of the LHS and RHS parts of the molecule.

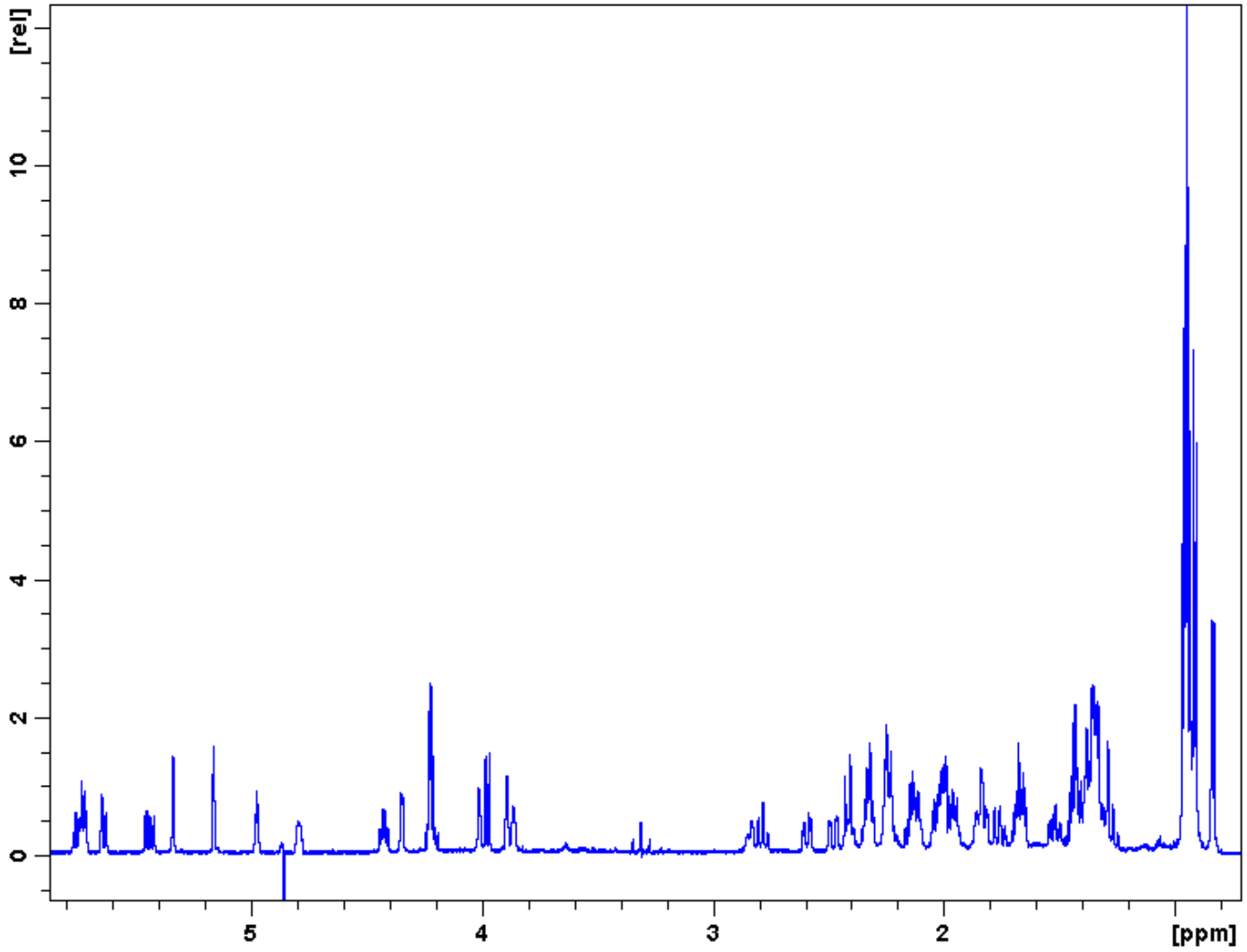

^{1}H NMR spectrum of AZA1 in CD_3OD

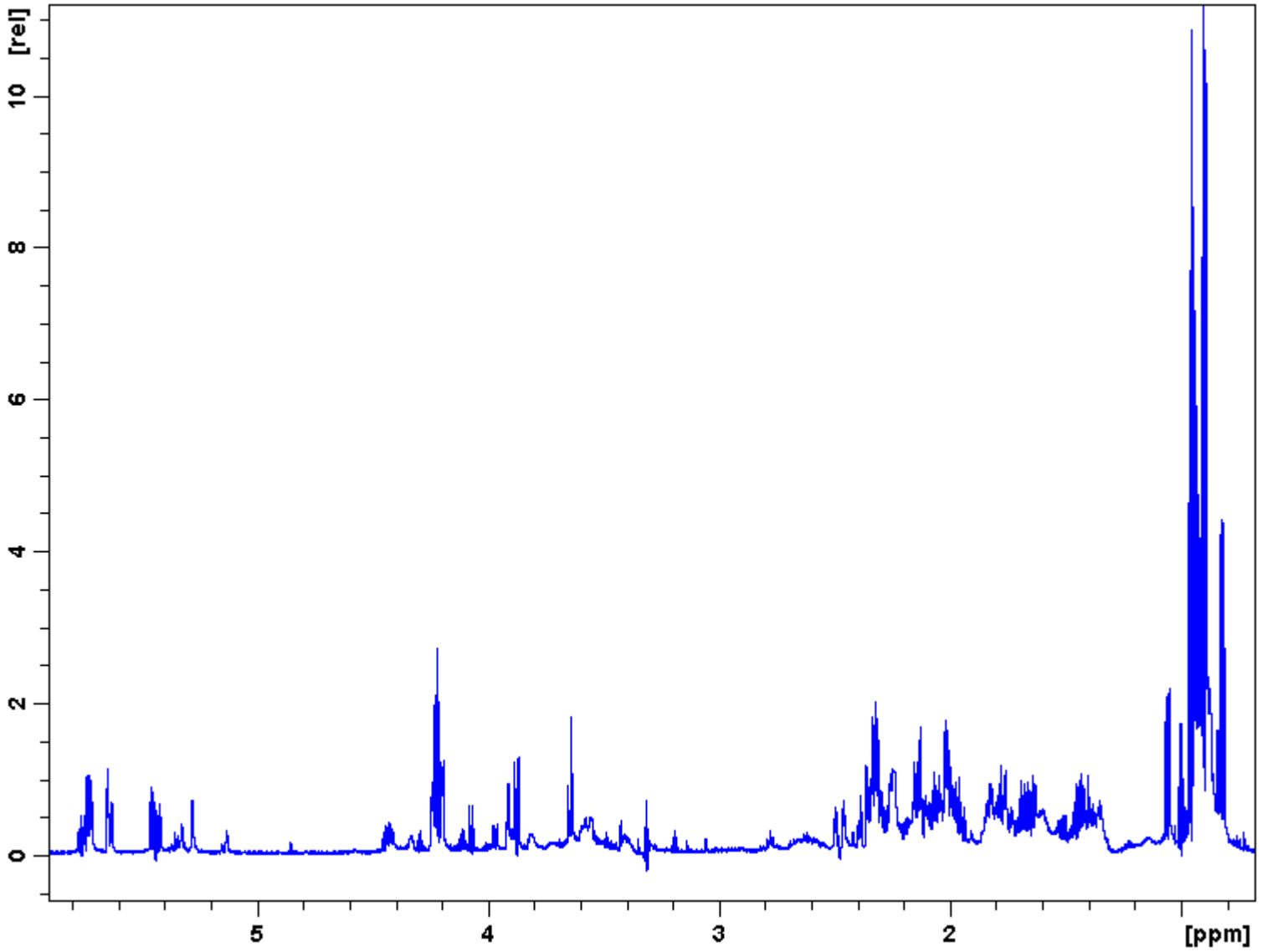

^{1}H NMR spectrum of 37-*epi*-AZA1 in CD_3OD

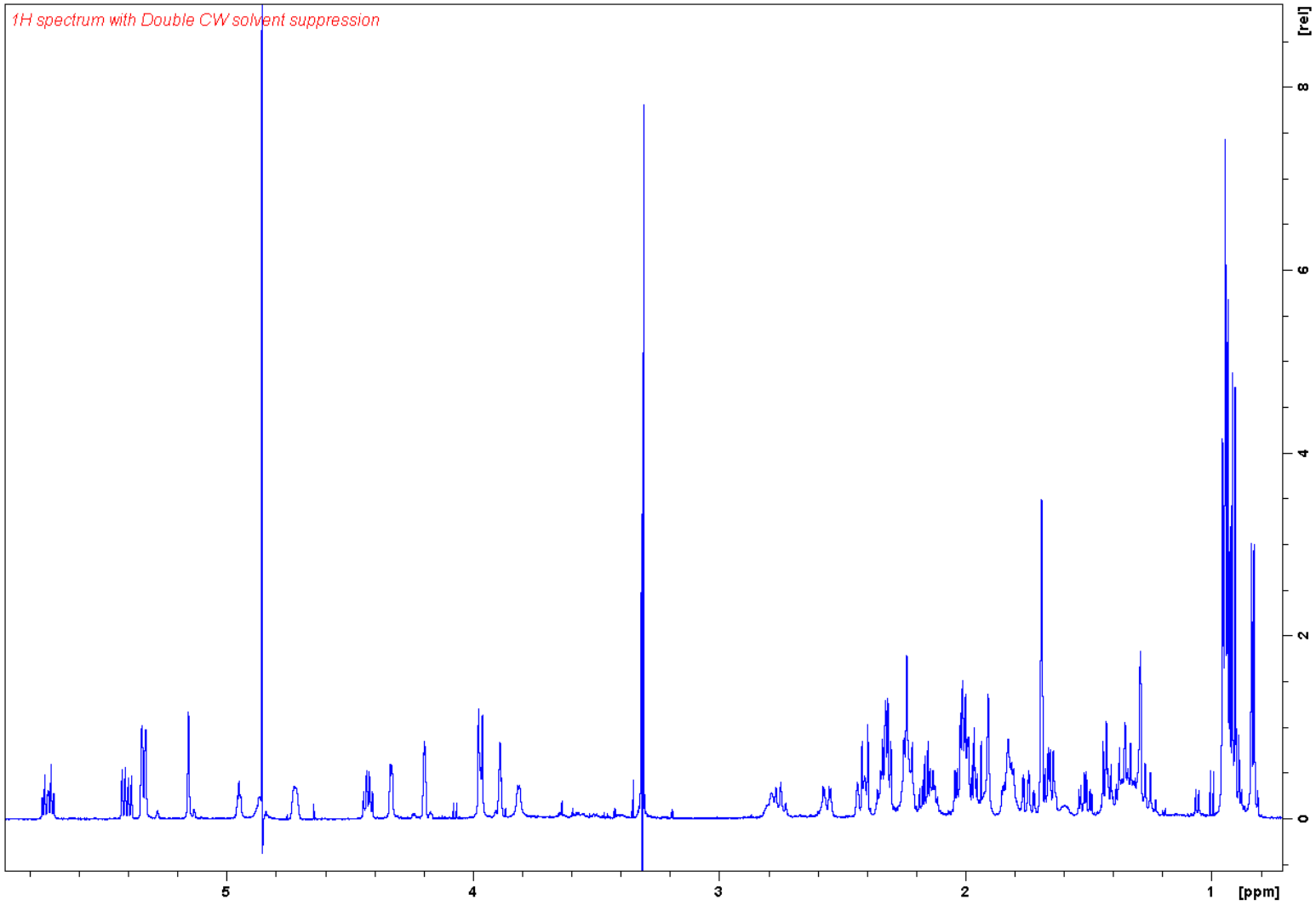

^{1}H NMR spectrum of AZA2

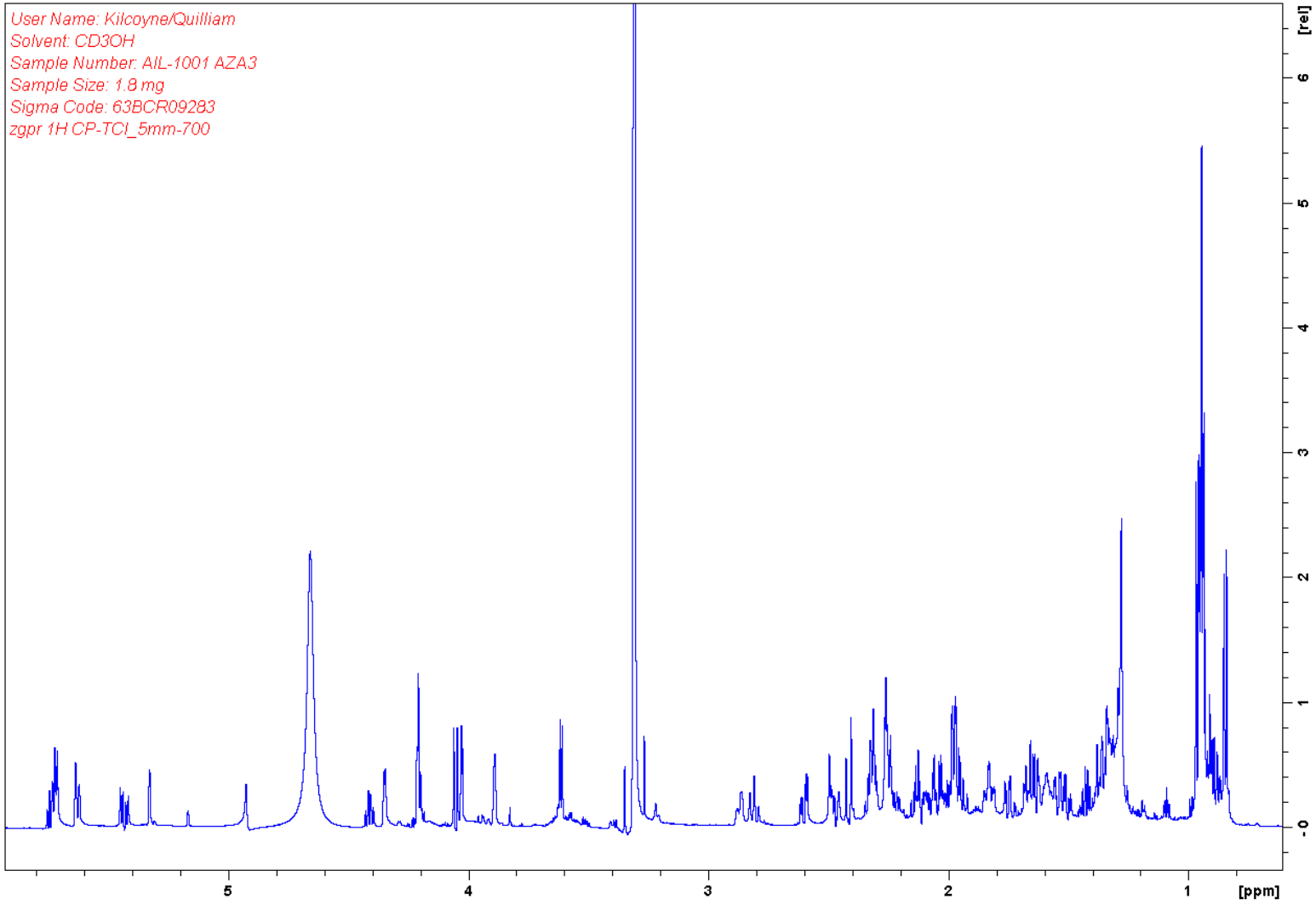

^{1}H NMR spectrum of AZA3

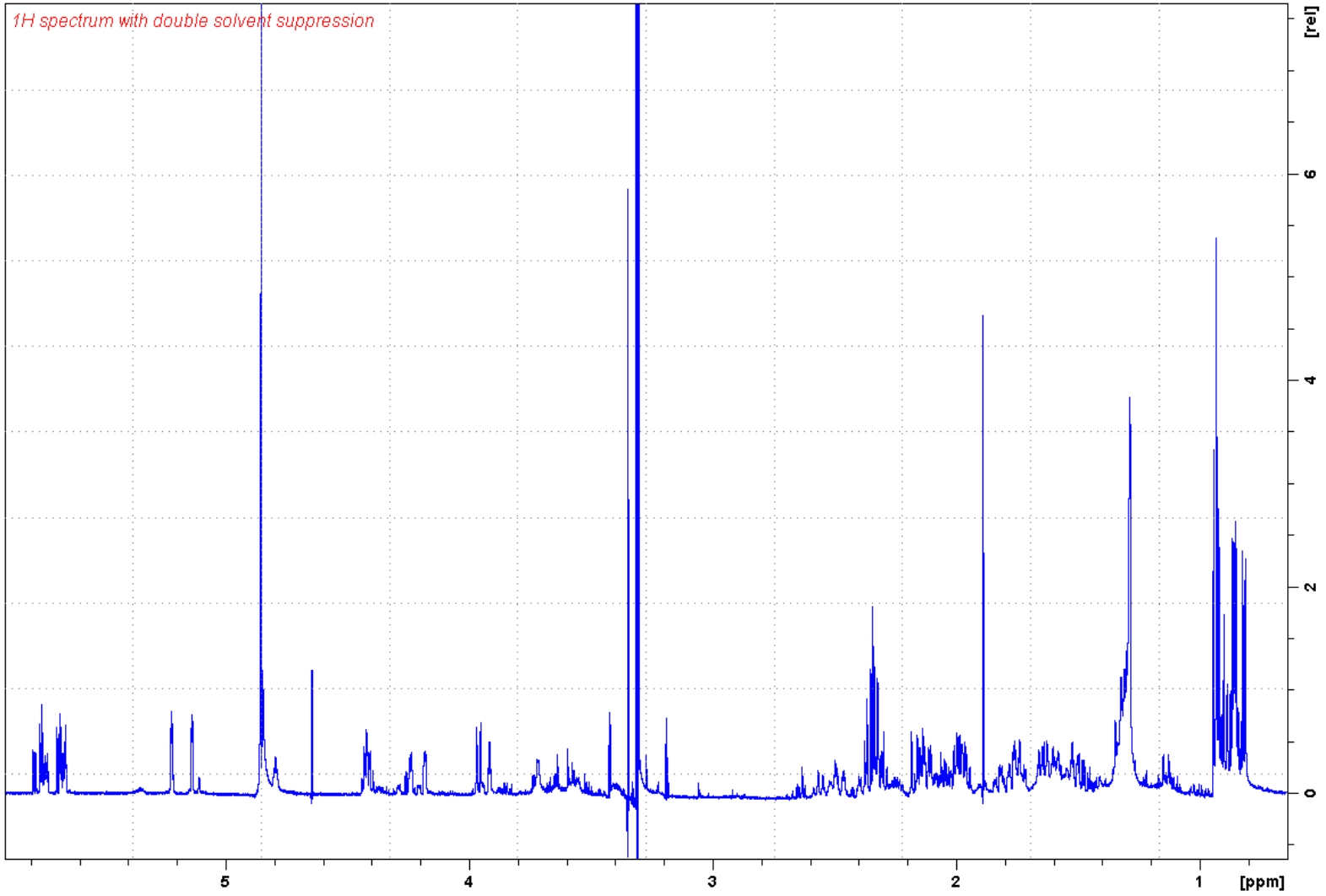

^{1}H NMR spectrum of AZA4

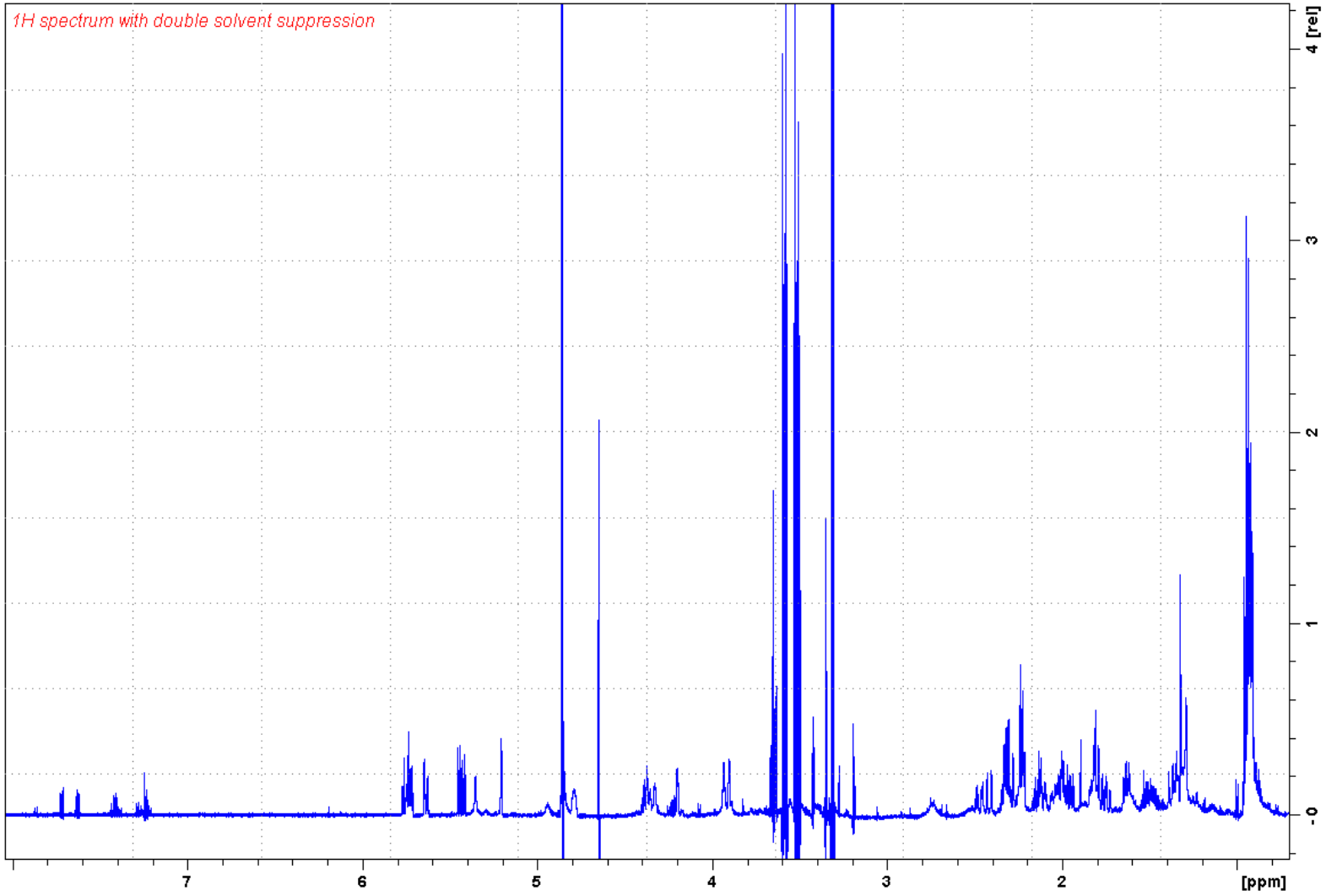

^{1}H NMR spectrum of AZA5

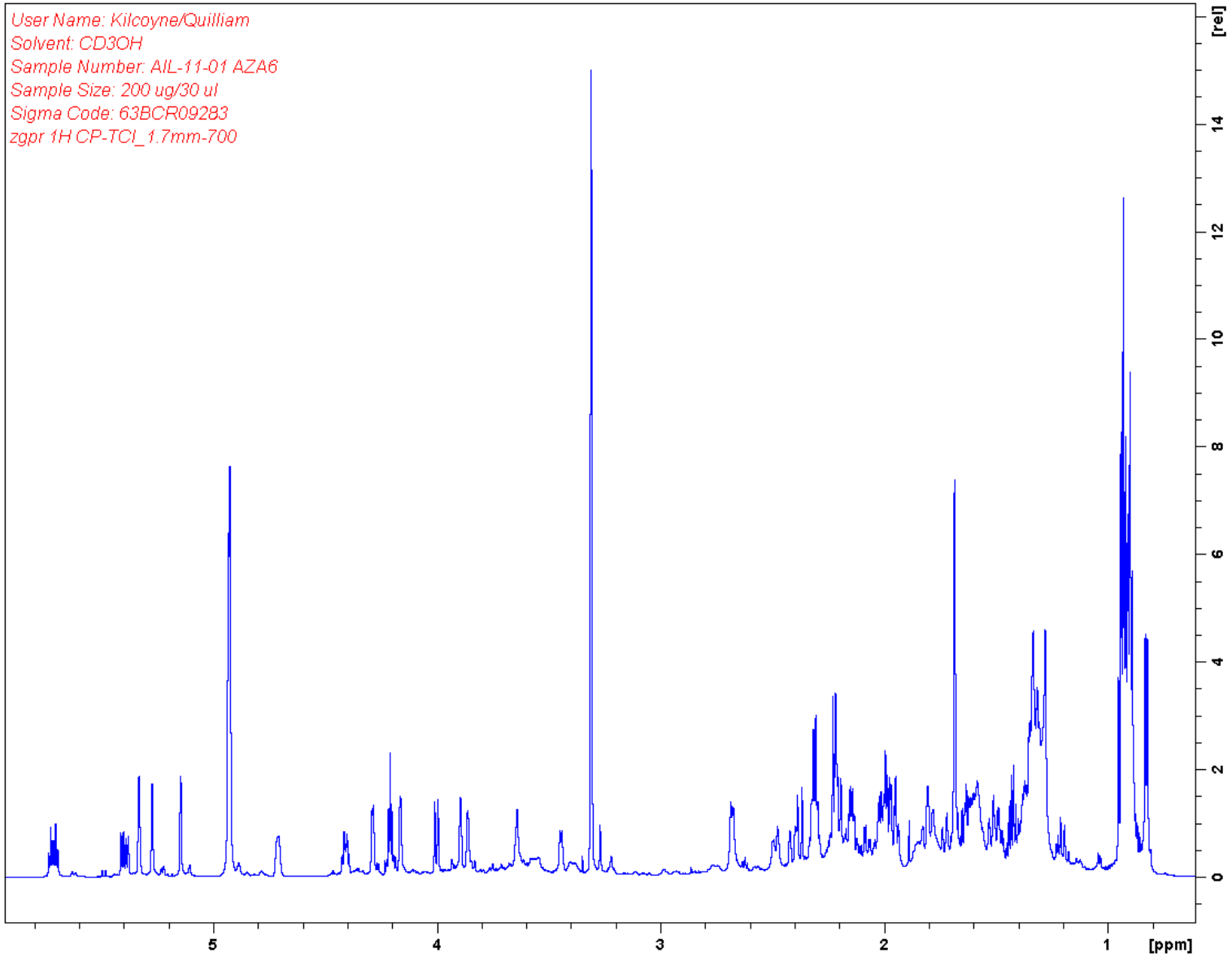

^{1}H NMR spectrum of AZA6

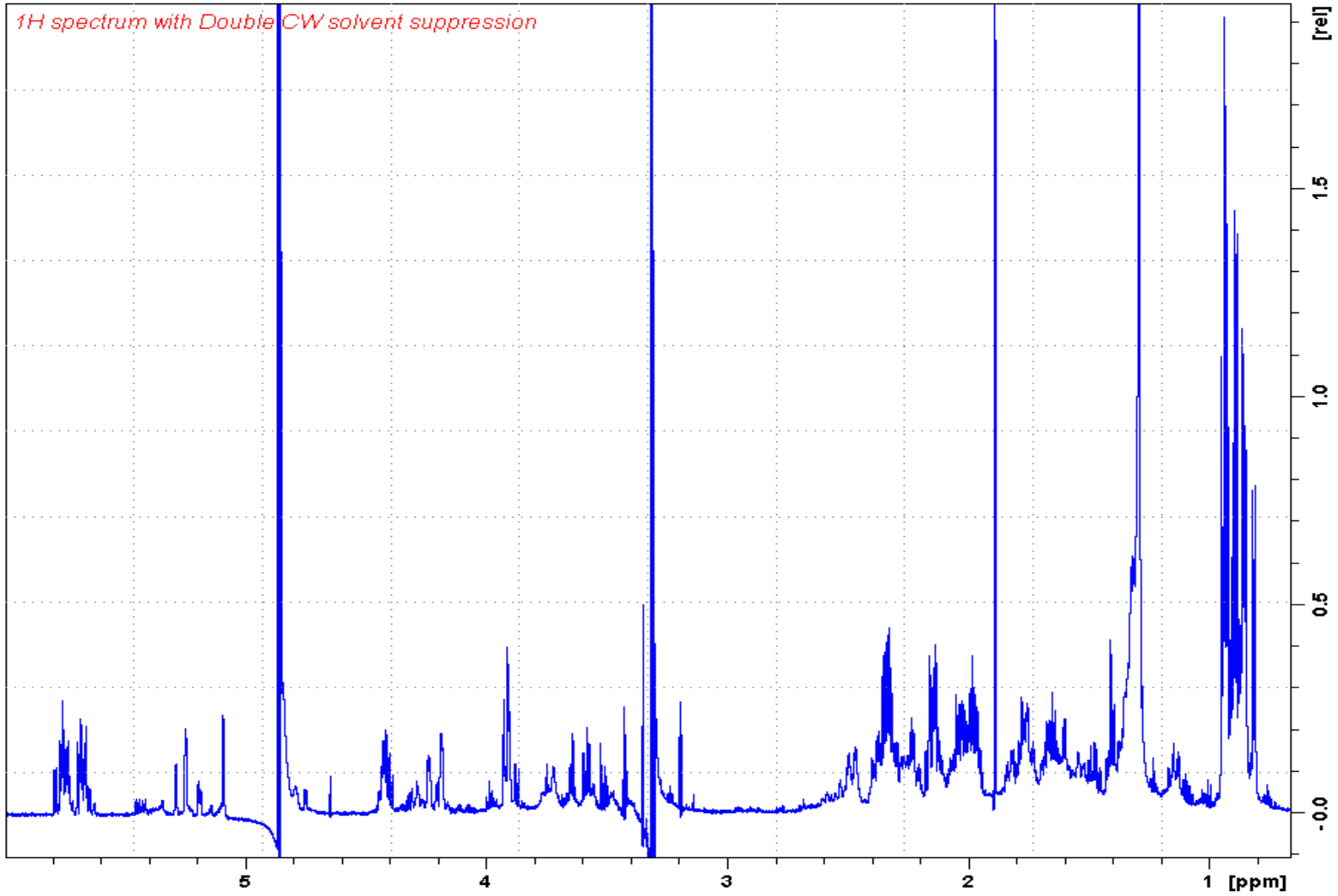

^{1}H NMR spectrum of AZA7

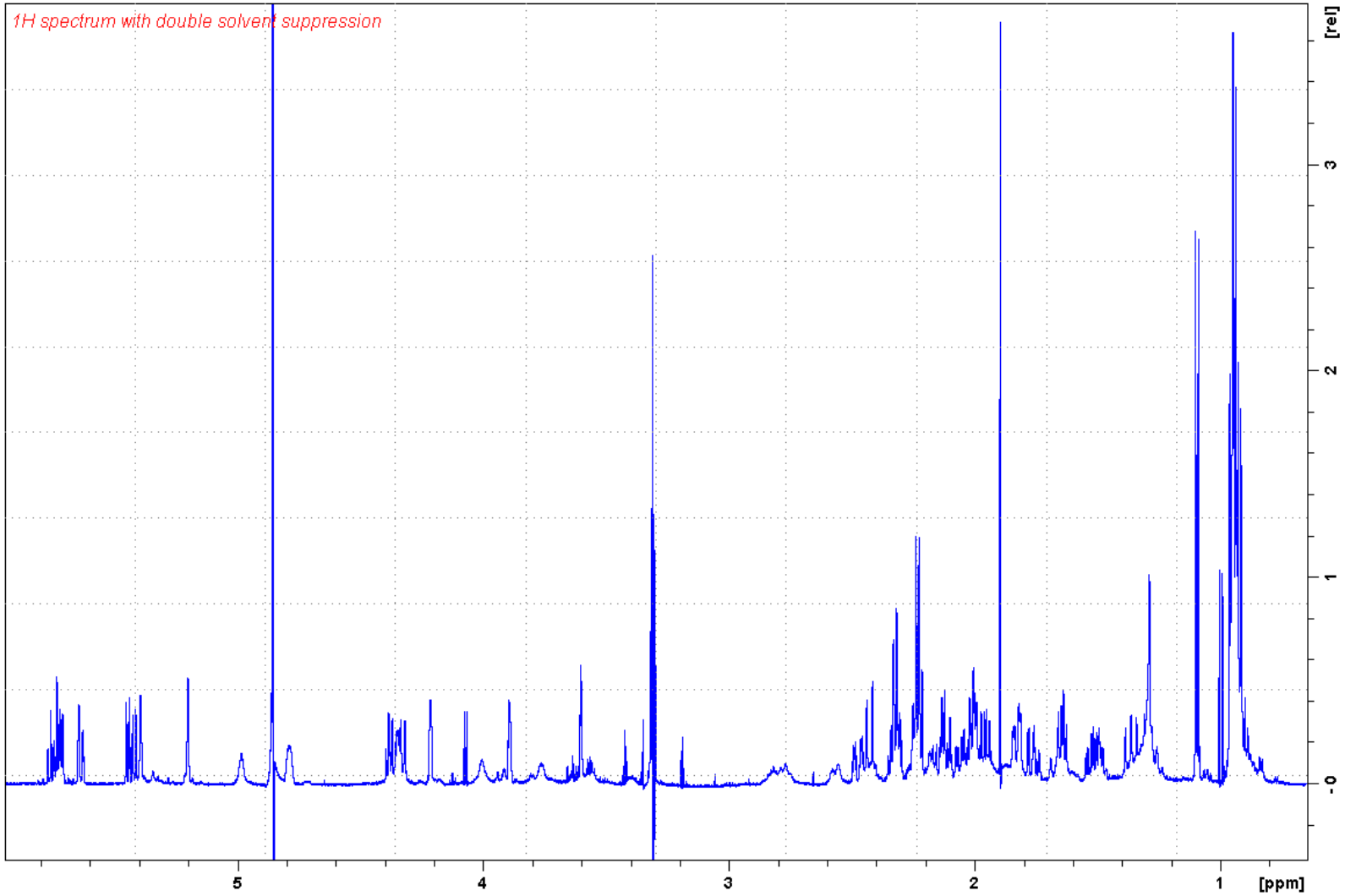

^{1}H NMR spectrum of AZA8

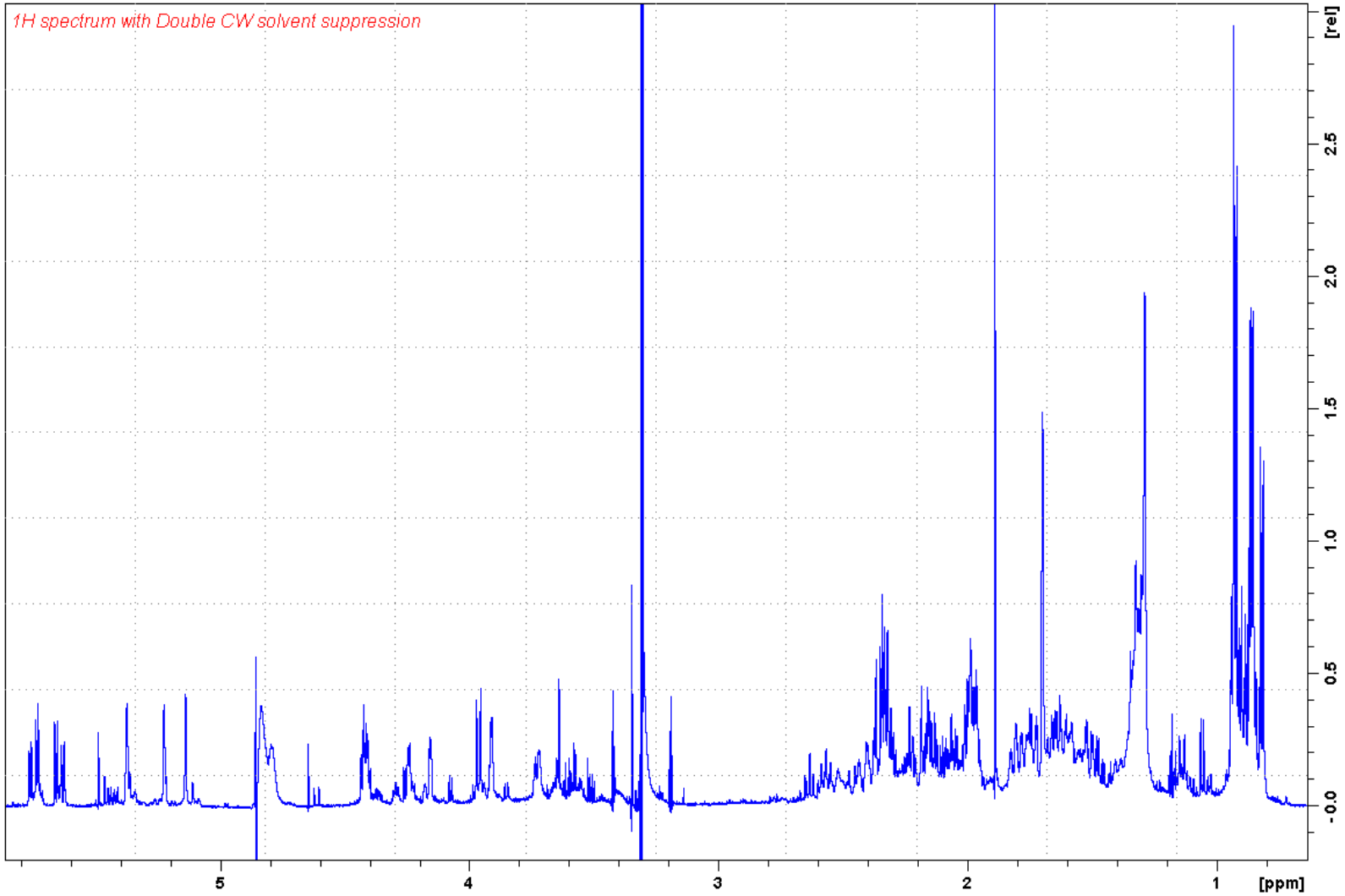

^{1}H NMR spectrum of AZA9

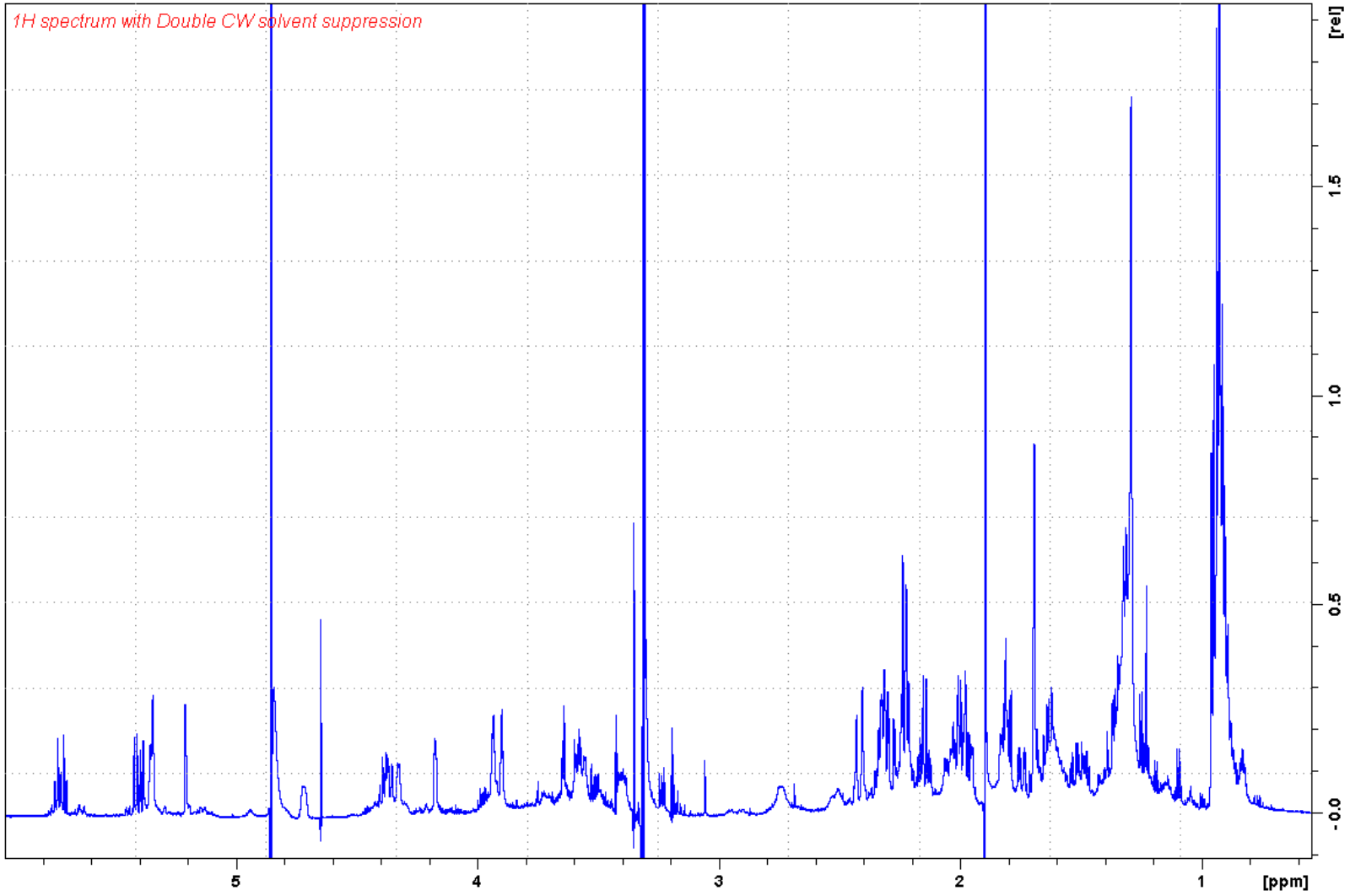

^{1}H NMR spectrum of AZA10

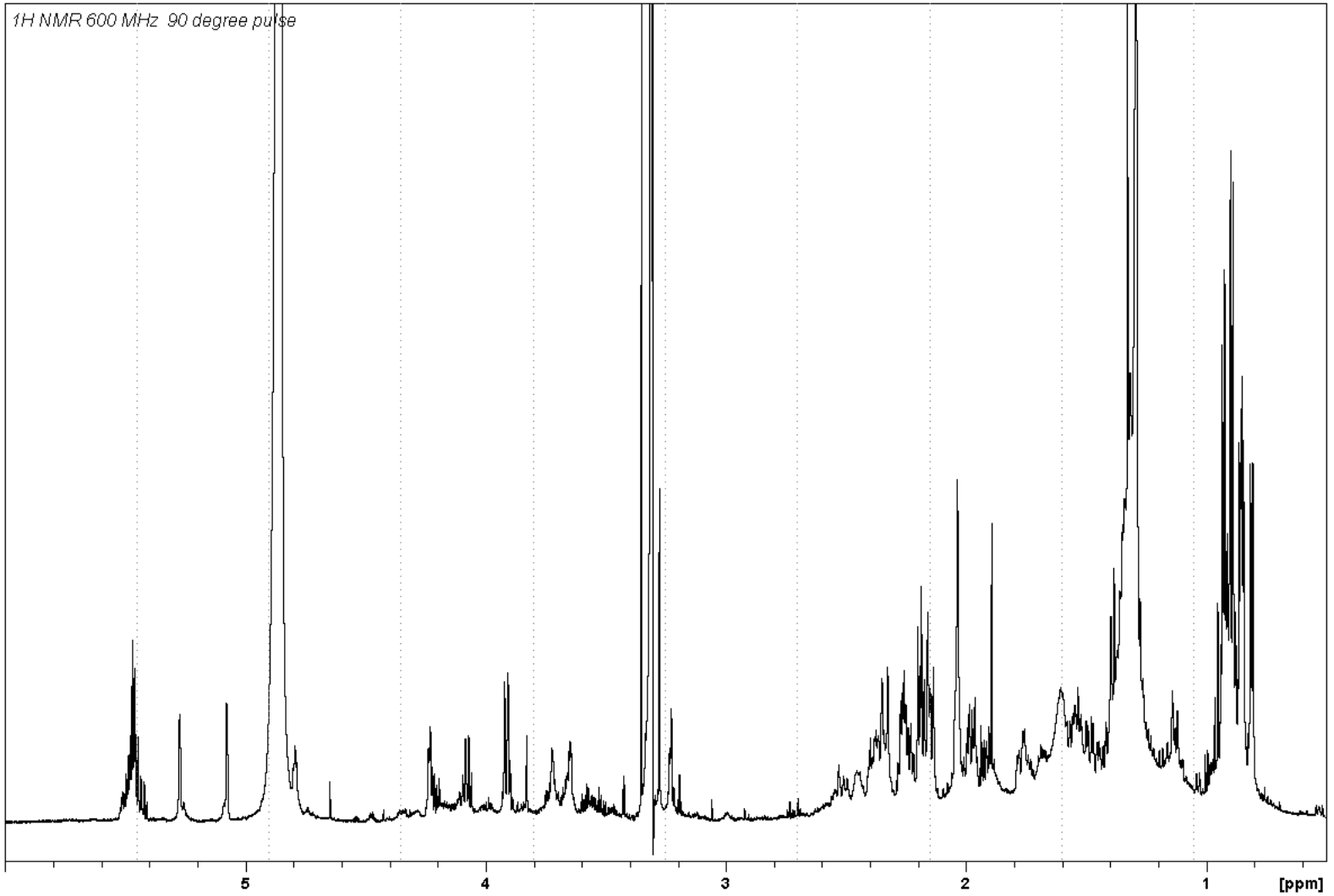

^{1}H NMR spectrum of AZA33 in CD_3OD

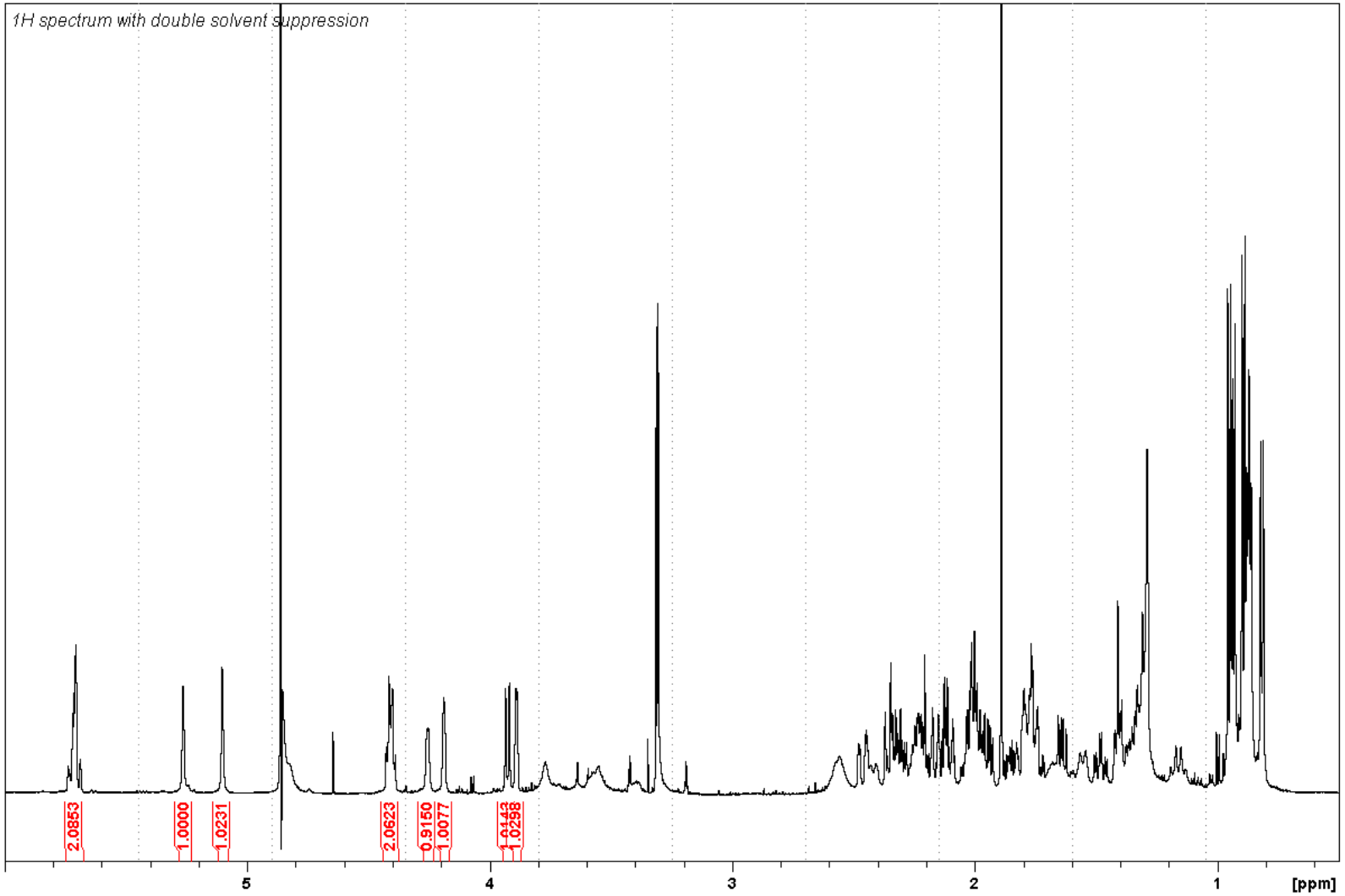

^{1}H NMR spectrum of AZA34 in CD_3OD